ROLE OF AKIRIN1 IN STRIATED MUSCLE

VANITHA VENKOBA RAO
(M.Sc), University of Madras

A THESIS SUBMITTED

FOR THE DEGREE OF DOCTOR OF PHILOSOPHY

DEPARTMENT OF BIOCHEMISTRY

NATIONAL UNIVERSITY OF SINGAPORE

2014

DECLARATION

I hereby declare that this thesis is my original work and it has been written by me in its entirety. I have duly acknowledged all the sources of information which have been used in the thesis.

This thesis has not been submitted for any degree in any university previously.

Vanitha Venkoba Rao

28 March 2014

ACKNOWLEDGEMENTS

Bertrand Russell once said, “The greatest of questions will lead you to the answer”. This quote strikes a nerve, as I near the end of my journey as a Ph.D student.

From Day 1, the Akirin1 project was a challenge that was spurred on by the innumerable questions that my mentor, Dr. Mridula Sharma and I had about this molecule. I would like to thank her first and foremost for her endless passion, her constant curiosity regarding the pleiotropic roles of this molecule and for constantly motivating the spirit of enquiry in me. I would also like to thank Dr. Ravi Kambadur, who has helped drive this project as well by his constructive and scientific opinions.

I am highly indebted to our collaborators Dr. Kazufumi Matsushita for sharing the Akirin1 knock-out mice without which this work would not have been possible.

I would also like thank Dr. Craig McFarlane for his critical thoughts and his helpful suggestions during lab meetings and otherwise.

Most importantly, I would like to thank the National University of Singapore and Yong Loo Lin school of Medicine for this opportunity and helping me to kick-start my scientific research career.

It would have been impossible for me to reach this juncture, had it not been for Dr. Xiaojia Ge, Dr. Ravi Kumar, Dr. Sudarsana Reddy and Dr. Sabeera who took the time out of their busy schedules to teach me the techniques at the very beginning.

The name that appears on this thesis is mine; however I am immensely grateful to Ms. Uma Maheswari and Ms. Kavitha Arockia Mary for their help with the experiments over the course of my Ph.D.

I would like to convey my gratitude to Dr. Himani Kukreti for sharing her perspective on this work and timely help with thesis correction.

I am grateful to the staff at the NTU animal facility for their help in maintaining the animals used in this study.

My heartfelt thanks to Mr. Kelvin Tan Suan Liang, Mr. Anantharaj and Ms. Subha for helping me with animal work.

I would like to extend my sincere gratitude to my Ph.D. Thesis Advisory Committee (TAC) members, Assoc. Prof. Markus R. Wenk and Dr. Takao Inoue for their critical and constructive advice on this work.

I would like to thank all the other members of the Functional Muscle genomics group for their inputs to my knowledge base and making the lab an enjoyable place to working.

My Ph.D. journey would not have been the same without my friends Mubashir, Upasna, Ritika, Devika, Nargis, Shruti, Sukanya and Indra Kumar. Thank you all for putting up with grumpy me when experiments failed. You guys definitely added sanity and peace into my life.

Last but not the least, I am highly indebted to my family for being there for me during all those hard times and supporting me both emotionally and financially.

TABLE OF CONTENTS

ABSTRACT

Akirin1 is a small (191 amino acid) ubiquitously expressed protein, which belongs to a family of highly conserved nuclear proteins called *akirins*. Due to its nuclear localization and propensity to interact with other proteins, Akirin1 is speculated to regulate transcription of its target genes as a cofactor. Previous studies have shown that Akirin1 is a downstream target of myostatin, which is a negative regulator of myogenesis. Akirin1 was expressed at higher levels in mice lacking myostatin and consistent over-expression of Akirin1 induced hypertrophy in C_2C_{12} myotubes *in vitro*.

To further elucidate the function of Akirin1 in striated muscle (skeletal muscle and cardiac muscle), an Akirin1 knock-out mouse model was used in this study. The results of this study show that Akirin1 knock-out mice did not show any obvious phenotypic change when compared to wild-type mice. The molecular analysis of important myogenic genes performed on Akirin1 knock-out skeletal muscle revealed that levels of myogenic genes were unchanged apart from myogenin.

Molecular analysis of sarcomeric genes like α-actin, Myosin heavy chain and troponins showed that Akirin1 knock-out skeletal muscle showed reduced levels of these proteins compared to the wild-type. Lack of Akirin1 also leads to reduced levels of certain cytoskeletal proteins like desmin and poly-glutamylated tubulin compared to the wild-type. These results indicate that Akirin1 plays an important role in maintaining the structural integrity in skeletal muscle.

One other important protein that helps in maintaining the sarcomere stability is MuRF1. Molecular analysis of MuRF1 in Akirin1 knock-out muscle showed

that MuRF1 mRNA and protein levels were down-regulated. Similarly, Akirin1 knock-out primary myoblast cultures also showed reduced MuRF1 mRNA and protein levels during differentiation. The results showed that Akirin1 regulates MuRF1 level in skeletal muscle. To determine how Akirin1 regulates MuRF1, we analyzed the promoter region of MuRF1. The promoter analysis showed FoxO3 and CREB-1 binding sites on MuRF1 promoter. Indeed, FoxO3 and CREB-1 protein levels were down-regulated in Akirin1 knock-out muscle compared to the Wild-type. Consistently, the levels of MuRF1, CREB-1 and FoxO3 were up-regulated when Akirin1 was over-expressed in C_2C_{12} myoblasts. Promoter-reporter assay results indicated that Akirin1 might be regulating the transcription of MuRF1 through CREB-1 and FoxO3.

One of the molecules important for maintaining the post-natal muscle mass and myoblast differentiation is serum response factor (SRF). We saw increased SRF levels in differentiating primary cultures compared to the wild-type. It is likely that Akirin1 negatively regulates SRF during differentiation because SRF, being a target of MuRF1, is not degraded due to lower MuRF1 levels.

Gene expression analysis showed that Akirin1 transcriptionally regulates the expression of different types of *Myh* genes. As a result of which, lack of Akirin1 makes the muscle less oxidative due to increase in *Myh2,* thus an increase in type IIa muscle fibers and decrease in *Myh7,* thus a decrease in type I muscle fibers. This shows a novel role of Akirin1 in maintaining the muscle fiber type and in turn regulating the metabolic activity of the muscle.

Akirin1 was found to have an interesting function in cardiac muscle. Histological analysis of Akirin1 knock-out heart showed larger ventricular cavity as seen in left ventricular hypertrophy (LVH). Absence of Akirin1 was shown to post-transcriptionally up-regulate serum response factor (SRF), which is known to affect the gene expression of cardiac hypertrophy inducing genes like β-MyHC and atrial natriuretic peptide (ANP) and miR-1. Our results showed that β-MyHC and ANP were transcriptionally up-regulated and miR-1 level was transcriptionally down regulated in Akirin1 knock-out cardiac muscle compared to the wild-type cardiac muscle. Thus, proposing that Akirin1 regulates SRF, which in turn maintains cardiac mass through regulating miR-1 expression. In summary, we speculate that Akirin1 regulates skeletal muscle metabolism and cardiac hypertrophy through different mechanisms.

LIST OF TABLES

LIST OF FIGURES

LIST OF SYMBOLS

%	Percentage
°C	Degree Celsius
3′	3 prime
5′	5 prime
A band	Anisotropic band
AA	Amino acid
ActRIIB	Activin type receptor IIB
ADP	Adenosine diphosphate
AF	Alexa Fluor
AIDS	Acquired Immuno Deficiency Syndrome
ALK4	Activin receptor-like kinase 4
AMP	Adenosine monophosphate
AMPK	AMP-activated protein kinase
Ang	Angiotensin
ANP	Atrial natriuretic peptide
ATCC	American Type Culture Collection
ATP	Adenosine triphosphate
bHLH	basic helix-loop-helix
BSA	Bovine Serum Albumin
BYM338	Bimagrumab
Ca^{2+}	Calcium
CAN	Ca^{2+} binding catalytic subunit
CBP	CREB binding protein
Cdk	Cyclin dependent kinase

cDNA	Complementary DNA
CE	Cytoplasmic extract
CEE	Chick embryo extract
ChIP	Chromatin Immunoprecipitation assay
CHO	Chinese hamster ovary
CKI	Cyclin dependent kinase inhibitor
cm	Centimeter
CNB	Ca^{2+} binding regulatory subunit
CO_2	Carbon dioxide
COOH	Carboxylic acid
DAPI	4',6-diamidino-2-phenylindole
DEPC	Diethylpyrocarbonate
dl	Deciliter
DmAkirin	Drosophila Akirin
DMD	Duchenne muscular dystrophy
DMEM	Dulbecco's Modified Eagle Medium
DMSO	Dimethyl sulfoxide
DNA	Deoxyribonucleic acid
DTT	Dithiothreitol
e.g.,	Example
ECM	Extra-cellular matrix
EMSA	Electrophoretic mobility shift assay
eMyHC	Embryonic MyHC
ER	Endoplasic reticulum
ERK	Extracellular signal-regulated kinase

ET	Endothelin
FBS	Fetal Bovine Serum
FGF	Fibroblast growth factor
FGFR1	FGF receptor 1
GDF-8	Growth and Differentiation Factor-8
GPCR	G-protein-coupled receptors
GPD	α-glycerophosphate dehydrogenase
HATs	Histone acetyltransferases
HGF	Hepatocyte growth factor
HRP	Horse radish peroxidase
HS	Horse Serum
I band	Isotropic band
IACUC	Institutional Animal Care and Use Committee
ICC	Immunocytochemistry
IGF-1	Insulin-like growth factor-I
IgG	Immunoglobulin G
JNK	c-Jun N-terminal kinase
KC1	Potassium chloride
kDa	Kilo Dalton
L	Liter
LAP	Latency-associated protein
LB	Luria Bertani
Lbx1	Ladybird homeobox 1
M	Molar
MAPK	Mitogen-activated protein kinase

MEF2	Myocyte enhancer factor-2
mg	Milligram
ml	Milliliter
MLC	Myosin light chain
mM	Millimolar
MOPS	3-(N-morpholino) propanesulfonic acid
Mrf4	Myogenic regulatory factor 4
MRFs	Myogenic Regulatory Factors
mRNA	Messenger ribonucleic acid
mtDNA	Mitochondrial Deoxyribonucleic acid
mTOR	Mammalian target of rapamycin
mTORC1	mTOR Complex 1
MuRF-1	Muscle ring finger-1
Myf5	Myogenic factor 5
MyHC	Myosin heavy chain
MyoD	Myogenic differentiation factor
Na_2-EDTA	Disodium ethylenediaminetetraacetic acid
NaCl	Sodium chloride
NaF	Sodium fluoride
NaOH	Sodium hydroxide
NBT	Nitro Blue Tetrazolium
NE	Nuclear extract
NF-κB	Nuclear factor-kappa B
NFAT	Nuclear factor of activated T-cells
ng	nanogram

NLS	Nuclear localization signal
nm	Nanometre
nmoles	Nanomoles
NP-40	Nonidet P-40
NSS	Normal sheep serum
NTU	Nanyang Technological University
nuDNA	Nuclear DNA
OCT	Optimal cutting temperature (embedding matrix)
OD	Optical density
P/S	Penicillin/Streptomycin
PAGE	Polyacrylamide gel electrophoresis
Pax	Paired box gene
PBS	Phosphate buffered saline
PBS-T	PBS-Tween 20
PCR	Polymerase Chain Reaction
PEG	Polyethylene glycol
PGC-1α	Peroxisome proliferator-activated receptor γ coactivator-1α
PI3-K	Phosphoinositide 3-kinase
PMSF	Phenylmethanesulfonylfluoride
PPARß/δ	Peroxisome proliferator-activated receptor ß/δ
PVP	Polyvinylpyrrolidone
Rb	Retinoblastoma
RBCC	RING/B box/Coiled coiled
RNA	Ribonucleic acid

RNAi	RNA interference
ROS	Reactive oxygen species
rpm	Revolution per minute
RT	Reverse Transcriptase
RT-qPCR	Real time-qualitative Polymerase Chain Reaction
SAPK	Stress-activated protein kinases
SC	Satellite cell
SDH	Succinate dehydrogenase
SDS	Sodium dodecyl sulphate
SEM	Standard Error of Mean
Smad	Small mothers against decapentaplegic
SmAkirin1	*Scophthalmus maximus* Akirin1
TA	*Tibialis anterior*
TAE	Tris-Acetate EDTA
TAK1	Transforming growth factor-ß-activated kinase 1
TBE	Tris Borate-EDTA
TBS	Tris buffered saline
TBS-T	Tris buffered saline – Tween 20
TE	Tris-EDTA
TGFβ	Transforming growth factor β
U	Units
USA	United Sates of America
UV	Ultraviolet
V	Volt

µg	Microgram
µl	Microliter
µM	Micromolar

OVERVIEW OF THE THESIS

Akirin1 is one of the relatively unstudied molecules in muscle biology, in terms of its potential role and the various facets that are still left to be explored. This small nuclear protein is evolutionarily conserved and known to be ubiquitously expressed in all the tissues. As Akirin1 has been previously established as an important pro-myogenic factor in myogenic cells (Marshall et al., 2008), our study involves understanding the role of Akirin1 in fully differentiated striated muscle (both skeletal and cardiac muscle).

As the emphasis of this study is in skeletal and cardiac muscle, relevant literature about skeletal and cardiac muscle structure, development and function and the various factors involved in these processes has been reviewed in chapter 1. The various materials and methods used in this study have been explained in chapter 2. The novel findings of this study are divided into three chapters in which the possible role of Akirin1 in myogenic differentiation, skeletal muscle and cardiac muscle has been discussed respectively.

Through this study we have established a novel role of Akirin1 in regulation of genes involved in maintenance of sarcomere structure and function. Additionally, we have shown an important function of Akirin1 in maintaining fiber-type composition and metabolic homeostasis in skeletal muscle. Furthermore in cardiac muscle, our results indicate an important role of Akirin1 in maintaining cardiac muscle mass via regulating miR-1 biogenesis. In summary, our study indicates a novel function of Akirin1 in both skeletal muscle and cardiac muscle albeit through different mechanisms.

CHAPTER 1

REVIEW OF LITERATURE

1. REVIEW OF LITERATURE

1.1 Skeletal muscle

Skeletal muscle is a highly contractile tissue derived from the mesodermal layer of embryonic germ cells. Skeletal muscle makes up to 40-50 % of the total body weight making it one of the largest organs. Vertebrates have three types of muscle tissue: skeletal, cardiac and smooth muscle. Skeletal and cardiac muscle are striated muscle while smooth muscle is non–striated. Although the three types of muscle share similar features, they vary from each other in their location, microscopic structure and how they are influenced by the nervous system. Skeletal muscle is controlled by somatic nervous system and thus is voluntarily controlled. This tissue is mostly attached to the skeleton via bundles of collagen fibers called tendons that aid in locomotion, stabilizing joints and posture maintenance. However, there are a few skeletal muscles that assist in the movement of other skeletal muscles or movement of certain internal organs. Skeletal muscle is metabolically active tissue playing a major role in carbohydrate and lipid metabolism and maintaining the energy homeostasis of the body.

1.1.1. Skeletal muscle structure

Skeletal muscle is a highly organized tissue composed of several distinct compartments of muscle fibers. An individual skeletal muscle is contained within a layer of connective tissue called the epimysium (Seeley et al., 2006) (Figure 1.1A). Skeletal muscle is further divided into smaller compartments by the perimysium called fascicle. In turn, a fasciculus contains bundles of muscle fibers encased by a layer of connective tissue called endomysium.

Each muscle fiber is a multinucleated single cell, enclosed by sarcolemma, and is predominantly made up of myofibrils (Seeley et al., 2006) (Figure 1.1B). Each myofibril in turn is made up of various types of proteins that form the contractile element of muscle called sarcomere (Seeley et al., 2006) (Figure 1.1C). Myofibrils basically contain three categories of proteins which function jointly leading to the contraction of the muscle: 1) Structural proteins, which give the frame work and elasticity to the muscle like titin and desmin; 2) Contractile proteins, which provide force during contraction of the muscle like actin and myosin; 3) Regulatory proteins, which regulate the process of contraction and relaxation of the muscle like troponins (Martini, 2006). The detailed structure of sarcomere will be later discussed in detail in section 1.1.1.1.

Apart from myofibrils, muscle fibers contain vital organelles like mitochondria, sarcoplasmic reticulum and myonuclei in sarcoplasm. Sarcoplasmic reticulum is made up of numerous transverse tubules and terminal cisterns filled with interstitial fluid. Two terminal cisterns and a transverse tubule form a triad, which invaginates from the sarcolemma to the center of the muscle fiber (Fung et al., 1981; Martini, 2006).

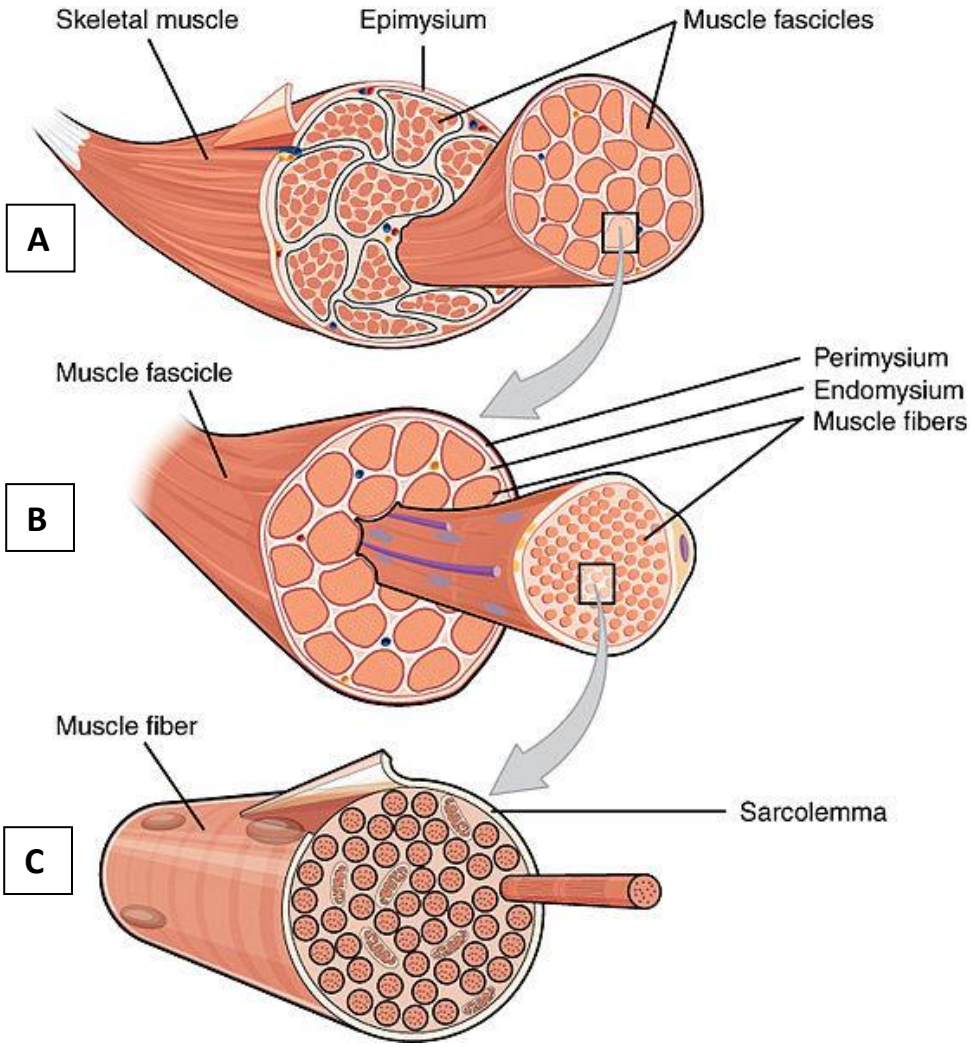

Figure 1.1 Skeletal muscle structure (A) Skeletal muscle is made up of fascicles, which are enclosed in the perimycium. The entire skeletal muscle is enclosed in the epimycium. (B) Fascicles are made up of muscle fibers, which are enclosed in the endomycium. (C) Muscle fiber is made up of myofibrils, which are in turn made up of sarcomeres enclosed in sarcolemma. Sarcomeres are mainly composed of actin and myosin filaments. Figure freely downloaded at http://commons.wikimedia.org/wiki/File:1007_Muscle_Fibes_%28large%29.jpg (Anatomy & Physiology, Connexions Web site. http://cnx.org/content/col11496/1.6/) on 29.12.2014.

1.1.1.1. Sarcomere structure

Sarcomere is the basic structural and functional element of skeletal muscle. It is defined by borders made of dense line of protein called Z-line. In between the Z line are series of thick and thin protein filaments, along with proteins that regulate the movement of thick and thin filaments. The thin actin filaments are 1-2 μm long and 8 nm in diameter, while thick myosin filaments are 1-2 μm long and 16 nm in diameter. Regular arrangement of these thick and thin filaments gives striated appearance to the muscle fiber. Due to differences in the density of thick and thin filaments, sarcomere shows dark A band at the center consisting of predominantly thick filaments and light I band at the periphery consisting of thin filaments. The center of the dark A band is bisected by M line of proteins which hold the thick filaments together. Under resting conditions, dark A band consists of two zones- H zone, which is the portion on either side of the M line consisting only of thick filaments; Zone of overlap, which is the portion where thick and thin bands overlap. During muscle contraction, due to increased overlapping of thick and thin filaments, the dark A band increases in size while light I band and H zone decreases, resulting in the shortening of the sarcomere (Campbell, 1996; Martini, 2006; Wakabayashi et al., 2010) (Figure 1.2A). The thick filament is predominantly made of rod-shaped protein called myosin. Each myosin molecule is made up of two myosin heavy chains (MyHC) and four myosin light chains (MLC). Myosin heavy chain protein has two catalytic globular heads at one end that binds to ATP, a regulatory neck region at the center made up of a pair of MLC and a tail at the other end. About 300 myosin molecules polymerize at the tail region to form the thick filament and the globular heads protrude from the

thick filament. The thin filament is predominantly made of globular proteins called actin. Many actin molecules polymerize and form long double helical structure called the thin filament. The globular heads of myosin interact with the actin filaments and lead to sliding of the filaments along each other eventually leading to contraction of the sarcomere. Apart from the structural proteins, a sarcomere contains regulatory proteins associated with the myofibrils that play important role in regulation of sarcomere contraction- Tropomyosin and troponin complex. Tropomyosin is a long myofibrillar protein that fits into the groove of two actin filaments and anchors Troponin complex. Troponins are a complex of three proteins- Troponin C, Troponin T and Troponin I. Troponin C contains a Ca^{2+} binding domain, troponin T interacts with tropomyosin and troponin I blocks the interaction of myosin and actin filaments (Figure 1.2B). When nerve impulses reach the neuromuscular junction, Ca^{2+} is released from the sarcoplasmic reticulum of the muscle fiber. Interaction of Ca^{2+} with Troponin C leads to conformational change in Troponin I as a result of which Troponin T is able to interact with tropomyosin and this allows interaction of myosin heads with actin filaments (Bagshaw, 1993; Campbell et al., 1996). According to sliding filament theory of muscle contraction, myosin head binds to adenosine triphosphate (ATP) and hydrolyzes ATP to adenosine diphosphate (ADP) and a phosphate ion. The energy released activates the myosin heads to interact with active site on the actin filaments creating a cross-bridge between thick and thin filaments. The hinge region of myosin molecule consisting of MLC acts as a regulatory lever for the myosin head domain. Myosin head then releases the ADP and phosphate ion while pulling the thin filament along. ADP on the myosin head

is recharged with ATP leading to dissociation of Myosin and actin bond, thus preparing for the next cycle. Many myosin heads together 'walk' on the actin filament leading to contraction of the sarcomere (Martini, 2006).

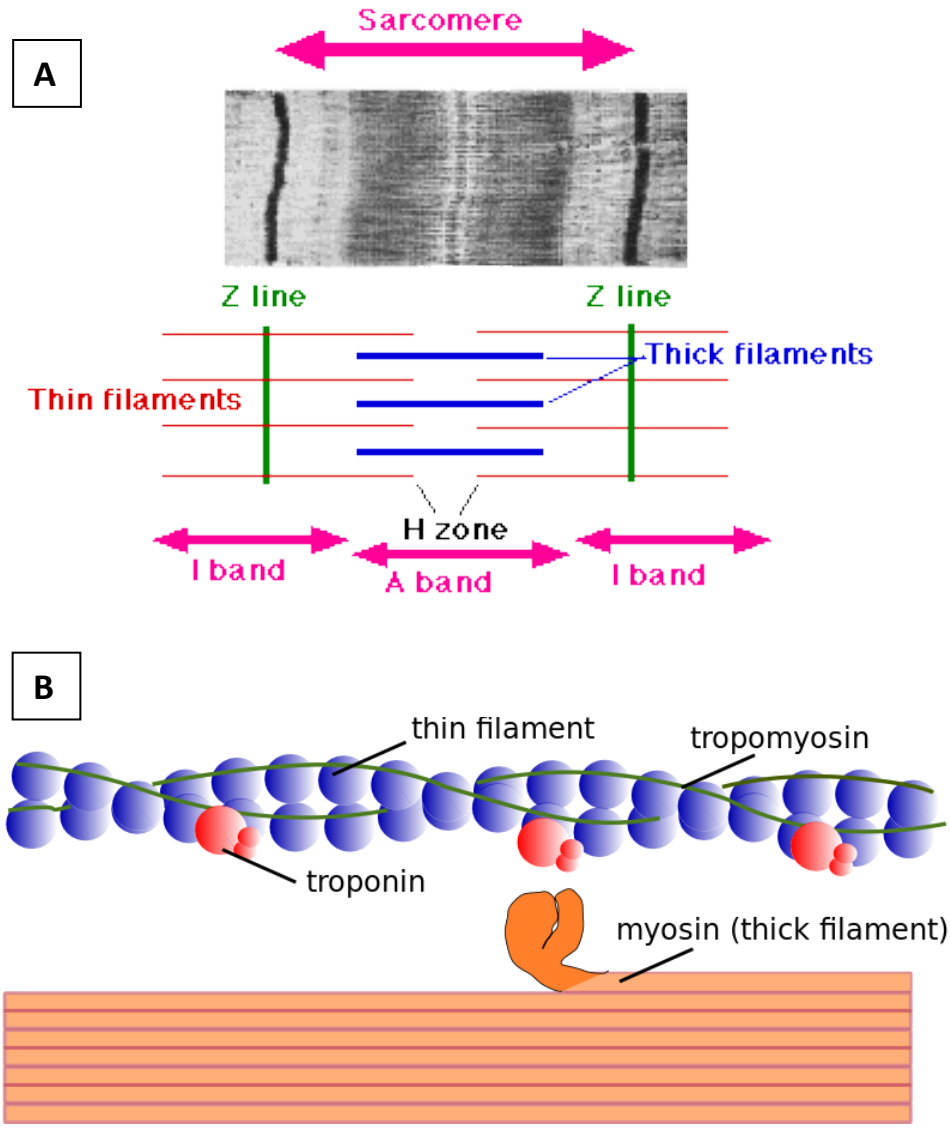

Figure: 1.2 Sarcomere structure and function. (A) Structure of sarcomere showing different regions during contraction. Figure freely downloaded from http://commons.wikimedia.org/wiki/File:Sarcomere.gif on 29.12.2014. (B) Sarcomere is mainly made up of actins, myosins and troponins that work in consort leading to the contraction of the sarcomere. Figure freely downloaded from http://commons.wikimedia.org/wiki/File:Myofilament.svg (Häggström, Mikael. "Medical gallery of Mikael Häggström 2014". *Wikiversity Journal of Medicine* 1(2). DOI:10.15347/wjm/2014.008. ISSN 20018762.) on 29.12.2014.

1.1.1.2. Sarcomeric proteins and their function

During muscle contraction, the highly organized assembly of hundreds of actin and myosin filaments of the sarcomere is anchored at the Z-line and M-band by important sarcomeric proteins. Some of the important sarcomeric proteins that anchor the actin and myosin filaments are discussed in the following paragraphs.

Titin is a giant protein that stabilizes the whole structure of the sarcomere by interacting with majority of the proteins at the Z-line and M-line (Tskhovrebova et al., 2003). It has been shown that myogenic cells lacking the titin protein have defective sarcomeric assembly (Person et al., 2000; Van der Ven et al., 2000). Obscurin**,** another important giant protein interacts with titin in the Z-line and ankyrin-1 in the sarcoplasmic reticulum, thus anchoring the myofibrillar assembly to the sarcoplasmic reticulum (Young et al., 2001; Kontrogianni-Konstantopoulos et al., 2003; Bagnato et al., 2003).

Muscle specific RING–finger proteins (MuRFs) belong to the family of RING/B box/Coiled coiled (RBCC) proteins consisting of three homologous MuRF genes i.e., MuRF1, MuRF2 and MuRF3 (Centner et al., 2001). The MuRF proteins are expressed in a tissue-specific manner and also homo- or heterodimerize through their coiled-coiled domain (Centner et al., 2001; Pizon et al., 2002). MuRF1 and MuRF2 are known to interact with titin protein at the M-line. Also, MuRF1 and MuRF3 interact with the sarcomeric proteins at the Z-line (Centner et al., 2001; Pizon et al., 2002). Thus, indicating that MuRF may be providing protein-protein interaction to various sarcomeric proteins in holding the sarcomere together. MuRFs have also been shown to interact with glutamylated tubulin present in the microtubules of the sarcomere

(Spencer et al., 2000; Pizon et al., 2002). Thus, it was shown that reduced MuRFs levels resulted in defective myofibrillar assembly and instability of the M-line structure of the sarcomere in cultured skeletal myocytes (Pizon et al., 2002; McElhinny et al., 2004). MuRFs have another distinct function of ubiquitinating the target proteins. It was shown that mice lacking MuRF1 are resistant to muscular atrophy and showed reduced E3 ubiquitin ligase activity in vitro (Fielitz et al., 2007; Bodine et al., 2001).

Desmin is an intermediate filament protein present specifically in striated muscle. This protein forms a scaffold in the Z-line connecting the sarcomere organelles together. Thus, desmin provides structural and mechanical stability to the myofibrillar assembly and the sarcomere in the muscles (Fuchs et al., 1994). It has been shown that lack of desmin leads to myofibrillar myopathy and muscular dystrophy (Fuchs et al., 1998) (Figure 1.3). There are other important sarcomeric proteins, which will not be discussed as they are beyond the scope of this project.

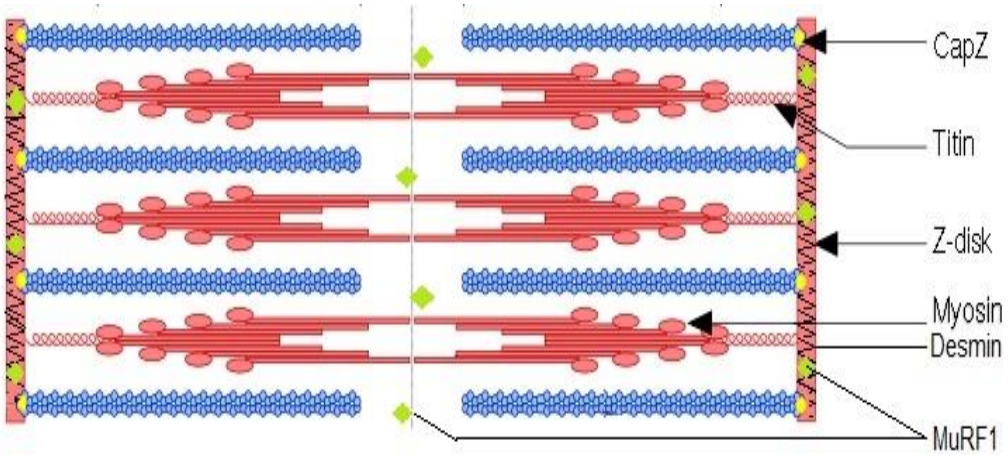

Figure 1.3 Important proteins in the sarcomere. Apart from actins and myosins, a sarcomere is made up of various structural, contractile and regulatory proteins which have specific function in the sarcomere. Figure freely downloaded and modified from http://commons.wikimedia.org/wiki/File:Sarcomere.svg (Richfield, David. "Medical gallery of David Richfield 2014". *Wikiversity Journal of Medicine* 1 (2). DOI:10.15347/wjm/2014.009. ISSN 2001-8762) on 29.12.14.

1.1.2. Muscle fiber types

Individual skeletal muscle is stimulated by numerous motor units, which is the functional unit of motor system. However, a motor unit controls a group of muscle fibers that have similar structural and functional properties within a muscle. Mammalian skeletal muscle is made up of different types of muscle fibers. This heterogeneity of muscle fibers is based on three structural and functional characteristics i.e., contraction speed due to nerve activity, type of MyHC expressed and density of mitochondria (type of metabolism). Muscle fibers that are controlled by smaller motor units and have low contraction speed are called slow twitch or type I fibers. As the slow twitch fibers contract less forcefully, they are highly resistant to fatigue. Slow twitch fibers have high mitochondrial density and thus are aerobic in nature. These fibers appear red in colour due to myoglobin, an oxygen carrying protein in the mitochondria. Type I fibers use triglycerides as energy source. Type I fibers express myosin isoform *Myh7* which is also expressed in cardiac muscle as cardiac beta MyHC (Talmadge et al., 1993; Lompre et al., 1984). Type II fibers are divided into type IIa and type IIb fibers. Both of these fibers are controlled by bigger motor units and have high contraction speed, thus generating greater force compared to type I fibers. Type IIa fibers have moderately high contraction speed and are anaerobic in nature and thus fairly resistant to fatigue. Type IIa fibers also have high density of mitochondria with increased oxidative potential; however they can metabolize glycogen and creatine phosphate as energy source. Type IIa fibers predominantly contain myosin isoform *Myh2* in mammals. Type IIb fibers have very high contraction speed and are anaerobic in nature, thus have low resistance to fatigue. Type

IIb fibers have low mitochondrial density and predominantly use glycogen and creatine phosphate as energy source. They are white in color due to lower amounts of myoglobin. Type IIb fibers predominantly contain myosin isoform *Myh4*. Muscle fibers that are neither Type IIa nor Type IIb fibers are called Type IIx or Type IId and have high expression in the diaphragm. These fibers have high contraction speed and low oxidative potential, with moderate mitochondrial density. Type IIx fibers contain myosin isoform *Myh1* (Westerblad et al., 2010, Schiaffino et al,. 1994). Fiber type switches occur with a change in function like, a change in murine masseter muscle to entirely type IIb fibers when the pups progress from suckling to mastication upon weaning (Gojo et al., 2002). Changes in fiber type also have been shown to occur with different training regimes in humans like type IIb fibers convert to type I in response to endurance training, however when training ceases these fibers revert back to Type IIb fibers. Thus heterogeneity of the muscle fibers in the skeletal muscle allows the same muscle to perform different tasks as per the requirement of the body.

1.1.3. Skeletal muscle function

Mammalian skeletal muscles exhibit different properties depending on their functional requirement. They have four important properties. 1. Contractility- ability to contract when stimulated by action potential. 2. Excitability- ability to respond to stimuli by producing electrical impulses. 3. Extensibility- ability to stretch without damage. 4. Elasticity- ability to return to its original length and shape after contraction and extension. Skeletal muscle can be divided into two classes depending on whether they are affected by gravitational pull or not. 1. Gravity muscles- which create movement and functions in the presence

of gravitational pull of the Earth through repeated cycles of contraction and relaxation like muscles required for locomotion e.g., *tibilas anterior*. 2. Anti-gravity muscles- which function even in the absence of gravitational pull through sustained contraction like muscles required for posture maintenance and breathing e.g., *Gluteus maximus* and diaphragm respectively (Martini, 2006). Apart from locomotion and posture maintenance, skeletal muscle has a role in thermogenesis, as contraction of muscle is a critical homeostatic mechanism for maintenance of normal body temperature. It is also important for the movement of substances within the body like contraction of skeletal muscle causes flow of lymph and helps in return of venous blood to the heart. Moreover, studies have revealed a novel function of skeletal muscle in maintaining the energy metabolism homeostasis (Wallimann et al., 1996).

1.2 Cardiac muscle

The heart wall is made up of three layers; the outer connective tissue called epicardium, the middle cardiac muscle tissue region called the myocardium and the inner simple squamous epithelium layer called endocardium. Cardiac muscle cells (cardiocytes), which form the myocardium, are uni-nucleated striated involuntary cells present only in the heart. Like skeletal muscle cells, cardiocytes also contain myofibrils i.e., the actin and myosin filaments, organized into sarcomeres (Figure 1.4). Cardiocytes are highly branched cells that are interconnected to each other by intercalated discs. These discs are made up of cell membranes of adjacent cardiocytes locked together by desmosomes, intercellular matrix and gap junctions. Electric impulses are uniformly and quickly conducted through these intercalated discs and help in coordinated contraction of the cardiocytes. Also, the intercalated discs hold the

cardiocytes together in place during contraction, thus maintaining the three-dimensional structure of the heart tissue (Martini, 2006).

Although cardiac muscle is a striated muscle, it is different from skeletal muscle in many ways. Some of the striking differences are as follows. 1. Cardiocytes are relatively smaller in size. 2. Unlike skeletal muscle cells, cardiocytes have very limited ability to repair and regenerate. Although cardiocytes are capable of dividing after a heart injury, the repair is usually insufficient leading to loss in cardiocyte function (Martini, 2006). 3. Cardiac muscles are involuntary in nature i.e., cardiac muscle is not controlled by somatic nervous system. But they have specialized cells called pacemaker cells that provide electric impulses and maintain a constant rate of contraction. 4. The cardiocytes contains T tubules that are short and broad and are not arranged in triads. 5. Cardiocytes are predominantly aerobic, as they need continuous supply of energy for uninterrupted contraction. Cardiocytes contain relatively large numbers of mitochondria and utilize glycogen and lipids as the main energy source. 6. Cardiocyte contraction lasts approximately 10 times longer than the skeletal muscle cell contraction and thus cardiocytes fatigue relatively lesser (Martini, 2006).

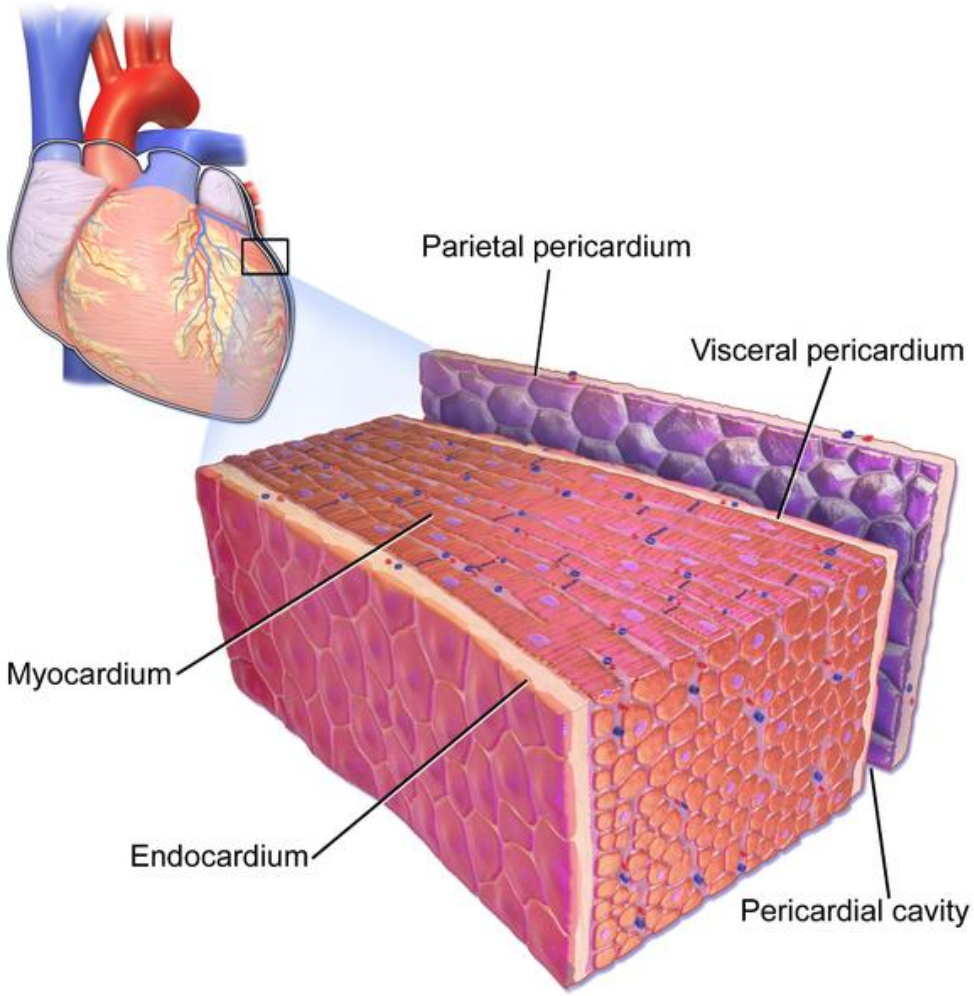

Figure 1.4 Cardiac muscle structure. Cardiac muscle sarcomeres are similar to skeletal muscle sarcomeres in their struture and function. Each cardiocytes is seperated by specialised membrane structures called intercalated discs that help in the conduction of electric impulses across the heart. Figure freely downloaded from http://commons.wikimedia.org/wiki/File:Blausen_0470_HeartWall.png (Blausen.com staff. "Blausen gallery 2014". *Wikiversity Journal of Medicine*. DOI:10.15347/wjm/2014.010. ISSN 20018762) on 29.12.2014.

1.2.1. Cardiac Hypertrophy

Cardiac muscle has the tendency to undergo structural changes in response to stress factors like hemodynamic load and/or cardiac injury. The process of cardiac muscle undergoing the structural changes, which eventually changes the dimension and function of the heart is termed as cardiac remodeling. Depending on the type of cardiac remodeling, the cardiac muscle can either increase in mass (hypertrophy) or decrease in mass (atrophy). Cardiac hypertrophy can be broadly classified into two types based on the type of hypertrophic stimulus- physiological hypertrophy and pathological hypertrophy (Cohn et al., 2000) (Figure 1.5). Physiological hypertrophy is a beneficial hypertrophy that occurs in response to physiological stimuli like exercise training or during pregnancy (Mone et al., 1996). When there is a hemodynamic load on the heart walls due to chronic physical exercise, the cardiomyocytes are stretched which leads to synthesis of new contractile proteins and usually the new sarcomeres are arranged in parallel. This increases the muscle thickness of the heart wall, thereby increasing the contractile ability and eventually the cardiac output (Wakatsuki et al., 2004). Thus, physiological hypertrophy is a compensated growth to normalize the wall stress and usually reverts back to normal on cessation of exercise regime (Zak et al., 1984). Physiological hypertrophy can be further subdivided into two categories depending on the type of hemodynamic overload. In case of aerobic exercises like running and swimming exerts volume load on the heart walls. This stimulates the addition of new sarcomeres next to each other in the cardiomyocytes leading to dilation of the heart walls. This kind of hypertrophy is called eccentric hypertrophy. On the contrary, during static exercise like

weight lifting, pressure load is exerted on the heart wall. This stimulates addition of new sarcomeres parallel to each other in the cardiomyocytes, increasing the thickness of the heart walls. This type of hypertrophy is called concentric hypertrophy (Pluim et al., 2000; Zak et al., 1984). Physiological hypertrophy is mainly induced by IGF1-phosphoinositide-3 kinase pathway. IGF-1 growth factor released in response to exercise training interacts with its receptor IGF1R. This further activates the PI3-K leading to activation of protein synthesis pathway resulting in cardiac cell growth (Toker et al., 1997). Mice having increased cardiac IGF-1/PI3-K have normal life span but develop physiological hypertrophy with increased cardiac output (Reiss et al., 1996; Shioi et al., 2000). On the contrary, mice with reduced IGF-1/PI3-K signaling show reduced heart size (Shioi et al., 2000; Luo et al., 2005).

A different kind of cardiac remodeling occurs in response to hemodynamic overload due to cardiomyopathies and chronic heart diseases like aortic stenosis and hypertension. This type of hypertrophy is known as pathological hypertrophy (Zak et al., 1984). In this kind of hypertrophy, the heart muscle wall increases in thickness due to the hemodynamic stress along with pathological stimuli such as production of collagen by cardiac fibroblasts, inflammation and apoptosis/necrosis of cardiomyocytes (Volders et al., 1993). All these factors together affect the contractility of the cardiac muscle and eventually the cardiac output. These changes are irreversible and eventually lead to heart failure and increased mortality (Olivetti et al., 1997). Re-expression of fetal genes like Atrial natriuretic peptide (ANP), βMyHC and skeletal alpha-actin are usually seen during pathological hypertrophy and not during physiological hypertrophy. In pathological hypertrophy, the

compensatory growth is eventually decompensated leading to dilated cardiomyopathy and heart failure (Pluim et al., 2000; Fagard et al., 1997). During pathological hypertrophy, chronic heart conditions like hypertension and aortic stenosis exerts pressure overload on the heart walls resulting in concentric hypertrophy (Grossman et al., 1975). Chronic heart condition like aortic regurgitation exerts volume overload on the heart walls leading to eccentric hypertrophy (Grossman et al., 1975; Pluim et al., 2000). Pathological hypertrophy is mainly induced through $G_{\alpha q}$ receptor belonging to G-protein-coupled receptors (GPCR) family of cell surface receptors (Seidman et al., 2001). Pathological stimulus induces secretion of cardiac factors like endothelin (ET)-1, angiotensin (Ang) II and noradrenaline leading to activation of $G_{\alpha q}$ receptor. This further activates overt Ca^{2+} signaling along with mitogen-activated protein kinases (MAPK) pathway together leading to pathological hypertrophy. Transgenic mice over-expressing $G_{\alpha q}$ receptor showed cardiac dysfunction and premature death (D'Angelo et al., 1997; Hein et al., 1997). On the contrary, mice lacking $G_{\alpha q}$ receptor in the cardiomyocytes failed to develop pathological hypertrophy even with pressure overload (Akhter et al., 1998; Wettschureck et al., 2001).

As pathological hypertrophy is of more clinical relevance, it has been extensively studied using artificial sympathomimetics drugs that mimic the effect of cardiac factors like ET-1, Ang II etc. Most widely used sympathomimetic drug is isoproterenol (ISO). It is clinically used to treat bradycardia (slow heart rate) and heart block. ISO is structurally similar to adrenaline and acts as a beta-adrenergic receptor agonist and induces pathological hypertrophy (Tse et al., 1979). However, it is also seen that there

can be crosstalk between these two main signaling pathways in developing either type of cardiac hypertrophy.

Studies have shown that myostatin is expressed in heart predominantly in the purkinje fibers and cardiomyocytes (Sharma et al., 1999). Myostatin is a well-studied negative growth factor and will be discussed in detail in section 1.6.3.1. Previous studies have shown that myostatin inhibits IGF-1 induced physiological hypertrophy in the heart, thus acting as a chalone for heart organ development (Shyu et al., 2005). Rodgers et al., on the contrary showed that myostatin null mice exhibited physiological hypertrophy and loss of myostatin induced eccentric hypertrophy with enhanced cardiac output (Rodgers et al., 2009). Also aged myostatin null mice have heavier hearts compared to the wild-type counterparts and showed physiological cardiac hypertrophy (Jackson et al., 2012).

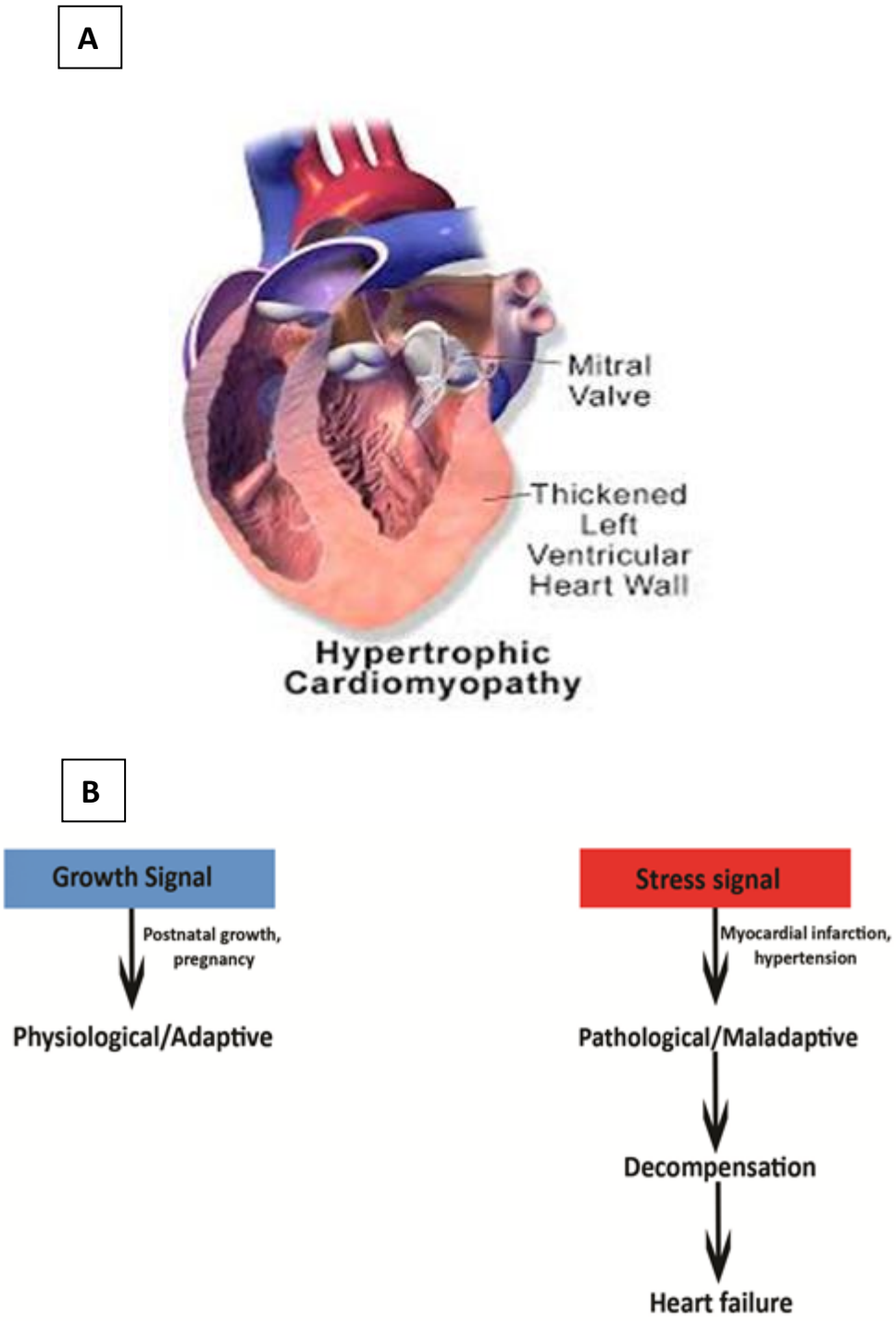

Figure 1.5 Types of cardiac hypetrophy. (A) Figure representing pathological cardiac hypertrophy. Figure freely downloaded from http://commons.wikimedia.org/wiki/File:Blausen_0166_Cardiomyopathy_Hypertrophic.png (Blausen.com staff. "Blausen gallery 2014". *Wikiversity Journal of Medicine*. DOI:10.15347/wjm/2014.010. ISSN 20018762) on 29.12.2014 (B) Image showing different stimuli responsible for physiological and pathological cardiac hypertrophy.

1.3 Skeletal Myogenesis

Skeletal muscle development is a highly coordinated event involving many factors functioning at specific time. This process of skeletal muscle formation is termed as myogenesis. There are two types of myogenesis depending on the time of development they occur, 1. Embryonic myogenesis- muscle development during embryogenesis 2. Post-natal myogenesis- muscle development after birth and also due to exercise training.

1.3.1. Embryonic myogenesis

In mammals, myogenic cells that are responsible for formation of muscle cells are derived from somites. Somites are bilaterally symmetric structures that are transiently formed from paraxial mesoderm of the embryo. They develop on either side of the neural tube and notochord in a rostro-caudal fashion (Buckingham et al., 2001). Initially somites are made of outer epithelium and mesenchymal core. However later, somites undergo the process of de-epithelialization to give rise to sclerotome ventrally and dermomyotome dorsally (Buckingham, 2001). The dorsal dermomyotome gives rise to skeletal muscles of body and limb while the ventral sclerotome gives rise to bone and cartilage of the body. Furthermore, the medial portion of dermomyotome, i.e., the epaxial dermomyotome, gives rise to deep back muscles and the lateral portion of dermomyotome i.e., the hypaxial dermomyotome, gives rise to rest of the musculature of the body and limbs (Figure 1.6). The first muscle mass to form in an embryo is the myotome, a layer of longitudinally arranged muscle cells between the dermomyotome and the sclerotome. Later, this mass of muscle cells is integrated into the trunk musculature. The uncommitted muscle precursor cells undergo delamination from the epithelium of the

dermomyotome and migrate to the limb buds, where they proliferate and differentiate to form skeletal muscles (Emerson, 1993).

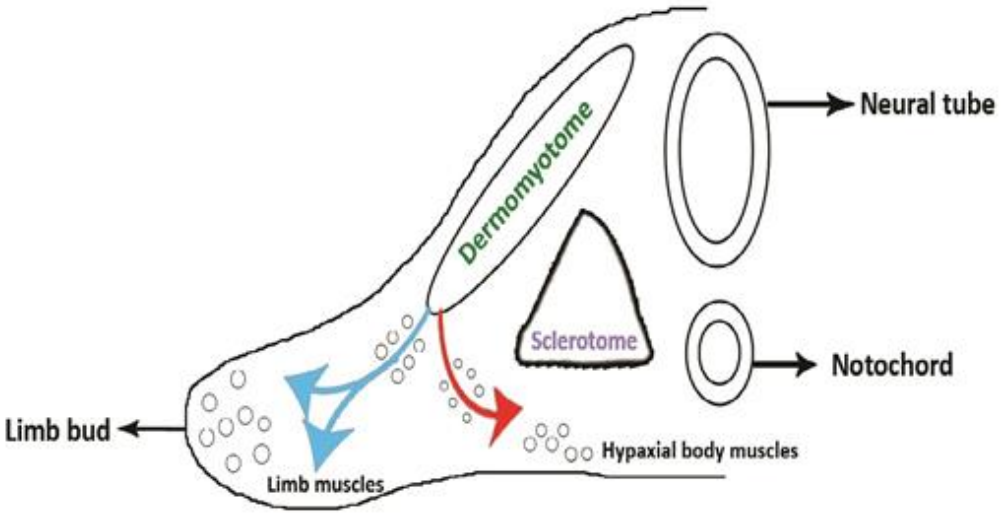

Figure 1.6 Embryonic myogenesis. Formation of skeletal muscle during embryogenesis. The dermomyotome gives rise to the epaxial myotome, which in turn gives rise to back musculature, and hypaxial myotome, which gives rise to limbs and body musculature.

1.3.1.1. Transcriptional factors involved in embryonic myogenesis

Myogenic Regulatory Factors (MRFs) and Myocyte enhancer factor-2 (MEF2) are two important classes of transcription factors that together orchestrate a highly regulated process of embryonic myogenesis.

MRFs are a group of four muscle-specific basic helix-loop-helix (bHLH) transcription factors namely MyoD, Myf5, myogenin and MRF4/ herculin/ Myf-6 that can convert non-myogenic cells to myogenic lineage when expressed ectopically (Choi et al., 1990; Miner at al., 1990; Edmondson et al., 1989). Studies in mice show that *Myf5* is the first bHLH transcription factor to be expressed during embryonic myogenesis and act upstream of *MyoD* along

with *Pax3* (Tajbakhsh et al., 1997). *MyoD* expression is followed by *myogenin* and lastly *MRF4* expression (Sassoon et al., 1989; Wright et al., 1989; Hannon et al., 1992). Mutations in *MyoD* gene results in delayed myogenesis with almost complete loss of muscle formation (Kablar et al., 1997), while mutations of *Myf5* gene results in normal musculature with slight reduction in muscle fiber size and muscle mass (Kablar et al., 1997). But when both *MyoD* and *Myf5* are mutated, mice show complete absence of skeletal muscle formation (Rudnicki et al., 1993). This indicates that MyoD and Myf5 functionally compensate for each other during embryonic myogenesis. Furthermore, mutations in myogenin show myoblasts that migrate normally but incapable of differentiation to form multinucleated myotubes (Venuti et al., 1995). Thus myogenin is indispensable for differentiation of skeletal muscle.

MRFs contain conserved bHLH domain with N-terminal and C-terminal transcriptional activation domains. It is the bHLH domain that binds to the DNA and dimerises with ubiquitously expressed E proteins to confer its role in skeletal myogenesis (Murre et al., 1989). The important E proteins expressed in skeletal muscle are E47, E12 and HEB. The MRFs characteristically bind to consensus sequence CANNTG called E-box, commonly found in the promoters of muscle specific genes like MLC1 and 3, desmin, creatine kinase, cardiac alpha actin, thus transactivating the downstream target genes (Li and Capetanaki, 1994; Amacher et al., 1993; Wentworth et al, 1991; Sartorelli et al., 1990).

MEF2 is another important class of transcription factors affecting the process of embryonic myogenesis. MEF2 is a family of MADS-box transcription

factors consisting of four members, MEF2A, MEF2B, MEF2C and MEF2D (Breitbart et al., 1993; Hidaka et al., 1995). The expression of MEF2 isoforms overlaps with MRFs expression in skeletal muscle although MEF2 is expressed in other tissues such as heart and brain (Edmondson et al., 1994; Molkentin et al., 1996). MEF2C is the predominantly expressed isoform in skeletal muscle (Edmondson et al., 1994).

The MADS- box of MEF2 proteins bind to conserved A/T-rich element in the promoters of muscle specific genes (Cserjesi and Olson, 1991; Gossett et al., 1989). MEF2 binding sites and E-boxes usually co-exist in the promoters of muscle specific genes (Black et al., 1995; Wan and Moreadith, 1995; Naidu et al., 1995; Edmondson et al., 1992). Thus MRFs and MEF2 family together influence the process of embryonic myogenesis. For example, MRF4 promoter in rat contains an E-box and a MEF2 binding site and both these sites are required for the maximum expression of MRF4 to drive the muscle specific expression (Black et al., 1995; Naidu et al., 1995). However in some instances, MRF and MEF2 can synergistically activate a promoter. For example, myogenin can interact with MEF2-DNA complex and transactivate muscle specific genes, even when the E-box is mutated. Thus mutation of the E-box does not eliminate the synergy between myogenin and MEF2 (Naidu et al., 1995). When both MRFs and MEF2 binding occurs in a promoter region, there appears to be a geometric restriction on the association of the two factors, with the two sites being found closely associated in the promoters of muscle specific genes (Fickett et al, 1996). Thus the synergistic interaction between the MRFs and MEF2 is an important mechanism for induction of muscle specific gene expression.

The ability of MRFs and MEF2 to activate muscle specific transcription is also regulated by their post-translational modification, specifically acetylation. MRFs and MEF2 can associate with histone acetyltransferases (HATs) and histone deacetylases (HDACs) which control the acetylation state of histones and therefore the condensation and accessibility of chromatin (Mal et al., 2001; Puri et al., 2001). Also, MyoD is known to can act as a substrate for HATs and HDACs (Mal et al., 2001; Puri et al., 2001; McKinsey et al., 2001; Eckner et al., 1996). Acetylation by HATs of histones results in the relaxation of nucleosomal structure allowing the access of transcriptional machinery into the chromatin (Garrett and Grisham, 1999). HAT activity is affected by numerous transcriptional activators such as p300 with CREB binding protein (CBP) and GRIP-1 (Eckner et al., 1996; Puri et al., 1997).

Deacetylated histones are associated with transcriptionally silent genes (Garrett and Grisham, 1999). There are two classes of HDACs containing eight known HDACs in humans; ubiquitously expressed Class I (-1, -2, -3, and -8); and Class II (-4, -5, -6, and -7) HDACs are highly expressed in adult heart, skeletal muscle and brain tissue (McKinsey et al., 2001; Zhou et al., 2000). HDAC act antagonistically to the function of HATs, and also influence the myogenic differentiation of C_2C_{12} myoblasts. The class I HDAC, HDAC-1, can target MyoD directly. HDAC1 binds to MyoD in undifferentiated cells, and can deacetylate MyoD, inhibiting its activity (Mal et al., 2001). The interaction of HDAC1 with MyoD is disrupted as the cell cycle regulatory protein pRb becomes hypo-phosphorylated during myogenic differentiation. Hypo-phosphorylated pRb forms a complex with HDAC1. A point mutation in pRb, making it incapable of binding HDAC1, prevents the disruption of the

MyoD-HDAC1 complex and inhibits muscle gene expression and myogenic differentiation (Puri et al., 2001; Lu et al., 2000). HDAC4, -5 and -7 associate with MEF2, via a HDAC class II specific domain in the amino-terminus, and inhibit MEF2 dependent transcription, suppressing myogenic differentiation (Zhang et al., 2002; Dressel et al., 2001; Lu et al., 2000). The interaction of HDACs with MEF2 mediates the inhibition of MyoD, as MyoD dependent transcription was affected when the E-box binding site was in close association with a MEF2 binding site (Lu et al., 2000). These studies indicate that HAT and HDAC proteins have the potential to play an important role in the regulation of transcription factors involved in embryonic myogenesis.

1.3.1.2. Growth factors involved in myogenesis

Along with transcription factors, various growth factors like Hepatocyte growth factor (HGF), Fibroblast growth factor (FGF), Bone morphogenetic protein (BMP) and Transforming growth factor β (TGFβ) play important role in both embryonic and post-natal myogenesis. HGF acts as a chemo-attractant and aids in migration of muscle precursor cells towards the limb bud. Mutations in either HGF or its receptor, c-met, results in failure of migration of muscle precursor cells eventually leading to absence of skeletal muscle in limbs (Francis-West et al., 2003; Bladt et al., 1995). HGF also suppresses the expression of myogenic regulatory factors like Myf5, MyoD and myogenin, and the muscle contractile protein Myosin heavy chain (MyHC) such that the migrating muscle precursor cells do not differentiate until they have reached the limb buds (Gal-Levi et al., 1998).

FGFs are other important factors required for the process of delamination and migration of myogenic precursor cells. FGFs including FGF-2,-4,-8 are

upstream of HGF expression. FGFs like HGF function as a chemo-attractant and help in the migration of myogenic precursor cells to the limb buds (Webb et al., 1997). FGFs also inhibit the expression of myogenic regulatory factors like Myf5 and MyoD to inhibit the differentiation of myogenic precursor cells until they have reached their appropriate destination. When the myogenic precursor cells have migrated to the limb buds, the predominant FGF receptor, FGF receptor 1 (FGFR1) is lost, followed by expression of myogenic regulatory factors like Myf5 and MyoD leading to the initiation of differentiation of myogenic cells (Itoh et al., 1996).

BMPs, BMP-2, -4 and -7 belong to TGFβ superfamily and inhibit myogenic differentiation. BMPs are produced in the developing limb bud and have varied function depending on their concentration. At low levels, BMPs induce and maintain the expression of Pax3 and inhibit the expression of MyoD. However at high concentrations, these BMPs prevent both Pax3 and MyoD expression and induce apoptosis (Amthor et al., 1998). The actions of BMPs are antagonized by Noggin, which is induced by Wnt signals from the dorsal neural tube (Reshef et al., 1998). It is the balance in expression of BMPs and Noggin that determine the expression of the myogenic regulatory factor genes such as Myf5 and MyoD (Emerson et al., 2000). Myostatin, another TGFβ superfamily member, also has important role in regulation of myogenesis. Myostatin, also known as Growth and Differentiation Factor-8 (GDF-8), is expressed in muscle precursors in the somite and this expression is continued into adult muscle (McPherron et al., 1997). Myostatin is shown to inhibit both proliferation and differentiation of myogenic precursor cells (Thomas et al.,

2000; Langley et al., 2002). The role of myostatin will be discussed in detail later in section 1.6.3.2.

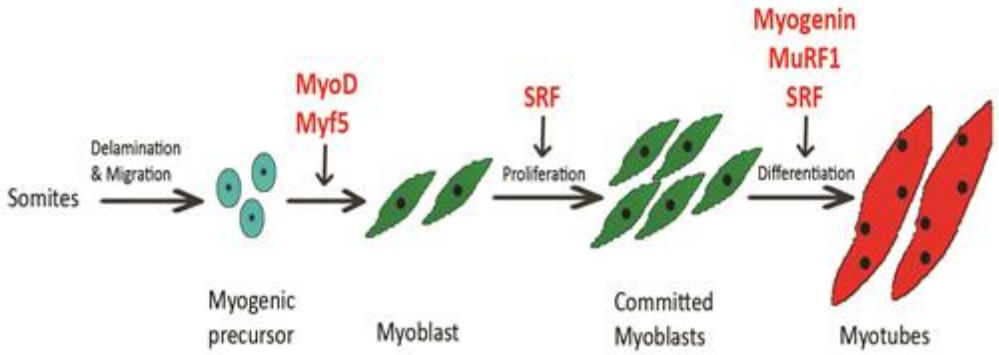

Figure 1.7 A schematic diagram showing the roles of certain important proteins during embryonic myogenesis used in this thesis.

1.3.2. Post-natal myogenesis

Once the muscle has formed, the myonuclei present in the myofibers are unable to divide to allow muscle maturation, growth and repair. For this purpose, skeletal muscle has a population of muscle precursor cells called satellite cells (SCs) that proliferate and provide growth and regenerative property to adult skeletal muscle. Satellite cells are mono-nucleated, quiescent precursor cells located between the basal lamina and the sarcolemma of the myofibers. SCs are usually in a quiescent state and possess a small cytoplasm and condensed chromatin. Thus they have a high nuclear to cytoplasmic ratio with minimum intracellular organelles (Bischoff, 1994; Muir et al., 1965). However, in case of myo-trauma, SCs are activated and migrate from their niche to the region of muscle injury. After reaching the area of injury, they re-enter the cell cycle, proliferate and either contribute myonuclei to the damaged myofibers or fuse among themselves to give rise to a nascent myofibers and

replace the damaged myofiber thus aiding in muscle regeneration and growth (McKinnell et al., 2004; Hawke et al., 2003). Simultaneously, the SCs also undergo the process of self-renewal to replenish the population of SCs within the muscle (Bischoff, 1994; Hawke et al., 2001; McCroskery et al., 2005) (Figure 1.8).

SCs express certain bona fide markers in response to activation. Quiescent SCs specifically express proteins like M-cadherin, CD34, Pax7, c-met, Sox8, Msx1 and myostatin (McCroskery et al., 2005; Fukada et al., 2004; Sajko et al., 2004; Cornelison et al., 2000; Cornelison et al., 1997) (Figure 1.8). Studies have shown that Pax7 is expressed in quiescent SCs and upon activation Pax7 expression is down-regulated. Thus, Pax7 has an important role in maintaining quiescence in SCs and maintaining the SC pool in skeletal muscle (Olguin et al., 2004). Mice lacking Pax7 showed a drastic reduction in SC number and muscle regenerative capacity. However, the postnatal muscle growth is not affected (Oustanina et al., 2004; Charge and Rudnicki et al., 2004). Upon activation, SCs begin to express Myf5, MyoD and desmin proteins, which are the markers of myogenic precursor cells (Cornelison et al., 1997). Mice studies have revealed that MyoD expression in SCs is critical for muscle regeneration, and MyoD null mice showed reduced muscle regeneration after muscle injury (Megeney et al., 1996) (Figure 1.8).

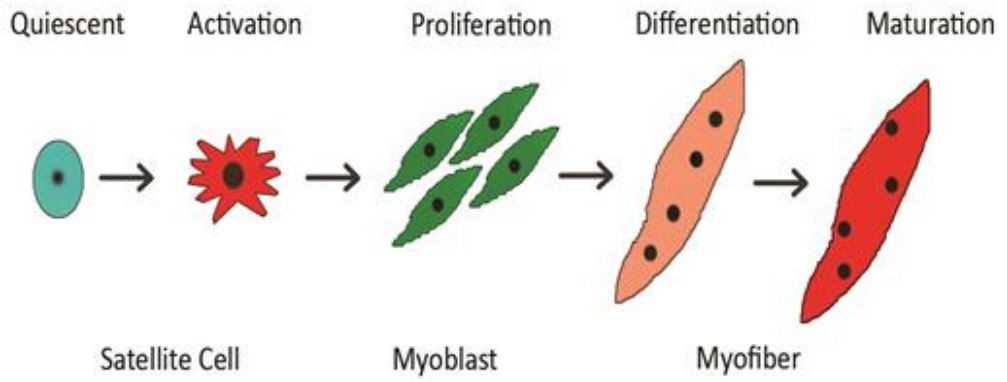

Figure 1.8 A schematic diagram depicting post-natal myogenesis. SCs normally exist in a quiescent state and are activated upon injury or myotrauma. Quiescent SCs express CD34, Pax7, Myf5 and β-gal. However, upon activation, MyoD expression is up-regulated along with the expression of Pax7. The SCs committed to differentiation express myogenin and fuse into myotubes and further mature into myofibers.

1.4 Muscle regeneration

Following post-natal muscle growth, satellite cells remain quiescent within the muscle. However in case of muscle trauma such as prolonged exercise or muscle injury, SCs are activated to regenerate and replenish the damaged muscle tissue. The process of skeletal muscle regeneration is divided into three phases- degeneration, regeneration and remodeling (Grefte et al., 2007). Due to muscle injury, the sarcolemma covering the myofibers is disrupted and myofibrils organization is lost. As a result, the intracellular muscle protein such as creatine kinase is released into the blood stream, which can be detected in the serum. The membrane damage also leads to influx of Ca^{2+} into the cell, stimulating the Ca^{2+} dependent proteases such as calpains that degrade the myofibrillar and cytoskeletal proteins. This necrotic muscle tissue releases chemotactic factors that initially recruit inflammatory neutrophils followed by macrophages to the injury site (McLennan, 1996; Tidball, 1995). The

macrophages phagocytose the necrotic tissue, allowing the muscle regeneration to occur. This phase of clearing the necrotic tissue is called degeneration. The inflammatory cells present at the site of injury, release cytokines and growth factors like HGF, FGF and TGFβ that activate and attract the SCs underneath the basal lamina from the distant uninjured sites to the site of injury (Schultz et al., 1985; Bischoff, 1997; Robertson et al., 1993). The activated SCs re-enter cell cycle and proliferate to increase in number and become myoblasts (McKinnell et al., 2004; Hawke et al., 2003). These SC derived myoblasts either fuse among themselves to form nascent myofibers or with the damaged myofiber, thus repairing or replacing myofibers. This phase of replenishing the damaged muscle tissue is called regeneration. The nascent myofibers show characteristic centrally located myonuclei and express embryonic MyHC (eMyHC). Upon maturation, the myofiber increase in size moving the myonuclei to the periphery of the myofiber. Thus, the regenerated myofibers become indistinguishable from the undamaged myofibers. Fibroblasts also infiltrate the site of injury and produce connective tissue resulting in scar tissue formation (Sato et al., 2003). This results in fibrosis in the muscle tissue, which affects the efficiency of muscle contraction (Fukushima et al., 2001; McCroskery et al., 2005). This phase of myofiber maturation followed by fibrosis is called remodeling.

1.5 Skeletal muscle metabolism

The fundamental role of skeletal muscle is to provide movement by contraction. Energy required for this contraction is obtained by metabolizing high-energy molecules like glucose, lipids, glycogen and phosphocreatine to release ATP (Sahlin et al., 1998). Skeletal muscle predominantly uses glucose

as the main energy source, which is stored in the form of polysaccharide chain of glucose molecules called glycogen (Graham et al., 2010). However, when glycogen reserves are low, the muscle fibers utilize fatty acids and amino acids to derive energy. During muscle activity, glycogen is broken down to release glucose and this catabolic process is termed as glycogenolysis. Glucose released is used as a substrate to generate ATP by two main processes 1) Anaerobic glycolysis in the cytoplasm 2) Aerobic oxidative metabolism in mitochondria. Firstly, glucose released from glycogen is anaerobically broken down into two pyruvate molecules in the cytoplasm, generating two molecules of ATP. This catabolic process is called glycolysis. Two pathways can metabolize the pyruvate formed through glycolysis:

1) Pyruvate can stay in the cytoplasm and continue to be broken down anaerobically to generate ATP and lactic acid. During strenuous exercise, ATP is predominantly generated anaerobically, and the lactic acid formed diffuses out of the muscles into the bloodstream, which is subsequently absorbed by the liver. Furthermore, the lactic acid in the liver can be converted back to pyruvate with the help of liver enzymes, thus providing substrate to generate more ATP. However, some of the lactic acid remaining in the muscle cell contributes to muscle fatigue.

2) Pyruvate enters mitochondria and is aerobically broken down by aerobic oxidative phosphorylation to generate almost 95% of the ATP demand of the contracting skeletal muscle.

Although the ATP requirement of the resting muscle is low, the muscle fibers absorb glucose, fatty acids and oxygen from the bloodstream. This leads to generation of excess amounts of ATP, as there is no limitation in oxygen

availability for the oxidative phosphorylation to occur in the mitochondria. These extra ATP molecules build up the glycogen and creatine phosphate reserves in the muscle fibers. At moderate levels of muscle activity, the ATP demand increases, which is met by breakdown of glycogen reserves followed by oxidative phosphorylation in the mitochondria. However, during high levels of muscle activity, the demand for ATP is very high which leads to inability of the mitochondria to cater to the demand. Thus, additional ATP is generated through anaerobic pathway discussed earlier.

1.6 Factors regulating post-natal skeletal muscle mass

Post-natally, skeletal muscle mass development is affected by various growth factors leading to either skeletal muscle atrophy or hypertrophy. These growth factors affect different stages of myogenesis leading to variation in skeletal muscle mass. Some growth factors have an impact on the rate of myoblast proliferation, which eventually determines the number of myoblasts present to undergo differentiation. Other growth factors influence the process of differentiation, affecting the timing and extent of myotube formation. Skeletal muscle undergoes wear and tear during its use. Growth factors play an important role in the regulation of skeletal muscle regeneration as well. Some of the important factors are discussed below.

1.6.1. Insulin-like growth factors (IGFs)

IGF family of growth factors consists of secreted proteins that positively regulate myogenesis. Two types of IGFs, IGF1 and IGFII are secreted by a wide variety of tissues including liver and skeletal muscle (Bondy et al., 1993; Alexandrides et al., 1989; Beck et al., 1988). IGF-I and -II have been shown

to enhance the proliferation and differentiation of myoblasts. Myoblasts treated with IGF-I show enhanced proliferation rates and cell survival (Lawlor et al., 2000; Semsarian et al., 1999); Engert et al., 1996). Expression of IGF-I and IGF-II increases during myoblast differentiation, indicating IGFs role in skeletal muscle differentiation (Yoshiko et al., 2002). As myoblasts differentiate, IGF-I enhances the differentiation process by inducing p21, MyoD and myogenin expression (Yang and Goldspink, 2002; Engert et al., 1996; Greene and Allen, 1991). This can lead to myotube hyperplasia- when myoblasts fuse and form new myotubes; as well as myotube hypertrophy- when myoblasts fuse with existing myotubes (Semsarian et al., 1999). Mice lacking IGF-I are significantly smaller compared to the wild type littermates and the muscle tissue is under-developed. In some strains of mice, lack of IGF-I results in death shortly after birth due to inability to breathe (Liu et al., 1993; Powell-Braxton et al., 1993). Conversely, overexpression of IGF-I (IGF-IEa) results in an increase in muscle mass (Mathews et al., 1989) and *in-vivo,* over-expression of IGF-I prevents muscle atrophy and induces exercise-induced muscle hypertrophy (Sacheck et al., 2004; Alzghoul et al., 2004; Paul and Rosenthal, 2002; Barton-Davis et al., 1998). There are two main isoforms of IGF-I expressed in skeletal muscle, IGF-IEa (mIGF-I) and MGF (IGF-IEc), both of which are splice variants of IGF-I gene. These two IGF-I splice variants appear to play different roles in skeletal muscle. MGF increased myoblast proliferation and inhibited myogenic differentiation, while IGF-IEa increased cell density and induced myoblasts to fuse to form myotubes (Goldspink et al., 2003; Yang and Goldspink, 2002).

IGF-II expression is necessary for myoblast survival and differentiation. Over-expression of IGF-II leads to up-regulation of myogenic markers such as myogenin, and an enhanced differentiation phenotype (Kaliman et al., 1998). Conversely, myoblasts lacking IGF-II undergo rapid cell death when switched to low mitogen media. The addition of IGF-I prevented this apoptosis, indicating that both IGF-I and IGF-II promote survival and differentiation of myoblasts (Lawlor and Rotwein, 2000).

IGFs bind to cell surface receptors to initiate signalling cascades to elicit their effect. There are three known receptors that bind IGFs. The insulin receptor, which predominantly binds insulin, can also bind related IGF-II and IGF-I to a far lesser extent. IGF-I and IGF-II appear to signal predominantly through the IGF-I receptor.

IGF-II receptor binds IGF-II with high affinity and can bind IGF-I to a much lesser extent. This IGF-II receptor is also known as the cation-independent mannose 6-phosphate receptor (Kiess et al., 1988).

IGF-II signaling via PI3K and Akt can activate the mTOR pathway and this signaling leads to skeletal muscle hypertrophy and inhibition of skeletal myogenic differentiation (Erbay et al., 2003; Sarker and Lee, 2004). Elevated IGF-II expression results in the phosphorylation of 4E-BP1 (PHAS1) and $p70^{S6K}$ via activation of the PI3K/Akt/mTOR pathway. Both 4E-BP1 and $p70^{S6K}$ are important factors required for translation. 4E-BP1 binds to eukaryotic initiation factor 4E in its un-phosphorylated state. Phosphorylation of 4E-BP1 by the PI3K/Akt/mTOR pathway results in the release of E4 in turn stimulating translation. The PI3K/Akt/mTOR can activate $p70^{S6K}$, which is a serine threonine protein kinase and phosphorylates and activates ribosomal

protein S6. The role of the ribosomal protein S6 is to recruit mRNAs to the ribosome and destine the proteins they encode to be expressed (Shah et al., 2000). Thus the phosphorylation of 4E-BP1 and $p70^{S6K}$ by IGFs via the PI3K/Akt/mTOR pathway results in increased translation within target cells. This in turn, results in increase in skeletal muscle protein synthesis over DNA synthesis leading to skeletal muscle hypertrophy.

1.6.2. Ca^{2+} signaling

Ca^{2+} released from the sarcoplasmic reticulum of skeletal muscle cells is required for skeletal muscle contraction. However, higher intracellular Ca^{2+}levels can trigger Ca2+/Calmodulin dependent protein phosphatase signaling called calcineurin signaling. Calcineurin is a cytoplasmic serine threonine protein phosphatase, which is made up of a heterodimer of 59kD catalytic subunit (CNA) and an auto-inhibitory 19kD Ca^{2+} binding regulatory subunit (CNB). At sustained higher intracellular Ca^{2+} levels, calcineurin binds to Ca^{2+} and is activated. Active calcineurin then binds to members of NFAT family of transcription factors and dephosphorylate them. This de-phosphorylation enables the translocation of NFAT transcription factors (NFATc1-c4) to the nucleus and affects the transcription of downstream target genes by interacting with factors like MEF2, GATA2 and AP-1 (Schulz and Yutzey, 2004; Olson and Williams, 2000; Musaro et al., 1999; Chin et al., 1998). Activation of calcineurin in myoblasts leads to up-regulation of slow fiber specific genes like slow MyHC, slow fiber specific troponin I and myoglobin (Delling et al., 2000; Chin et al., 1998). On the contrary, inactivation of calcineurin promotes fiber type switch from slow fibers to fast fibers (Chin et al., 1998). Calcineurin also has a role in IGF-1 induced skeletal

muscle hypertrophy (Musaro et al., 1999; Zheng et al., 2004). Increased phosphatase activity of calcineurin leads to interaction of GATA2 transcription factor with NFATc1 in the nucleus. This results in transcriptional up-regulation of hypertrophy-associated genes contributing to IGF-1 induced skeletal muscle hypertrophy (Semsarian et al., 1999; Musaro et al., 1999). NFAT proteins translocate to the nucleus at different times in skeletal muscle formation, indicating a specific role for each in the process of myogenesis. NFATc3 is expressed in the nuclei of myoblasts, NFATc2 is localized in the nucleus in nascent myotubes, and NFATc1 is found in the nuclei of nascent and mature myotubes (Schulz and Yutzey, 2004; Delling et al., 2000). NFATc2 null mice show reduced muscle size due to decrease in muscle fibre cross sectional area. NFATc3 null mice also show reduced skeletal muscle mass but this is due to decrease in myofibre number, indicating different NFATs play different roles in myogenesis (Kegley et al., 2001).

1.6.3. Transforming Growth Factor βs (TGFβ)

TGFβ is a superfamily of growth factors consisting of nearly 30 members that play important roles in the process of myogenesis affecting the skeletal muscle mass. Some of the important TGFβ superfamily members are TGFβs, BMPs, Growth and Differentiation Factors (GDFs), Activins and Inhibins. TGFβ family of secreted signaling molecules mainly affects determination, proliferation, differentiation, adhesion, apoptosis and migration of skeletal muscle. TGFβ superfamily members possess certain characteristic features. They contain a secretion signal at the amino-terminal of the protein, followed by a latency-associated peptide (LAP) that which can be cleaved at the RSRR

cleavage site present in the carboxyl-terminal of the protein making it active as a signaling molecule. The carboxyl-terminal portion of the molecule contains nine conserved cysteine residues that form the cysteine knot structure typical of the superfamily (Mehra and Wrana, 2002; Massague et al., 2000; Vitt et al., 2001; 2001; Gaddy-Kurten et al, 1995; Daopin et al., 1993). TGFβ1 and 2 can inhibit myoblast proliferation and induce or inhibit differentiation depending on culture conditions (Liu et al., 2001; Cusella-De Angelis et al., 1994; Greene and Allen, 1991). TGFβ prevents myoblast proliferation by up-regulating a cell cycle inhibitor, p21 (Li et al., 1995). TGFβ in low serum media inhibits terminal differentiation of myoblasts by inhibiting the activity and expression of MyoD and myogenin (Liu et al., 2001; Vaidya et al., 1989; Massague et al., 1986). However in high serum media, TGFβ can induce the differentiation of myoblasts (Zentella and Massague, 1992). TGFβ also induces embryonic stem cells into myogenic lineage (Slager et al., 1993). During skeletal muscle myogenesis, TGFβ appears to be required for the mediation of signals from the neural tube that is required for myogenesis (Pirskanen et al., 2000). In addition, TGFβ can act as a chemotactic factor for satellite cells in regenerating muscle (Bischoff et al, 1997). Thus TGFβ appears to play an important role in the regulation of the skeletal muscle mass both pre- and post-natally.

1.6.3.1. Myostatin

Myostatin also known as Growth and Differentiation Factor-8 (GDF-8) was discovered in 1997 in mice as a TGF-β superfamily member that specifically regulates skeletal muscle growth (McPherron et al., 1997). Myostatin is

expressed in skeletal muscle and acts as a negative regulator of both proliferation and differentiation of myoblasts (McCroskery et al., 2005; Langley et al., 2004; Langley et al., 2002; Thomas et al., 2000; Kambadur et al., 1997; McPherron et al., 1997). Furthermore, myostatin also acts as a negative regulator of muscle regeneration and hypertrophy, thus regulating all stages of muscle myogenesis. Thus myostatin becomes one of the key players in the regulation of myogenesis of skeletal muscle. Apart from skeletal muscle, myostatin has been detected in adipose tissue (McPherron et al., 1997) and in cardiomyocytes and purkinje fibers of the heart (Sharma et al., 1999). But the function of myostatin in other tissues is largely unknown.

Mutations in myostatin, as in myostatin null mice and cattle, results in 2-3 fold increased muscle mass than wild type, termed as "double-muscling" phenotype (Schuelke et al., 2004; Lee and McPherron, 1999; Kambadur et al., 1997). This increase in muscle mass is due to both muscle fiber hypertrophy and hyperplasia (McPherron et al., 1997). Moreover, myostatin null mice showed increased proportion of type II or glycolytic fibers (Girgenrath et al., 2005). In addition to targeted disruption of *Mstn* in mice, several naturally occurring mutations have been identified in other species including the double-muscled cattle breeds such as Belgian Blue (Figure 1.9) and Piedmontese (Grobet et al., 1998; Kambadur et al., 1997; McPherron et al., 1997) and the whippet racing dog breed (Mosher et al., 2007). *Mstn* mutation has been discovered in humans that resulted in dramatic hypertrophy of skeletal muscle (Schuelke et al., 2004).

Figure 1.9 Double muscling phenotype. Natural mutations in myostatin lead to lack of functional myostatin resulting in double muscling phenotype in cattle. Figure freely downloaded from http://commons.wikimedia.org/wiki/File:GEURTZ16.JPG#filelinks (privates Foto auf einem deutschen Zuchtbetrieb, wo ich einen Bullen gekauft habe, dieses Foto wurde von mir selbst gemacht, summer 2005) on 29.12.2014.

Like other TGFβ superfamily members, myostatin is synthesized as a 52kD inactive precursor protein (pre-proprotein). After synthesis, the precursor protein consists of a homodimer linked by disulphide bonds. The precursor myostatin undergoes two proteolytic cleavage events to generate the mature protein. In the first cleavage, the 24 amino acid amino terminal signal peptide is cleaved which targets the protein for secretion from the Golgi complex (pro-protein). In the second cleavage, the proprotein is cleaved at the RSRR proteolytic cleavage site to give rise to 12.5kD carboxy terminal mature myostatin protein and 26kD amino terminal Latency associated protein (LAP)

(Lee and McPherron, 2001; Sharma et al., 2001; Thomas et al., 2000). The mature myostatin contains nine conserved cysteine residues, out of which eight cysteine residues form disulphide bond within the protein and the ninth residue forms a covalent bond between the homodimers. The bonding between these cysteine residues forms a typical structure of TGFβ superfamily called as the cysteine knot. This cysteine knot is required for the functioning of the mature myostatin protein (McPherron et al., 1997).

TGFβ superfamily members elicit its biological response by binding to serine threonine kinase receptor activin type IIB (ActRIIB) (Rebbapragada et al, 2003). Mice over-expressing dominant negative form of ActRIIB showed increased muscle mass comparable to myostatin null mice (Lee and McPherron et al., 2001). Another study showed that the mstn-mediated activation of ActRIIB receptor leads to phosphorylation of the type I receptors, i.e., activin receptor-like kinase 4 (ALK4) or ALK5 (Rebbapragada et al., 2003). Once Mstn binds to Type II and Type I receptors, downstream molecules like Smad2 and/or Smad3 are activated (Rebbapragada et al., 2003). Smad 2/3 binds to co-smad called smad4 and together translocates to the nucleus and regulates expression of various downstream target genes (Rebbapragada et al., 2003). Thus, mstn signals canonically through Smads to affect the skeletal muscle mass. In addition, it is also reported that Mstn can signal via non-canonical pathways through p38 mitogen activated protein (MAPK), ERK1/2, c-Jun N-terminal Kinase (JNK) and Wnt signaling (Allendorph et al., 2006; Elkasrawy and Hamrick, 2010; Huang et al., 2007). It was shown that myostatin induces p38 MAPK phosphorylation through TGFβ activated kinase-1 (TAK1) in myoblasts and has been proposed to be

involved in myostatin mediated myoblast growth inhibition (Philip et al., 2005). Thus, the regulation of skeletal muscle mass by myostatin is attributed mainly to these above-mentioned pathways.

It had clearly been established that myostatin is a negative regulator of skeletal muscle formation and muscular hypertrophy (Grobe et al., 1997; Kambadur et al., 1997; McPherron et al., 1997). Addition of myostatin protein to C_2C_{12} or primary bovine myoblasts in culture results in an inhibition of proliferation in a dose dependent manner. Furthermore, this inhibition did not result in overt myotube formation, did not result in increased apoptosis and was reversible (Thomas et al, 2000). Treatment of myoblasts with myostatin results in an up-regulation of the Cyclin dependent kinase inhibitor (CKI), p21, without altering the levels of other CKIs (Rios et al., 2001; Thomas et al., 2001; Thomas et al., 2000). Thomas et al. (2000) proposed that the mechanism of this cell cycle inhibition involves the up-regulation of p21. p21, in turn inhibits the activity of the Cyclin-cdk2 complex, in addition a slight down-regulation of cdk2 expression occurs, overall this results in an inhibition of cdk2 activity. This loss of cdk2 activity results in hypo-phosphorylation of the retinoblastoma protein (Rb). This active hypo-phosphorylated Rb inhibits cell cycle progression from G1-S phase, thus stalling the myoblasts at G1 phase resulting in reduced number of myoblasts (Thomas et al., 2000).

It has been well established that myostatin regulates skeletal myogenesis by inhibiting differentiation of myoblasts in a dose dependent manner (Langley et al., 2002; Rios et al., 2002; Joulia et al., 2003). Furthermore, myostatin was shown to signal through smad3 protein and down-regulate MyoD protein expression as well as activity (Langley et al., 2002).

In addition to regulating skeletal muscle mass, myostatin also has an important role in muscle repair and regeneration. The process of muscle regeneration is described in section 1.4. Myostatin was shown to negatively regulate regeneration by keeping satellite cells quiescent until necrosis and inflammation has occurred and in the absence of myostatin the regenerative process is accelerated (McCroskery et al., 2005).

It has been shown that antagonists to myostatin could be potentially useful pharmalogical treatments for disorders associated with overt degeneration and regeneration such as muscular dystrophies (McCroskery et al., 2005; Bartoli et al., 2007; Ohsawa et al., 2007). Treatment of mdx mice, a model for Duchenne muscular dystrophy (DMD), with myostatin inactivating antibody lead to an increase in body weight, muscle size and muscle strength alleviating the dystrophic phenotype (Bogdanovich et al., 2002). Also, similar improvement in muscle strength was seen in mdx mice crossed into myostatin null lineage (Wagner et al., 2005). Myostatin is also shown to inhibit satellite cell migration and proliferation during muscle regeneration. Thus inactivation of myostatin could be used as a potential therapeutic target to alleviate muscular dystrophy symptoms. Recently, a novel myostatin antagonist, human ActRIIb antibody called Bimagrumab (BYM338) was developed. This antibody binds to human myostatin and Activin A and blocks the canonical signaling pathways of myostatin, thus stimulating differentiation of primary human myoblasts leading to hypertrophy. BYM338 is also shown to inhibit glucocorticoid-induced muscle wasting and induce muscle hypertrophy in mice (Lach-Trifilieff et al., 2014). Similarly, it was shown that short-term antagonism of myostatin with truncated myostatin protein called mstn-ant1,

improved the muscle regeneration after muscle injury during sarcopenia (Siriett et al., 2007). Inhibition of myostatin resulted in increased activation of satellite cells with MyoD expression and enhanced regeneration after muscle injury in sarcopenic muscle (Siriett et al., 2007). This suggests that antagonism of myostatin can act as a potential therapeutic strategy to ameliorate sarcopenia.

In addition to inhibiting the process of myogenesis, myostatin has been implicated in the induction of muscle wasting. Increased myostatin expression has been detected in atrophic conditions like sarcopenia (Schulte and Yarasheski, 2001; Yarasheski et al., 2002); muscle disuse, including chronic human muscle disuse atrophy (Reardon et al., 2001; Zachwieja et al., 2000), hind limb unloading (Carlson et al., 1999) and space flight (Lalani et al., 2000) and during progression of cachexia (Zimmers et al., 2002). Ma et al., (2003) demonstrated that injection of a glucocorticoid like dexamethasone in rats induces skeletal muscle atrophy and elevated myostatin RNA and protein expression. Furthermore, inhibition of dexamethasone by a glucocorticoid agonist RU-486, resulted in down-regulation of myostatin levels and alleviating muscle wasting (Ma et al., 2003).

In addition to an associative role during various skeletal muscle wasting pathologies, myostatin has been directly demonstrated to induce cachexia in mice. Specifically, injection of CHO cells over-expressing myostatin into the mice resulted in 33% reduction in total body weight within 16 days compared to the control mice (Zimmers et al., 2002). Furthermore in the same study it was demonstrated that the severe body mass loss was alleviated by injection of

myostatin antagonists like follistatin or myostatin pro-peptide (Zimmers et al., 2002).

Myostatin-induced skeletal muscle wasting has been shown to result in down-regulation of myogenic gene expression. Over-expression of myostatin results in reduced expression of myogenic structural genes like MyHC and desmin (Durieux et al., 2007). Furthermore, myostatin–mediated muscle wasting resulted in down-regulation of MRFs including MyoD and myogenin (Durieux et al., 2007; McFarlane et al., 2006). A reduction in these MRFs would further worsen the muscle wasting phenotype by potentially impairing post-natal myogenesis and muscle regeneration. Concomitant with the down-regulation of MRFs, myostatin via smad3 signaling stimulates the activity of FoxO transcription factors to induce the transcription of atrophy-related genes like atrogin-1, MuRF1 and E214K which degrade the sarcomeric proteins through ubiquitin-proteasome pathway (McFarlane et al., 2006; Ge et al., 2011; Lokireddy et al., 2011). Furthermore, it was demonstrated that treatment of C_2C_{12} myotubes with recombinant myostatin protein inhibited PI3-K/Akt phosphorylation by down-regulating the IGF-I/PI3-K/Akt pathway thereby inhibiting the protein synthesis and inducing muscle atrophy (Trendelenburg et al., 2009). These evidences show myostatin as a potent inducer of skeletal muscle wasting.

Myostatin has also shown to induce increased production of reactive oxygen species (ROS) by activating TNF alpha signaling pathway thus inducing skeletal muscle wasting phenotype in skeletal muscle cells (Sriram et al., 2011). It was also shown that increased ROS in turn induces increased myostatin expression in a feed-forward mechanism and increased myostatin

levels in turn activate the ubiquitin-proteasome pathway leading to sarcomeric protein degradation (Sriram et al., 2011).

Recently, another important ubiquitin ligase protein called Mul1 was shown to induce loss of mitochondria as a response to muscle wasting in mice (Lokireddy et al., 2012). Furthermore, it was shown in the same study that during muscle wasting, Mul1 targets an important mitochondrial biogenesis protein called Mfn1 to ubiquitin-proteasomal degradation resulting in mitochondrial fission and eventually mitophagy (Lokireddy et al., 2012).

1.7 Akirin1

To understand the function of myostatin in skeletal muscle, novel downstream signaling molecules of myostatin have been identified. Suppressive subtraction hybridization of mRNA expressed between wild type and myostatin knockout muscle identified a novel gene called *mighty* (Marshall et al., 2008). Later this gene was renamed as Akirin1. The gene name 'akirin' is taken from a Japanese phrase '*akiraka ni suru'* meaning 'making things clear' due to presence of a strong nuclear localization signal (NLS) at the N terminus of the protein. Due to the presence of clear NLS, akirin family of proteins is shown to be highly conserved nuclear proteins (Goto et al., 2008). Akirin1 is a 191 amino acid protein with a molecular weight of 21 kD and isoelectric point of 9.05 (Macqueen et al., 2009; Yang et al., 2011). Akirin1 is ubiquitously expressed in all the tissues, but is negatively regulated by myostatin in skeletal muscle (Marshall et al., 2008). Evolutionarily, akirin gene underwent a gene duplication event in vertebrates to give rise to two homologues, Akirin1 and Akirin2 (Macqueen et al., 2009). Akirin2 is similar to Drosophila Akirin (DmAkirin) and has a role in providing innate immunity against gram-

negative bacteria (Goto et al., 2008). In rats, Akirin2 was shown to interact with 14-3-3 repressor-protein complex and promote carcinogenesis (Macqueen et al., 2009).

It was shown that when Akirin1 is over expressed in C_2C_{12} cells, the myoblasts withdraw from cell cycle and show increased fusion of myoblasts compared to the control C_2C_{12} myoblasts. This increased fusion of myoblasts results in hypertrophy of myotubes (Marshall et al., 2008). The hypertrophy phenotype is contributed by premature expression of MyoD with increased production of IGF-II (Marshall et al., 2008). Akirin1 expression was up regulated in myostatin null muscle compared to the wild type muscle (Marshall et al., 2008). On the contrary, differentiated C_2C_{12} myotubes that were treated with myostatin showed reduced levels of Akirin1 expression (Marshall et al., 2008). Furthermore, expression of Akirin1 in mdx mice resulted in muscle fibers with increased myofiber size (Marshall et al., 2008). Thus showing that Akirin1 is an important pro-myogenic protein that functions downstream of myostatin (Marshall et al., 2008). During muscle regeneration, Akirin1 is expressed earlier i.e., after two days of muscle injury and is shown to have a role in satellite cell activation (Salerno et al., 2009). Also, over expression of Akirin1 led to increased chemotactic efficiency of myoblasts and macrophages during muscle regeneration (Salerno et al., 2009). Thus it was shown that Akirin1 has a very prominent role during the process of skeletal muscle regeneration.

Contemporarily, a few research groups were independently studying akirin under different aliases in different animal models like fly, ticks and fish. In drosophila, when genome–wide high-throughput RNA interference (RNAi)

screen was performed to identify new components of Imd pathway, a novel gene called *DmAkirin* was identified (Goto et al., 2008). DmAkirin (also called *bhringi*), functions along with NF-κB transcription factor in Imd pathway to provide innate immunity to drosophila by producing attacin, an antibacterial protein that acts against gram-negative bacteria (Goto et al., 2008). Nowak et al. discovered another important function of akirin as a cofactor in drosophila. It was shown that Akirin physically interacts with muscle transcription factor twist, and regulate transcription of twist-regulated genes in drosophila. Akirin protein also co-localizes with Brahma SWI/SNF complex subunits which is a chromatin remodeling complex. Thus, akirin is predicted to link twist and chromatin remodeling complex resulting in remodeling of chromatin assembly, affecting the expression of twist-regulated genes (Nowak et al., 2012).

Akirin was discovered in ticks as well. It was shown that when ticks were infected with bacterial pathogens, they produce a protective protein called subolesin. This protein was identified to be similar in structure and function to Akirin (Zivkovic et al., 2010).

Evolutionarily, *Akirin* gene underwent a few gene duplication events in teleost lineage to give rise to eight homologues of *Akirin* (Macqueen et al., 2009). In Atlantic salmon fish, the various homologues of Akirin have been shown to play significant roles in myoblast proliferation and differentiation (Macqueen et al., 2010). Akirin in *Scophthalmus maximus* (turbot) was identified as a nuclear-localized protein that was expressed ubiquitously in all the tissues with maximum expression in the brain and spleen (Yang et al., 2011). Also, *Scophthalmus maximus* Akirin1 (SmAkirin1) was identified as a member of

NF-κB signaling pathway induced in response to bacterial and viral infection (Yang et al., 2011).

Recently Dong et al. showed that Akirin1 was down regulated by increased expression of myostatin in dexamethasone-induced muscle atrophy in mice (Dong et al., 2013). Furthermore, reduced Akirin1 levels affected the proliferation and differentiation of satellite cell both *in-vitro* and *in-vivo,* contributing to muscle atrophy during dexamethasone treatment. On the contrary, when myostatin was down regulated in dexamethasone-treated mice, both Akirin1 levels and satellite cell activation increased, leading to improved skeletal muscle regeneration and growth. Also, when Akirin1 was over expressed in dexamethasone-treated myoblasts, satellite cell activation improved leading to up-regulation of myogenic markers like MyoD and myogenin. Thus, by inducing Akirin1, a pro-myogenic factor, dexamethasone-induced satellite cell dysfunction and muscle atrophy could be alleviated (Dong et al., 2013).

1.8 Aims and Objectives

Akirin1 is one of the new exciting molecules in Muscle biology, in terms of its potential role and the various facets that are still left to be explored. A number of research groups have studied the roles of Akirin as a transcriptional co-activator in invertebrates, namely Drosophila, and vertebrates such as Atlantic salmon fish. *Akirin* gene has two homologues (*Akirin1* and *Akirin2*) in mice. Previous work from our lab showed a novel role of Akirin1 as a pro-myogenic protein in differentiating C_2C_{12} myotubes. Therefore, to delineate the exact function of Akirin1 in fully differentiated striated muscle (skeletal and cardiac muscle), we have used Akirin1 gene knock-out mice. Through this study, we aim to achieve the following:

1. Understand the function of Akirin1 during skeletal myogenesis.

   As over-expression of Akirin1 in C_2C_{12} myoblasts lead to enhanced differentiation of myoblasts, we wanted to study the effect of lack of Akirin1 during myogenic differentiation using Akirin1 knock-out mice.

2. Characterize the skeletal muscle phenotype in Akirin1 knock-out mice.

   Previous work showed that Akirin1 over-expression increased the protein synthesis leading to hypertrophy of myotubes. So we wanted to study the skeletal muscle phenotype of Akirin1 knock-out mice by exploring important aspects in fully differentiated skeletal muscle such as the levels of various skeletal muscle sarcomeric proteins and myogenic genes that are important for myogenesis and energy metabolism.

3. Characterize the cardiac muscle phenotype in Akirin1 knock-out mice.

   Knowing that cardiac muscle is a highly oxidative tissue and Akirin1 may have a role in energy metabolism, we wanted to study the effect of Akirin1 in cardiac muscle by studying the cardiac muscle sarcomeric proteins and molecules involved in cardiac hypertrophy signaling.

CHAPTER 2

MATERIALS AND METHODS

2. MATERIALS AND METHODS

This chapter details the general materials and methods used in this thesis, which includes reagents, chemicals, solutions, oligonucleotides, antibodies and relevant protocols.

2.1 Materials

This section provides the general materials used in this thesis.

2.1.1. Oligonucleotides

All oligonucleotides used in this thesis were synthesized by Sigma-Aldrich, Singapore. The stock solutions (100µM) were stored at -20^{o}C. The working concentration of primers used was 2.5 µM for Reverse Transcriptase-quantitative Polymerase Chain Reaction (RT-qPCR) and 10 µM for genotyping PCR. The oligonucleotides used are listed in table 2.1 and 2.2.

Table 2.1 RT-qPCR primers

Gene	**Forward primer 5'-3'**	**Reverse primer 5'-3'**
Myh1	CACGCTGGATGCTGAGATTA	AGGTGCAGCTGAGTGTCCTT
Myh 2	CTCGTTTGCCAGTAAGGGTCT	GGCCTCGATTCGCTCCTTT
Myh4	CAAGTCATCGGTGTTTGTGG	GGCCATGTCCTCAATCTTGT
Myh7	GCTGGCACTGTGGACTACAA	CTTTCTTTGCCTTGCCTTTG
MuRF1	ACGAGAAGAAGAGCGAGCTG	CTTGGCACTTGAGAGGAAGG
PGC1α	GAGAGACAACCCTGGGATCA	GTGGCCAGCATTATTTCACAG
U6	CTCGCTTCGGCAGCACA	AACGCTTCACGAATTTGCGT

Pri- miR-1	GGTGGGCTGCTTCATGTT	TTTCCTTTAGCTTCTTCTTGGC
Myogenin	TGGTACCCAGTGAATGCAACTC	GGACCAAACTCCAGTGCATTG
Cyclophilin	TTGCCATTCCTGGACCCAAA	ATGGCACTGGTGGCAAGTCC
Akirin1	ATAACCATTCCCACAGTTCCACAGC	TAAAAGAGCACTGGTGGGCTCTCA
β-MyHC/Myh7	TGCAAAGGCTCCAGGTCTGAGGGC	GCCAACACCACCCTGTCCAAGTTC
ANP	CCAGGCCATATTGGAGCAAA	GAAGCTGTTGCAGCCTAGTC
Cardiac troponin C	TGCAGGCCACAGGTGAGACCA	GAACAGGCGCAGGCAACCGT
Cardiac troponin I	AAAGCAGCGATGCGGCTGGG	TTCTTGGCGTGTGGCTCGGT
Cardiac troponin T	GGCCAAGGAGCTGTGGCAGA	CGCCCGGTGACTTTGGCCTT
mature miR-1	TGGAATGTAAAGAAGTATGTAT	TTTTTTTTTTTTTTTTTT
mt DNA	CCTATCACCCTTGCCATCAT	GAGGCTGTTGCTTGTGTGAC
nu DNA	ATGGAAAGCCTGCCATCATG	TCCTTGTTGTTCAGCATCAC
α-actin	CTGAGCGTGGCTATTCCTTGTGC	GCAGCGGTGGCCATCTCATTCT
Desmin	GTCCTCCTACCGCCGCACCTT	CGTGCGCGACACCTGGTACAC
AMPKα2	CGCCTCTAGTCCTCCATCAG	ATGTCACACGCTTTGCTCTG
PPARα	GGACCTTCGGCAGCTGGT	TCGGACTCGGTCTTCTTGATG
HDAC4	CAGATGGACTTTCTGGCCG	CTTGAGCTGCTGCAGCTTC
MEF2C	CCATCAGCCATTTCAACAAC	GATGGCGGCATGTTATGTAG
FoxO3	AGCCGTGTACTGTGGAGCTT	TCTTGGCGGTATATGGGAG

MyHC	CATCGCCGCAGACTTTGG	GGGCCTCCTTCTGGGATGCCT
p21/WAF1	CGGTGGAACTTTGACTTCGT	CAGGGCAGAGGAAGTACTGG
MyoD	GACAGGGAGGAGGGGTAGAG	TGCTGTCTCAAAGGAGCAGA
CREB-1	TCTAGTGCCCAGCAACCAAG	ACGCCATAACAACTCCAGGG
SRF	TACCAGGTGTCGGAGTCTGACA	GGCAGGTTGGTGACTGTGAA

Table 2.2 Genotyping primers

Gene	**Forward primer 5'-3'**	**Reverse primer 5'-3'**
Akirin1 WT	AGTGATACCAGGGTGTTAGGA ACTTCC	GTTGAAGTACTGTGACAGCCA TCTTGG
Akirin1 knock-out	AACCAACTACCCACTTCAAAG CCATACC	TGTCTATTCCTGCCACATTCAC TGTGC

2.1.2. Antibodies

All antibodies used in this project were purchased from the following companies: Santa Cruz Biotechnology Inc (Santa Cruz Biotechnology Inc, Santa Cruz, CA), Developmental Studies Hybridoma Bank (DSHB, Iowa City, IA), Cell Signaling (Cell Signaling Technology, Inc. Danvers, MA), BD Pharmingen (BD Pharmingen, San Diego, CA, R&D System (R&D Systems Inc, Minneapolis, MN, USA, Abnova (Taipei City, Taiwan), Abcam (Cambridge, UK Dako (Dako, Glostrup, Denmark), Sigma (Sigma, St. Louis, MO), mouse anti-MuRF1 and rabbit anti-atrogin-1 antibodies were gifted from Regeneron Company, USA.

The primary and secondary antibodies used in this project are listed in table 2.3.

Table 2.3 Western antibodies and dilutions

Antibody	**Catalogue No.**	**Source**	**Dilution used**
4eBP1	sc-9977	Santa Cruz	1:500
Akirin1	Ab 77074	Abcam	1:250
Akt	sc-8312	Santa Cruz	1:2000
AMPKα	2550	Cell signaling	1:500
ANP	sc-80686	Santa Cruz	1:500
Atrogin-1	Gift	Regeneron	1:2000
Atrogin-1	PAB15627	Abnova	1:3000
Cardiac troponin I	TI-1	DSHB	1:1000
Cardiac troponin T	CT3	DSHB	1:1000
Cdk4	sc-601	Santa Cruz	1:200
CREB-1	sc-240	Santa Cruz	1:500
Cyclin D1	sc-8396	Santa Cruz	1:200
Desmin	D76	DSHB	1:500
FoxO3	sc-11351	Santa Cruz	1:400
GAPDH	sc-166545	Santa Cruz	1:10000
GSK3β	612312	BD Pharmingen	1:500

HDAC4	2072	Cell signaling	1:500
IGF-1	sc-9013	Santa Cruz	1:300
Cyclin E	sc-481	Santa Cruz	1:400
MEF2C	sc-13266	Santa Cruz	1:200
mTOR	2983	Cell signaling	1:300
MuRF1	Gift	Regeneron	1:200
MuRFI	sc-27642	Santa Cruz	1:200
MyHC	MF20	DSHB	1:5000
MyoD	sc-304	Santa Cruz	1:400
Myogenin	sc-576	Santa Cruz	1:400
p-ERK1/2 (thr202/tyr204)	sc-16982	Santa Cruz	1:500
p-4eBP1 (ser65/thr70)	sc-12884	Santa Cruz	1:500
p-Akt (ser473-R)	sc-7985-R	Santa Cruz	1:500
p-CREB-1 (ser133)	sc-7978	Santa Cruz	1:500
p-FoxO3 (ser253)	sc-101683	Santa Cruz	1:100
p-GSK3β (ser9)	9336	Cell signaling	1:500
p-MEF2C (thr300)	sc-130201	Santa Cruz	1:200
p-mTOR (ser2448)	2971	Cell signaling	1:300
p-p38 MAPK (T180/Y182)	4511	Cell signaling	1:1000

pPI3Kp85(tyr458)/p55(tyr199)	4228	Cell signaling	1:200
p21(WAF1/CDK inhibitor-1)	556430	BD Pharmingen	1:400
P38 MAPK	4292	Cell signaling	1:2000
p-JNK (T183/Y185)	9251	Cell signaling	1:1000
PGC1α	sc-13067	Santa Cruz	1:500
JNK	9252	Cell signaling	1:400
PI3Kp85	4292	Cell signaling	1:500
Polyglutamylated tubulin	T9822	Sigma	1:3000
PPARα	sc-9000	Santa Cruz	1:500
SRF	5147	Cell signaling	1:1000
Troponin C	sc-48347	Santa Cruz	1:200
Troponin I	TI-4	DSHB	1:500
Troponin T-SS	sc-8122	Santa Cruz	1:500
Ubiquitin	sc-8017	Santa Cruz	1:10000
ERK1/2	sc-94	Santa Cruz	1:500
α-actin	sc-58670	Santa Cruz	1:1000
α-Myh (cardiac)	Ab50967	Abcam	1:100
α-tubulin	T9026	Sigma	1:10000
β-Myh (cardiac MYH7)	sc- 71575	Santa Cruz	1:200

Table 2.4 Primary antibodies used for Immunohistochemistry (IHC)

Antibody	Catalogue no.	Source	Dilution used
Myh fast 2A	2F7	DSHB	1:25
Myh fast 2B	10F5	DSHB	1:25
Myh slow (type I)	A4.840	DSHB	1: 25

Table 2.5 Secondary antibodies

Antibody	Catalogue no.	Source	Dilution used	Usage
Alexa Fluor 488 (AF 488) donkey anti-mouse lgG	A-21202	Invitrogen	1:400	IHC
Goat anti-mouse lgG HRP conjugate	170-6516	Bio-Rad	1:5000	Western blot
Goat anti-rabbit lgG HRP conjugate	170-6515	Bio-Rad	1:5000	Western blot
Goat anti-rat lgG HRP conjugate	sc-2006	Santa Cruz	1:2000	Western blot

2.1.3. Reagents and chemicals

Sigma-Aldrich, St. Louis, MO, USA: Methylene blue, Collagenase type 1A, Aprotinin, Bovine serum albumin (BSA), low-gelling temperature agarose, PVP (Polyvinylpyrrolidone), PEG (Polyethylene glycol), DMSO (Dimethyl sulphoxide).

PAA Laboratories: DMEM (Dulbecco's Modified Eagle Medium).

BD Biosciences, Franklin Lakes, New Jersey, USA: Matrigel.

HyClone Laboratories, Inc., Logan, Utah, USA: Fetal Bovine Serum (FBS) and HEPES pH 7.8

Gibco, Carlsbad, CA, USA: Penicillin/Streptomycin (P/S), Trypsin-EDTA and HS (Horse serum).

US Biologicals, Swampscott, MA, USA: Chick embryo extract (CEE) and Dithiothreitol (DTT).

Bio-Rad Laboratories: Bradford assay reagent, Ssofast Evagreen and nitrocellulose membrane.

Santa Cruz Biotechnology, Inc, Santa Cruz, CA, USA: PhenylmethanesulfonyIfluoride (PMSF).

1st Base Pte. Ltd.: EDTA (Ethylenediaminetetraacetic acid).

GE Healthcare Life Sciences: Nucleic acid blotting nylon membrane (Hybond-N+).

Fluka, St. Louis, MO, USA: lgepal (NP-40).

Merck & Co, Inc., NJ, USA: Ethanol, Formaldehyde, HCl, methanol, acetone.

Invitrogen: NSS (Normal sheep serum) and DAPI (4',6-diamidino-2-phenylindole).

2.1.4. Enzymes

All restriction enzymes were acquired from New England Biolabs (NEB, USA) or Fermentas (Maryland, USA). All restriction enzyme buffers were supplied by the respective companies. The remaining enzymes used in this study are listed in table 2.6.

Table 2.6 Enzymes

Enzymes	**Source**
Proteinase K	Invitrogen
iScript Reserve Transcriptase	Biorad
Taq DNA polymerase	Fermentas

2.1.5. Plasmid DNA

All plasmids were stored at -20^{o}C or 4^{o}C in either TE buffer or Milli-Q water. Bacterial stocks were maintained in 25% autoclaved glycerol and stored at -80^{o}C. Plasmid DNA constructs and their sources are given in the table 2.7.

Table 2.7 Plasmid constructs

Construct name	**Vector backbone**	**source**
Akirin1 pcDNA3.1	pcDNA3.1	Invitrogen
pRL-TK	Renilla	Promega
MuRF1-Luc	pGL4.1	Gift

2.1.6. Solutions

The solutions used in this project are listed in table 2.8**.**

Table 2.8 Composition of solutions used

Solution	**Working concentration**	**Composition**
Formal saline fixative	10% Formaldehyde 0.9% Saline	37% Formaldehyde - 250 ml NaC1-8.7g Milli-Q water - 750 ml
Sodium borate buffer	0.01 M (pH 8.7)	Sodium tetraborate - 7.63g Milli-Q water - 2 L Adjust pH to 8.7

Methylene blue stain	1% methylene blue	Methylene blue - 1g 0.01 M borate buffer (pH 8.5)- 100 ml
1 M HC1	1 M	37% fuming HCl - 8.33 ml Milli-Q water - 100 ml
HC1:Ethanol	1:1 0.1 M HC1: Ethanol	Absolute ethanol - 500 ml 1 M HC1 - 50 ml Milli-Q water - 450 ml
Ethanol:formaldehyde:Acetic acid	20:2:1	Absolute ethanol - 87 ml 37% Formaldehyde - 8.7 ml Glacial acetic acid - 4.3 ml
0.1% HC1	0.1%	37% fuming HC1 - 0.1 ml Milli-Q water - 99.9 ml
Scott's tap water	-	Sodium bicarbonate - 3.5 g $MgSO_4$. $7H_2O$ - 20g Milli-Q water - 1 L
Collagenase 1A solution	0.2%	Collagenase 1A (490U) - 40mg DMEM - 20ml Freshly prepared. Filter sterilized.
Matrigel	10%	Matrigel - 0.4 ml Cold DMEM - 3.6 ml
RIPA buffer	Aprotinin 1.5 mM Sodium vanadate 2 mM NaF 5 mM Na_2-EDTA 1X protease inhibitor stock 2 mM PMSF (add just before using)	1.7 mg/ml Aprotinin- 0.4 ml 700 mM Sodium vanadate- 30 µl 500 mM NaF- 1.4 ml 0.5 M EDTA- 140 µl 50 X protease inhibitor stock- 400 µl Make up to14 ml with Milli-Q water 100 mM PMSF- 140 µl

Solutions for cytoplasmic and nuclear extract isolation (freshly prepared):

Lysis buffer	50 mM KCl 0.5% Igepal-NP-40 25 mM HEPES (pH 7.8) - 125 µM DTT 1 mM PMSF	1 M KCl - 250 µl Igepal-NP-40 - 25 µl 1 M HEPES (pH 7.8) - 125 µl 1.7 mg/ml Aprotinin - 58.8 µl 250 mM DTT - 2.5 µl 100 mM PMSF - 50 µl Milli-Q water - 4.48 ml
Wash buffer	50 mM KCl 25 mM HEPES (pH 7.8) - 125 µM DTT 1 mM PMSF	1 M KCl - 250 µl 1 M HEPES (pH 7.8) - 125 µl 1.7 mg/ml Aprotinin - 58.8 µl 250 mM DTT - 2.5 µl 100 mM PMSF - 50 µl Milli-Q water - 4.51 ml
Extraction buffer	0.5 M KCl 25 mM HEPES (pH 7.8) - - 125 µM DTT 1mM PMSF	1 M KCl – 2.5 ml 1 M HEPES (pH 7.8) - 125 µl 50% glycerol - 1 ml 1.7 mg/ml Aprotinin - 58.8 µl 250 mM DTT - 2.5 µl 100 mM PMSF - 50 µl Milli-Q water- 1.26 ml
10% Buffered formalin	Sodium phosphate, monobasic Sodium phosphate, dibasic 37% Formaldehyde	4 g 6.5 g 100 ml Milli-Q water- 900 ml
SDH staining reagent	Sodium succinate Nitroblue tetrazolium (NBT)	50mM 0.6mM Prepared in 1X PBS
GPD staining reagent	rac-Glycerol 1-phosphate disodium salt hexahydrate	9.3 mM 0.24 mM

	NBT	Prepared in 0.2 M Tris-HCl buffer (pH7.4).
Tris-glycine SDS running buffer	Tris Glycine 10% SDS	30g 18.8 g 10 ml Make up to1000 ml with Milli-Q water.
Western blot transfer buffer	Tris Glycine Methanol	15.1 g 75 g 1000 ml Make up to 5000 ml with Milli-Q water.
Stacking protein gel (4%)	30% Acrylamide Tris HCl pH 6.8 10%SDS 10% APS TEMED	1ml 750 µl 60 µl 60 µl 10 µl Milli-Q water- 4.1 ml
Separating protein gel (6%) for high molecular weight proteins.	30% Acrylamide Tris HCl pH 8.8 10%SDS 10% APS TEMED	4 ml 7.5 ml 200 µl 200 µl 20 µl Milli-Q water- 8.1 ml
Separating protein gel (10%) for low molecular weight proteins.	30% Acrylamide Tris HCl pH 8.8 10%SDS 10% APS TEMED	6.7 ml 7.5 ml 200 µl 200 µl 10 µl Milli-Q water- 5.4 ml
MES-SDS running buffer	1X	20X MES-SDS - 50 ml Make up to 1000 ml with Milli-Q water.

Western blot transfer buffer	-	Tris - 3.03 g Glycine - 14.4 g Methanol - 200 ml Make up to 1000 ml with Milli-Q water. Store at 4°C.
TBS (Tris buffered saline)	0.05 M Tris-HC1 (pH 7.5) 150 mM NaCl 1X	1 M Tris-HCl (pH 7.5) = 50 ml 5 M NaCl = 30 ml Make up to 1000 ml with Milli-Q water.
TBS-T (1X)	0.05 M Tris-HC1 (pH 7.5) 150 mM NaCl 0.1% Tween-20	1 M Tris-HCl (pH 7.5) - 50 ml 5 M NaCl - 30 ml Tween 20 - 1 ml Make up to 1000 ml with Milli-Q water.
Western blot milk blocker	5% non-fat milk in 1X TBS-T	Non-fat milk powder - 5 g 1X TBS-T - 100 ml
Western blot BSA blocker	5% BSA in 1X TBS-T	BSA - 5 g 1X TBS-T - 100 ml

Solutions and reagents for EMSA:

Tris-borate EDTA (TBE) buffer	0.5X	10X TBE - 100 ml Make up to 2000 ml with Milli-Q water. Freshly prepared.
5% TBE gel	-	30% Acrylamide - 1.66 ml 10X TBE - 0.5 ml 10% Ammonium persulfate (freshly prepared) - 0.1 ml TEMED - 10 µl Make up to 10 ml with Milli-Q water.
Binding buffer	100 mM Tris 500 mM KCl 10 mM DTT	Tris - 60.57 mg KCl - 186.32 mg DTT - 7.71 mg

	pH 7.5	Milli-Q water - 5 ml Adjust pH to 7.5. Store at -20°C.
DNA Loading dye	5X	Bromophenol blue - 25 mg Xylene cyanol - 25 mg 0.2 M Na_2-EDTA - 5 ml 30% glycerol - 3 ml Make up to 10 ml with Milli-Q water. Store at -20°C.
Tris-acetate EDTA (TAE) buffer	1X	10X TAE - 100 ml Make up to 1000 ml with Milli-Q water.
Sodium acetate	3 M (pH 5.0)	Sodium acetate – 2.460 g Milli-Q water - 10 ml Adjust pH to 5.0
DNA extraction buffer	0.1 M NaCl 1 mM Na2-EDTA 1% SDS	NaCl- 292.2 mg Na2-EDTA- 18.61 mg 10% SDS- 5 ml Make up to 50 ml with 10 mM Tris-HCl (pH 8.0)
DAPI	0.2 µg/ml DAPI in 1 X PBS	1 mg/ml DAPI - 2 µl Make up to 10 ml with 1X PBS.
Proteinase K	5 µg/ml Proteinase K 20 mM Tris and 1 mM Na_2-EDTA pH 7.5	19.2 mg/ml Proteinase K - 2.6 µl Tris - 24.2 mg Na_2-EDTA - 3.7 mg Make up to 10 ml with Milli-Q water. Adjust pH to 7.5.
PBS-T	1X PBS 0.05 % Tween-20	1X PBS - 10 ml Tween-20 - 5 µl
Na_2-EDTA	0.5 M	Na_2-EDTA - 18.6 g Milli-Q water - 100 ml

2.1.7 Cell lines

The cell lines used in this project are listed in the table 2.9.

Table 2.9 Cell lines

Cell line	Species	Cell type	Source
C_2C_{12}	Mouse	Myoblast	ATCC (Yaffe and Saxel, 1977).
Clone 7 (Akirin1 over-expressing stable clone)	Mouse	Myoblasts	Marshall et al., 2008

2.2 Methods

This section describes the basic protocols employed in the thesis.

2.2.1. Mice breeding

Heterozygote and homozygous breeding pairs of Akirin1 knock-out and wild-type mice (C57BL/6 and SV129 mixed strain background) used in this project were obtained from Dr. Kazufumi Matsushita (Osaka University, Japan). Mice were housed at the Nanyang Technological University (NTU) Animal House, Singapore and maintained on standard chow diet at a constant temperature (20°C) under a 12/12 hour artificial light/dark cycle with unlimited access to water. All experiments were performed as per the approved protocols of Institutional Animal Ethics Committee (IACUC), Singapore.

2.2.2. Genotype analysis

Genotype analysis of the Akirin1 transgenic mice was performed according to Ge et al., 2011. A 0.2 x 0.2 cm^2 section of mouse ear tissue was digested in 300 µl of tissue lysis buffer containing 10 mM Tris-HCl (pH 8.0), 100 mM Na_2EDTA, 0.5% SDS and 100 µg/ml Proteinase K for 2 hour at 56°C. The tissue digest was centrifuged at 13,000 rpm at room temperature for 10 minutes. The supernatant was transferred to a new tube and 500 µl of

isopropanol was added followed by 1 ml ice-cold 70% ethanol. The mixture was centrifuged at 13,000 rpm at room temperature for 10 minutes. The supernatant was decanted and DNA pellet was washed with 1 ml of 70% ethanol. After air-drying, the pellet was re-suspended in 100 µl of 10 mM Tris-HCl (pH 8.0) for 5 minutes at 65°C. Semi-quantitative PCR was performed to identify wild type, heterozygous, Akirin1 homozygous knock-out alleles using the oligonucleotides listed in table 2.2. PCR reaction conditions were as follows: 5 minutes at 94°C, 35 amplification cycles (30 seconds at 94°C, 1 minute at 67°C, and 1 minute at 72°C) and 10 minutes at 72^{o}C. PCR products were separated on 1% agarose gel in 1X TAE running buffer.

2.2.3. DNA gel electrophoresis

Agarose gels (0.8-2% depending on the size of the fragments to be separated) were made in 1X TAE buffer. Ethidium bromide was added for visualization of the DNA bands. DNA samples were mixed with 5X DNA loading dye before loading and run in 1X TAE running buffer. DNA molecular markers were run beside the DNA samples. Electrophoresis was carried out at 100 V until the desired separation of bands was obtained. The separated DNA was then visualized under ultraviolet (UV) light using the Gel Doc system (G:BOX, Syngene, Synoptics Ltd., England) and photos were printed.

2.2.4. Isolation of primary myoblasts

Primary myoblasts were cultured from hind-limb muscles using a modified method published by McCroskery et al., 2003. Muscles were minced in PBS and centrifuged at 3000 rpm for 10 minutes to remove PBS. The minced

muscles were digested in 0.2% collagenase type 1A in Dulbecco's Modified Eagle Medium (DMEM; Invitrogen, USA) at 37°C with shaking (70 rpm) for 90 minutes and then centrifuged at 3000 rpm for 10 minutes. The pellet was re-suspended in 12 ml PBS and passed through 100 µm filter (BD falcon 100 µm nylon cell strainers) and then centrifuged at 3000 rpm for 10 min. The pellet was re-suspended in 8 ml of warm primary myoblasts proliferation media containing 20% Fetal Bovine Serum (FBS), 10% Horse Serum (HS), 1% chicken embryo extract (CEE), 100 units/ml penicillin and 100 µg/ml streptomycin in DMEM (Invitrogen, USA), and pre-plated on uncoated 10 cm plates for 3 hours at 37°C and 5% CO_2 to remove fibroblasts. After 3 hours primary myoblasts were transferred to 10% Matrigel (BD Biosciences, USA) coated 10 cm plates and incubated for 12 hours at 37°C and 5% CO_2. Isolated primary myoblasts were later washed with PBS and maintained for subsequent experiments.

2.2.5. Cell culture

The established ATCC mammalian (murine) cell line C_2C_{12} myoblasts were used (Yaffe and Saxel 1977). The cell stocks were stored in C_2C_{12} proliferation media Dulbecco's Modified Eagle Medium (DMEM) (PAA Laboratories, Inc., Pasching, Austria), 10% Fetal Bovine Serum (FBS) (HyClone Laboratories, Inc., Logan, Utah, USA), 1% Penicillin / Streptomycin (P/S) (Gibco, Carlsbad, CA, USA) media with 5% Dimethyl Sulfoxide (DMSO) (Sigma-Aldrich, St. Louis, MO, USA) in liquid nitrogen. The cells were passaged in proliferation media and differentiated in C_2C_{12} low serum differentiation media: DMEM, 2% Horse Serum (HS) (Gibco, Carlsbad, CA, USA), 1% P/S was used to differentiate the myoblasts to myotubes.

2.2.6. Myoblast proliferation assay

Myoblast proliferation was assessed as described according to Thomas et al, 2000. Myoblasts were seeded on 96-well plates at a density of 1,000 cells per well and incubated at 37°C and 5% CO_2. Proliferating myoblasts were subsequently fixed at 24-hour intervals in 100 µl formal saline fixative (10% Formaldehyde, 0.9% NaCl). Proliferation was assessed using the methylene blue photometric end-point assay (Oliver et al., 1989). Briefly the fixative was removed and myoblasts were washed with 1X PBS for two times. Then myoblasts were incubated at room temperature for 30 minutes in 100 µl methylene blue stain (1% methylene blue in 0.01 M sodium tetraborate, pH 8.5). Each well was washed four times with 200 µl of borate buffer to remove excess stain. Following this, 200 µl of 0.1 M HC1: 70% ethanol (1:1) was added and the absorbance of the cells was read on xMark Microplate Absorbance Spectrophotometer (Bio-Rad, USA) reader at 655 nm. The absorbance is directly proportional to final myoblast number.

2.2.7. Myoblast differentiation assay

Primary myoblasts from wild-type and Akirin1 knock-out were seeded in 6-well plates (for protein and RNA) or on Thermanox coverslips (for Hematoxylin and Eosin staining) coated with 10% Matrigel (BD Biosciences) at a density of 25,000 cells/cm² in proliferation medium containing DMEM, 20% FBS, 10% HS, 1% CEE, 100 units/ml penicillin and 100 µg/ml streptomycin at 37°C and 5% CO_2. After an overnight attachment period, myoblasts were induced to differentiate in low serum media containing DMEM, 2% HS, 100 units/ml penicillin and 100 µg/ml streptomycin. Myotubes in 6-well plates were washed twice with 1X PBS and collected in

TRIzol for RNA or RIPA buffer for total protein respectively. Myotubes on the coverslips were fixed at 24-hour intervals in 0.5 ml fixative containing 70% ethanol; formaldehyde; acetic acid (20:2:1) for 30 seconds and washed with 1X PBS three times for Hematoxylin and Eosin (H & E) staining.

2.2.8. Muscle sample collection

Mice were terminated by CO_2 asphyxiation and the muscles were dissected and frozen in liquid nitrogen. Body weights and the weights of individual muscles, including *M tibialis anterior*, *M gastrocnemius*, *M soleus*, *M quadriceps*, heart, masseter and diaphragm were recorded before sample collection.

2.2.9. Protein lysate isolation and quantitation

The myoblasts or myotubes were collected in appropriate volume of RIPA buffer and homogenized by passing through 27G gauge needle at least 20 times. The lysate was incubated for 15 minutes on ice and centrifuged at 12,000 rpm for 15 minutes. Skeletal muscle protein lysates were prepared by homogenizing muscles in RIPA buffer (1 ml buffer for 50 mg muscle tissue) using the Yellowline 1KA DI 25 Base Homogenizer (Fisher Scientific, USA) at 9,500 - 24,000 rpm for 1 minute at each speed keeping on ice. The protein lysate was kept on ice for 15 minutes and then centrifuged at 12,000 rpm for 15 minutes at 4°C. The supernatant was collected and the protein concentration was measured using Bradford's protein assay reagent (Bio-Rad, USA) against BSA standard (Bio-Rad, USA) detected at 595 nm.

2.2.10. Cytoplasmic and nuclear fraction extraction

C_2C_{12} and Clone7 cells were differentiated and collected at respective time-points. The cells were trypsinized and centrifuged at 1,500 rpm for 5 minutes at 37°C following 1X PBS was twice. The cell pellets were stored at -80°C to be processed later or were processed immediately for isolation of cytoplasmic and nuclear extracts as previously described (Ye et al. 1996). Wild-type and Akirin1 knock-out quadriceps muscle samples were homogenized in ice-cold 1X PBS and processed immediately for isolation of cytoplasmic and nuclear extracts as previously described (Ye et al., 1996). To the cell pellet or muscle homogenate, 300 µl of lysis buffer was added, mixed well and incubated on ice for 4 minutes. The tubes were then centrifuged at 10,000 rpm for 1 minute at 4°C. The supernatant was collected as cytoplasmic extract (CE). The pellet in the tubes were washed with 300 µl of wash buffer followed by centrifugation at 10,000 rpm for 1 minute at 4°C. The supernatant was discarded and the pellet was re-suspended in appropriate volume (100 µl for cells; 250 µl for muscles) of extraction buffer. The pellet was pipetted up and down several times in the extraction buffer. The mixture was centrifuged at 14,000 rpm for 5 minutes at 4°C. The supernatant was collected as nuclear extract (NE). The protein concentrations of the nuclear and cytoplasmic extracts were measured by Bradford's assay (Bradford 1976) (Bio-Rad).

2.2.11. SDS-PAGE and western blotting

Equal amount of proteins, usually 20-30 µg, were mixed with 4X protein loading dye (Invitrogen, CA, USA) with β-Mercaptoethanol (βMe) (loading dye:βMe = 3:1, V:V) . The mixed protein samples were boiled at 100°C for 5 min and separated in SDS-PAGE (NuPage 4-12% gradient Bis-Tris pre-cast

polyacrylamide gels, Invitrogen, USA) at 200V (125mA). After electrophoresis, SDS-PAGE gels were transferred to TransBlot (Bio-Rad, USA) nitrocellulose membrane by electroblotting using Xcell II blot module (Invitrogen). The membranes were then stained with Ponceau S (Fluka, Sigma-Aldrich) to determine equal protein loading and transfer efficiency. After de-staining in 1X TBS-T, membranes were blocked overnight with 5% milk in TBS-T at 4°C, or blocked in PVP blocker or BSA blocker for 1 hour at room temperature. Blocking was followed by incubation with specific primary (3 hours for milk and BSA blocker or overnight in PVP blocker) and secondary antibodies (1 hour). Membranes were washed with 1X TBS-T for 5 times (5 minutes each) after each incubation. Primary and secondary antibodies used in this project are listed in table 2.3 and 2.5 respectively. HRP activity was detected using Western Lighting™ Chemiluminescence Reagent Plus (NEL104; PerkinElmer Life Sciences, Waltham, MA, USA). Films (Kodak) were exposed to the membranes and the developed films were analyzed using Quantity One imaging software (Bio-Rad, USA).

2.2.12. RNA extraction and electrophoresis

Total RNA from cells or skeletal muscle tissue was isolated using TRIzol (Invitrogen, CA, USA) according to the manufacturer's protocol. 1 ml of TRIzol was used for 100 mg muscle or 1 million cells. After homogenization, samples were incubated for 5 minutes at room temperature and centrifuged for 10 minutes at 4°C (12,000 rpm). After mixing with chloroform (200 µl for 1 ml TRIzol), samples were vigorously shaken for 15 seconds. Following 3 minutes incubation at room temperature, samples were centrifuged for 15 minutes at 12,000 rpm. The aqueous phase was transferred into fresh tubes

and mixed with isopropanol (500 µl for 1 ml TRIzol) for RNA precipitation. Total RNA was collected by centrifuging (12,000 rpm) for 10 minutes, and the resulting pellet was washed with 75% ethanol and then re-suspended in DEPC-treated H_2O (0.1% diethylpyocarbonate). The re-suspended RNA was incubation at 55°C for 10 minutes aided the solubilisation of RNA. After quantification with NanoDrop® spectrophotometer (ND-1000; NanoDrop Technologies Inc., DE, USA), RNA samples were stored at -80°C. RNA quality was checked by electrophoresis. Equal amount of RNA samples (1 µg), mixed with 2X RNA loading dye, were separated in 1.5% agarose gel (UltraPure™, Invitrogen, USA) in 1X MOPS running buffer with formaldehyde.

2.2.13. cDNA synthesis and quantitative PCR analysis

One µg of RNA was used for cDNA synthesis using iScript™ cDNA Synthesis Kit (Bio-Rad, USA) according to the manufacturer's instruction. RNA samples were mixed with 5X iScript reaction buffer and 1 µ1 of iScript reverse transcriptase (RT). The reaction mixture was incubated for 5 minutes at 25°C, followed by 30 minutes at 42°C and finally for 5 minutes at 85°C. After incubation, synthesized cDNA was stored at -20°C prior to use. Quantitative real time PCR was carried out in triplicates using SsoFast™ EvaGreen supermix and CFX96 Real Time System (Bio-Rad, USA). PCR reaction conditions were as follows: 3 minutes at 98°C and 45 amplification cycles (3 seconds at 98°C, 10 seconds at 60°C, and 10 seconds at 72°C). Gene expression levels were analyzed as fold change using the ΔΔCT (threshold cycle) method, normalized to *cyclophilin* expression. Details about the oligonucleotides used in this project are listed in table 2.1.

2.2.14. Tissue preparation for cryosectioning for histological analysis

Muscle tissue processing was performed according to Ge et al., 2011. For histological analysis, muscles and whole heart were embedded with liquid Optimal Cutting Temperature (OCT) compound and then frozen in isopentane cooled with liquid nitrogen. Transverse sections of 10 µm thick were cut using Rotary Cryostat Microtome (RM2265, Leica) and mounted on slides for further histological analysis.

2.2.15. Hematoxylin and Eosin (H&E) staining of primary cultures

Hematoxylin and Eosin staining of mouse muscle primary cultures was performed according to McFarlane et al., 2008. Wild-type and Akirin1 knock-out primary myoblasts were seeded on 10% Matrigel (BD Biosciences) coated Thermanox coverslips (Thermo Scientific, USA) at a density of 25,000 cells/cm². After overnight incubation at 37°C and 5% CO_2, myoblasts were induced to differentiate in low Serum differentiation medium for 96 hours. Myotubes were subsequently fixed at 24-hour intervals in 70% ethanol formaldehyde: acetic acid (20:2:1) for 30 seconds and washed with 1X PBS three times, and then stained with Hematoxylin solution (Merck Chemicals, Germany) for 3 minutes and rinsed in 0.1% HCl solution for 2 seconds. Myotubes were then washed in Scott's tap water for 5 times (1 minute each), and stained in Eosin solution (Merck Chemicals, Germany) for 3 minutes. After Eosin incubation, slides were dehydrated in 100% ethanol three times (5 minutes each) and mounted with DPX solution (Merck Chemicals, Germany).

2.2.16. Measurement of myotube number, myotube area and fusion index

To assess if Akirin1 knock-out primary myoblasts differentiate differently compared to the wild-type primary myoblasts, the cells were first seeded on Thermanox coverslips (Thermo Scientific, USA) at a density of 25,000 cells/cm². Primary myoblasts were induced to differentiate in DMEM with 2% horse serum and 1% penicillin/streptomycin. At the indicated time points, the cultures were fixed with ethanol:formaldehyde:glacial acetic acid (20:2:1) and stained with Hematoxylin and 1% Eosin. Myotubes containing two, three or more than three myonuclei were considered for measuring the myotube number using the Image-Pro Plus analysis software package (Media Cybernetics, Bethesda, MD, USA). Fusion index was determined by counting the number of nuclei within myotubes over the total number of nuclei (represented as percentage). Myotubes containing equal or more than three myonuclei were considered for measuring the myotubes number and area. The myotubes area was represented as μm^2. Myotube number myotubes area and fusion index were assessed in six random images taken from two coverslips each per genotype.

2.2.17. Hematoxylin and Eosin (H & E) staining of muscle sections

Firstly, 10 µm thick sections were cut at the mid-belly region of *tibialis anterior* muscle and then Hematoxylin and Eosin staining was performed. The sections were stained in Hematoxylin solution for 1 minute and rinsed in tap water until sections were clear. This was followed by rinsing the sections in Scott's tap water for 2 minutes and then rinsed with tap water. The muscle sections were further stained with Eosin solution for 2 minutes and rinsed with tap water until the sections were clear. The sections were serially dehydrated

in 50% ethanol three times, 70% ethanol three times, 90% ethanol for 2 minutes and 100% ethanol for 2 times (2 minutes each). The stained sections were cleared in xylene two times (5 minutes each) and air-dried. The dry sections were mounted using DPX mounting solution and allowed to dry overnight at room temperature. Images were captured using the Leica CTR 6500 microscope, equipped with the Leica DFC 310 FX camera and Image Pro Plus software (Media Cybernetics, Bethesda, MD).

2.2.18. Succinate dehydrogenase (SDH) and α-glycerophosphate dehydrogenase (GPD) staining on *tibialis anterior* sections

SDH and α-GPD activity was measured by a colorimetric assay described by Masuda et al., 2009 with slight modification. In brief, for SDH staining, sections were air-dried for 30 minutes and then incubated in pre-warmed PBS buffer containing 50nM sodium succinate and 0.6 mM Nitro Blue Tetrazolium (NBT) (Sigma N5514) for 30 minutes at 37^{o}C. For a-GPD staining, the sections were incubated in pre-warmed 0.2 M Tris-HCl buffer (pH7.4) containing 9.3 mM rac-glycerol-1-phosphate disodium salt hexahydrate (Sigma G6014) and 0.24 mM NBT for 45 minutes at 37^{o}C after air-drying. The reaction was terminated by thoroughly rinsing the sections with Milli-Q water. After dehydration and clearance by xylene, the sections were mounted by DPX (Sigma). Images were captured using the Leica CTR 6500 microscope, equipped with the Leica DFC 310 FX camera and Image Pro Plus software (Media Cybernetics, Bethesda, MD). The enzyme activities were measured for the mean grey value by Image J software (National Institute of Health, USA) and expressed as the mean optical density (OD) of the entire *tibialis anterior* section.

2.2.19. Fiber typing of *tibialis anterior* sections

10 µm thick *tibialis anterior* sections were cut and blocked with blocking mixture made of 0.5% Triton X-100, 0.2% BSA and 10% normal sheep serum (NSS) in 1X PBS for one hour at room temperature with shaking. Further, the sections were treated with appropriate primary myosin heavy chain type antibody in a diluent made of 0.2% BSA, 5% normal sheep serum and 0.1% PBS-Tween 20 at 4^{o}C overnight with shaking. The primary antibody dilution used for the various myosin heavy chain types is listed in table 2.4. Next day, the sections were washed with 1X PBS three times for five minutes each. The primary antibody staining was fixed by treating the sections with 10% buffered formalin for 5 minutes and then washed three times with 1X PBS for five minutes each. Further, sections were treated with secondary antibody diluent containing biotinylated sheep anti-mouse IgG antibody in 1:200 dilution along with 0.2% BSA, 5% normal sheep serum in 0.1%PBS-Tween 20 for one hour at room temperature with shaking followed by washing thrice with 1X PBS for five minutes each. Tertiary antibody streptavidin anti-mouse IgG Alexa Fluor 488 (AF 488) was used at 1:400 dilution along with 0.2% BSA and 0.1% PBS-Tween 20 for one hour at room temperature in dark. Then the sections were washed with 1X PBS thrice for five minutes each. Myonuclei were stained with DAPI made in 1X PBS at 1:10,000 dilution for five minutes and then rinsed with 1X PBS and air-dried. The dry sections were mounted using ProLong Gold Antifade solution (Invitrogen) and allowed to dry overnight at room temperature. Images were captured using the Leica CTR 6500 microscope, equipped with the Leica DFC 310 FX camera and Image Pro Plus software (Media Cybernetics, Bethesda, MD).

2.2.20. Transformation of competent cells and isolation of single bacterial colonies

Transformation of DH5α competent cells was achieved by addition of 5-10 ng of plasmid DNA to 50 µl of the competent cells. The DNA competent cell mixture was incubated on ice for 20 minutes, followed by a heat shock at 42°C for 48 seconds, then further 2 minute incubation on ice. Following this, 950 µl of room temperature LB broth (without antibiotic) was added to the transformed cells and incubated at 37°C for 90 minutes with gentle shaking (~150 rpm). The culture was spread over LB agar plates, which contained the appropriate antibiotic, and grown for 16-24 hours at 37°C. Single colonies were seeded in 4 ml (for miniprep) or 100 ml (for maxiprep) of LB broth with the appropriate antibiotic. The cultures were grown at 37°C with shaking (~250 rpm) for 12-18 hours.

2.2.21. Plasmid isolation

Plasmid DNA used in this study was isolated using two procedures explained below.

2.2.21.1. Miniprep plasmid isolation

Plasmid DNA was extracted and purified using the QIAprep spin miniprep system (Qiagen), according to the manufacturer's protocol. Bacteria were harvested by centrifugation at 3500 rpm for 5 minutes in a 1.5 ml eppendorf tube. The bacterial pellet was re-suspended in 250 µl of Buffer P1 followed by 250 µl of Buffer P2, the sample was then mixed by inverting four-six times and allowed to incubate at room temperature for no more than 5 minutes. After incubation 350 µl of Buffer P3 was added. After the addition of Buffer

P3, the tube was again inverted four-six times to mix. The extract was centrifuged (20,000 x g for 10 minutes) and the supernatant transferred to a QIAprep spin column. The spin column was centrifuged at 20,000 x g for 1 minute, washed with 0.75 ml Buffer PE and centrifuged twice to remove any traces of Buffer PE. Plasmid DNA was eluted in 50 µl Buffer EB by centrifugation (20,000 x g for 1 minute).

2.2.21.2. Maxiprep plasmid isolation

Large-scale purification of plasmid DNA was performed using the Qiagen Plasmid Maxi kit (Qiagen) as per the protocol. Firstly, 250 ml of overnight culture was harvested by centrifugation at 6,000 x g for 15 minutes. The pellet was then re-suspended in 10 ml of buffer P1, mixed with 10 ml of Buffer P2 and incubated on ice for 20 minutes on addition of Buffer P3. The mix was then centrifuged for 30 minutes at 20,000 x g followed by a second spin at 20,000 x g for 15 minutes to remove any contaminants. The plasmid DNA containing supernatant was passed through a pre-equilibrated Qiagen-column by gravity flow. Plasmid DNA bound to the column was washed twice with Qiagen Buffer QC and eluted with Qiagen elution buffer. The eluted DNA was precipitated with 0.7 volumes of isopropanol and pelleted by centrifugation at 20,000 x g for 10 minutes. The pellet was washed twice with 70% ethanol, dried and re-suspended in an appropriate volume of TE buffer.

2.2.22. Transfection and Luciferase assay

C_2C_{12} myoblasts were plated at a density of 15,000 cells/cm² in 6 well plates. Following overnight attachment, the C_2C_{12} myoblasts were transfected with either pGL4.1 or rat MuRF1 promoter construct along with pcDNA3.1 or

pcDNA3.1-Akirin1 expression vector together with the control Renilla Luciferase vector pRL-TK using Lipofectamine 2000 (Invitrogen) as per the manufacturer's guidelines. Following overnight transfection, the medium was replaced with fresh differentiation medium and the cells were incubated and collected at respective time points. The cells were lysed using 1X passive lysis buffer (Promega, USA). Luciferase assays were performed using the Dual Luciferase Assay System, as per the manufacturer's protocol (Promega). Relative luciferase activity in each of the extracted protein samples was measured in triplicate using the Fluoroskan Ascent Microplate Fluorometer and Luminometer (Thermo Fisher Scientific Inc.,).

2.2.23. Electrophoretic Mobility Shift Assay (EMSA)

Oligonucleotides which contain the CREB-1 consensus binding site 5'-TGACATTA-3' on rat MuRF1 promoter i.e., forward oligonucleotide 5'-CGTGGTGGTGACTGGGGGTGTGTAGTGACATTATTTTGT-3' and reverse oligonucleotide 5'-ACAAAATAATGTCACTACACACCCCCAGTC ACCACCACG-3' were hybridized and labeled at the 3' end with Biotin Tetraethyleneglycol (TEG) (Sigma-Aldrich, St. Louis, MO, USA). The EMSA was performed using the Lightsift Chemiluminescent EMSA kit (Thermo Scientific Pierce Biotechnology, Rockford, IL, USA). Nuclear extracts obtained from wild-type and Akirin1 knock-out *quadriceps* muscle and Clone 7 cells were incubated with the biotin labeled probe (working concentration 1nM) in final volume of 20 µl containing binding buffer (100 mM Tris, 500 mM KC1, 10 mM DTT, pH 7.5), glycerol, $MgC1_2$, poly (dl-dC) and NP-40. After 20 minutes of incubation at room temperature, samples were subjected to electrophoresis on a 5% acrylamide gel containing Tris-

Borate-EDTA (TBE) (Promega Corporation, Madison, W1, USA) at 80V at 4ºC. The samples were then transferred to a nylon membrane at 200 mA for 2 hours at 4ºC and UV-crosslinked after transfer. The membrane was probed with stabilized Streptavidin-Horseradish Peroxidase conjugate and developed using the Lightshift Chemiluminescent EMSA kit (Thermo Scientific Pierce Biotechnology, Rockford, 1L, USA).

To confirm the presence of CREB-1 protein in the shifted complex, nuclear extracts from cells and *quadriceps* muscle were pre-incubated for 20 minutes at room temperature with 4 µg of CREB-1 (sc-240) antibody before incubation with the labeled probe for another 20 minutes at room temperature. The samples were then subjected to EMSA as mentioned above.

2.2.24. Genomic and mitochondrial DNA isolation from differentiating primary myoblasts

Primary myoblasts were seeded in 6-well plates and differentiated in low serum differentiation media. Myotubes were collected at 24-hour intervals in 100 µl of DNA extraction buffer per well. Then the cells were digested with 10mg/ml Proteinase K for 1.5 hours at 56^{o}C with shaking. The volume of the digested sample was made to 500 µl using DNA extraction buffer. From this mixture, 250 µl was taken for DNA extraction by phenol-chloroform method. One volume of Phenol:Chloroform:Isoamyl alcohol (25:24:1) (Invitrogen, USA) was added to the digested mixture and shaken well followed by centrifuging at 14,000 rpm for 5 minutes. The top aqueous phase containing the DNA was collected in a new tube and precipitated by adding 2 volumes of 100% ethanol. To this, 1/10 volume of 3 M sodium acetate (pH 5) was added and centrifuged at 14,000 rpm for 10 minutes. The DNA pellet was washed

with 150 µl of 70% ethanol and then air-dried. The DNA pellet was re-suspended in 50 µl of 10 mM Tris–HCl (pH 8) and the DNA concentration was checked using NanoDrop® spectrophotometer (ND-1000; NanoDrop Technologies Inc., DE, USA).

2.2.25. Mitochondrial DNA (mtDNA) copy number per nuclear DNA (nuDNA) ratio quantification by qPCR

Relative copy number of mitochondrial DNA (mtDNA) per nuclear DNA (nuDNA) ratio was measured using a protocol described by Chen et al., 2010. The set of primers for mtDNA, forward primer: 5'-CCTATCACCCT TGCCATCAT-3'; reverse primer: forward primer: 5'-CCTATCACCCT TGCCATCAT-3'; reverse primer: 5'GAGGCTGTTGCTTGTGTGAC-3' and for nuDNA, forward primer: 5'-ATGGAAAGCCTGCCATCATG-3'; reverse primer: 5'-TCCTTGTTGTTCAGCATCAC-3' were used. Quantification of the relative ratio of mtDNA per nuDNA was analyzed using the threshold cycle ΔΔCT method.

2.2.26. cDNA synthesis and quantitative real time PCR analysis of mature miR-1

One µg of RNA was used for cDNA synthesis using Taqman® MicroRNA Reverse Transcription Kit (Applied Biosystems®, USA) according to the manufacturer's instruction. Quantitative real time PCR was carried out in duplicates using Taqman® PCR Kit protocol as per manufacturer's instruction in CFX96 Real Time System (Bio-Rad, USA). PCR reaction conditions were as follows: 2 minutes at 50°C, 10 minutes at 95^{o}C and 40 amplification cycles (15 seconds at 95°C and 1 minute at 60°C). Gene expression levels were

analyzed as fold change using the ΔΔCT (threshold cycle) method, normalized to *U6* expression. Details about the oligonucleotides used in this project are listed in table 2.1.

2.2.27. Statistical analysis

Statistical analysis was performed using one–way ANOVA, two-tailed Student's t-test Results were considered significant at $p<0.05$ (*), $p<0.01$ (**), or $p<0.001$ (***). Results were expressed as mean ± SE of 3 or 4 independent experiments. Non-parametric Mann-Whitney U test was used to calculate the level of significance for ± SE n=2 experiments and the results were considered significant at $p<0.05$ (*), $p<0.01$ (**), or $p<0.001$ (***)

CHAPTER 3

ROLE OF AKIRIN1 IN MYOGENESIS

3. ROLE OF AKIRIN1 IN MYOGENESIS

This chapter explains the results that help us in understanding the role of Akirin1 during myogenesis. The materials and methods used in this chapter are discussed in chapter 2 of this thesis.

RESULTS

3.1 Identification of Akirin1 knock-out mice by genotyping and confirming the absence of Akirin1 in these mice.

In this study, Akirin1 knock-out mice were used as the animal model to understand the in-vivo function of Akirin1. Akirin1 knock-out mice was generated by deleting exon 1 of Akirin1 gene in C57BL6J/SV129 mouse embryos by *loxP-cre* system (Goto et al., 2008). C57BL6J/SV129 (wild-type) mice were used as controls in this study. Mice were bred and genomic DNA was isolated from the ear tissue. To identify the wild-type and Akirin1 knock-out pups, semi-quantitative PCR was performed with specific primers (Table 2.2). Wild-type mice were identified by an amplicon band of 413 base pairs while Akirin1 knock-out mice were identified by an amplicon band of 650 base pairs (Figure 3.1A).

To confirm the absence of Akirin1 gene in Akirin1 knock-out mice, real time-quantitative PCR was performed on wild-type and Akirin1 knock-out *quadriceps* RNA using Akirin1 specific primers (Table 2.1). The *Akirin1* Ct values were normalised to *cyclophilin* Ct values. This result clearly indicated that Akirin1 gene is indeed significantly down-regulated in Akirin1 knock-out muscle compared to the wild-type muscle (Figure 3.1B).

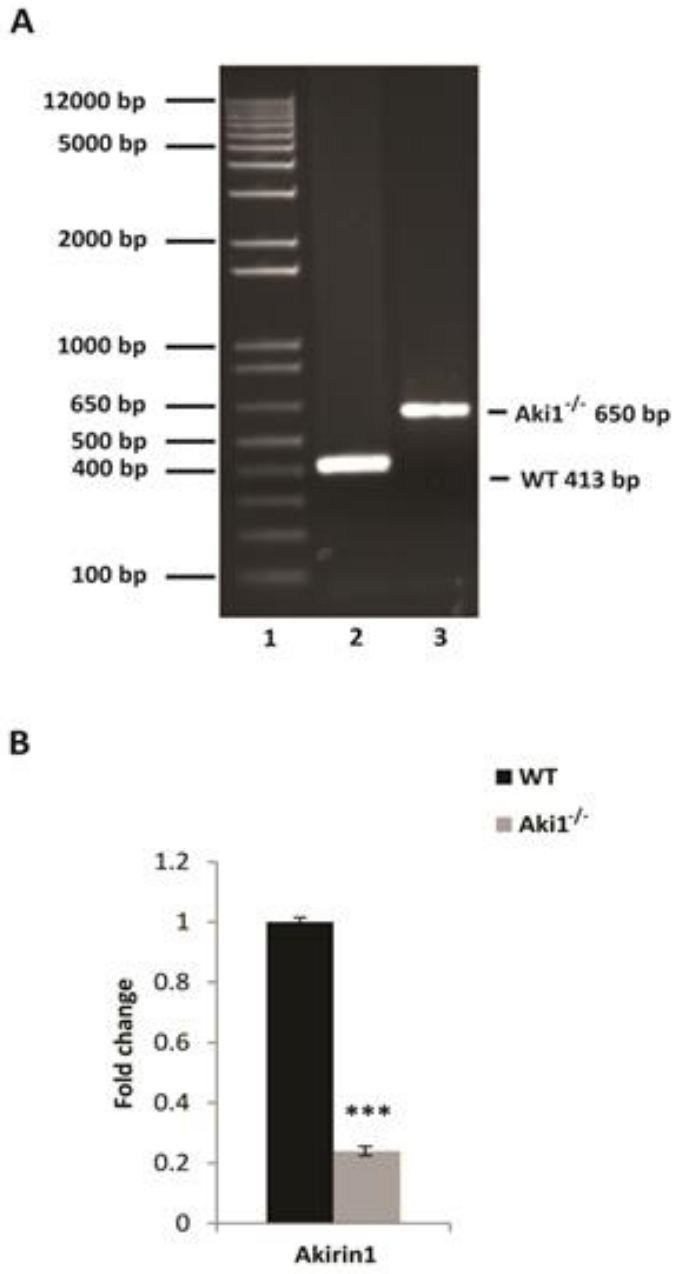

Figure 3.1 Identification of Akirin1 knock-out mice by genotyping and confirming the absence of Akirin1 in these mice. (A) Agarose gel electrophoresis was performed on the PCR amplification products from Akirin1 knock-out and wild-type ear explants. 1 kb plus ladder was loaded as reference (Lane 1). Wild-type allele was identified by the amplicon product size at 413 base pairs (lane 2). Akirin1 knock-out allele was identified by the amplicon product size at 650 base pairs (lane 3). (B) Confirmation of absence of Akirin1 in Akirin1 knock-out muscles. The mRNA expression for *Akirin1* was determined in *quadriceps* muscle obtained from Akirin1 knock-out and wild-type mice. The values are mean ± S.E. of four different animals. ***$p<0.001$ denotes significant fold change difference in Akirin1 mRNA expression relative to the wild-type.

3.2 Absence of Akirin1 leads to reduced proliferation of primary myoblasts.

Marshall et al., showed that over-expression of Akirin1 in C_2C_{12} myoblasts led to increased proliferation compared to the control C_2C_{12} myoblasts (Marshall et al., 2008). So, we wanted to see if the rate of proliferation was affected in the absence of Akirin1 in skeletal muscle. To investigate this, methylene blue photometric end-point assay was performed on proliferating Akirin1 knock-out and wild-type primary myoblasts. Methylene blue stains the myoblasts in the culture dish and the optical density obtained at 655nm will be proportional to the number of myoblasts in the culture dish.

The results revealed that Akirin1 knock-out primary myoblasts cultures showed significantly reduced number of primary myoblasts at 24, 36, 48 hour of proliferation compared to that of the wild-type primary myoblasts (Figure 3.2A).

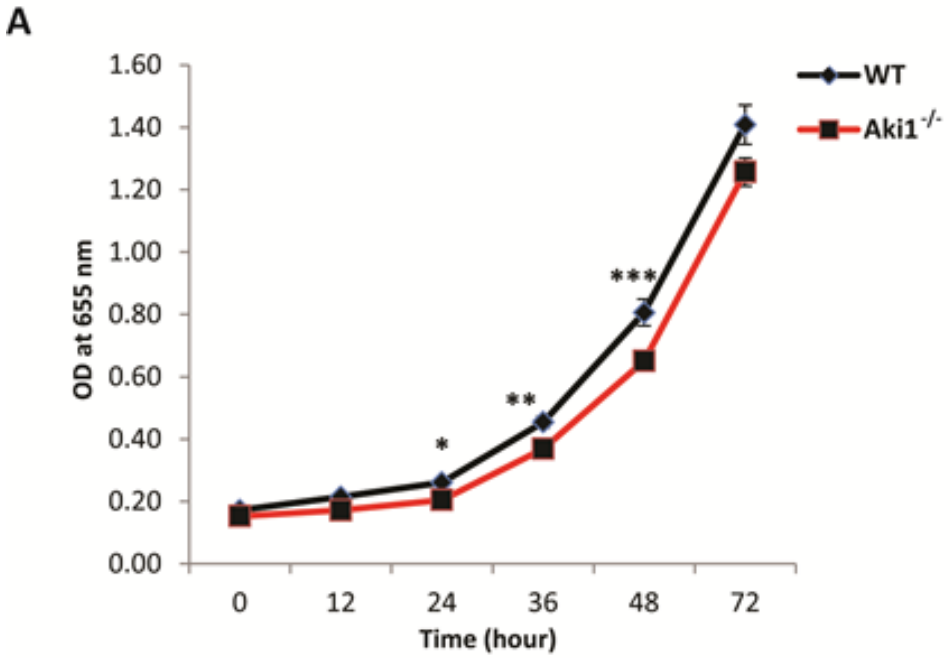

Figure 3.2 Absence of Akirin1 leads to reduced proliferation of primary myoblasts. (A) Akirin1 knock-out and wild-type primary myoblasts were allowed to proliferate and fixed at the indicated time point and methylene blue photometric end-point assay was performed (*$p<0.05$, **$p<0.01$ and ***$p<0.001$) (n=4, where n is the number of primary myoblast culture isolations done and for each primary myoblast culture isolation four mice per genotype were used).

3.3 Lack of Akirin1 alters the levels of cell cycle regulators during proliferation.

As Akirin1 knock-out primary myoblasts proliferated slower than the wild-type, we analyzed the protein level of an important cyclin–dependent kinase inhibitor (CKI), p21 also known as WAF1/CDK inhibitor-1. p21 binds and inhibits the activity of cyclin-cdk complexes thus inhibiting G1-S phase transition (Gartel et al., 2005). Akirin1 knock-out and wild-type primary myoblasts were allowed to proliferate and cells were collected at 24-hour intervals. Protein lysates were subjected to western blotting with anti-p21 antibody. The results showed that proliferating Akirin1 knock-out primary myoblasts have significantly higher level of p21 protein compared to the wild-type primary myoblasts (Figure 3.3A and B).

Next, we wanted to investigate the levels of various cell cycle regulators that play important roles in different stages of cell cycle progression. Cyclins and cyclin dependent kinases (Cdk) are the important regulators of cell cycle checkpoint progression. Proliferating Akirin1 knock-out and wild-type primary myoblast protein lysates were subjected to western blotting with anti-cyclin D1, anti-cyclin E and anti-cdk4 antibodies. Proliferating Akirin1 knock-out primary myoblasts showed significantly higher protein levels of cyclin E, cyclin D1 compared to the wild-type primary myoblasts (Figure 3.3A, C and D). However, cdk4 levels were not significantly up-regulated (Figure 3.3A and E).

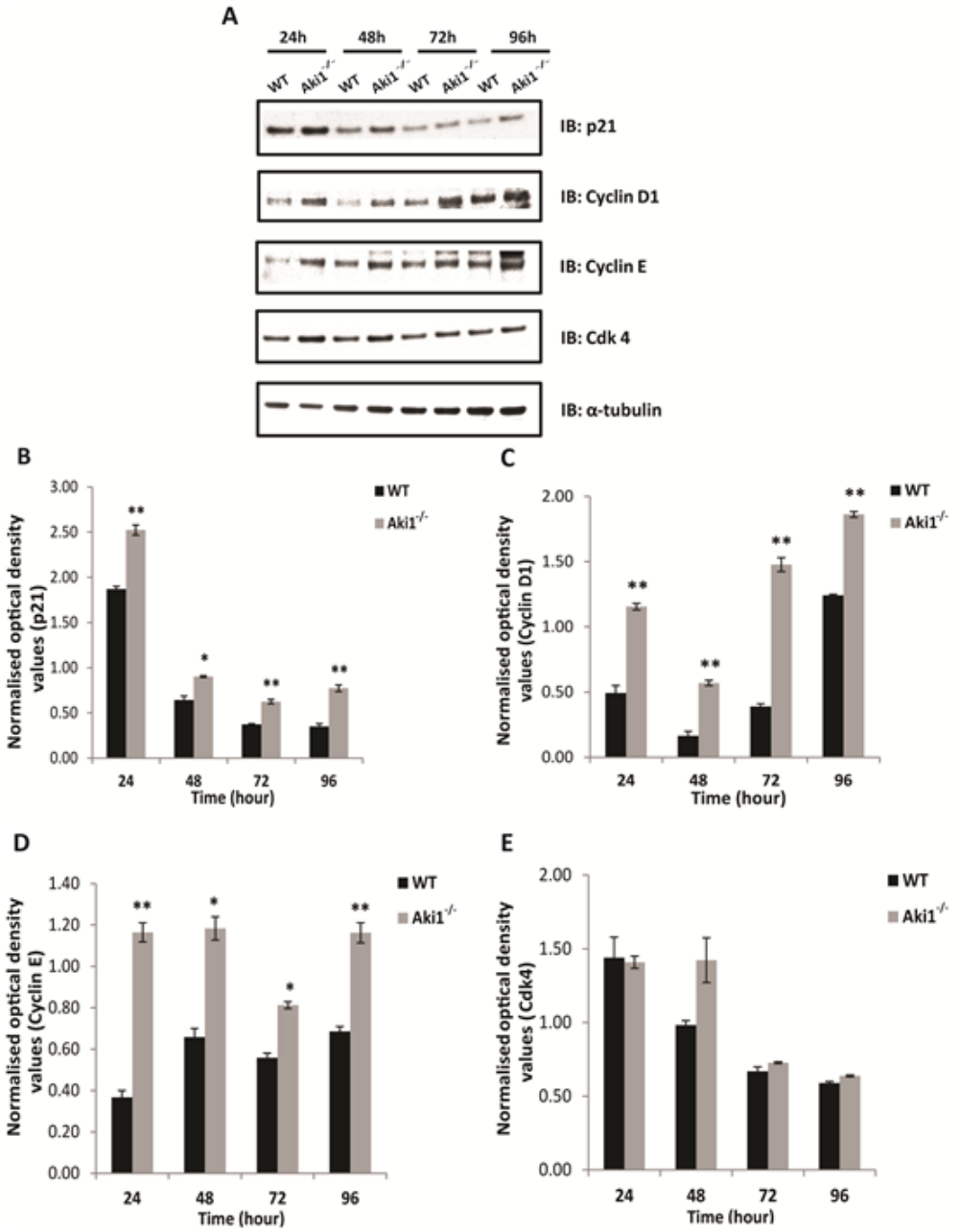

Figure 3.3 Lack of Akirin1 alters the levels of cell cycle regulators during proliferation. Western blotting analysis was performed on Akirin1 knock-out and wild-type proliferating primary myoblasts protein lysates. (A) A representative immunoblot showing protein level of p21, cyclin D1, cyclin E and Cdk4. α-tubulin was used as the internal control for equal protein loading on the gel. (B), (C), (D) and (E) Corresponding densitometry graph of p21, cyclin D1, cyclin E and Cdk4 in Akirin1 knock-out and wild-type primary myoblasts during proliferation. Level of significance was calculated by non-parametric Mann-Whitney U test (*$p<0.05$ and **$p<0.01$) ($n=2$, where n is the number of primary myoblast culture isolations done and for each primary myoblast culture isolation four mice per genotype were used).

3.4 Proliferating Akirin1 knock-out primary myoblasts have increased levels of Serum response factor (SRF) protein.

Serum response factor (SRF) is a MADS box containing transcription factor that binds to serum response element (SRE) on the promoters of target genes and stimulates their transcription. It has been shown that SRF is indispensable for myoblast proliferation (Soulez et al., 1996). Therefore, protein lysates from Akirin1 knock-out and wild-type proliferating primary myotubes were used to perform western blotting with anti-SRF antibody. The results showed that Akirin1 knock-out primary myoblasts showed significantly increased levels of SRF protein when compared to wild-type myoblasts at 24, 48, 72 and 96 hours of proliferation [Figure 3.4A(i) and A(ii)].

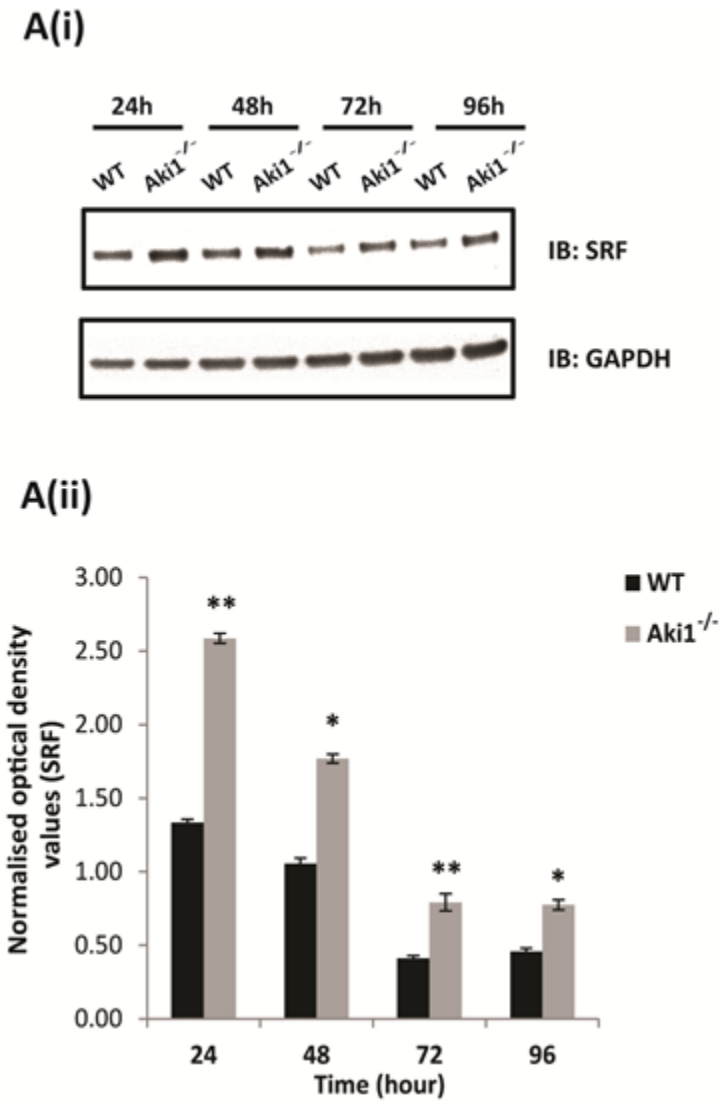

Figure 3.4 Proliferating Akirin1 knock-out primary myoblasts have increased levels of Serum response factor (SRF) protein. Western blotting analysis was performed on Akirin1 knock-out and wild-type primary myoblasts protein lysates. A(i) A representative immunoblot showing protein level of SRF in proliferating Akirin1 knock-out and wild-type primary myoblasts. GAPDH was used as the internal control for equal protein loading on the gel. A(ii) Corresponding densitometry graph of SRF showing significant increase in the protein content in Akirin1 knock-out primary myoblasts at 24, 48, 72 hours of proliferation. Level of significance was calculated by non-parametric Mann-Whitney U test (*$p<0.05$ and **$p<0.01$) (n=2, where n is the number of primary myoblast culture isolations done and for each primary myoblast culture isolation four mice per genotype were used).

3.5 Akirin1 knock-out primary myoblasts show increased myoblast fusion.

Previous results have shown that over-expression of Akirin1 in C_2C_{12} myoblasts led to enhanced differentiation compared to the control C_2C_{12} myoblasts (Marshall et al., 2008). So, we wanted to see if the rate of differentiation was affected in the absence of Akirin1 in skeletal muscle. To investigate this, Akirin1 knock-out and wild-type primary myoblasts were allowed to differentiate in low serum media and collected at 24-hour intervals and stained with hematoxylin and eosin. Akirin1 knock-out primary culture showed increased myoblast fusion and formed highly branched and elongated myotubes especially at 48 and 72 hours of differentiation compared to the wild-type primary culture (Figure 3.5A).

To further investigate if Akirin1 knock-out primary myoblasts showed earlier fusion, we estimated the fusion index in differentiating Akirin1 knock-out and wild-type primary culture. Fusion index reflects the extent of fusion of myoblasts with each other to form myotubes. This index is estimated by the ratio of number of nuclei inside the myotubes to total number of myonuclei. Akirin1 knock-out primary cultures showed significantly increased fusion index at 24, 48 and 72 hours of differentiation compared to the wild-type primary cultures (Figure 3.5B). We also investigated the number of myotubes formed during differentiation in Akirin1 knock-out and wild-type primary cultures. Akirin1 knock-out primary culture formed significantly reduced number of myotubes at 48 and 72 hours of differentiation compared to the wild-type primary culture (Figure 3.5C). The area of the myotubes formed at each time point were calculated using ImagePro software and the frequency

distribution of the myotubes formed showed that Akirin1 knock-out primary cultures formed bigger myotubes compared to the wild-type at 24 hours of differentiation (Figure 3.5D). However at 72 hours of differentiation, no significant difference in myotubes area between Akirin1 knock-out and wild-type primary cultures was observed (Figure 3.5E).

These results together suggest that Akirin1 knock-out primary myoblasts have the tendency to fuse early compared to the wild-type primary myoblasts to formed less myotubes.

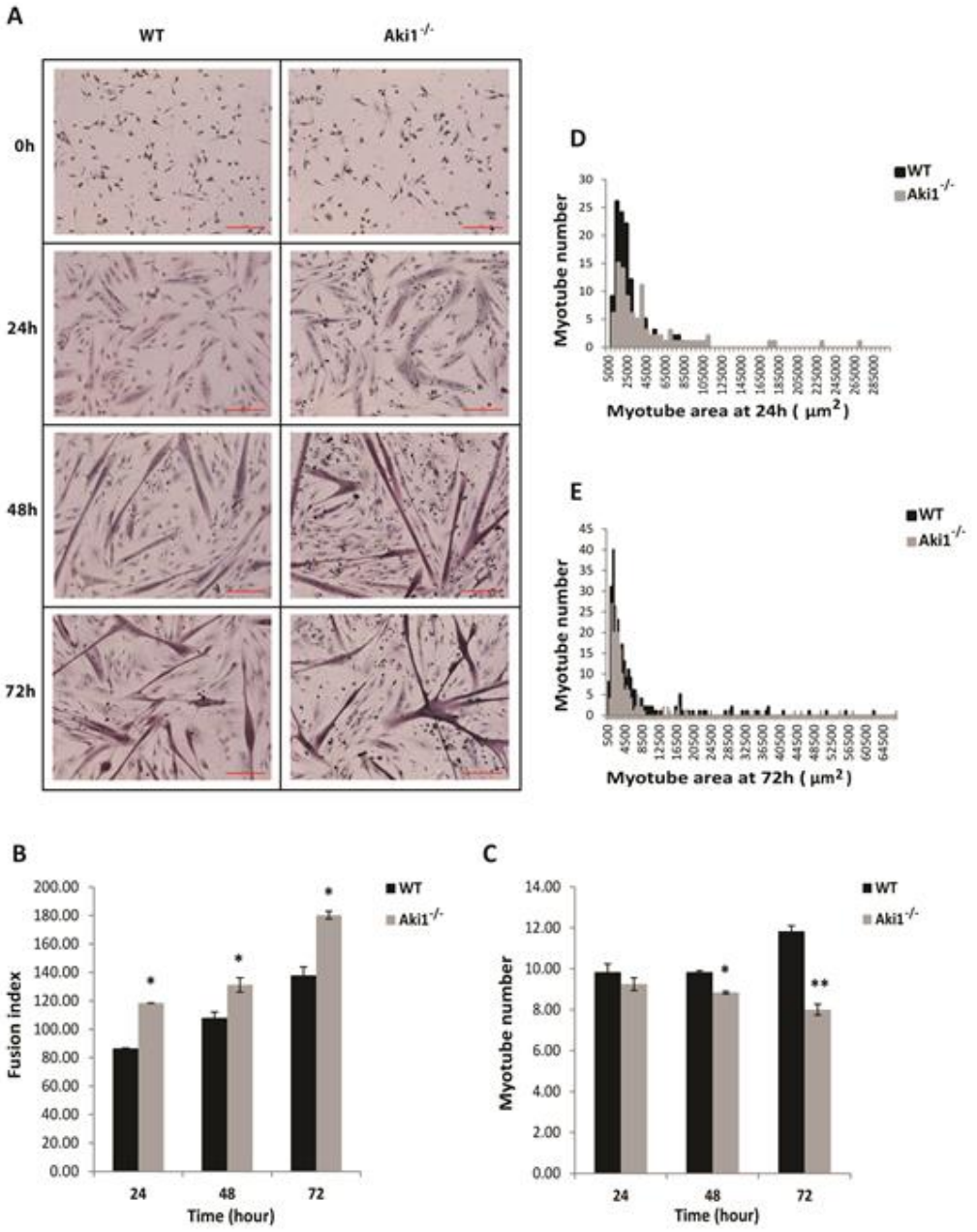

Figure 3.5 Akirin1 knock-out primary myoblasts show increased myoblast fusion. Akirin1 knock-out and wild-type primary myoblasts were allowed to differentiate in low serum media. (A) The cells were fixed and stained with hematoxylin and eosin and images were taken using Leica upright bright field microscope under 10X magnification. Scale bar of the representative images represents 500 µm. (B) and (C) Graphs showing fusion index and myotube number respectively (*$p<0.05$ and **$p<0.01$) (n=3, where n is the number of times the differentiation assay was performed and for each differentiation assay four mice per genotype were used). (D) and (E) Frequency distribution graphs of area of myotubes formed by Akirin1 knock-out and wild-type primary cultures during 24 hour and 72 hour of differentiation.

Figure 3.6 Akirin1 knock-out primary myotubes show increased p21 levels while the levels of other myogenic regulators were unchanged. Western blotting analysis was performed on Akirin1 knock-out and wild-type primary myotube protein lysates. A(i) A representative immunoblot showing protein levels of myogenic regulators like MyoD, p21, myogenin and MyHC. α-tubulin was used as the internal loading control. A(ii), A(iii), A(iv) and A(v) Corresponding densitometry graphs of MyoD, p21, myogenin and MyHC respectively. Level of significance was calculated by non-parametric Mann-Whitney U test (*$p<0.05$, **$p<0.01$ and $p<0.001$) (n=2, where n is the number of primary myoblast culture isolations done and for each primary myoblast culture isolation four mice per genotype were used).

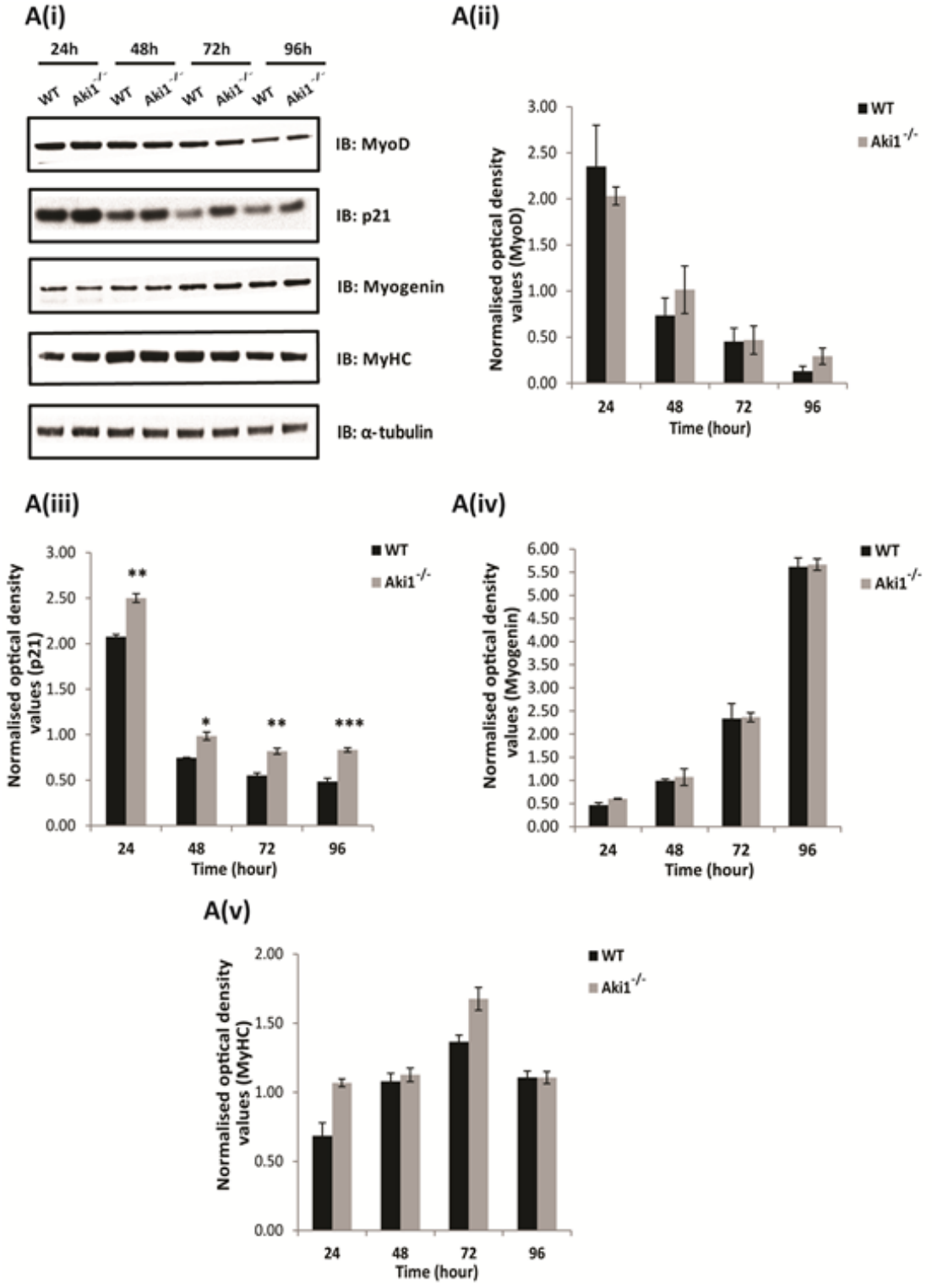
A(i)
24h
48h
72h
96h
WT
Aki1-/-
IB: MyoD
IB: p21
IB: Myogenin
IB: MyHC
IB: α-tubulin
A(ii)
Normalised optical density values (MyoD)
Time (hour)
WT
Aki1-/-
A(iii)
Normalised optical density values (p21)
Time (hour)
A(iv)
Normalised optical density values (Myogenin)
Time (hour)
A(v)
Normalised optical density values (MyHC)
Time (hour)

3.6 Akirin1 knock-out primary myotubes show increased p21 levels while the levels of other myogenic regulators were unchanged.

The process of myogenic differentiation is profoundly affected by important myogenic regulators like MyoD, p21 (WAF1/CDK inhibitor-1), Myogenin and MyHC. First of all, induction of MyoD expression leads the myoblasts into differentiation program. Later, p21 expression inhibits the cell cycle progression leading to withdrawal of myoblasts from cell cycle. Followed by p21 is myogenin, an important protein responsible for the fusion of myoblasts with each other to form myotubes is expressed. Lastly, MyHC is expressed leading to the maturation of myotubes.

Protein lysates of differentiating primary myotubes were subjected to immunoblotting with anti-p21 antibody. Akirin1 knock-out primary myotubes showed significantly increased levels of p21 protein at 24, 48,72 and 96 hours of differentiation compared to the wild-type primary myotubes [Figure 3.6A(i) and A(iii)].

The western blotting for MyoD, myogenin and MyHC in Akirin1 knock-out and wild-type primary myotubes were performed with anti-MyoD, anti-myogenin and anti-MyHC antibodies. The results showed no significant difference in the protein levels of MyoD, myogenin and MyHC between Akirin1 knock-out and wild-type primary myotubes during 24, 48,72 and 96 hours of differentiation [Figure 3.6A(i), A(ii), A(iv) and A(v)]. These results together suggest that the earlier fusion of myoblasts may be due to increased p21 protein in Akirin1 knock-out primary myotubes compared to the wild-type myotubes.

3.7 Lack of Akirin1 leads to increased levels of Serum Response Factor (SRF) protein during differentiation.

As our previous results showed that Akirin1 knock-out primary myoblasts showed increased myoblast fusion, we investigated the level of SRF during myogenic differentiation. It has been shown that SRF is necessary for myoblast fusion and differentiation into myotubes in C_2C_{12} myoblasts (Soulez et al., 1996).

Akirin1 knock-out and wild-type differentiating primary myotubes protein lysates were subjected to western blotting with anti-SRF antibody. Similar to the *quadriceps* muscle results, protein levels of SRF were elevated in cell lysates of differentiating primary myotubes derived from Akirin1 knock-out mice compared to the wild-type [Figure 3.7A(i) and A(ii)].

Further, *SRF* mRNA levels were quantified by real time-qPCR in wild-type and Akirin1 knock-out differentiating primary myotubes and normalised to *cyclophilin* Ct values. The results obtained showed no significant change in the mRNA level of *SRF* gene in Akirin1 knock-out primary myotubes compared to the wild-type primary myotubes during 24, 48, 72 and 96 hours of differentiation (Figure 3.7B). These results together suggest a post-transcriptional role of Akirin1 in regulating SRF levels during myoblast differentiation.

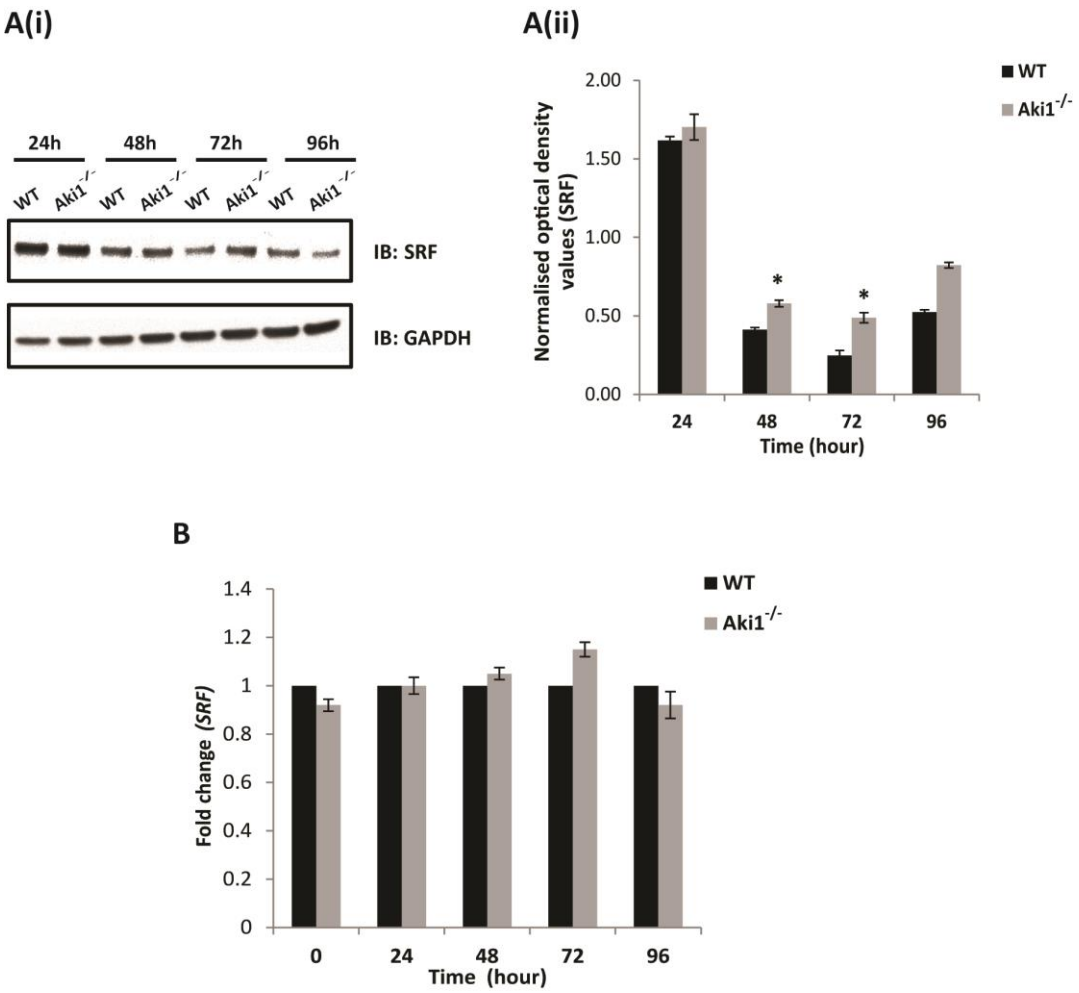

Figure 3.7 Lack of Akirin1 leads to increased levels of Serum Response Factor (SRF) protein during differentiation. Western blotting analysis was performed on protein lysates of Akirin1 knock-out and wild-type primary myotubes at 24, 48, 72 and 96 hours of differentiation. A(i) A representative immunoblot showing the protein level of SRF. GAPDH was used as the internal control for equal protein loading on the gel. A(ii) A graph showing corresponding densitometry analysis of SRF protein levels. Level of significance was calculated by non-parametric Mann-Whitney U test (*$p<0.05$, $p<0.001$) (n=2, where n is the number of primary myoblast culture isolations done and for each primary myoblast culture isolation four mice per genotype were used). (B) A graph showing the fold change mRNA expression of *SRF* in differentiating Akirin1 knock-out and wild-type primary myotubes (n=2, where n is the number of primary myoblast culture isolations done and for each primary myoblast culture isolation four mice per genotype were used).

3.8 Lack of Akirin1 leads to lower MuRF1 levels in differentiating primary myotubes.

Another important protein that is shown to be important for the process of myogenic differentiation is MuRF1 (Spencer et al., 2000). Also, our results in section 4.6 showed that absence of Akirin1 in fully differentiated skeletal muscle like *quadriceps* lead to reduced MuRF1 levels. Therefore, we wanted to check the levels of MuRF1 during differentiation. For this, protein lysates from Akirin1 knock-out and wild-type differentiating primary myotubes were subjected to western blotting with anti-MuRF1 antibody. Consistent with the quadriceps muscle results, Akirin1 knock-out myotubes also showed lower protein levels of MuRF1 compared to the wild-type myotubes during 24, 48, 72 and 96 hours of differentiation [Figure 3.8A(i) and A(ii)]. However, Akirin1 knock-out myotubes did not indicate any significant difference in other ubiquitin ligases like atrogin-1 when compared to the wild-type myotubes during 24, 48, 72 and 96 hours of differentiation [Figure 3.8A(i) and A(iii)].

As *MuRF1* mRNA level was down-regulated in Akirin1 knock-out *quadriceps* muscle, we investigated if *MuRF1* mRNA level was also down-regulated in Akirin1 knock-out primary myotubes using real time-qPCR. Consistent with the reduced MuRF1 protein levels, Akirin1 knock-out primary myotubes showed significantly lower levels of *MuRF1* mRNA levels compared to the wild-type primary myotubes at 48, 72 and 96 hours of differentiation (Figure 3.8B). These results together indicate that Akirin1 regulates transcription of MuRF1 in primary myotubes.

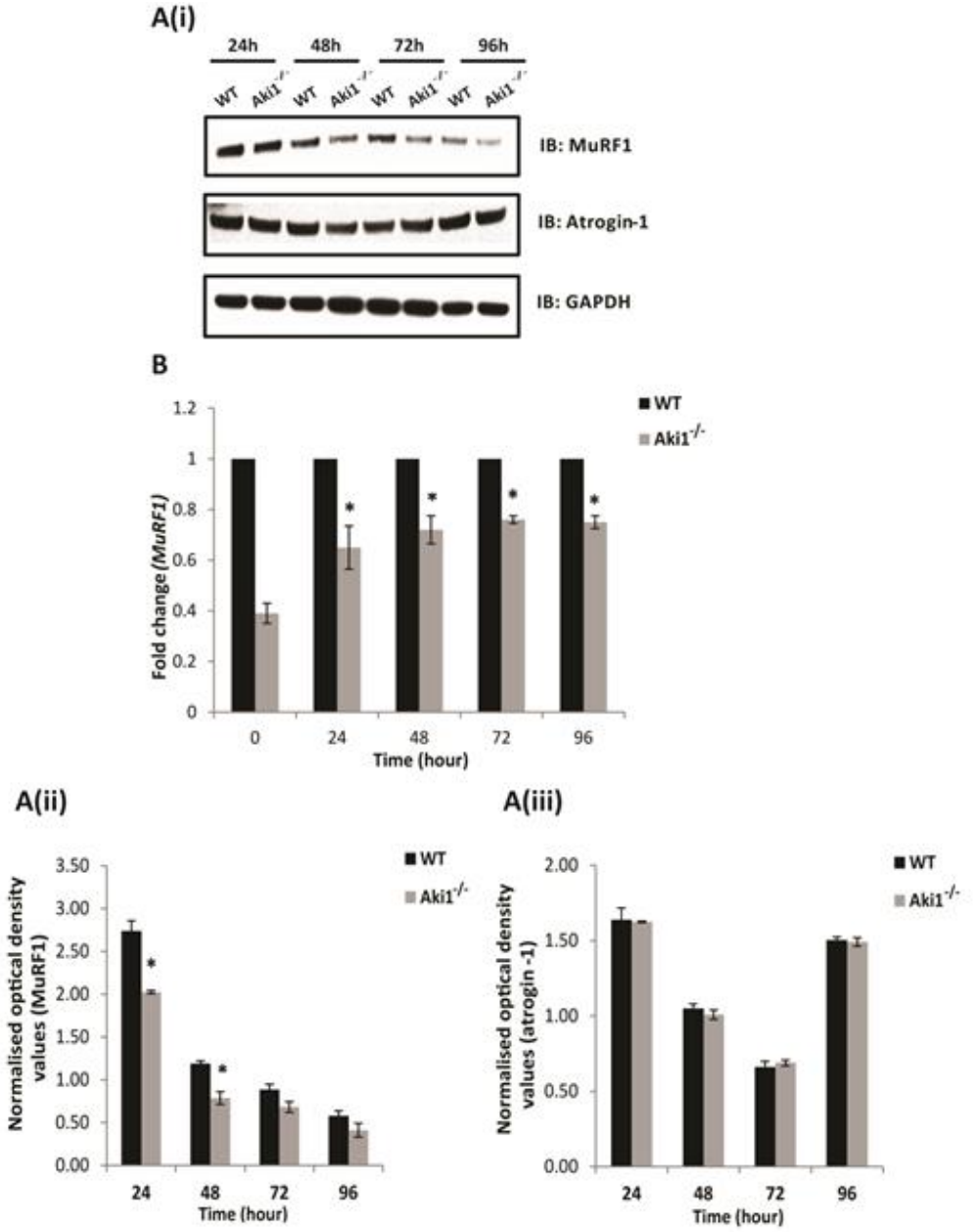

Figure 3.8 Lack of Akirin1 leads to lower MuRF1 levels in differentiating primary myotubes. Western blotting analysis for MuRF1 and atrogin-1 was performed on protein lysates of Akirin1 knock-out and wild-type primary myotubes during differentiation. A(i) A representative immunoblot showing the protein levels of MuRF1 and atrogin1. GAPDH was used as the internal control for equal protein loading on the gel. A(ii) and A(iii) Graphs showing corresponding densitometry analysis of MuRF1 and atrogin1 respectively (*$p<0.05$) (n=3, where n is the number of primary myoblast culture isolations done and for each primary myoblast culture isolation four mice per genotype were used). (B) Graph showing the fold change *MuRF1* mRNA expression in Akirin1 knock-out primary myotubes compared to the wild-type primary myotubes during 0, 24, 48, 72 and 96 hours of differentiation (n=3, where n is the number of primary myoblast culture isolations done and for each primary myoblast culture isolation four mice per genotype were used). Level of significance was compared to wild-type primary myotubes (*$p<0.05$).

3.9 Akirin1 regulates the phosphorylation of FoxO3 protein in differentiating primary myotubes.

An important upstream transcription factors that binds to and activates transcription of MuRF1 promoter is FoxO3 protein. As differentiating Akirin1 knock-out myotubes showed reduced levels of MuRF1 compared to the wild-type, the proteins levels of phospho-FoxO3 as well as total FoxO3 were estimated in Akirin1 knock-out and wild-type differentiating primary myotubes using anti-phospho FoxO3 (ser253) and anti-FoxO3 antibodies. The results showed that Akirin1 knock-out primary myotubes have increased phospho-FoxO3 protein and reduced total FoxO3 protein compared to the wild-type primary myotubes during 24, 48, 72 and 96 hours of differentiation [Figure 3.9A(i), A(ii) and A(iii)]. Densitometry analysis confirmed that the ratio of phospho-FoxO3 (inactive form) to total FoxO3 is significantly more in differentiating Akirin1 knock-out primary myotubes compared to the wild-type [Figure 3.9A(iv)]. These results suggested that lack of Akirin1 leads to phosphorylation of FoxO3 protein there by leading to reduced MuRF1 levels during differentiation.

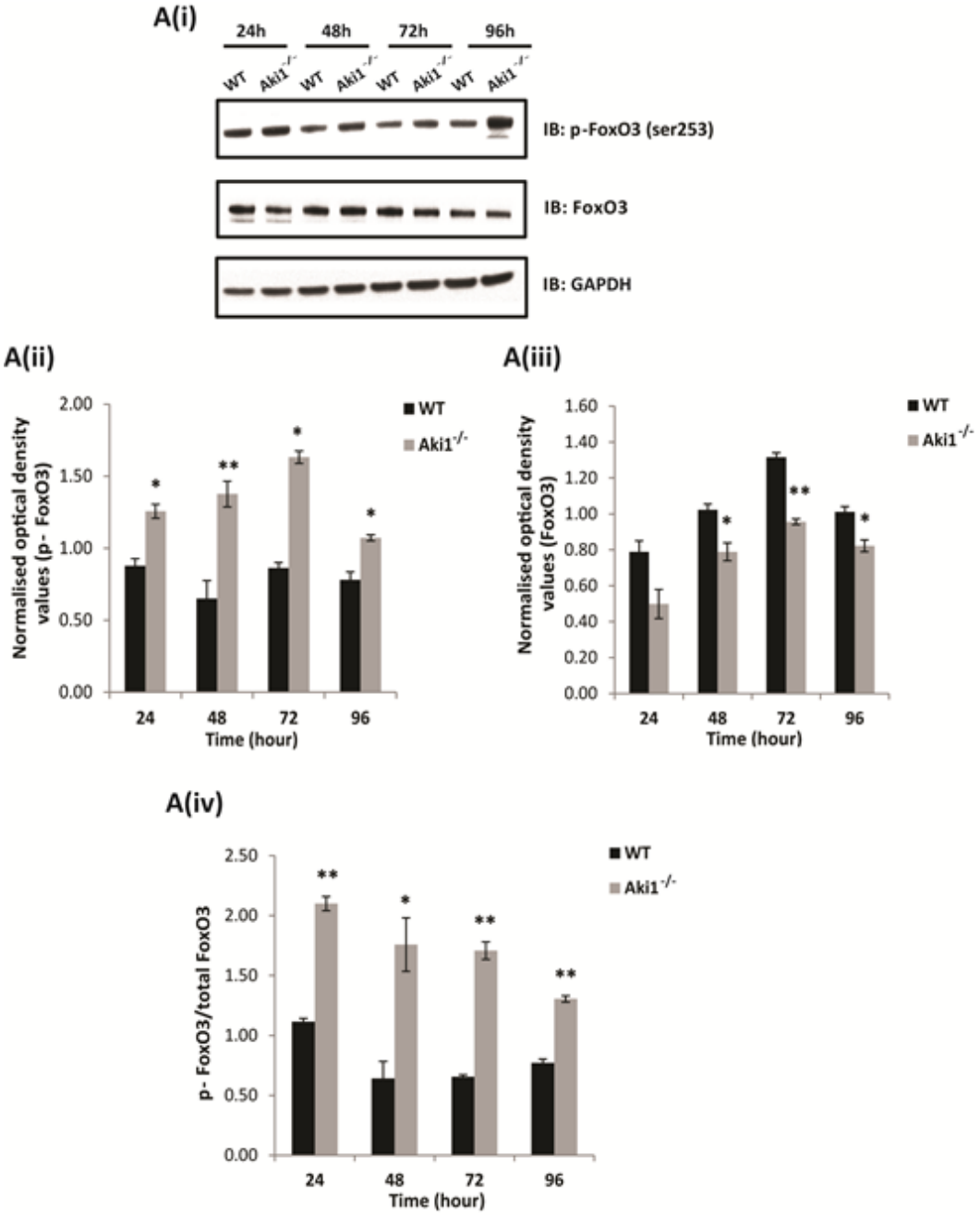

Figure 3.9 Akirin1 regulates the phosphorylation of FoxO3 protein in differentiating primary myotubes. Western blotting analysis for phospho-FoxO3 (ser 253) and total FoxO3 was performed on protein lysates of Akirin1 knock-out and wild-type primary myotubes at 24, 24, 72 and 96 hours of differentiation. A(i) A representative immunoblot showing the protein levels of phospho-FoxO3 (ser 253) and total FoxO3. GAPDH was used as the internal control for equal protein loading on the gel. A(ii) and A(iii) Graphs showing corresponding densitometry analysis of phospho-FoxO3 (ser 253) and total FoxO3 respectively. A(iv) A graph representing the ratio of phospho-FoxO3 (ser 253) to total FoxO3 levels. (*$p<0.05$ and **$p<0.01$) (n=3, where n is the number of primary myoblast culture isolations done and for each primary myoblast culture isolation four mice per genotype were used).

3.10 Akirin1 regulates CREB-1 protein levels during differentiation.

Another transcription factor that is known to bind to MuRF1 promoter and regulate MuRF1 transcription is CREB-1 (Tobimatsu et al., 2009). CREB-1 is known to regulate cellular energy metabolism in skeletal muscle (Thomson et al., 2007; St-Pierre et al., 2003). To investigate if Akirin1 regulates CREB-1 levels in differentiating primary myotubes, Akirin1 knock-out and wild-type differentiating myotubes protein lysates were subjected to western blotting using phospho-CREB-1 (ser 133) and total CREB-1 antibodies. The results showed that Akirin1 knock-out primary myotubes have reduced phospho-CREB-1 (active form) and total CREB-1 levels and compared to the wild-type primary myotubes during 24, 48, 72 and 96 hours of differentiation [Figure 3.10A(i); A(ii) and A(iii)]. Densitometry analysis also confirmed that the ratio of phospho-CREB-1 (ser 133) (active) and total CREB-1 is significantly reduced in differentiating Akirin1 knock-out primary myotubes compared to the wild-type [Figure 3.10A(iv)]. These results suggest that lack of Akirin1 leads to reduced CREB-1 levels as a result of which MuRF1 is down-regulated in differentiating primary myotubes.

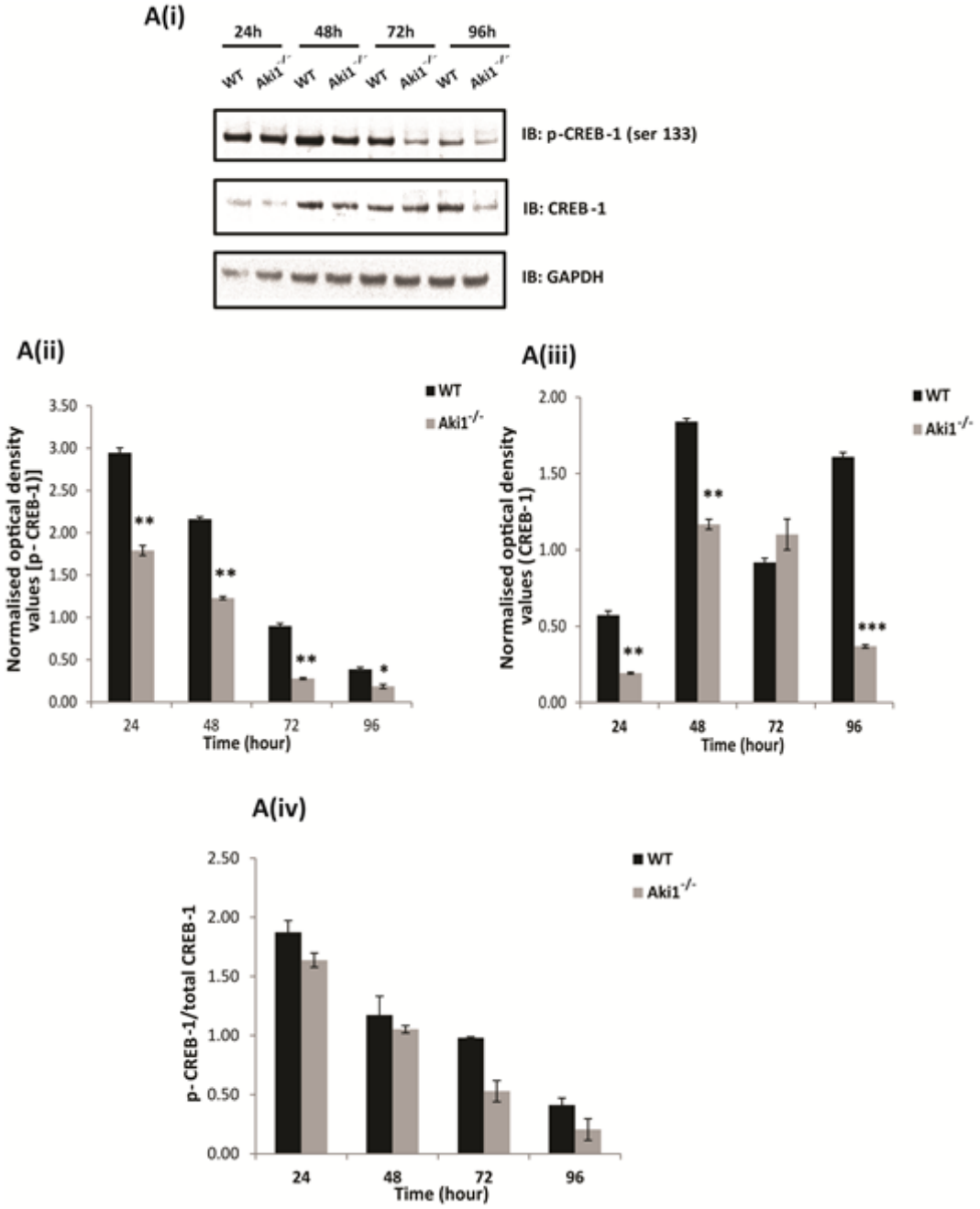

Figure 3.10 Akirin1 regulates CREB-1 protein levels during differentiation. Western blotting analysis for phospho-CREB-1 (ser 133) and total CREB-1 was performed on protein lysates of Akirin1 knock-out and wild-type primary myotubes at 24, 24, 72 and 96 hours of differentiation. A(i) A representative immunoblot showing the protein levels of phospho-CREB-1 (ser 133) and total CREB-1. GAPDH was used as the internal control for equal protein loading on the gel. A(ii) and A(iii) Graphs showing corresponding densitometry analysis of phospho-CREB-1 (ser 133) and total CREB-1 respectively. A(iv) A graph representing the ratio of phospho-CREB-1 (ser 133) to total CREB-1 levels (*$p<0.05$ and **$p<0.01$) (n=3, where n is the number of primary myoblast culture isolations done and for each primary myoblast culture isolation four mice per genotype were used).

3.11 Absence of Akirin1 leads to reduced mitochondrial DNA copy number in differentiating primary myotubes.

Reduced level of CREB-1 has been shown to down-regulate the expression of its other downstream target genes like PPARα and PGC1α. Reduced levels of these proteins are shown to reduce the oxidative potential of the skeletal muscle thus affecting the metabolic activity of the muscle (Thomson et al., 2007; St-Pierre et al., 2003). We know that amount of ATP generation through oxidative phosphorylation occurs in the mitochondria, which is strictly dependent on the mitochondrial DNA copy number (Chen et al., 2010; Dickinson et al., 2013). So, we estimated the copy number of mitochondrial DNA (mtDNA) per nuclear DNA (nuDNA) ratio by performing real time-qPCR with specific set of primers for mtDNA and nuDNA. Akirin1 knock-out differentiating primary myotubes contained significantly lower mtDNA per nuDNA ratio compared to the wild-type (Figure 3.11A). Thus showing that lack of Akirin1 reduces the mitochondrial DNA copy number during differentiation.

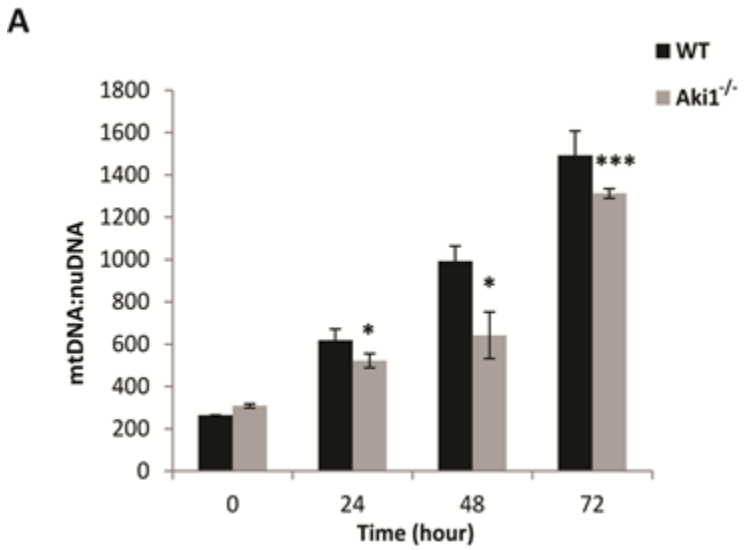

Figure 3.11 Absence of Akirin1 leads to reduced mitochondrial DNA copy number in differentiating primary myotubes. (A) Graph showing the ratio of mitochondrial DNA (mtDNA) copy number per nuclear DNA (nuDNA) in differentiating Akirin1 knock-out and wild-type primary myotubes. Level of significance was calculated by non-parametric Mann-Whitney U test (*$p<0.05$ and ***$p<0.001$) (n=2, where n is the number of primary myoblast culture isolations done and for each primary myoblast culture isolation four mice per genotype were used).

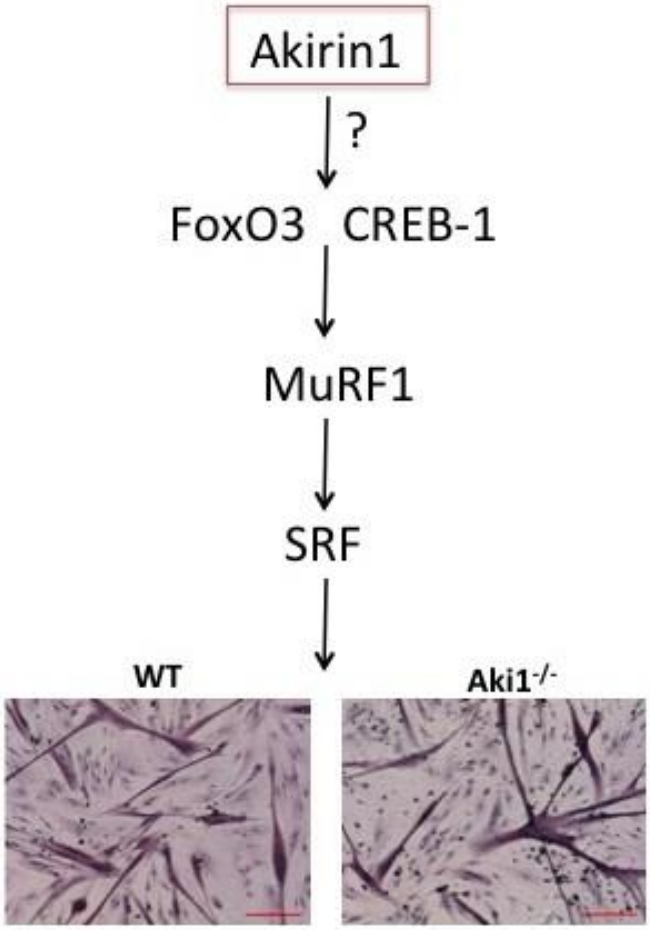

Figure 3.12 A schematic diagram summarizing the various results obtained in understanding the possible role of Akirin1 during myogenesis.

CHAPTER 4

ROLE OF AKIRIN1 IN SKELETAL MUSCLE

4. ROLE OF AKIRIN1 IN SKELETAL MUSCLE

This chapter explains the results, which help us in understanding the role of Akirin1 in skeletal muscle. The materials and methods used in this chapter are discussed in chapter 2 of this thesis.

RESULTS

4.1 Analysis of Akirin1 knock-out skeletal muscle.

To understand if lack of Akirin1 alters skeletal muscle characteristics, firstly we investigated the body size of Akirin1 knock-out and wild-type mice. The body size of all the Akirin1 knock-out mice that were investigated in this thesis was comparable to that of the wild-type mice (Figure 4.1A). Also, we looked at the limb skeletal muscle mass in Akirin1 knock-out and wild-type mice. Akirin1 knock-out mice muscle mass was comparable to that of the wild-type (Figure 4.1B). Furthermore, to investigate the effect of Akirin1 on muscle fiber histology, *tibialis anterior* muscles were sectioned and stained with hematoxylin and eosin (Figure 4.1C). No significant difference in myofiber number was seen between Akirin1 knock-out and wild-type mice (Figure 4.1D). We also looked at the weights of *quadriceps* muscle of Akirin1 knock-out and compared to the wild-type *quadriceps* muscle (Figure 4.1E). These results showed that absence of Akirin1 did not affect the body size, skeletal muscle mass or individual muscle weight in mice.

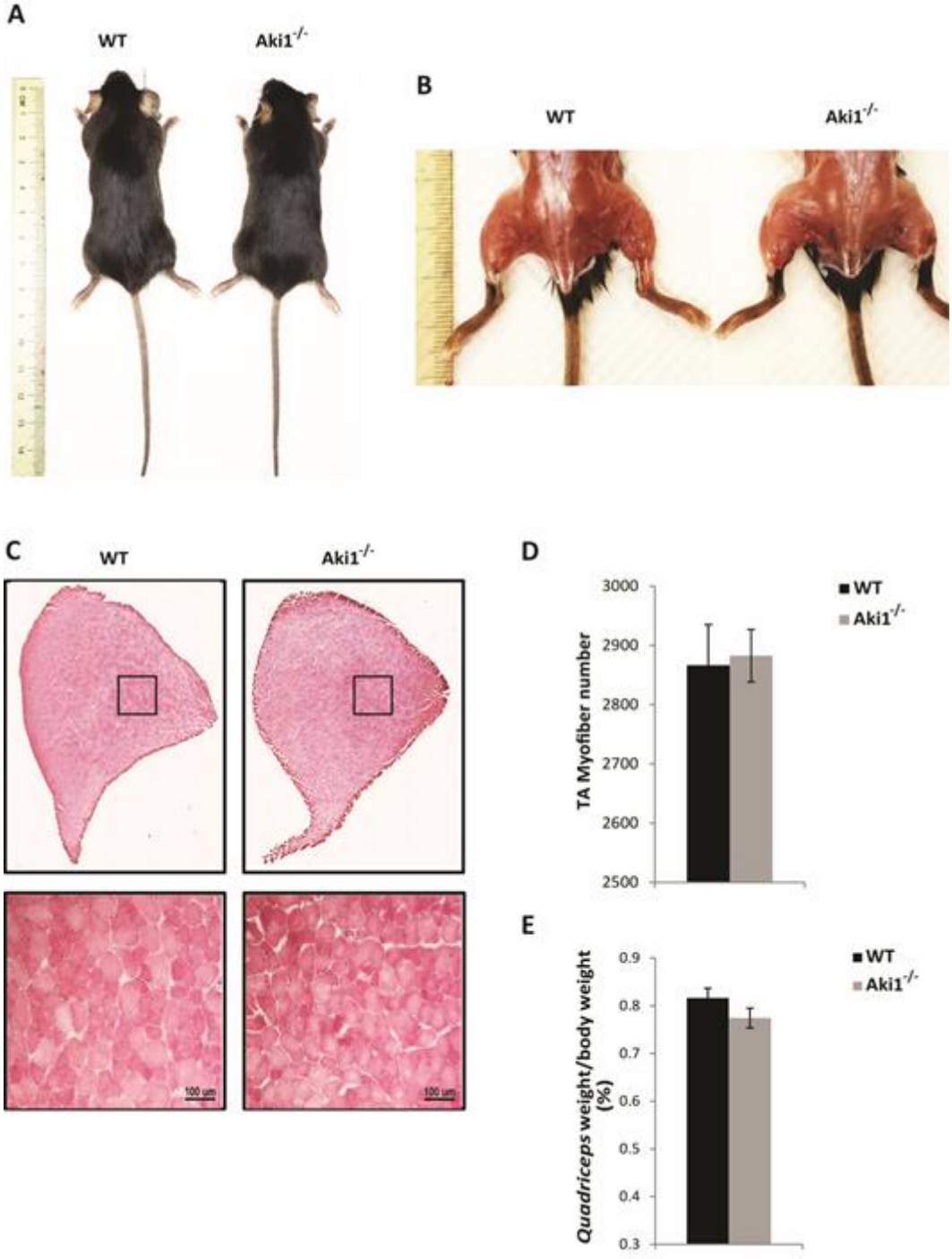

Figure 4.1 Analysis of Akirin1 knock-out skeletal muscle. (A) Representative images of body size of Akirin1 knock-out and wild-type mice. (B) Representative images of limb skeletal muscle mass of Akirin1 knock-out and wild-type mice. (C) Representative images of hematoxylin and eosin stained Akirin1 knock-out and wild-type *tibialis anterior* muscle. Scale bar represents 100 μm. (D) Total muscle fiber number in TA muscles from Akirin1 knock-out and wild-type mice. The values are mean ± S.E. of three animals. (E) *Quadriceps* muscle weights of Akirin1 knock-out and wild-type mice expressed as a percentage of total body weight. The values are mean ± S.E. of six animals.

4.2 Lack of Akirin1 affects the levels of myogenic genes in *quadriceps* muscle.

The process of muscle development is predominantly affected by myogenic regulatory factors (MRFs). It was previously shown by Marshall et al. that Akirin1 is a pro-myogenic protein that is downstream of myostatin, and is negatively regulated by myostatin (Marshall et al., 2008). So, to investigate if lack of Akirin1 affects the process of myogenesis through modifying the expression of important MRFs, protein lysates made from wild-type and Akirin1 knock-out *quadriceps* muscle were subjected to western blotting using anti-MyHC, anti-MyoD and anti-Myogenin antibodies (Figure 4.2A). Densitometry analysis clearly indicated that Akirin1 knock-out muscle showed significantly reduced protein levels of myogenin compared to the wild-type muscle, while the amounts of other MRFs like MyHC and MyoD were comparable to that of the wild-type muscle [Figure 4.2B(i), B(ii) and B(iii)]. In order to see if myogenin was down-regulated transcriptionally as well, *myogenin* mRNA level was quantified in wild-type and Akirin1 knock-out muscle. Consistent with the reduced protein level, *myogenin* mRNA levels were also significantly reduced in Akirin1 knock-out muscle compared to the wild-type [Figure 4.2C(iii)], while the mRNA levels of other MRFs did not change which were consistent with their protein levels [Figure 4.2C(i) and C(ii)].

Figure 4.2 Lack of Akirin1 affects the level of myogenic genes in *quadriceps* muscle. Myogenic regulatory factors (MRFs) profile in Akirin1 knock-out and wild-type skeletal muscle. Western blotting analysis was performed on Akirin1 knock-out and wild-type *quadriceps* muscle protein lysates. A(i) A representative immunoblot showing protein levels of important myogenic genes i.e., MyHC, MyoD and myogenin. GAPDH was used as the internal control for equal protein loading on the gel. B(i), B(ii), B(iii) and B(iv) Corresponding densitometry graphs of MyHC, MyoD and myogenin respectively showing significant decrease or no change in the protein content in skeletal muscle (*$p<0.05$) (n=4). (C) mRNA expression for *MyHC*, *MyoD* and *myogenin* was determined in Akirin1 knock-out and wild-type *quadriceps* muscle. The values are mean ± S.E. of four different animals. **$p<0.01$ denotes significant fold change difference in *Akirin1* mRNA expression relative to the wild-type.

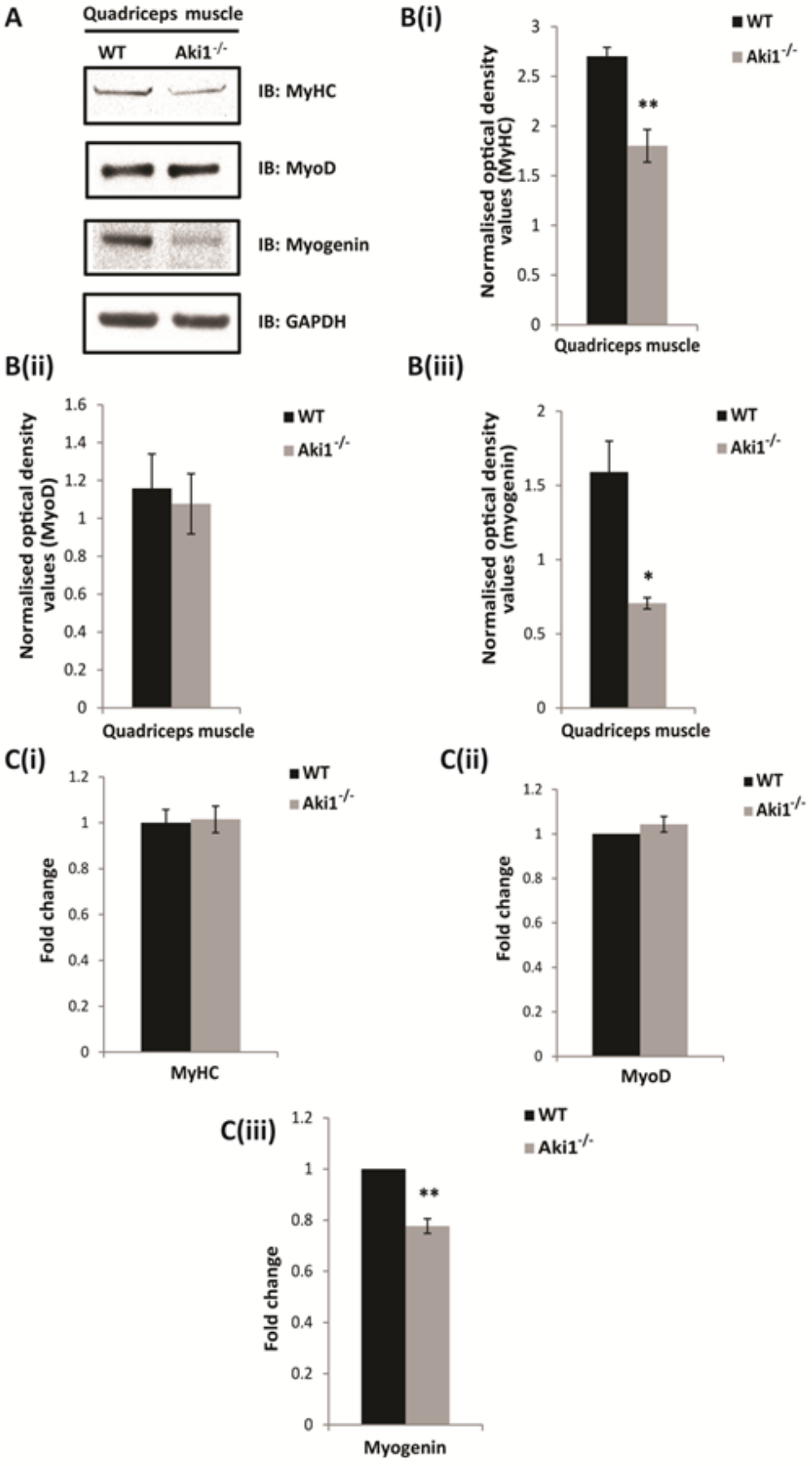
A
Quadriceps muscle
WT
Aki1-/-
IB: MyHC
IB: MyoD
IB: Myogenin
IB: GAPDH
B(i)
Normalised optical density values (MyHC)
Quadriceps muscle
WT
Aki1-/-
**
B(ii)
Normalised optical density values (MyoD)
Quadriceps muscle
WT
Aki1-/-
B(iii)
Normalised optical density values (myogenin)
Quadriceps muscle
WT
Aki1-/-
*
C(i)
Fold change
MyHC
WT
Aki1-/-
C(ii)
Fold change
MyoD
WT
Aki1-/-
C(iii)
Fold change
Myogenin
WT
Aki1-/-
**

4.3 Akirin1 does not regulate the levels of MEF2C class of myogenic regulators.

Apart from Myogenic Regulatory Factors (MRFs), another family of transcription proteins called the MEF2s is known to influence the process of muscle development. And among the MEF2 family of transcription factors, it has been shown that MEF2C plays an important role in muscle development (Edmondson et al., 1994). So, we investigated if lack of Akirin1 affected the MEF2C levels by subjecting the wild-type and Akirin1 knock-out *quadriceps* muscle protein lysates to immunoblotting with anti-phospho-MEF2C (thr300) (active) and anti-MEF2C antibodies. Densitometry analysis showed slightly reduced but non-significant levels of both total and phospho-MEF2C [Figure 4.3A, B(i) and B(ii)]. Consistent with the protein levels, the mRNA expression levels of *Mef2c* in Akirin1 knock-out was comparable to that of the wild-type (Figure 4.3C). Thus suggesting that, Akirin1 does not affect MEFC2 class of myogenic transcription factors.

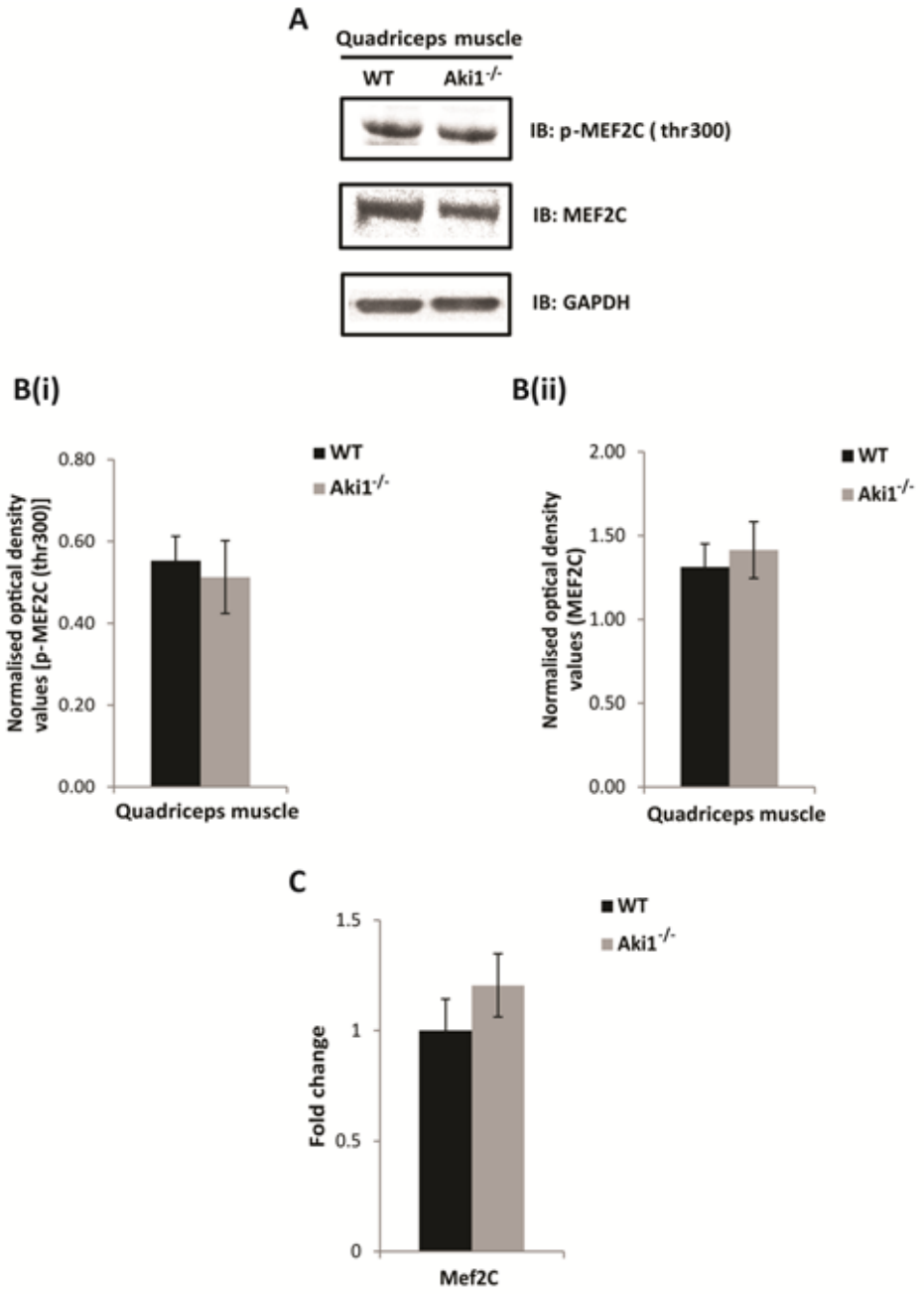

Figure 4.3 Akirin1 does not regulate the levels of MEF2C class of myogenic regulators. Analysis of another class of myogenic regulators, MEF2C in Akirin1 knock-out and wild-type quadriceps muscle. Western blotting analysis was performed on protein lysates of Akirin1 knock-out and wild-type quadriceps muscle. (A) A representative immunoblot showing the protein levels of both phospho-MEF2C (thr300) and total MEF2C. GAPDH was used as the internal control for equal protein loading on the gel. B(i) and B(ii) graphs showing corresponding densitometry analysis of phospho-MEF2C (thr300) and total MEF2C respectively (n=4). mRNA expression of *Mef2c* was determined in Akirin1 knock-out and wild-type quadriceps muscle. (C) A graph showing the fold change mRNA expression of *Mef2c* in Akirin1 knock-out quadriceps muscle compared to the wild-type. The values are mean ± S.E. of four different animals.

4.4 Akirin1 regulates the protein levels of important sarcomeric proteins in the skeletal muscle.

As explained in section 1.1.1.1, sarcomeres are the contractile units of a muscle. A sarcomere consists of three categories of proteins which function jointly leading to the contraction of the muscle. 1) Structural proteins, such as desmin, which give the frame work and elasticity to the muscle 2) Contractile proteins like actin and myosin, which provide force during contraction of the muscle 3) Regulatory proteins like troponins, which regulate the process of contraction and relaxation of the muscle. Troponin T binds to tropomyosin and facilitates sarcomere contraction, troponin I regulates the contraction of the sarcomere by either turning on or off the interaction between the actin and myosin filaments and troponin C binds to Ca^{2+} ions released from the sarcoplasmic reticulum to initiate contraction (Martini, 2006). To investigate if Akirin1 has a novel role in maintaining the levels of the regulatory proteins, immunoblotting was performed on protein lysates of wild-type and Akirin1 knock-out *quadriceps* muscle using anti-troponin T, anti-troponin I and anti-troponin C antibodies. Densitometry analysis showed that troponin T was significantly lower in Akirin1 knock-out muscle compared to the wild-type muscle. Another regulatory protein, Troponin I, was also significantly down-regulated in the Akirin1 knock-out muscle compared to the wild-type muscle. However the level of troponin C was unchanged [Figure 4.4A, B(i), B(ii) and B(iii)].

Further, the protein levels of α-actin, desmin and MyHC, movement of which leads to the contraction of the sarcomere, were also estimated. Akirin1 knock-out and wild-type *quadriceps* muscle protein was probed with anti-α-actin and

anti-desmin antibody. Densitometry analysis showed that Akirin1 knock-out muscle showed significantly lower levels of α-actin, MyHC and desmin when compared to the wild-type muscle [Figure 4.4C, D(i) and D(ii)]. These results together suggest that absence of Akirin1 leads to reduced levels of important sarcomeric proteins, thus implying a novel role of Akirin1 in maitaining the sarcomeric intergrity of skeletal muscle.

Figure 4.4 Akirin1 regulates the protein levels of important sarcomeric proteins in the skeletal muscle. Analysis of the different sarcomeric contractile and regulatory proteins in Akirin1 knock-out and wild-type *quadriceps* muscle. Western blotting analysis was performed on Akirin1 knock-out and wild-type *quadriceps* muscle protein lysates. (A) A representative immunoblot showing the protein levels of sarcomeric contractile proteins like α-actin and desmin in Akirin1 knock-out and wild-type *quadriceps* muscle. GAPDH was used as an internal control for equal protein loading on the gel. B(i) and B(ii) Corresponding densitometry graphs of α-actin and desmin respectively (**$p<0.01$ and ***$p<0.001$) (n=4). (C) A representative immunoblot showing the sarcomeric regulatory protein levels i.e., troponin T, troponin I and troponin C in Akirin1 knock-out and wild-type *quadriceps* muscle. D(i), D(ii) and D(iii) Graphs showing the densitometry analysis of troponin T, troponin I and troponin C respectively (**$p<0.01$) (n=4).

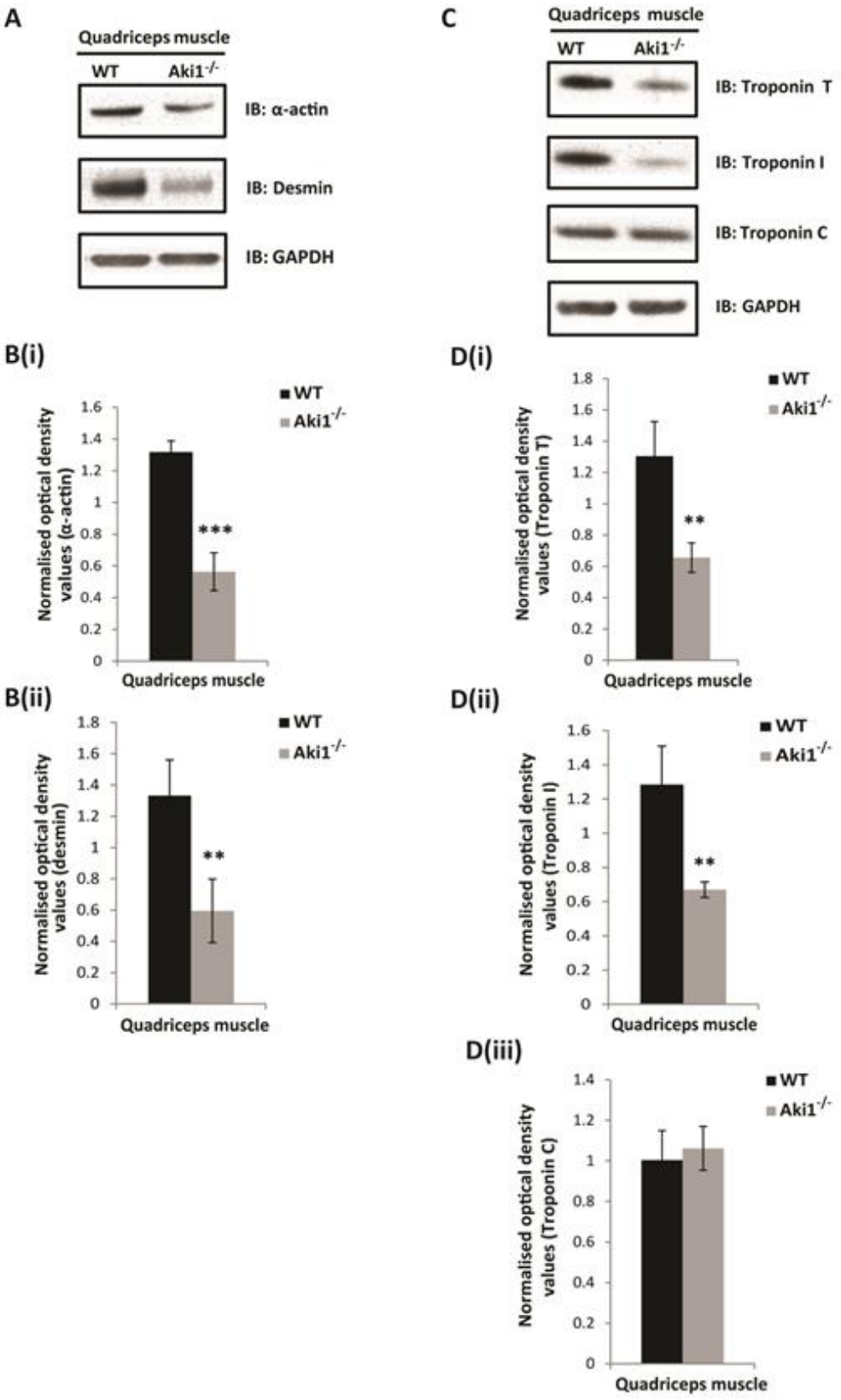
A
Quadriceps muscle
WT
Aki1-/-
IB: α-actin
IB: Desmin
IB: GAPDH
C
Quadriceps muscle
WT
Aki1-/-
IB: Troponin T
IB: Troponin I
IB: Troponin C
IB: GAPDH
B(i)
Normalised optical density values (α-actin)
WT
Aki1-/-
***
Quadriceps muscle
B(ii)
Normalised optical density values (desmin)
WT
Aki1-/-
**
Quadriceps muscle
D(i)
Normalised optical density values (Troponin T)
WT
Aki1-/-
**
Quadriceps muscle
D(ii)
Normalised optical density values (Troponin I)
WT
Aki1-/-
**
Quadriceps muscle
D(iii)
Normalised optical density values (Troponin C)
WT
Aki1-/-
Quadriceps muscle

4.5 Akirin1 regulates α-actin and desmin proteins in the sarcomere post-transcriptionally.

Although Akirin1 regulates the protein levels of the sarcomeric proteins like α-actin and desmin, the mRNA levels of both α-*actin* and *desmin* in the Akirin1 knock-out muscle were not significantly different from wild-type muscle (Figure 4.5A and B). This shows that Akirin1 regulates α-actin and desmin post-transcriptionally in skeletal muscle.

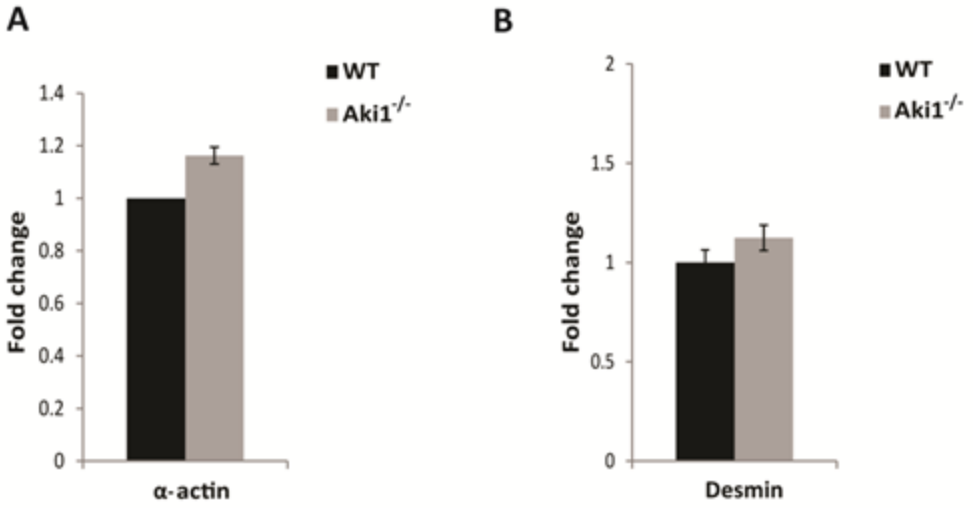

Figure 4.5 Akirin1 regulates α-actin and desmin proteins in the sarcomere post-trancriptionally. Gene expression analysis of sarcomeric proteins like *α-actin* and *desmin,* in Akirin1 knock-out and wild-type *quadriceps* muscle. (A) and (B) Graphs showing the fold change mRNA expression of *α-actin* and *desmin* in Akirin1 knock-out *quadriceps* muscle compared to that of the wild-type. The values are mean ± S.E. of four different animals.

Figure 4.6 Absence of Akirin1 regulates MuRF1, but not atrogin1 in skeletal muscle. Analysis of skeletal muscle specific E3 ubiquitin ligases, MuRF1 and atrogin1 in Akirin1 knock-out and wild-type *quadriceps* muscle. Western blotting analysis for MuRF1 and atrogin1 was performed on protein lysates of Akirin1 knock-out and wild-type *quadriceps* muscle. A(i) A representative immunoblot showing the protein levels of MuRF1 and atrogin1. GAPDH was used as the internal control for equal protein loading on the gel. A(ii) and A(iii) Graphs showing corresponding densitometry analysis of MuRF1 and atrogin1 respectively (***$p<0.001$) (n=4). Expression analysis of MuRF1 in Akirin1 over-expressing myoblasts. Western blotting was performed on protein lysates from differentiating Akirin1 over-expressor myoblasts and control C_2C_{12} myoblasts. B(i) A representative immunoblot showing the protein levels of MuRF1. B(ii) A graph showing the corresponding densitometry analysis of MuRF1 protein levels in Akirin1 over-expressor myoblasts and control C_2C_{12} myoblasts. The graph is representative of at least two independent experiments. Level of significance was compared to control C_2C_{12} myoblasts (*$p<0.05$ and **$p<0.01$).

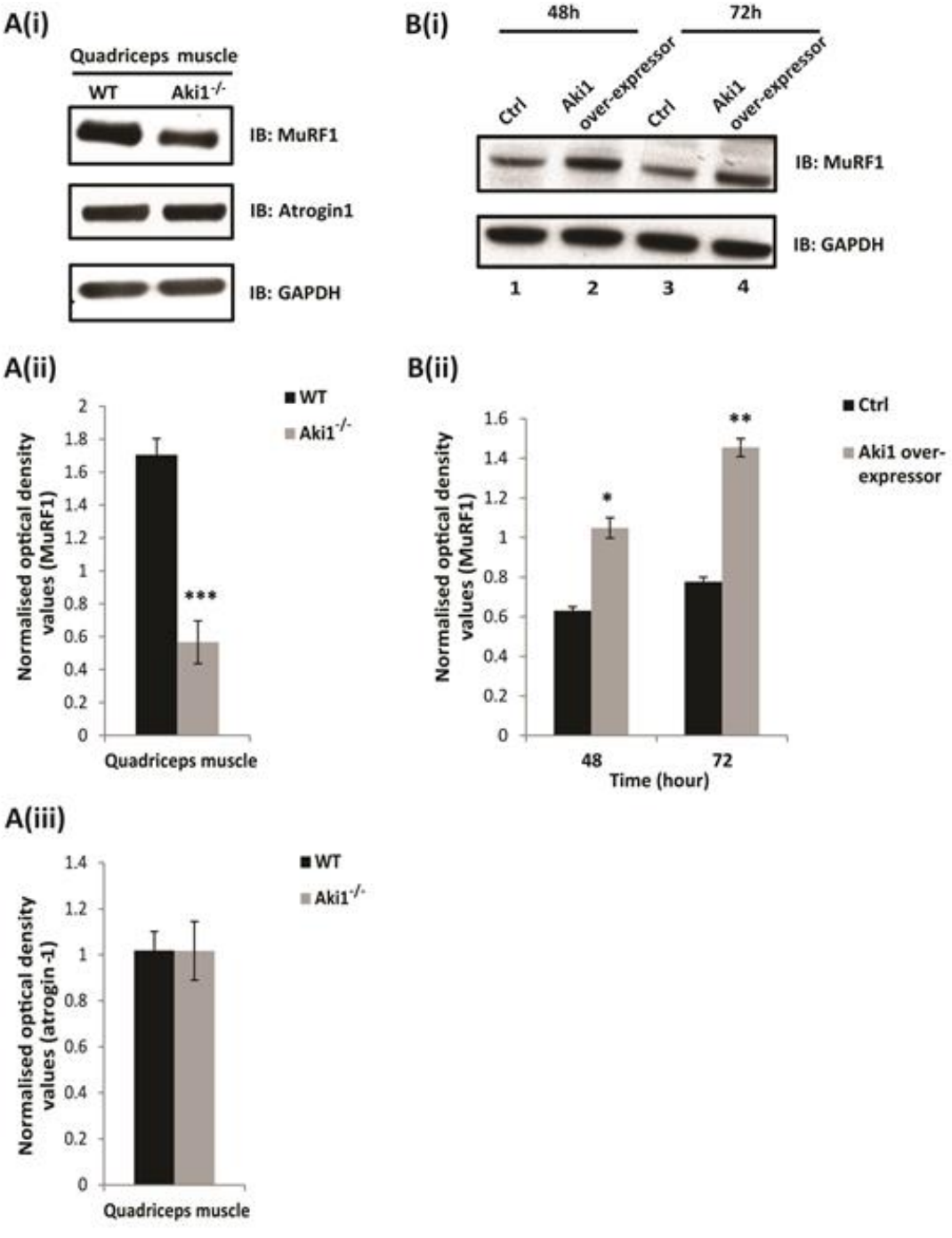
A(i)
Quadriceps muscle
WT
Aki1-/-
IB: MuRF1
IB: Atrogin1
IB: GAPDH
B(i)
48h
72h
Ctrl
Aki1 over-expressor
Ctrl
Aki1 over-expressor
IB: MuRF1
IB: GAPDH
1
2
3
4
A(ii)
WT
Aki1-/-
Normalised optical density values (MuRF1)
***
Quadriceps muscle
B(ii)
Ctrl
Aki1 over-expressor
Normalised optical density values (MuRF1)
*
**
48
72
Time (hour)
A(iii)
WT
Aki1-/-
Normalised optical density values (atrogin-1)
Quadriceps muscle

4.6 Absence of Akirin1 regulates MuRF1, but not atrogin1 in skeletal muscle.

Loss of skeletal muscle mass is attributed to two important muscle atrogenes called MuRF1 and atrogin1. Marshall et al. showed that over-expression of Akirin1 in C_2C_{12} myoblasts lead to increased fusion of myoblasts resulting in hypertrophy of myotubes (Marshall et al., 2008). As the results in section 4.5 showed reduced levels of sarcomeric proteins, we wanted to quantify the protein levels of atrogenes- MuRF1 and atrogin1. For this, western blotting was performed on wild-type and Akirin1 knock-out *quadriceps* muscle protein lysates and probed with anti-MuRF1 and anti-atrogin1 antibody. Although the protein levels of atrogin1 remained unchanged between wild-type and Akirin1 knock-out muscle (Figure 4.6A(i) and C), the levels of MuRF1 protein was significantly down-regulated in Akirin1 knock-out compared to the wild-type muscle [Figure 4.6A(i) and A(ii)].

A C_2C_{12} cell line that stably over-expresses Akirin1 was generated by Marshall et al., 2008. Using this Akirin1 over-expression model, we further studied the results obtained above. MuRF1 protein level was estimated in Akirin1 over-expressor cells with C_2C_{12} cells as control. Contrary to the results obtained in Akirin1 knock-out model, MuRF1 protein level was indeed up-regulated in Akirin1 over-expressor cells compared to the control cells at 48 and 72 hours of differentiation [Figure 4.6B(i) lanes 2 and 4]. Densitometry analysis confirmed that MuRF1 levels were significantly up-regulated in Akirin1 over-expressor cells compared to the control C_2C_{12} cells during differentiation [Figure 4.6B(ii)].

4.7 Akirin1 transcriptionally regulates the levels of MuRF1 in both C_2C_{12} myoblasts and skeletal muscle.

As we observed reduced MuRF1 protein levels in the absence of Akirin1, we wanted to further investigate if MuRF1 was down-regulated at the transcriptional level. For this, *MuRF1* mRNA levels were quantified by real time-qPCR in wild-type and Akirin1 knock-out *quadriceps* muscle and normalised to *cyclophilin* Ct values. Consistent with the reduced MuRF1 protein levels, Akirin1 knock-out muscle showed significantly lower levels of *MuRF1* mRNA levels compared to the wild-type muscle (Figure 4.7A). On the contrary, MuRF1 mRNA levels were up-regulated upon Akirin1 over-expression during differentiation when compared to control C_2C_{12} cells. Consistent with the increased MuRF1 protein levels, Akirin1 over-expressor cells clearly showed significantly increased MuRF1 mRNA levels compared to the control C_2C_{12} cells during differentiation (Figure 4.7B).

Knowing that Akirin1 regulates the level of MuRF1 mRNA, it was necessary to investigate if Akirin1 regulates MuRF1 transcriptionally. To achieve this, MuRF1 promoter-luciferase plasmid was co-transfected with Akirin1 expression plasmid into C_2C_{12} myoblasts and the luciferase activity was quantified. C_2C_{12} myoblasts transfected with both MuRF1 promoter-luciferase plasmid and Akirin1 expression plasmid showed nearly two fold significant increase in luciferase activity when compared to luciferase activity of C_2C_{12} myoblasts transfected with MuRF1 promoter alone (Figure 4.7C). These findings together demonstrate a novel function of Akirin1 in regulating MuRF1 in skeletal muscle.

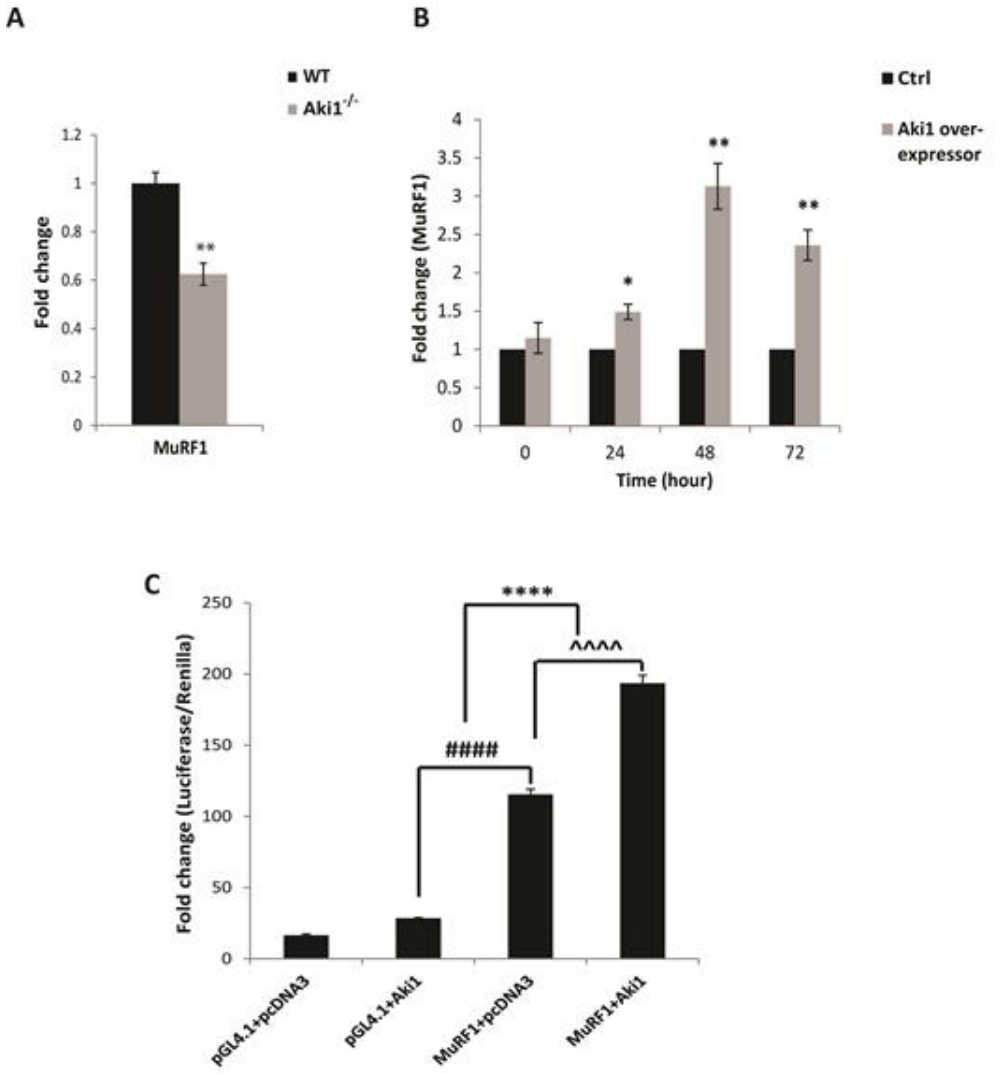

Figure 4.7 Akirin1 transcriptionally regulates the levels of MuRF1 in both C_2C_{12} myoblasts and skeletal muscle. (A) A graph showing the fold change *MuRF1* mRNA expression in Akirin1 knock-out *quadriceps* muscle compared to the wild-type. The values are mean ± S.E. of four different animals. Level of significance was compared to wild-type (*$p<0.05$). (B) A graph showing fold change *MuRF1* mRNA expression in Akirin1 over-expressor myoblasts and control C_2C_{12} myoblasts during differentiation. The graph is representative of at least two independent experiments. Level of significance was compared to control C_2C_{12} myoblasts (*$p<0.05$ and **$p<0.01$). (C) A graph showing promoter-luciferase reporter activity in C_2C_{12} myoblasts transfected with either pGL4.1 or pcDNA3.1 empty vectors or MuRF1 promoter (MuRF1-pGL4.1) and Akirin1 expression vector (Akirin1-pcDNA3.1), together with control Renilla luciferase vector pRL-TK. The graph is representative of four independent experiments. ($^{\#\#\#\#}p<0.0001$, ****$p<0.0001$ and ^^^^$p<0.0001$).

4.8 Akirin1 regulates MuRF1 expression via modulating the phosphorylation of FoxO3 protein in skeletal muscle.

One of the important upstream transcription factors that bind to and activate transcription of MuRF1 promoter is FoxO3 protein. FoxO3 protein belongs to the family of fork-head transcription factors that bind to DNA with their fork-head DNA-binding domain. FoxO3 protein possesses the ability to be phosphorylated leading to its translocation out of the nucleus thus down-regulating the down-stream target genes. To investigate if MuRF1 expression is down-regulated through FoxO3 protein, Akirin1 knock-out and wild-type *quadriceps* muscle protein lysates were subjected to immunoblotting using anti-phospho FoxO3 (ser253) and anti-FoxO3 antibodies. The results revealed that Akirin1 knock-out mice have increased phospho-FoxO3 protein (inactive form) and reduced total FoxO3 protein compared to the wild-type [Figure 4.8.1A(i), A(ii) and A(iii)]. Densitometric analysis also confirmed that the ratio of phospho-FoxO3 (inactive form) to total FoxO3 is significantly more in Akirin1 knock-out muscle compared to the wild-type [Figure 4.8.2A(iv)]. This shows that lack of Akirin1 leads to phosphorylation of FoxO3 leading to reduced active FoxO3 protein in skeletal muscle.

To see if the expression profile of phospho-FoxO3 and total FoxO3 proteins changes when Akirin1 was over-expressed, control C_2C_{12} and Akirin1 over-expressor cell protein lysates were subjected to western blotting and probed with anti-phospho FoxO3 (ser253) and anti-FoxO3 antibodies. The results clearly show that Akirin1 over-expressor cells showed reduced phospho-FoxO3 protein and increased total FoxO3 protein compared to the control C_2C_{12} cells [Figure 4.8.1B(i) lanes 2 and 4, B(ii) and B(iii)]. Densitometry

analysis also shows that the ratio of phospho-FoxO3 to total FoxO3 is significantly reduced in Akirin1 over-expressor compared to the control C_2C_{12} cells [Figure 4.8.2B(iv)]. This shows that over-expression of Akirin1 leads to reduced FoxO3 phosphorylation that would allow its translocation to the nucleus and binding to the MuRF1 promoter thereby activating MuRF1 transcription.

FoxO3 mRNA levels were quantified by real time-qPCR in wild-type and Akirin1 knock-out *quadriceps* muscle and normalised to *cyclophilin* Ct values. The *FoxO3* mRNA level in Akirin1 knock-out skeletal muscle was similar to that of the wild-type. (Figure 4.8.2C). These findings together suggest that Akirin1 may regulate the expression of MuRF1 by modulating FoxO3 phosphorylation in skeletal muscle.

Figure 4.8.1 Akirin1 regulates MuRF1 expression via modulating the phosphorylation of FoxO3 protein in skeletal muscle. Western blotting analysis for phospho-FoxO3 (ser 253) and total FoxO3 was performed on protein lysates of Akirin1 knock-out and wild-type *quadriceps* muscle. A(i) A representative immunoblot showing the protein levels of phospho-FoxO3 (ser 253) and total FoxO3. GAPDH was used as the internal loading control. A(ii) and A(iii) Graphs showing corresponding densitometry analysis of phospho-FoxO3 (ser 253) and total FoxO3 respectively. (*$p<0.05$) (n=4). Expression analysis of FoxO3 in Akirin1 over-expressor myoblasts. Western blotting was performed on protein lysates from differentiating Akirin1 over-expressor myoblasts and control C_2C_{12} myoblasts. B(i) A representative immunoblot showing the protein levels of phospho-FoxO3 (ser 253) and total FoxO3. B(ii) and B(iii) Graphs showing the corresponding densitometry analysis of phospho-FoxO3 (ser 253) and total FoxO3 protein levels in Akirin1 over-expressor myoblasts and control C_2C_{12} myoblasts. All the graphs are representative of at least two independent experiments. Level of significance was compared to control C_2C_{12} myoblasts (*$p<0.05$).

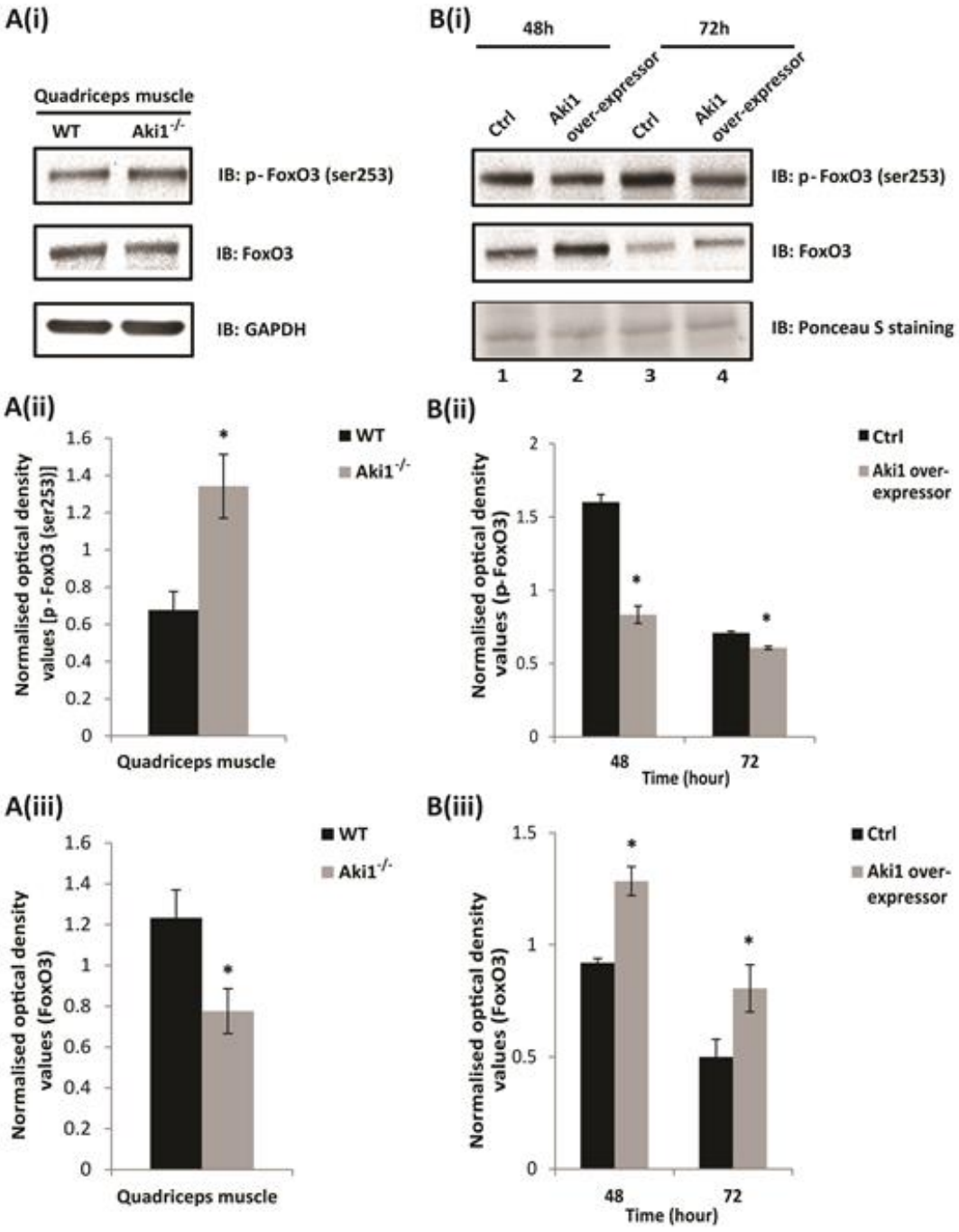
A(i)
Quadriceps muscle
WT
Aki1-/-
IB: p-FoxO3 (ser253)
IB: FoxO3
IB: GAPDH
B(i)
48h
72h
Ctrl
Aki1 over-expressor
Ctrl
Aki1 over-expressor
IB: p-FoxO3 (ser253)
IB: FoxO3
IB: Ponceau S staining
1
2
3
4
A(ii)
Normalised optical density values [p-FoxO3 (ser253)]
WT
Aki1-/-
Quadriceps muscle
B(ii)
Normalised optical density values (p-FoxO3)
Ctrl
Aki1 over-expressor
48
72
Time (hour)
A(iii)
Normalised optical density values (FoxO3)
WT
Aki1-/-
Quadriceps muscle
B(iii)
Normalised optical density values (FoxO3)
Ctrl
Aki1 over-expressor
48
72
Time (hour)

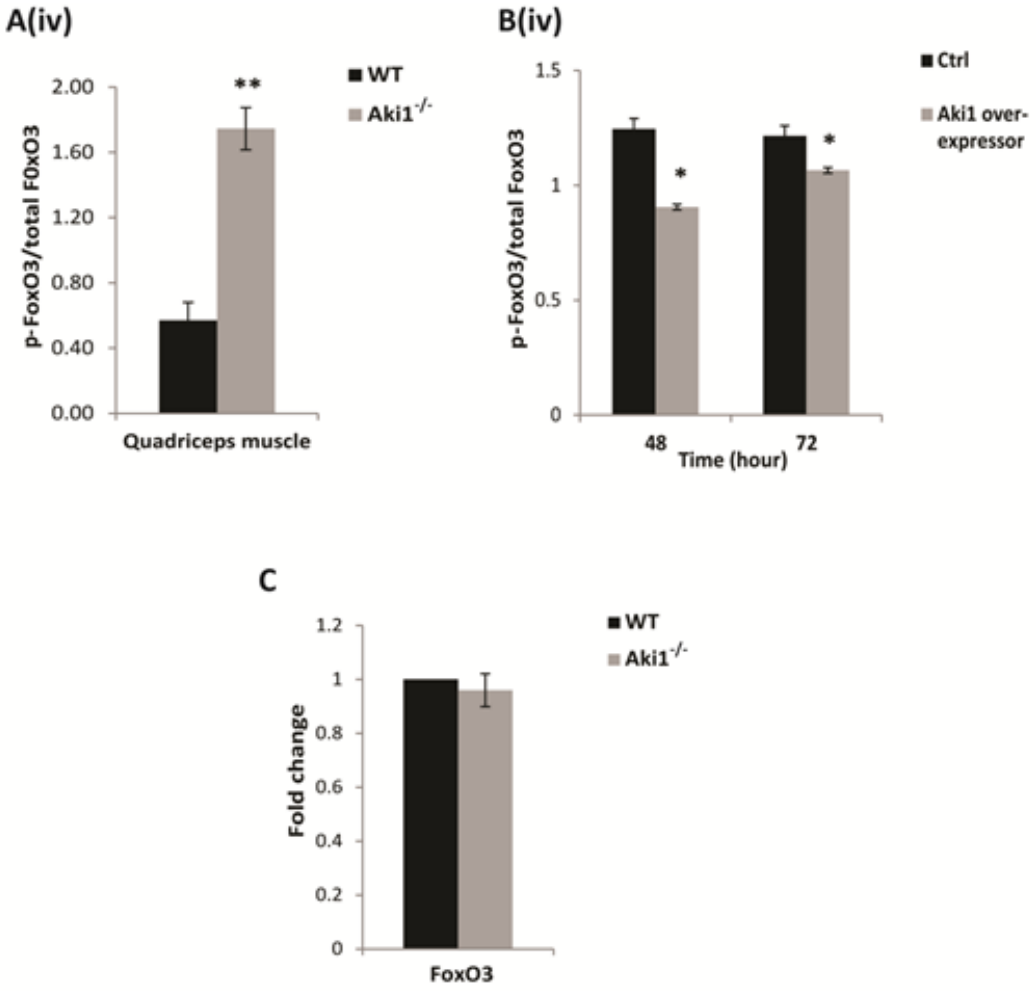

Figure 4.8.2 Akirin1 regulates the levels of active form of FoxO3 protein post-trancriptionally. A(iv) A graph representing the ratio of phospho-FoxO3 (ser 253) to total FoxO3 levels. (*p<0.05) (n=4). B(iv) A graph representing the ratio of phospho-FoxO3 (ser 253) to total FoxO3 levels. All the graphs are representative of at least two independent experiments. Level of significance was compared to control C_2C_{12} myoblasts (*p<0.05 and **p<0.01). (C) A graph showing the fold change mRNA expression of *FoxO3* in Akirin1 knock-out *quadriceps* muscle compared to that of the wild-type. The values are mean ± S.E. of four different animals.

4.9 Lack of Akirin1 affects the extent of glutamylation of tubulin molecules due to reduced MuRF1 levels.

MuRF1 is also known to be an important sarcomeric protein that binds to microtubules and stabilize them. Binding of MuRF1 molecules to the microtubules lead to the addition of glutamic acid to the tubulin molecules there by making them resistant to depolymerisation and facilitating myoblast fusion (Spencer et al., 2000). As our previous data from section 4.7 revealed that Akirin1 knock-out *quadriceps* muscle have reduced MuRF1 expression, we wanted to investigate the level of glutamylation of tubulin proteins. For this, Akirin1 knock-out and wild-type *quadriceps* muscle protein lysates were probed with anti-poly-glutamylated tubulin and α-tubulin antibody. The results obtained showed that Akirin1 knock-out muscle have significantly lower levels of poly-glutamylated tubulin proteins compared to the wild-type muscle while the α-tubulin levels were unchanged (Figure 4.9A and B). Thus, suggesting that reduced MuRF1 protein level indeed leads to reduced glutamylation of tubulin molecules in the absence of Akirin1.

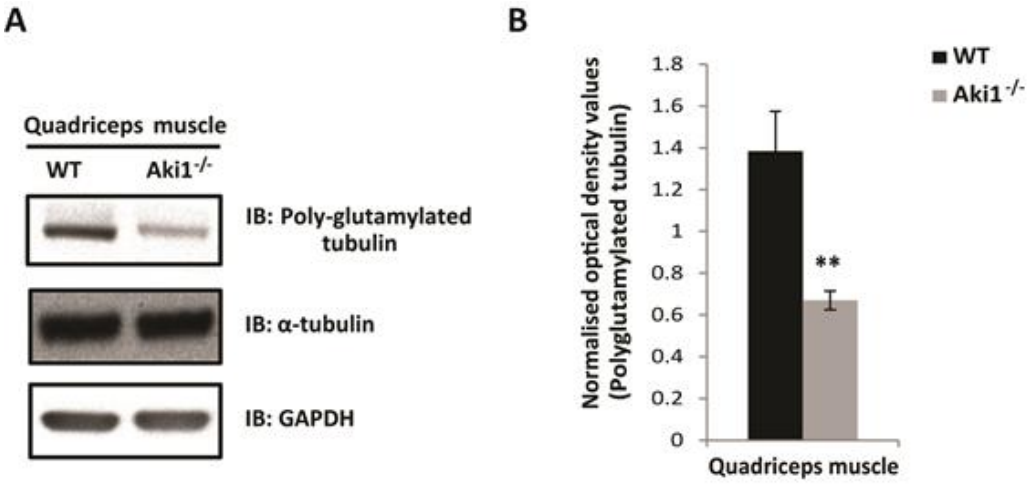

Figure 4.9 Lack of Akirin1 affects the extent of glutamylation of tubulin molecules due to reduced MuRF1 levels. Analysis of poly-glutamylated tubulin in Akirin1 knock-out and wild-type *quadriceps* muscle. Western blotting analysis was performed on protein lysates of Akirin1 knock-out and wild-type *quadriceps* muscle. (A) A representative immunoblot showing the protein levels of poly-glutamylated tubulin and α-tubulin. GAPDH was used as the internal control for equal protein loading on the gel. (B) A graph showing corresponding densitometry analysis of poly-glutamylated tubulin. (**$p<0.01$) (n=4).

4.10 Lack of Akirin1 leads to reduced ubiquitination of various cellular proteins due to reduced MuRF1 activity.

Another known function of MuRF1 is to mark the target proteins that are destined to be degraded, by adding ubiquitin molecules, which later, are degraded by the proteasomes. As our results showed lower MuRF1 levels in the absence of Akirin1, we wanted to study the ubiquitination profile of various cellular proteins in the Akirin1 knock-out muscle. Protein lysates from Akirin1 knock-out and wild-type *quadriceps* muscle were probed with anti-ubiquitin antibody. Results showed that Akirin1 knock-out muscle have significantly lower extent of ubiquitination of the cellular proteins when compared to the wild-type muscle (Figure 4.10A and B). This suggests that due to reduced MuRF1 levels, the normal turn-over of the various cellular proteins may be affected in Akirin1 knock-out muscle.

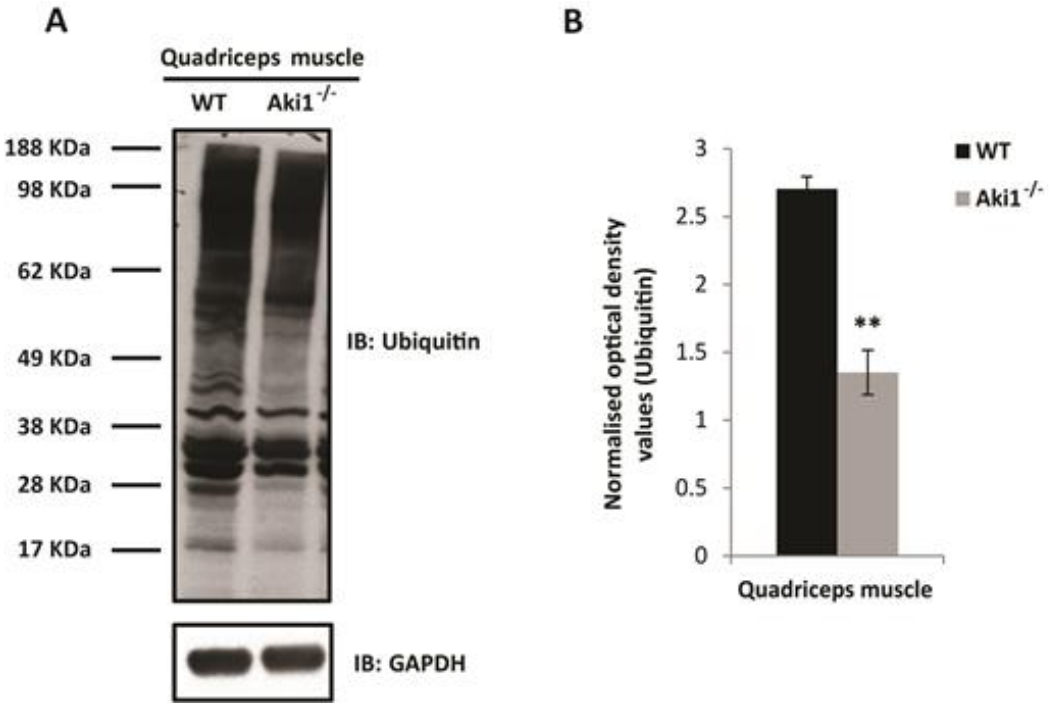

Figure 4.10 Lack of Akirin1 leads to reduced ubiquitination of various cellular proteins due to reduced MuRF1 activity. Analysis of ubiquitination of cellular proteins in Akirin1 knock-out and wild-type *quadriceps* muscle. Western blotting analysis was performed on protein lysates of Akirin1 knock-out and wild-type *quadriceps* muscle. (A) A representative immunoblot showing the extent of ubiquitination of cellular proteins in Akirin1 knock-out and wild-type *quadriceps* muscle. GAPDH was used as the internal control for equal protein loading on the gel. (B) A graph showing corresponding densitometry analysis of ubiquitination in Akirin1 knock-out and wild-type *quadriceps* muscle. (**$p<0.01$) (n=4).

4.11 Absence of Akirin1 leads to reduced levels of CREB-1 protein in skeletal muscle.

One of the important transcription factors that are known to bind to MuRF1 promoter and regulate MuRF1 transcription is CREB-1 (Tobimatsu et al., 2009). But, apart from regulating the expression of MuRF1, CREB-1 is also known to regulate important genes like PPARα and PGC1α, which are involved in cellular energy metabolism homeostasis in skeletal muscle (Thomson et al., 2007; St-Pierre et al., 2003). So, to investigate the regulation of CREB-1 by Akirin1 in fully-differentiated muscle, protein lysates from Akirin1 knock-out and wild-type *quadriceps* muscle were probed with phospho-CREB1 (ser133) and CREB-1 antibodies. The results showed that the protein levels of both phospho-CREB-1 (active form) and total CREB-1 was significantly reduced compared to the wild-type muscle [Figure 4.11.1A(i)]. Densitometry analysis confirmed that both phospho-CREB1 (ser133) (active form) and total CREB-1 protein levels were significantly lower in Akirin1 knock-out *quadriceps* muscle compared to the wild-type [Figure 4.11.1A(ii) and A(iii)]. Further, no significant difference was observed in the ratio of phospho-CREB-1 (active form) to total CREB-1 levels between the Akirin1 knock-out and wild-type muscle [Figure 4.11.2A(iv)]. These results indicate that lack of Akirin1 affects the total CREB-1 protein levels in skeletal muscle. Due to reduced CREB-1 protein levels, the regulation of metabolically important genes like PPARα and PGC1α may further be affected.

On the contrary, when control C_2C_{12} and Akirin1 over-expressors cell protein lysates were subjected to western blotting with anti-phospho-CREB1 (ser133) and anti-CREB-1 antibodies, the results showed reduced levels of phospho-

CREB-1 (active form), while the total CREB-1 protein levels were significantly increased in Akirin1 over-expresssor myoblasts compared to the control C_2C_{12} myoblasts [Figure 4.11.1B(i) lanes 2 and 4, B(ii) and B(iii)]. Futhermore, the ratio of phospho-CREB-1 (active form) to total CREB-1 levels, which is indicative of the inactive CREB-1 levels was significantly reduced in Akirin1 over-expressor myoblasts compared to the control C_2C_{12} myoblasts [Figure 4.11.2A(iv)].

As the CREB-1 protein level was reduced in the absence of Akirin1, we wanted to further investigate the *Creb-1* mRNA expression level. The *Creb-1* mRNA levels were quantified by real time-qPCR and the *Creb-1* Ct values were normalised to *cyclophilin* Ct values. The results showed that there was no significant difference in the amount of *Creb-1* mRNA between Akirin1 knock-out and wild-type *quadriceps* muscles (Figure 4.11.2C). These above findings clearly suggest that Akirin1 regulates CREB-1 protein at the post-transcriptional level in skeletal muscle.

Figure 4.11.1 Absence of Akirin1 leads to reduced levels of CREB-1 protein in skeletal muscle. Western blotting analysis for phospho-CREB-1 (ser 133) and total CREB-1 was performed on protein lysates of Akirin1 knock-out and wild-type *quadriceps* muscle. A(i) A representative immunoblot showing the protein levels of phospho-CREB-1 (ser 133) and total CREB-1. GAPDH was used as the internal loading control. A(ii) and A(iii) Graphs showing corresponding densitometry analysis of phospho-CREB-1 (ser 133) and total CREB-1 levels respectively. (*$p<0.05$ and **$p<0.01$) (n=4). Western blotting was performed on protein lysates from differentiating Akirin1 over-expressor myoblasts and control C_2C_{12} myoblasts. B(i) A representative immunoblot showing the protein levels of phospho-CREB-1 (ser 133) and total CREB-1. B(ii) and B(iii) Graphs showing the corresponding densitometry analysis of phospho-CREB-1 (ser 133) and total CREB-1 protein levels in differentiating Akirin1 over-expressor myoblasts and control C_2C_{12} myoblasts. The graphs are representative of at least two independent experiments. Level of significance was compared to control C_2C_{12} myoblasts (*$p<0.05$ and **$p<0.01$).

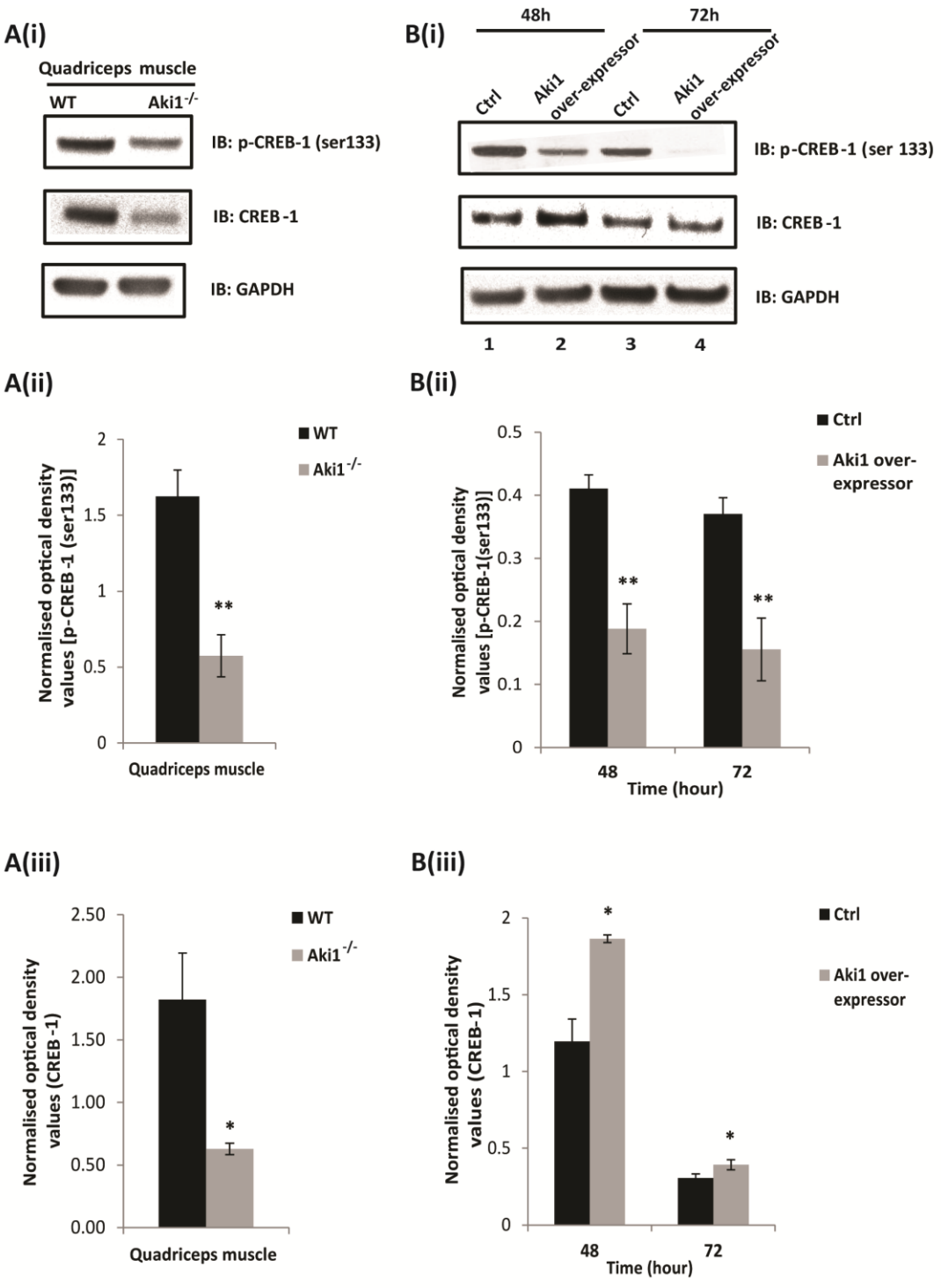
A(i)
Quadriceps muscle
WT
Aki1-/-
IB: p-CREB-1 (ser133)
IB: CREB-1
IB: GAPDH
B(i)
48h
72h
Ctrl
Aki1 over-expressor
Ctrl
Aki1 over-expressor
IB: p-CREB-1 (ser 133)
IB: CREB-1
IB: GAPDH
1
2
3
4
A(ii)
Normalised optical density values [p-CREB-1 (ser133)]
WT
Aki1-/-
Quadriceps muscle
B(ii)
Normalised optical density values [p-CREB-1(ser133)]
Ctrl
Aki1 over-expressor
48
72
Time (hour)
A(iii)
Normalised optical density values (CREB-1)
WT
Aki1-/-
Quadriceps muscle
B(iii)
Normalised optical density values (CREB-1)
Ctrl
Aki1 over-expressor
48
72
Time (hour)

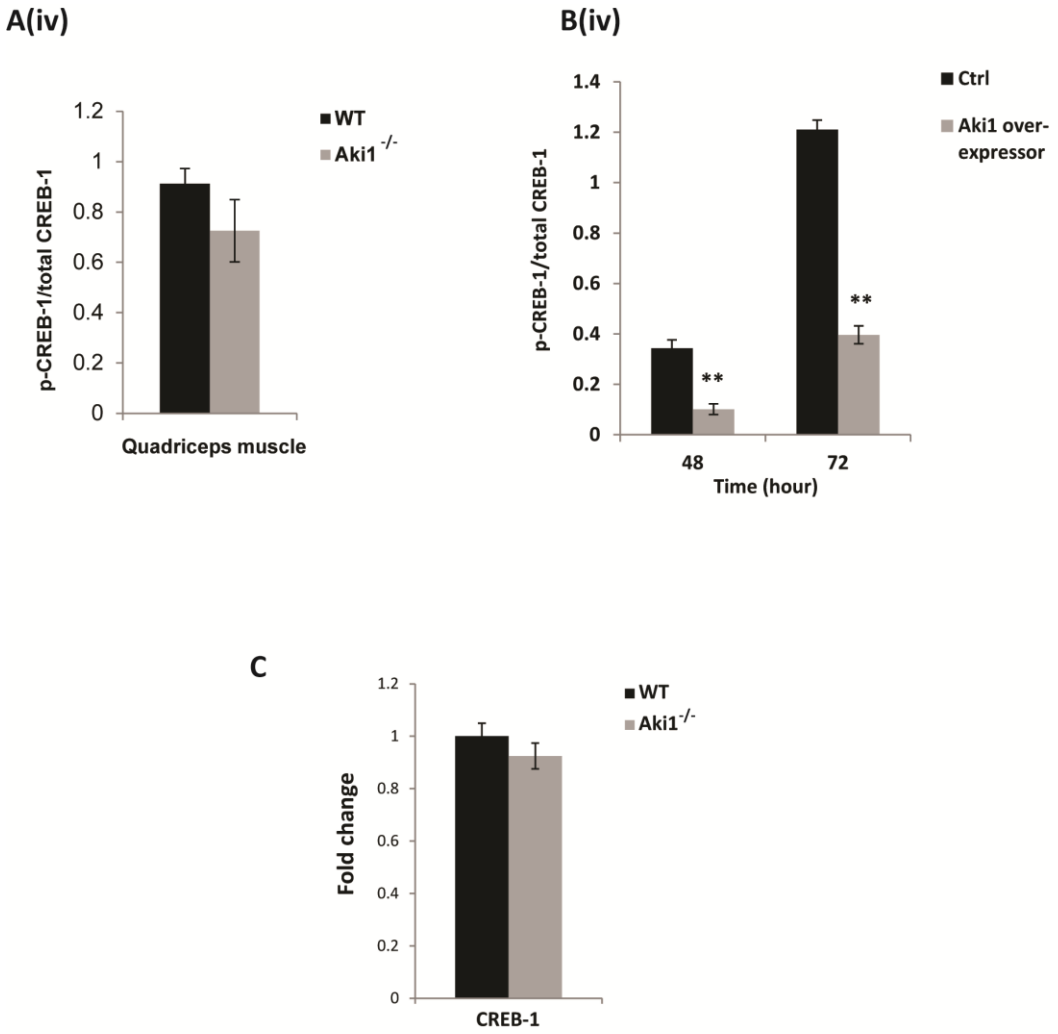

Figure 4.11.2 Akirin1 regulates the levels of active form of CREB-1 protein post-trancriptionally. A(iv) A graph representing the ratio of phospho-CREB-1 (ser 133) to total CREB-1 levels in skeletal muscle (n=4). B(iv) A graph representing the ratio of phospho-CREB-1 (ser 133) to total CREB-1 levels in Akirin1 over-expressor cells. This graph is representative of at least two independent experiments. Level of significance was compared to control C_2C_{12} myoblasts (**$p<0.01$). (C) A graph showing the fold change mRNA expression of *Creb-1* in Akirin1 knock-out *quadriceps* muscle compared to the wild-type. The values are mean ± S.E. of four different animals. Level of significance was compared to wild-type.

4.12 Lack of Akirin1 leads to reduced binding of CREB-1 protein on MuRF1 promoter.

CREB-1 is a leucine zipper protein that binds to cAMP responsive element and initiate transcription of its down-stream target genes like MuRF1. Results in section 4.11 showed that Akirin1 knock-out muscle have lower levels of both total and phospho-CREB-1 protein compared to the wild-type muscle. To further investigate if reduced levels of CREB-1 protein binding to MuRF1 promoter leads to reduced MURF1 levels, Electrophoretic Mobility Shift Assay (EMSA) was performed. Oligonucleotides containing the CREB-1 consensus-binding region on MuRF1 promoter were designed. Nuclear extracts from wild-type and Akirin1 knock-out *quadriceps* muscles were isolated and EMSA was performed using CREB-1 antibody. The results showed significantly lower amounts of CREB-1 protein binding activity in Akirin1 knock-out muscle nuclear extracts compared to the wild-type muscle nuclear extracts (Figure 4.12A lane 2 and 4). The specificity of the band obtained was confirmed by addition of increasing concentration of CREB-1 antibody i.e. 2µg CREB-1 antibody in lane 4 and 5; 4µg CREB-1 antibody in lane 6 and 7. The amount of DNA-CREB-1 complex reduces proportional with increasing concentration of CREB-1 antibody (Figure 4.12A lane 4, 5, 6 and 7). This shows that in the absence of Akirin1, CREB-1 transcription factor binding on MuRF1 promoter is reduced, there by resulting in reduced MuRF1 transcription.

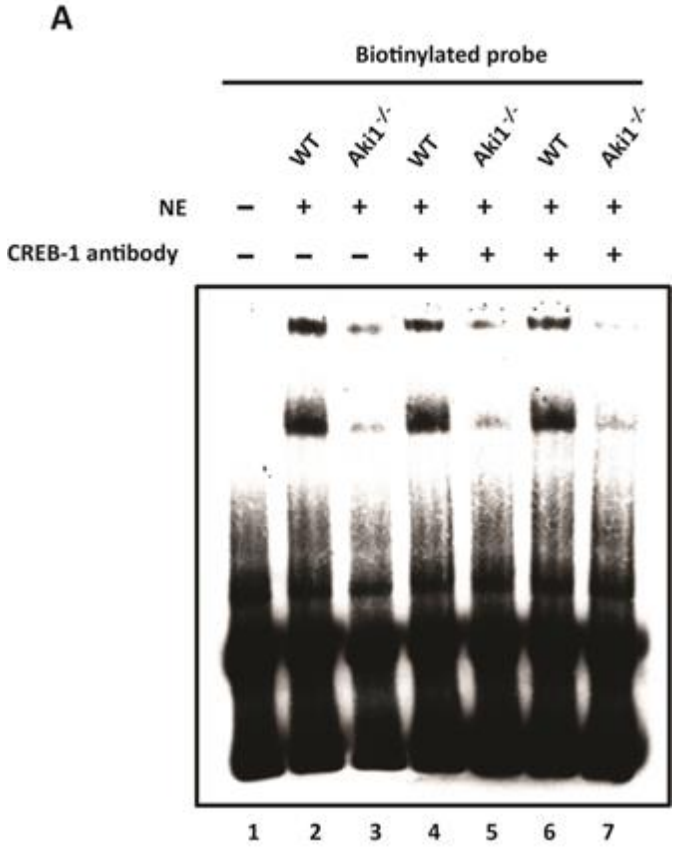

Figure 4.12 Lack of Akirin1 leads to reduced binding of CREB-1 protein on MuRF1 promoter. EMSA was performed using nuclear lysates from Akirin1 knock-out and wild-type *quadriceps* muscle with or without CREB-1 antibody. (A) A representative gel showing reduced CREB-1 binding in Akirin1 knock-out muscle compared to the wild-type as indicated by the shifted band in lane 3 (lane 1-oligo only, lane 2-wild type and lane 3-Akirin1 knock-out). The diminishing band intensity of CREB-1 specific band with increasing CREB-1 antibody concentration (lane 4 and 6).

4.13 Lack of Akirin1 does not significantly affect the Serum Response Factor (SRF) expression in the skeletal muscle.

SRF, a transcription factor belonging to MADS box family of transcription factors, binds to serum response element (SRE) on the promoters of target genes and stimulates its transcription. Also, SRF has been known to be targeted for degradation by MuRF1 (Patterson et al., 2011). As we observed reduced MuRF1 levels in the absence of Akirin1, we investigated the SRF levels in Akirin1 knock-out and wild-type *quadriceps* muscle. Although Akirin1 knock-out muscle showed slightly elevated SRF protein levels compared to wild-type muscle, this increase was not statistically significant [Figure 4.13A(i) and (ii)].

Also, when Akirin1 was over-expressed, no significant difference in SRF protein levels in Akirin1 over-expressor myoblasts was observed compared to control C_2C_{12} myoblasts at 48 and 72 hours of differentiation [Figure 4.13B(i) lane 2 and 4; B(ii)].

SRF mRNA levels were quantified by real time-qPCR in wild-type and Akirin1 knock-out *quadriceps* muscle and normalised to *cyclophilin* Ct values. The results showed that Akirin1 knock-out muscle showed no significant difference in the mRNA level of *SRF* gene when compared to the wild-type muscle (Figure 4.13C).

Figure 4.13 Lack of Akirin1 does not significantly affect the Serum Response Factor (SRF) expression in the skeletal muscle. Analysis of SRF in Akirin1 knock-out and wild-type *quadriceps* muscle. Western blotting analysis was performed on protein lysates of Akirin1 knock-out and wild-type *quadriceps* muscle. A(i) A representative immunoblot showing the protein level of SRF. GAPDH was used as the internal loading control. A(ii) A graph showing corresponding densitometry analysis of SRF protein levels (n=3). Expression analysis of SRF in Akirin1 over-expressor myoblasts. Western blotting was performed on protein lysates from differentiating Akirin1 over-expressor myoblasts and control C_2C_{12} myoblasts. B(i) A representative immunoblot showing the protein level of SRF. B(ii) A graph showing the corresponding densitometry analysis of SRF protein level in Akirin1 over-expressor myoblasts and control C_2C_{12} myoblasts. All the graphs are representative of at least two independent experiments. Level of significance was compared to control C_2C_{12} myoblasts. mRNA expression of *SRF* was determined in Akirin1 knock-out and wild-type *quadriceps* muscle. (C) A graph showing the fold change mRNA expression of *SRF* in Akirin1 knock-out *quadriceps* muscle compared to the wild-type (n=4). Level of significance was compared to wild-type.

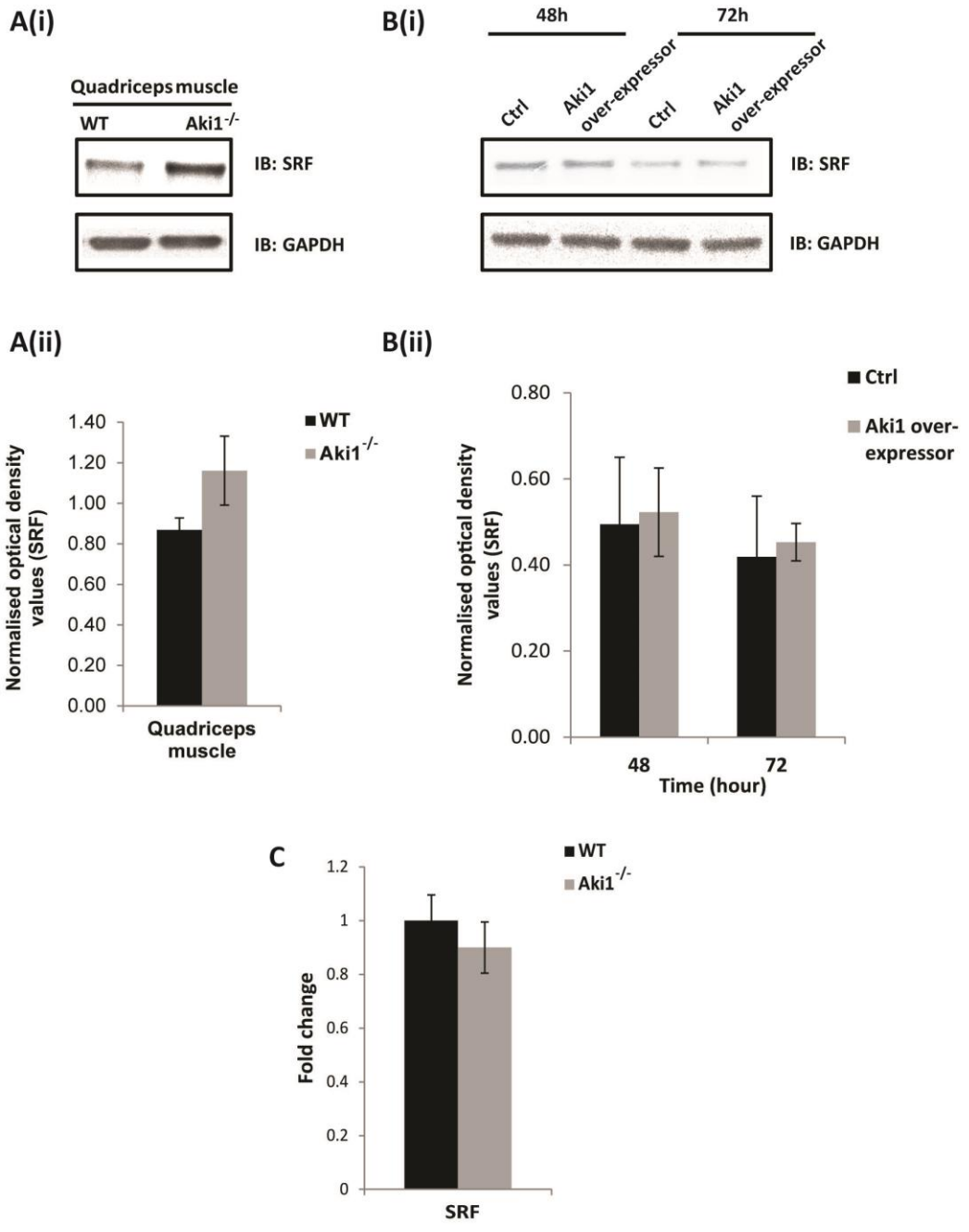
A(i)
Quadriceps muscle
WT
Aki1-/-
IB: SRF
IB: GAPDH
B(i)
48h
72h
Ctrl
Aki1 over-expressor
Ctrl
Aki1 over-expressor
IB: SRF
IB: GAPDH
A(ii)
Normalised optical density values (SRF)
1.40
1.20
1.00
0.80
0.60
0.40
0.20
0.00
WT
Aki1-/-
Quadriceps muscle
B(ii)
Normalised optical density values (SRF)
0.80
0.60
0.40
0.20
0.00
Ctrl
Aki1 over-expressor
48
72
Time (hour)
C
Fold change
1.2
1
0.8
0.6
0.4
0.2
0
WT
Aki1-/-
SRF

4.14 Lack of Akirin1 results in a fiber type switch, from oxidative to fast oxidative fibers in *tibialis anterior* muscle.

Our previous results in quadriceps muscle showed that absence of Akirin1 affected the levels of certain important metabolic proteins like CREB-1, MuRF1 and SRF. So, we wanted to investigate the metabolic profile in a muscle made up of mixed types of fibers such as *tibialis anterior*. As explained in section 1.1.2, a muscle is made up of four types of muscle fibers in mice, which use different metabolic pathways to derive energy for muscle contraction (Talmadge et al., 1993; Lompre et al., 1984). One of the ways to study the metabolic pattern in the skeletal muscle is by identifying the type of MyHC expressed in different muscle fiber types through fiber-typing studies. To investigate this, immunohistochemistry was performed on *tibialis anterior* muscle sections with anti-MyHC type I, anti-MyHC type IIa and anti-MyHC type IIb antibodies which recognize myofibers containing specific type of MyHC protein. Fiber typing images revealed that Akirin1 knock-out *tibialis anterior* muscle sections have significantly lower number of MyHC type I fibers compared to the wild-type *tibialis anterior* muscle sections. Also, Akirin1 knock-out muscle sections showed significantly higher number of MyHC type IIa fibers compared to the wild-type muscle sections. However the number of MyHC type IIb fibers remain the same in Akirin1 knock-out compared to wild-type muscle sections (Figure 4.14.1A and B).

To investigate whether the fiber type switch was due to differential gene expression of MyHC type in the muscle fibers, real time-qPCR was performed on Akirin1 knock-out and wild-type *quadriceps* muscle which is also a mixed fiber type muscle. Consistent with the immunohistochemistry results, Akirin1

knock muscle showed significantly lower *Myh7* (MyHC type I) mRNA expression compared to the wild-type muscle (Figure 4.14.2A). Furthermore, the mRNA level of *Myh2* (MyHC type IIa) was also significantly higher in Akirin1 knock-out muscle when compared to the wild-type muscle (Figure 4.14.2B). However, the mRNA levels of *Myh4* (MyHC type IIb) was unchanged Figure 4.14.2C). All these results suggest that lack of Akirin1 results in a fiber type switch, from oxidative (type I) to fast oxidative (type IIa) fibers in the skeletal muscle.

Figure 4.14.1 Lack of Akirin1 results in a fiber type switch, from oxidative to fast oxidative fibers in *tibialis anterior* muscle. (A) Panel showing the different types of MyHC (type I, type IIa and type IIb) staining on Akirin1 knock-out and wild-type *tibialis anterior* muscle sections. (B) Quantification of number of myofibers stained positive for different MyHC types (type I, type IIa and type IIb) in Akirin1 knock-out and wild-type *quadriceps* muscle sections. The values are mean ± S.E. of two animals. Level of significance was compared to Wild-type (***$p<0.001$).

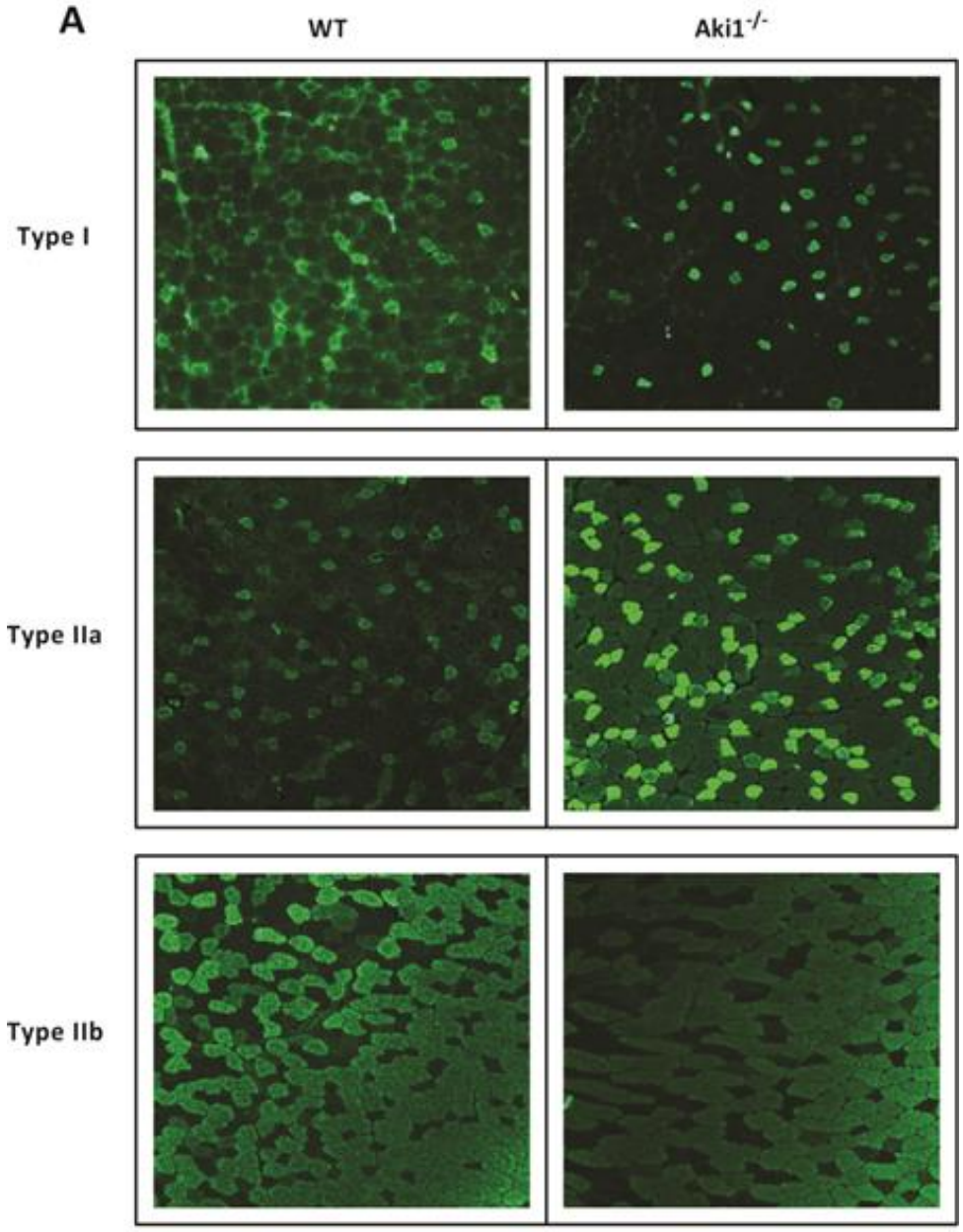
A
WT
Aki1-/-
Type I
Type IIa
Type IIb

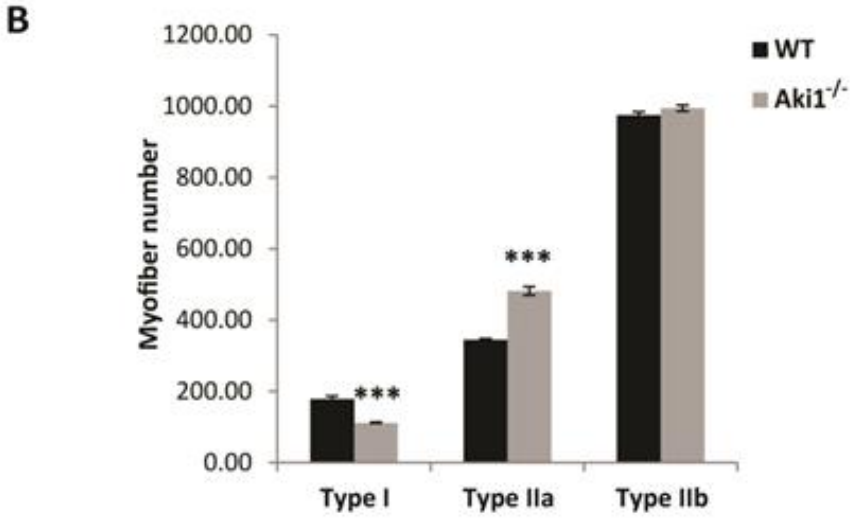
B
1200.00
1000.00
800.00
600.00
400.00
200.00
0.00
Myofiber number
WT
Aki1-/-
***
***
Type I
Type IIa
Type IIb

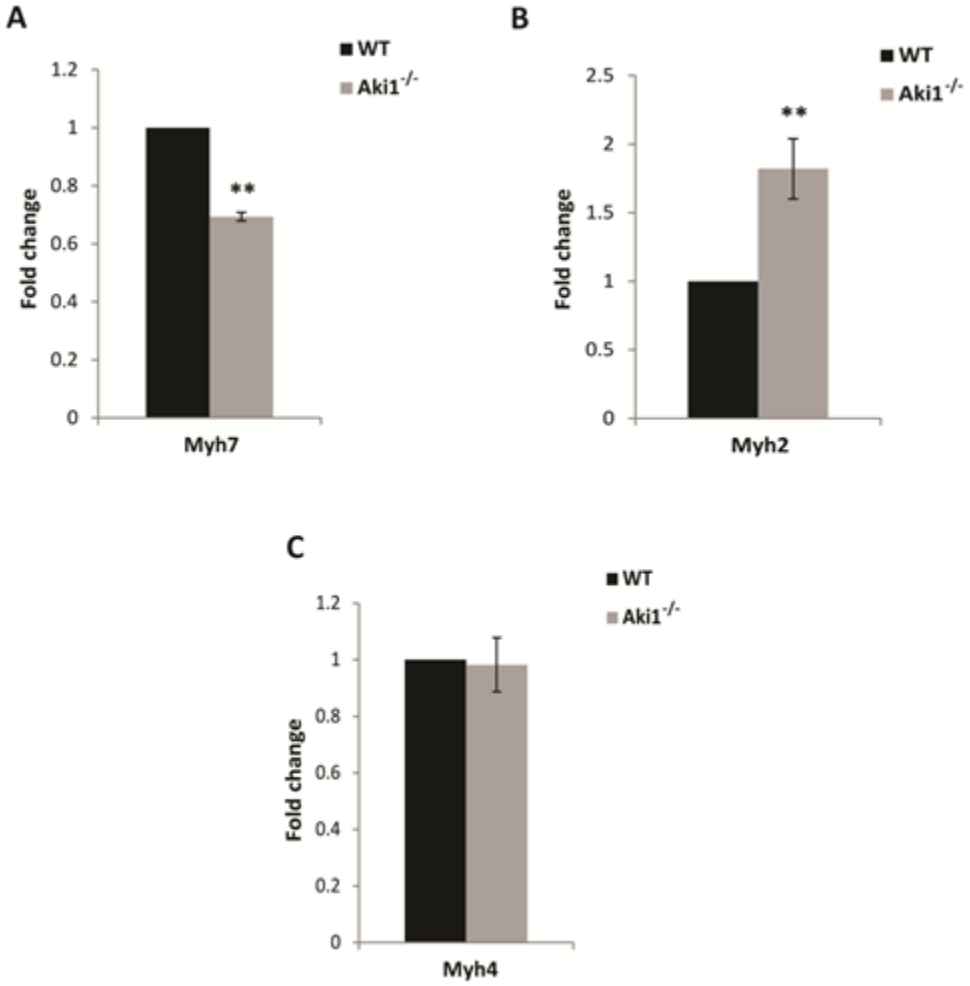

Figure 4.14.2 Gene expression profile of different types of *Myh* genes in Akirin1 knock-out *quadriceps* muscle. mRNA expression of *Myh7, Myh2* and *Myh4* was determined in Akirin1 knock-out and wild-type *quadriceps* muscle. (A), (B) and (C) Graphs showing the fold change mRNA expression of *Myh7, Myh2* and *Myh4* in Akirin1 knock-out *quadriceps* muscle respectively. The values are mean ± S.E. of four different animals. Level of significance was compared to wild-type (**p<0.01).

4.15 Lack of Akirin1 makes the muscle fibers less oxidative.

To further confirm that lack of Akirin1 affects the oxidative potential of the skeletal muscle, Akirin1 knock-out and wild-type muscle *tibialis anterior* sections were stained for succinate dehydrogenase (SDH), an important enzyme in citric acid cycle and α-glycerophosphate dehydrogenase (α-GPD), an important enzyme in glycolysis pathway. Histochemistry results revealed that Akirin1 knock-out muscle sections have significantly lower SDH staining compared to the wild-type sections (Figure 4.15A). The normalised optical density also showed significant reduction of SDH staining in Akirin1 knock-out muscle sections compared to the wild-type (Figure 4.15B). However, there was no significant difference in α-GPD staining between Akirin1 knock-out and wild-type muscle sections (Figure 4.15C and D).

Figure 4.15 Lack of Akirin1 makes the muscle fibers less oxidative. (A) Panel showing representative succinate dehydrogenase (SDH) staining in Akirin1 knock-out and wild-type *tibialis anterior* muscle sections. Scale bar represents 100 μm. (B) Quantification of optical density of SDH staining in Akirin1 knock-out and wild-type *tibialis anterior* muscle sections. The values are mean ± S.E. of three animals. Level of significance was compared to wild-type (***$p<0.001$). (C) Panel showing representative α-glycerophosphate dehydrogenase (α-GPD) staining in Akirin1 knock-out and wild-type *tibialis anterior* muscle sections. Scale bar represents 100 μm. (D) Quantification of optical density of α-GPD staining in Akirin1 knock-out and wild-type *tibialis anterior* muscle sections. The values are mean ± S.E. of three animals.

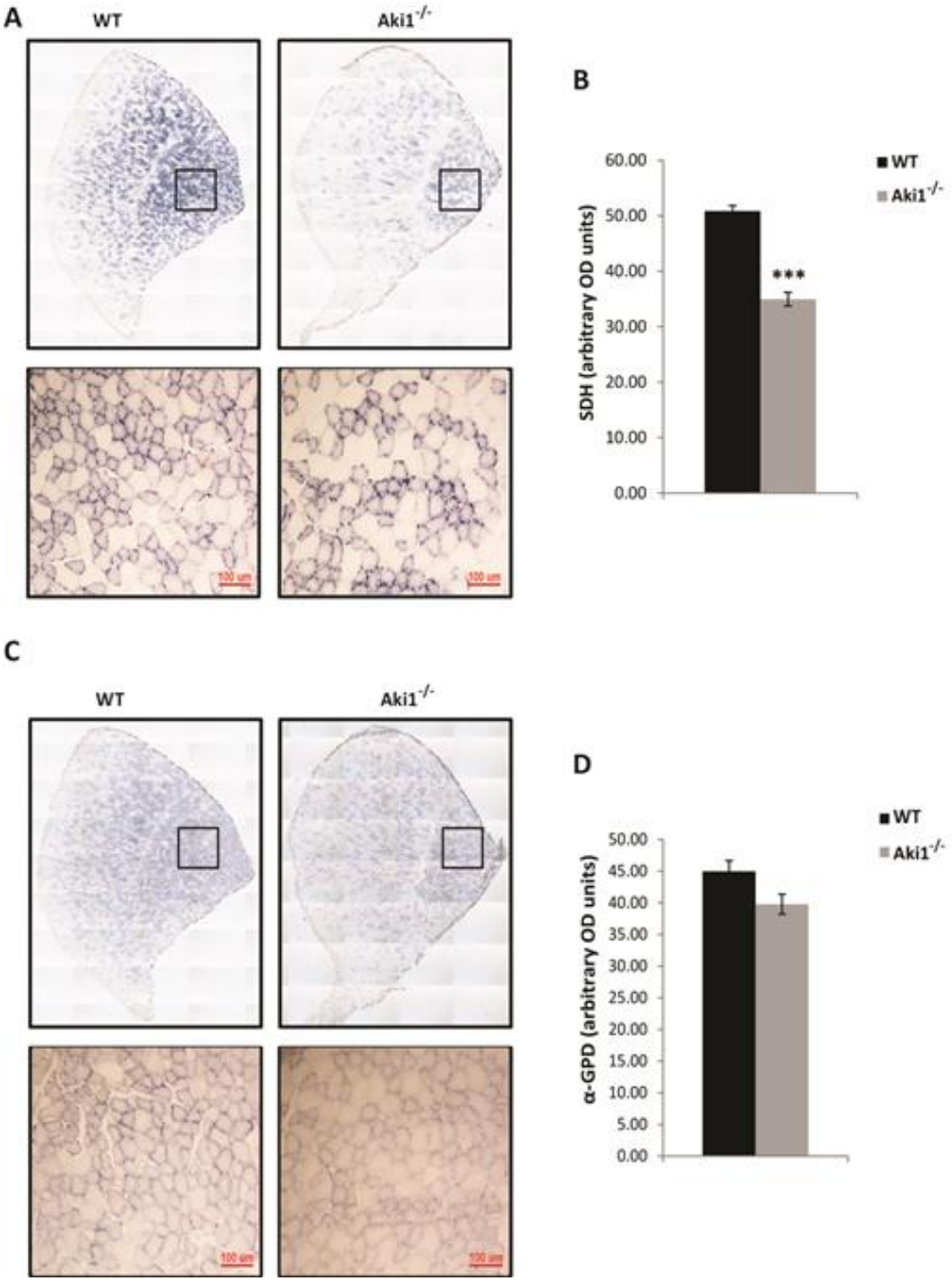
A
WT
Aki1-/-
100 um
100 um
B
60.00
50.00
40.00
30.00
20.00
10.00
0.00
SDH (arbitrary OD units)
***
WT
Aki1-/-
C
WT
Aki1-/-
100 um
100 um
D
50.00
45.00
40.00
35.00
30.00
25.00
20.00
15.00
10.00
5.00
0.00
α-GPD (arbitrary OD units)
WT
Aki1-/-

4.16 Absence of Akirin1 leads to reduced mitochondrial DNA copy number in skeletal muscle.

Reduced CREB-1 levels have been shown to down-regulate its target genes like PPARα and PGC1α. Thus, leading to reduced oxidative potential of the skeletal muscle and affecting the energy homeostasis (Thomson et al., 2007; St-Pierre et al., 2003). Other research groups have also shown that the amount of ATP generated through oxidative phosphorylation in the mitochondria is proportional to the mitochondrial DNA copy number (Chen et al., 2010; Dickinson et al., 2013). So, copy number of mitochondrial DNA (mtDNA) per nuclear DNA (nuDNA) ratio was estimated by performing real time-qPCR with specific set of primers for mtDNA and nuDNA. The results showed that Akirin1 knock-out *quadriceps* muscle contained significantly lower mtDNA per nuDNA ratio compared to the wild-type muscle (Figure 4.16A). Thus showing that lack of Akirin1 reduces the mitochondrial DNA copy number in skeletal muscle, there by affecting the oxidative potential of the skeletal muscle.

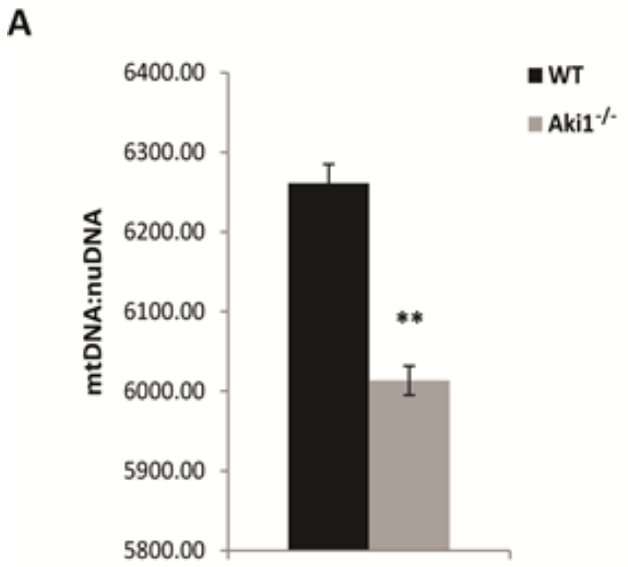

Figure 4.16 Absence of Akirin1 leads to reduced mitochondrial DNA copy number in skeletal muscle. (A) Graph showing the copy number of mitochondrial DNA (mtDNA) per nuclear DNA (nuDNA) ratio in Akirin1 knock-out and wild-type *quadriceps* muscle. (**p<0.01) (n=3).

Figure 4.17 Lack of Akirin1 regulates the protein levels of AMPK in skeletal muscle. Western blotting analysis for AMPKα was performed on protein lysates of Akirin1 knock-out and wild-type *quadriceps* muscle. A(i) A representative immunoblot showing the protein level of AMPKα. GAPDH was used as the internal control for equal protein loading on the gel. A(ii) A graph showing corresponding densitometry analysis of AMPKα level. (*$p<0.05$) (n=4). Expression analysis of AMPKα in Akirin1 over-expressor myoblasts during differentiation. Western blotting was performed on protein lysates from differentiating Akirin1 over-expressor myoblasts and control C_2C_{12} myoblasts. B(i) A representative immunoblot showing the protein level of AMPKα. B(ii) A graph showing the corresponding densitometry analysis of AMPKα protein level in differentiating Akirin1 over-expressor myoblasts and control C2C12 myoblasts. All the graphs are representative of at least two independent experiments. Level of significance was compared to control C_2C_{12} myoblasts (*$p<0.05$). mRNA expression of *AMPKα2* was determined in Akirin1 knock-out and wild-type *quadriceps* muscle. (C) A graph showing the fold change mRNA expression of *AMPKα2* in Akirin1 knock-out *quadriceps* muscle compared to the wild-type. The values are mean ± S.E. of four different animals.

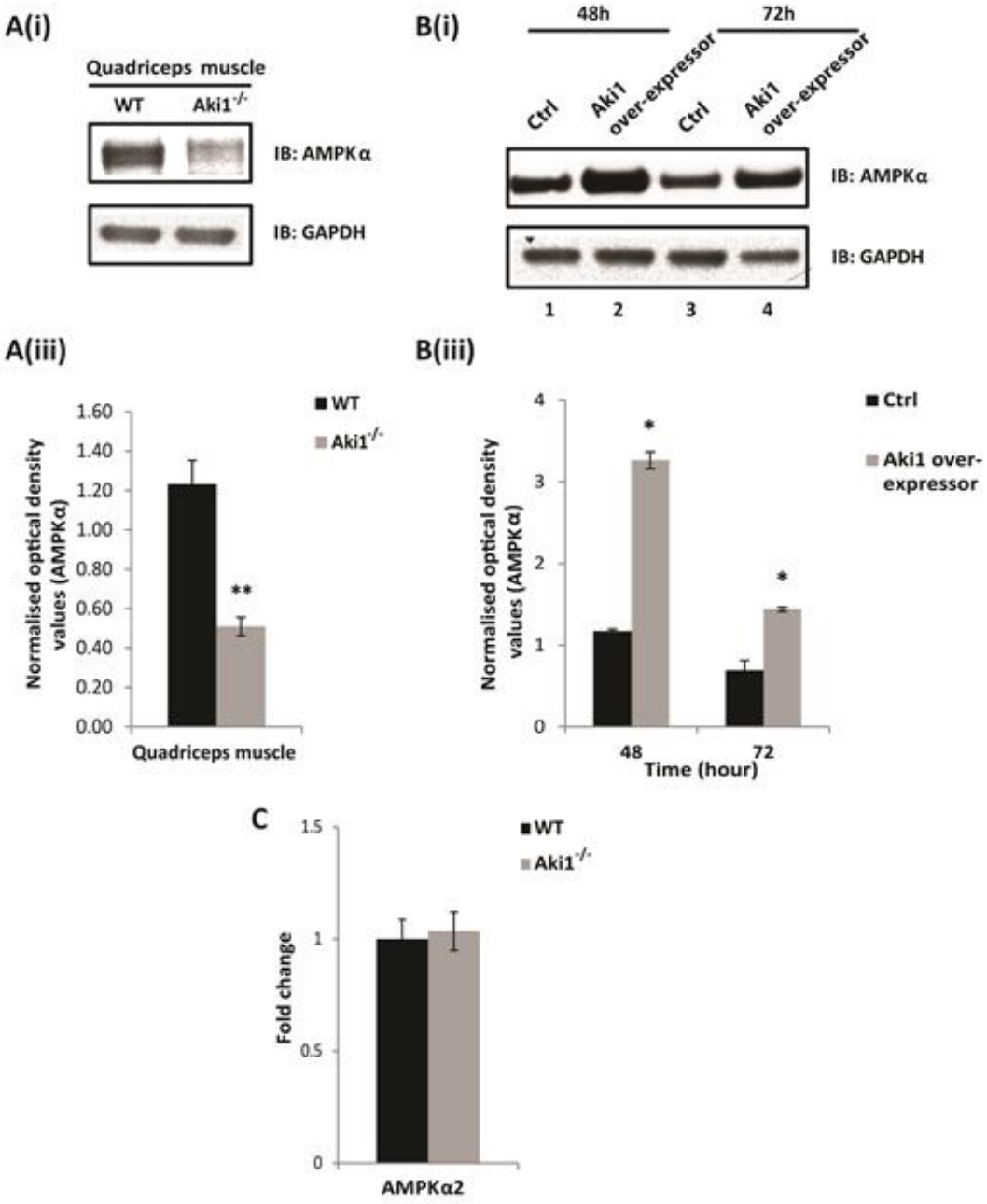
A(i)
Quadriceps muscle
WT
Aki1-/-
IB: AMPKα
IB: GAPDH
B(i)
48h
72h
Ctrl
Aki1 over-expressor
Ctrl
Aki1 over-expressor
IB: AMPKα
IB: GAPDH
1
2
3
4
A(iii)
WT
Aki1-/-
Normalised optical density values (AMPKα)
1.60
1.40
1.20
1.00
0.80
0.60
0.40
0.20
0.00
**
Quadriceps muscle
B(iii)
Ctrl
Aki1 over-expressor
Normalised optical density values (AMPKα)
4
3
2
1
0
*
*
48
72
Time (hour)
C
WT
Aki1-/-
Fold change
1.5
1
0.5
0
AMPKα2

4.17 Lack of Akirin1 regulates the protein levels of AMPK in skeletal muscle.

Skeletal muscle is a highly metabolic tissue that quickly responds and adapts to the various energy fluctuations in the body. One of the most important proteins that help in maintaining the energy metabolism in skeletal muscle is AMPK. Being known as a "metabolic master switch", AMPK senses the ATP levels and mediates the cellular adaptation to nutritional and environmental variations. As results from section 4.15 and 4.16 showed that Akirin1 knock-out muscle is less oxidative compared to the wild-type muscle, we wanted to investigate the AMPKα protein level in Akirin1 knock-out muscle. Protein levels of AMPKα were reduced in Akirin1 knock-out *quadriceps* muscle compared to the wild-type [Figure 4.17A(i) and A(ii)].

To validate if AMPK protein levels are indeed regulated by Akirin1, we analyzed AMPK levels in Akirin1 over-expressor cells and control C_2C_{12} cells. Akirin1 over-expressor cells showed significantly higher levels of AMPKα protein levels at 48 and 72 hours of differentiation [Figure 4.17B(i) lanes 2 and 4; B(ii)] .

As AMPKα protein level was reduced in Akirin1 knock-out muscle, we wanted to investigate if the *AMPKα2* expression was down-regulated at mRNA level in the absence of Akirin1. For this, *AMPKα2* mRNA levels were quantified by real time-qPCR and the *AMPKα2* Ct values were normalised to *cyclophilin* Ct values. Results showed that there was no significant difference in the amount of *AMPKα2* mRNA between Akirin1 knock-out and wild-type muscles (Figure 4.17C). These results together indicate that Akirin1 regulates the expression of AMPKα post-transcriptionally in skeletal muscle.

4.18 Protein levels of PPARα and PGC1α are affected in the absence of Akirin1 in skeletal muscle.

Activation of AMPK triggers a number of downstream effectors, which together maintain the energy homeostasis. The important downstream molecules of AMPK that play an important role in ATP synthesis through oxidative phosphorylation are Peroxisome Proliferator Activated Receptor-α (PPARα) and its coactivator Peroxisome proliferator-activated receptor gamma coactivator 1-alpha (PGC-1α). These two proteins interact and induce transcription of various genes, making the skeletal muscle oxidative in nature. Other studies have shown that over-expression of PPARα result in fiber-type switch, from glycolytic (type II) to oxidative (type I) (Holst et al., 2003).

As Akirin1 knock-out muscle is less oxidative, we wanted to ascertain if downstream signaling of AMPK is affected via PPARα and PGC1α. For this, Akirin1 knock-out and wild-type *quadriceps* muscle protein lysates were subjected to western blotting with anti-PPARα and anti-PGC1α antibodies. The results showed that Akirin1 knock-out muscle showed significantly lower levels of both the proteins compared to the wild-type muscle [Figure 4.18.1A(i), A(ii) and A(iii)].

On the contrary, PGC1α protein level was significantly up-regulated when Akirin1 was over-expressed compared to control C_2C_{12} myoblasts at 48 and 72 hours of differentiation. However, PPARα protein level was unchanged. [Figure 4.18.1B(i) lane 2 and 4; B(ii) and B(iii)].

As the absence of Akirin1 down-regulated the protein levels of PPARα and PGC1α in *quadriceps* muscle, we analyzed the expression of these two genes by real time-qPCR in wild-type and Akirin1 knock-out *quadriceps* muscle and

normalised to *cyclophilin* Ct values. The results showed that Akirin1 knock-out muscle showed no significant difference in the mRNA levels of both *PPARα* and *PGC1α* genes when compared to the wild-type muscle (Figure 4.18.2 A and B). These results together suggest that Akirin1 regulates PPARα and PGC1α post-transcriptionally.

Figure 4.18.1 Akirin1 regulates the downstream target of AMPK, PPARα and PGC1α, thus affecting the transcription of energy homeostasis genes in skeletal muscle. Analysis of PPARα and PGC1α levels in Akirin1 knock-out *quadriceps* muscle and Akirin1 over-expressor myoblasts. Western blotting analysis for PPARα and PGC1α was performed on protein lysates of Akirin1 knock-out and wild-type *quadriceps* muscle. A(i) A representative immunoblot showing the protein levels of PPARα and PGC1α. GAPDH was used as the internal control for equal protein loading on the gel. A(ii) and A(iii) Graphs showing corresponding densitometry analysis of PPARα and PGC1α levels respectively. (**$p<0.01$) (n=4). Expression analysis of PPARα and PGC1α in Akirin1 over-expressing myoblasts. Western blotting was performed on protein lysates from differentiating Akirin1 over-expressor myoblasts and control C_2C_{12} myoblasts. B(i) A representative immunoblot showing the protein levels of PPARα and PGC1α. B(ii) and B(iii) Graphs showing the corresponding densitometry analysis of PPARα and PGC1α protein levels in Akirin1 over-expressor myoblasts and control C_2C_{12} myoblasts. All the graphs are representative of at least two independent experiments. Level of significance was compared to control C_2C_{12} myoblasts (*$p<0.05$).

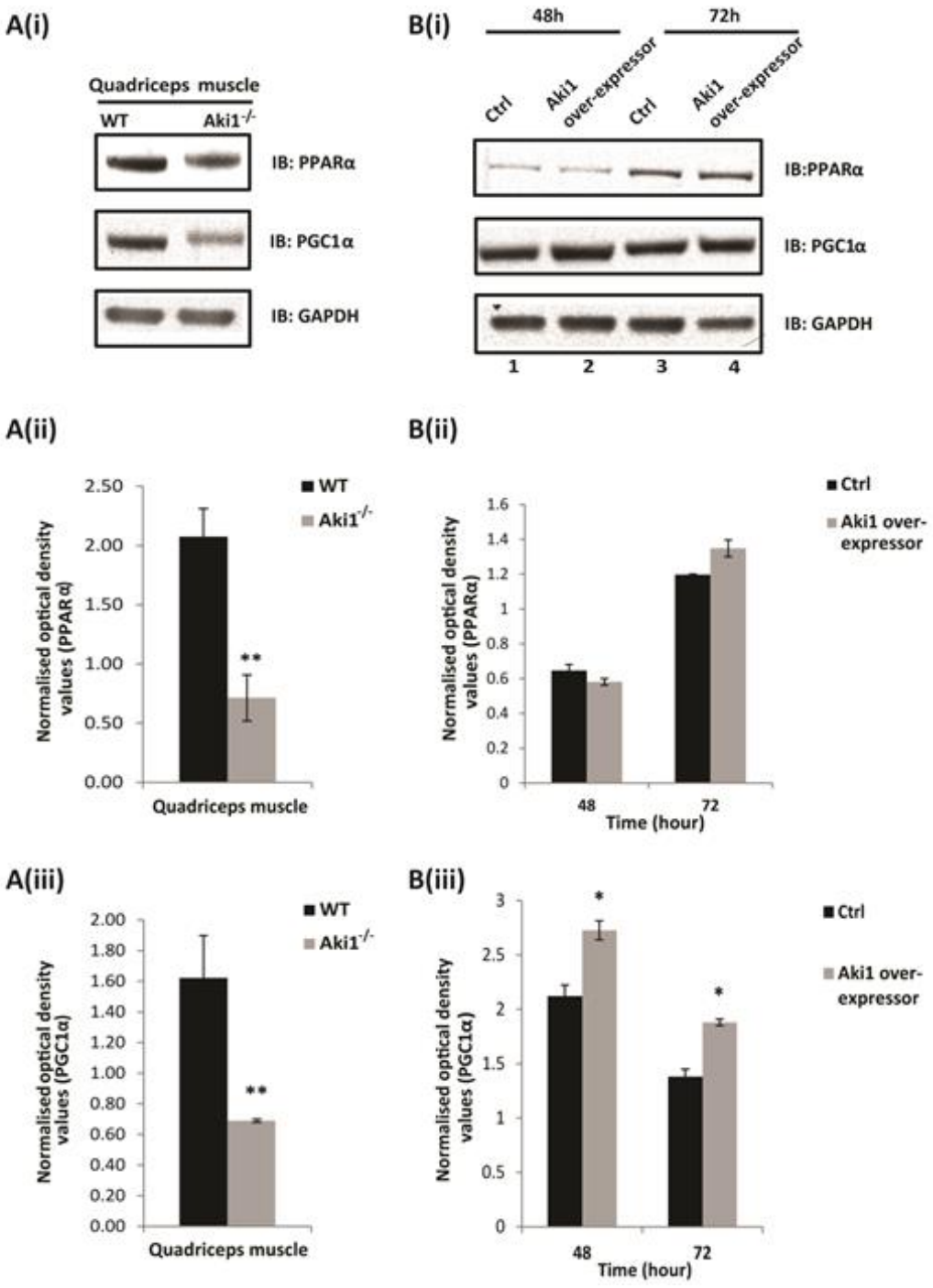
A(i)
Quadriceps muscle
WT
Aki1-/-
IB: PPARα
IB: PGC1α
IB: GAPDH
B(i)
48h
72h
Ctrl
Aki1 over-expressor
Ctrl
Aki1 over-expressor
IB:PPARα
IB: PGC1α
IB: GAPDH
1
2
3
4
A(ii)
WT
Aki1-/-
Normalised optical density values (PPAR α)
2.50
2.00
1.50
1.00
0.50
0.00
**
Quadriceps muscle
B(ii)
Ctrl
Aki1 over-expressor
Normalised optical density values (PPARα)
1.6
1.4
1.2
1
0.8
0.6
0.4
0.2
0
48
72
Time (hour)
A(iii)
WT
Aki1-/-
Normalised optical density values (PGC1α)
2.00
1.80
1.60
1.40
1.20
1.00
0.80
0.60
0.40
0.20
0.00
**
Quadriceps muscle
B(iii)
Ctrl
Aki1 over-expressor
Normalised optical density values (PGC1α)
3
2.5
2
1.5
1
0.5
0
*
*
48
72
Time (hour)

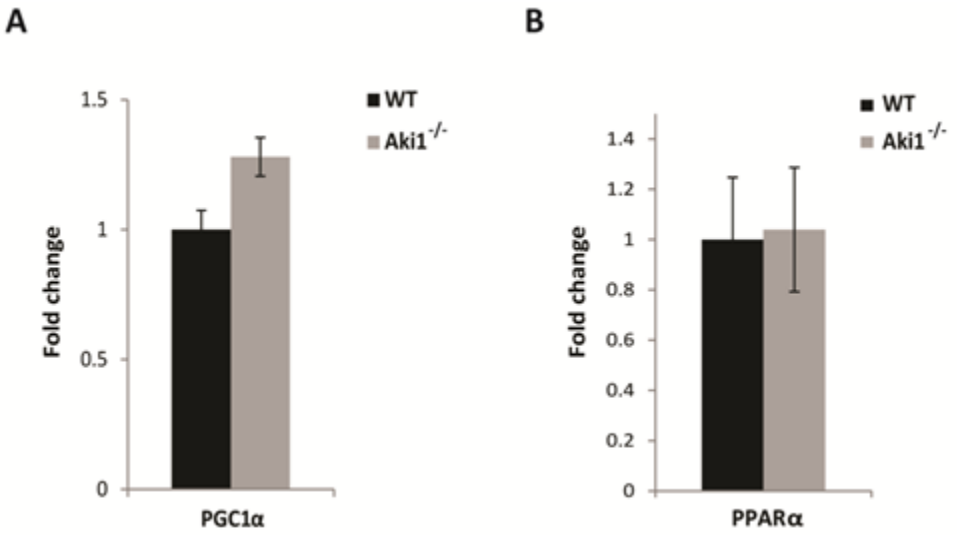

Figure 4.18.2 Akirin1 post-trancriptionally regulates PPARα and PGC1 α in skeletal muscle. mRNA expression of *PPARα* and *PGC1α* was determined in Akirin1 knock-out and wild-type *quadriceps* muscle. (A) and (B) Graphs showing the fold change mRNA expression of *PPARα* and *PGC1α* in Akirin1 knock-out *quadriceps* muscle respectively. The values are mean ± S.E. of four different animals.

4.19 Akirin1 negatively regulates HDAC4 in skeletal muscle.

Histones play an important function in epigenetic regulation of transcription thus affecting various processes like developmental events and cell cycle progression etc. Histones can be acetylated or deacetylated leading to conformational changes in chromosome structure and restricting the access of transcription factors to the DNA. One of the most important histone modifying enzymes is HDAC4, which belong to class II histone deacetylase family. HDAC4 possess the ability to deacetylated the histone proteins and thus repressing the transcription of various promoters. One of the upstream regulators of HDAC4 is AMPK. As we observed reduced levels of AMPK in Akirin1 knock-out mice (Figure 4.17), we wanted to investigate the levels of HDAC4. For this, western blotting was performed on Akirin1 knock-out and wild-type *quadriceps* muscle protein lysates with anti-HDAC4 antibody. The results showed significantly increased levels of HDAC4 protein in Akirin1 knock-out muscle when compared to wild-type muscle [Figure 4.19A(i) and (ii)].

On the contrary, when Akirin1 was over-expressed, HDAC4 protein levels were significantly down-regulated in Akirin1 over-expressor myoblasts compared to control C_2C_{12} myoblasts at 48 and 72 hours of differentiation [Figure 4.19B(i) lane 2 and 4; B(ii)].

HDAC4 mRNA levels were quantified by real time-qPCR in wild-type and Akirin1 knock-out *quadriceps* muscle and normalised to *cyclophilin* Ct values. The results showed no significant difference in the mRNA level of *HDAC4* gene between Akirin1 knock-out and wild-type muscle (Figure 4.19C). These results suggest that Akirin post-transcriptionally regulates HDAC4 expression in skeletal muscle.

Figure 4.19 Akirin1 negatively regulates HDAC4 in skeletal muscle. Analysis of HDAC4 levels in Akirin1 knock-out *quadriceps* muscle and Akirin1 over-expressor myoblasts. Western blotting analysis for HDAC4 was performed on protein lysates of Akirin1 knock-out and wild-type *quadriceps* muscle. A(i) A representative immunoblot showing the protein level of HDAC4. GAPDH was used as the internal control for equal protein loading on the gel. A(ii) A graph showing corresponding densitometry analysis of HDAC4 protein level. (***$p<0.001$) (n=4). Expression analysis of HDAC4 in Akirin1 over-expressor myoblasts. Western blotting was performed on protein lysates from differentiating Akirin1 over-expressor myoblasts and control C_2C_{12} myoblasts. B(i) A representative immunoblot showing the protein level of HDAC4. B(ii) A graph showing the corresponding densitometry analysis of HDAC4 protein level in Akirin1 over-expressor myoblasts and control C_2C_{12} myoblasts. All the graphs are representative of at least two independent experiments. Level of significance was compared to control C_2C_{12} myoblasts (*$p<0.05$). mRNA expression of *Hdac4* was determined in Akirin1 knock-out and wild-type *quadriceps* muscle. (C) A graph showing the fold change mRNA expression of *Hdac4* in Akirin1 knock-out *quadriceps* muscle compared to the wild-type. The values are mean ± S.E. of four different animals.

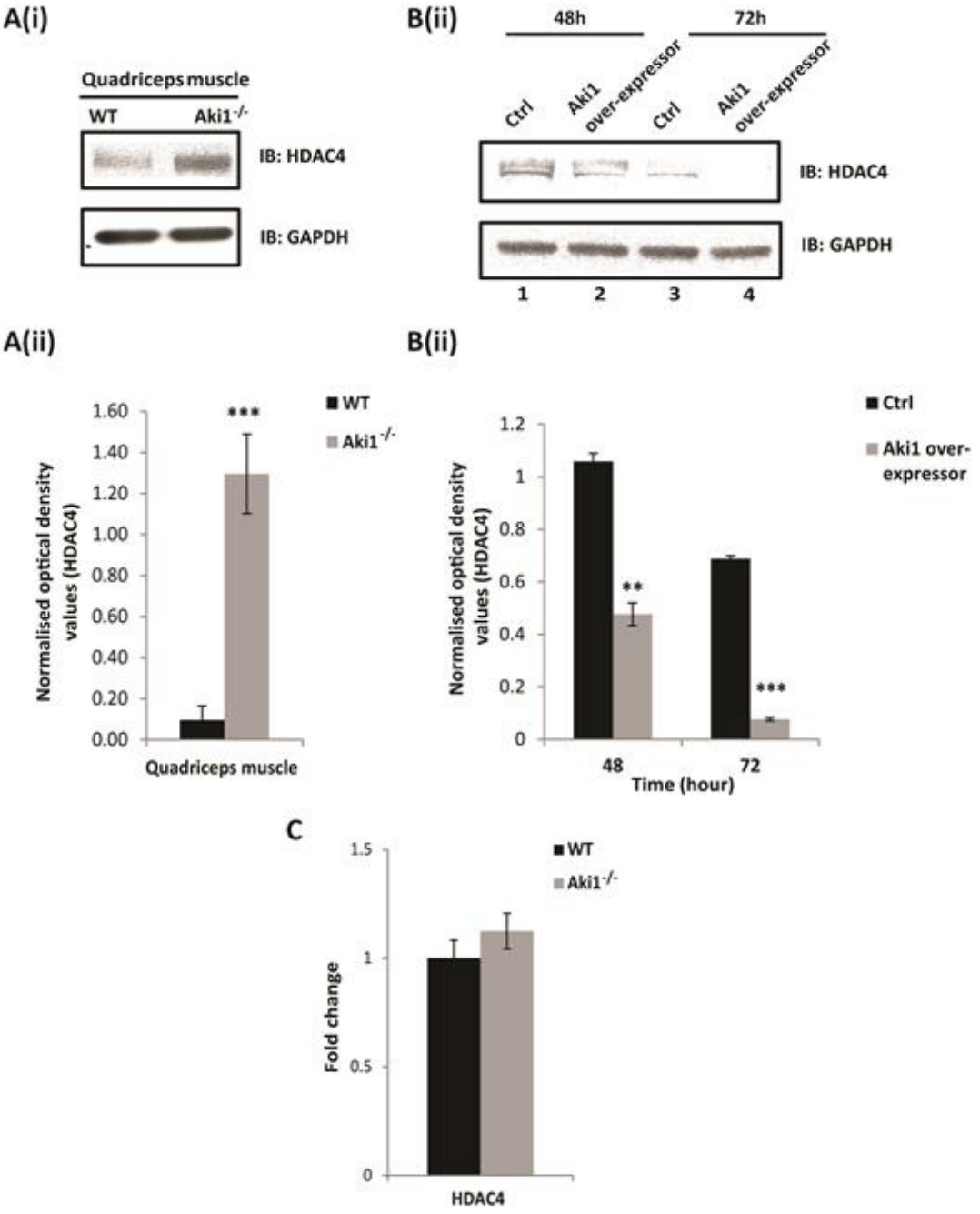
A(i)
Quadriceps muscle
WT
Aki1-/-
IB: HDAC4
IB: GAPDH
B(ii)
48h
72h
Ctrl
Aki1 over-expressor
Ctrl
Aki1 over-expressor
IB: HDAC4
IB: GAPDH
1
2
3
4
A(ii)
Normalised optical density values (HDAC4)
1.60
1.40
1.20
1.00
0.80
0.60
0.40
0.20
0.00
***
WT
Aki1-/-
Quadriceps muscle
B(ii)
Normalised optical density values (HDAC4)
1.2
1
0.8
0.6
0.4
0.2
0
**
***
Ctrl
Aki1 over-expressor
48
72
Time (hour)
C
Fold change
1.5
1
0.5
0
WT
Aki1-/-
HDAC4

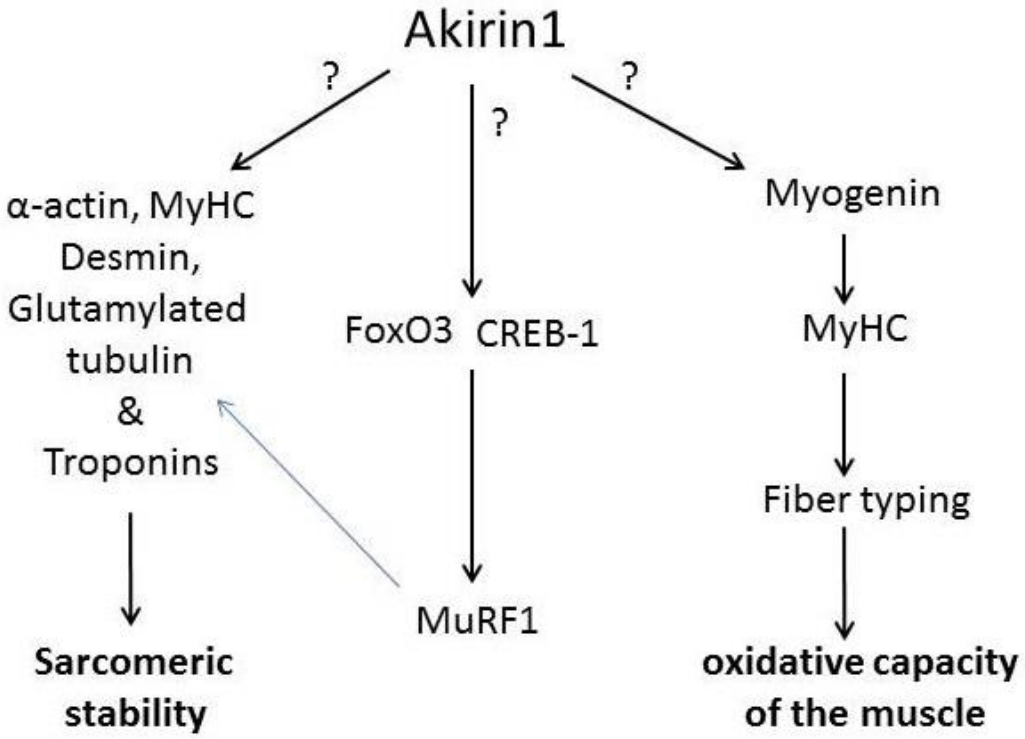

Figure 4.20 A schematic diagram summarizing the various results obtained in understanding the possible role of Akirin1 in fully differentiated skeletal muscle.

CHAPTER 5

ROLE OF AKIRIN1 IN CARDIAC MUSCLE

5. ROLE OF AKIRIN1 IN CARDIAC MUSCLE

This chapter explains the results, which help us in understanding the role of Akirin1 in cardiac muscle. The materials and methods used in this chapter are discussed in chapter 2 of this thesis.

RESULTS

5.1 Lack of Akirin1 leads to cardiac hypertrophy.

To understand the effect of Akirin1 in cardiac muscle, we primarily investigated the size of Akirin1 knock-out and wild-type hearts. Ex-vivo Akirin1 knock-out heart showed no significant difference in heart size compared to the wild-type (Figure 5.1A). We examined the weights of the heart and calculated as percentage body weight. The results showed no significant difference in the heart weights between Akirin1 knock-out and wild-type mice (Figure 5.1B). Further, to investigate the effect of Akirin1 on cardiac muscle histology, whole hearts were transversely and longitudinally sectioned and stained with hematoxylin and eosin. The histology images revealed that the ventricular cavities were larger in Akirin1 knock-out heart compared to the wild-type heart (Figure 5.1C).

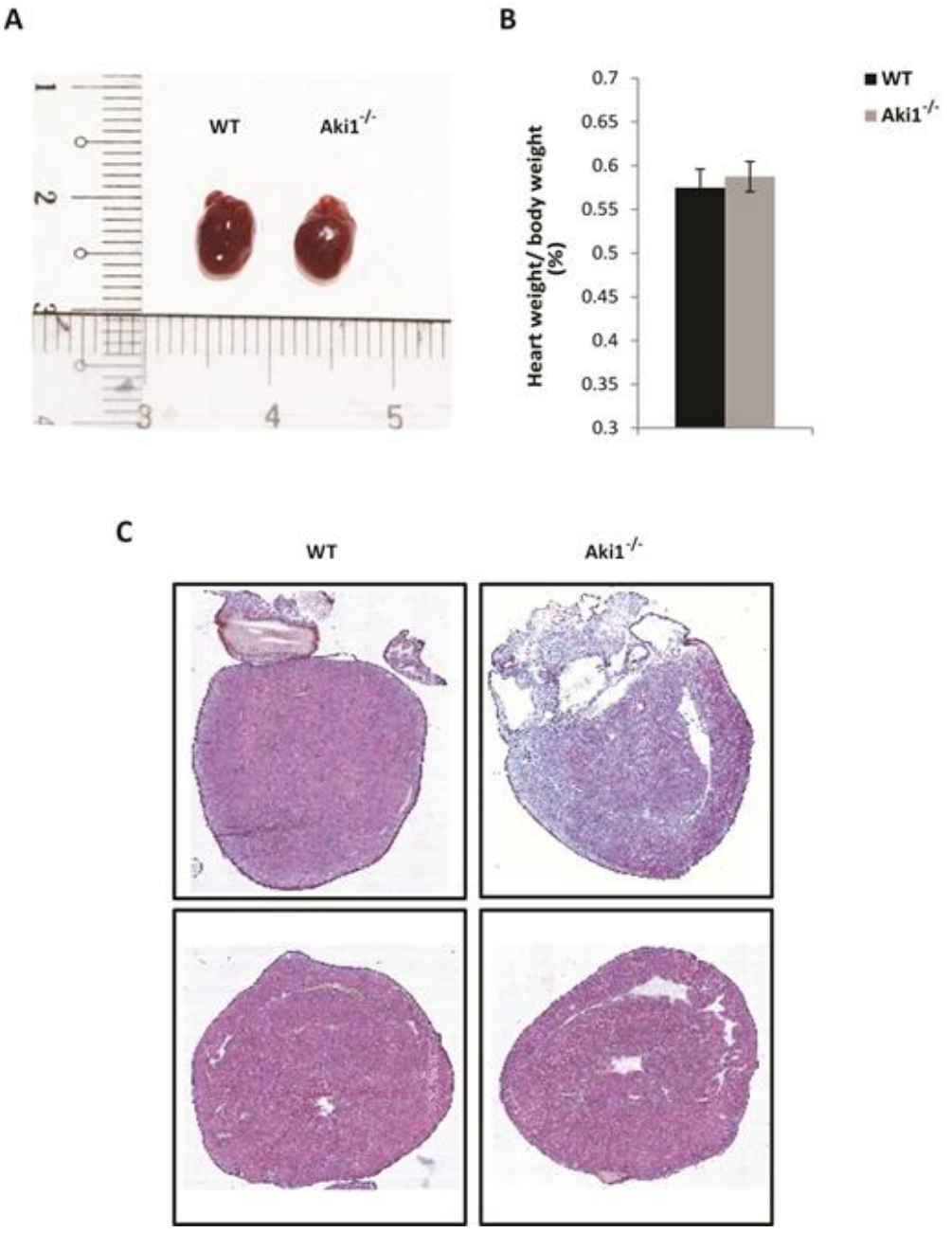

Figure 5.1 Lack of Akirin1 leads to cardiac hypertrophy. (A) A representative image of ex-vivo Akirin1 knock-out and wild-type heart. (B) Graph showing the heart weights of Akirin1 knock-out and wild-type mice calculated as percentage of total body weight. The values are mean ± S.E. of ten animals. (C) Longitudinal and transverse images of Akirin1 knock-out and wild-type hearts stained with hematoxylin and eosin showing larger ventricular cavities in Akirin1 knock-out heart compared to the wild-type heart.

Figure 5.2.1 Lack of Akirin1 up-regulates the sarcomeric proteins in the cardiac muscle. Western blotting analysis was performed on Akirin1 knock-out and wild-type cardiac muscle protein lysates. A(i) A representative immunoblot showing the protein levels of various sarcomeric contractile proteins (α-actin, α-MyHC, β-MyHC and desmin). GAPDH was used as an internal control for equal protein loading on the gel. A(ii), A(iii), A(iv) and A(v) are corresponding densitometry graphs of α-actin, α-MyHC, β-MyHC and desmin showing significant increase in protein content in Akirin1 cardiac muscle compared to the wild-type respectively (**$p<0.01$ and ***$p<0.001$).

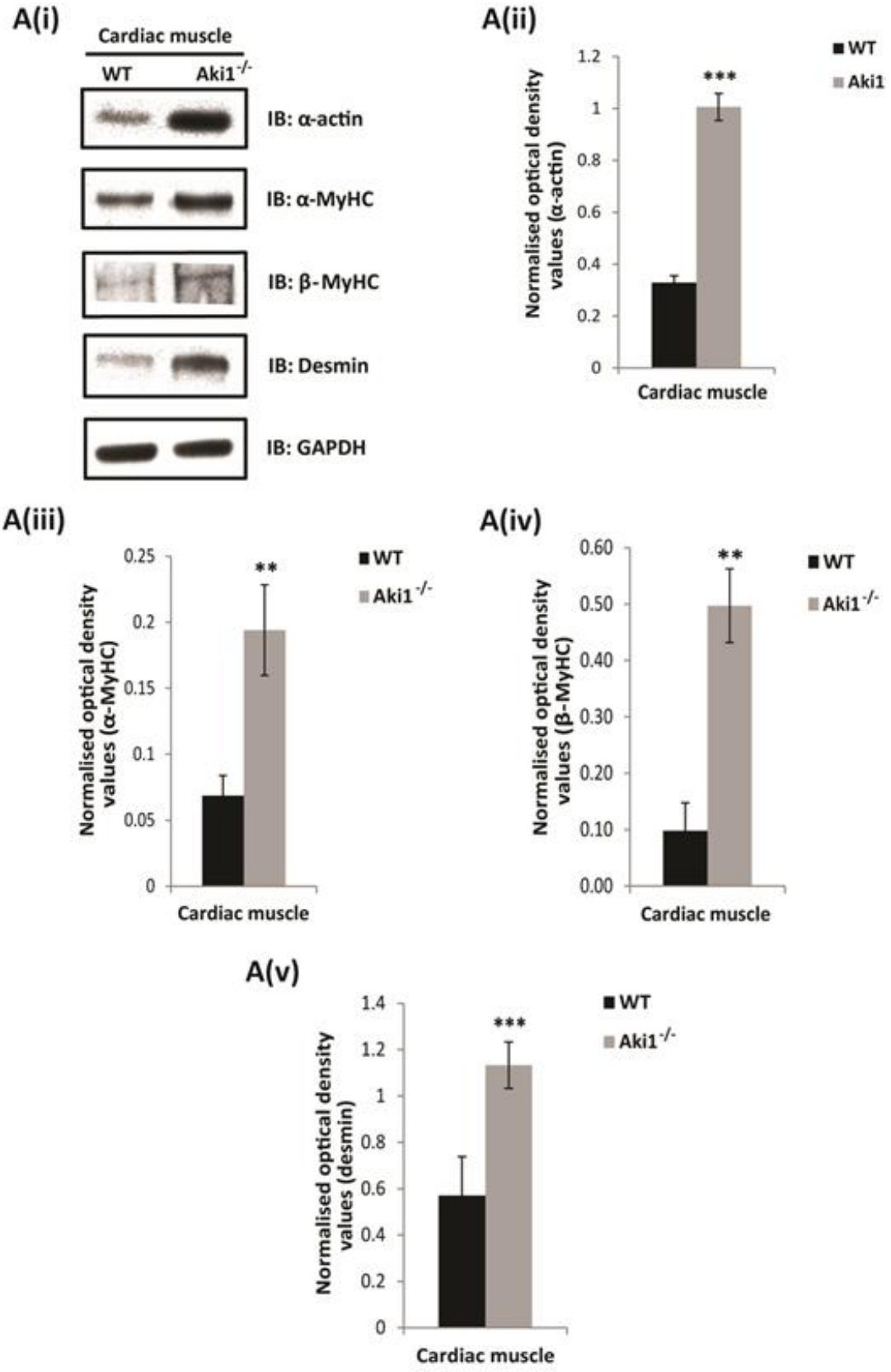
A(i)
Cardiac muscle
WT
Aki1-/-
IB: α-actin
IB: α-MyHC
IB: β-MyHC
IB: Desmin
IB: GAPDH
A(ii)
Normalised optical density values (α-actin)
1.2
1
0.8
0.6
0.4
0.2
0
***
WT
Aki1
Cardiac muscle
A(iii)
Normalised optical density values (α-MyHC)
0.25
0.2
0.15
0.1
0.05
0
**
WT
Aki1-/-
Cardiac muscle
A(iv)
Normalised optical density values (β-MyHC)
0.60
0.50
0.40
0.30
0.20
0.10
0.00
**
WT
Aki1-/-
Cardiac muscle
A(v)
Normalised optical density values (desmin)
1.4
1.2
1
0.8
0.6
0.4
0.2
0
***
WT
Aki1-/-
Cardiac muscle

5.2 Lack of Akirin1 up-regulates the sarcomeric protein levels in the cardiac muscle.

Our results in section 4.4 suggested that lack of Akirin1 in skeletal muscle lead to reduced levels of sarcomeric proteins. So, we wanted to investigate if the expression of the important cardiac contractile proteins were also affected in the absence of Akirin1. For this, Akirin1 knock-out and wild-type cardiac muscle protein lysates were subjected to immunoblotting with anti-α-actin, anti-β-MyHC, anti-α-MyHC and anti-desmin antibodies. Protein analysis results revealed that Akirin1 knock-out cardiac muscle indeed show significantly increased levels of major sarcomeric proteins like α-actin, β-MyHC, α-MyHC and desmin compared to the wild-type cardiac muscle [Figure 5.2.1A(i), A(ii), A(iii), A(iv) and A(v)].

Next, we wanted to determine if the increase in sarcomeric protein levels corresponded to increased gene expression. For this, we quantified the *α-actin*, *Myh7/β-MyHC* and *desmin* mRNA expression in Akirin1 knock-out and wild-type cardiac muscle by real-time qPCR. The gene expression analysis revealed that *α-actin* and *Myh7/β-MyHC* mRNA levels were significantly up-regulated in the Akirin1 knock-out cardiac muscle compared to the wild-type cardiac muscle [Figure 5.2.2A and B]. However the *desmin* mRNA levels were unchanged in Akirin1 knock-out and wild-type cardiac muscle [Figure 5.2.2C]. These results suggest that Akirin1 knock-out mice show signs of cardiac hypertrophy due to increased expression of sarcomeric proteins.

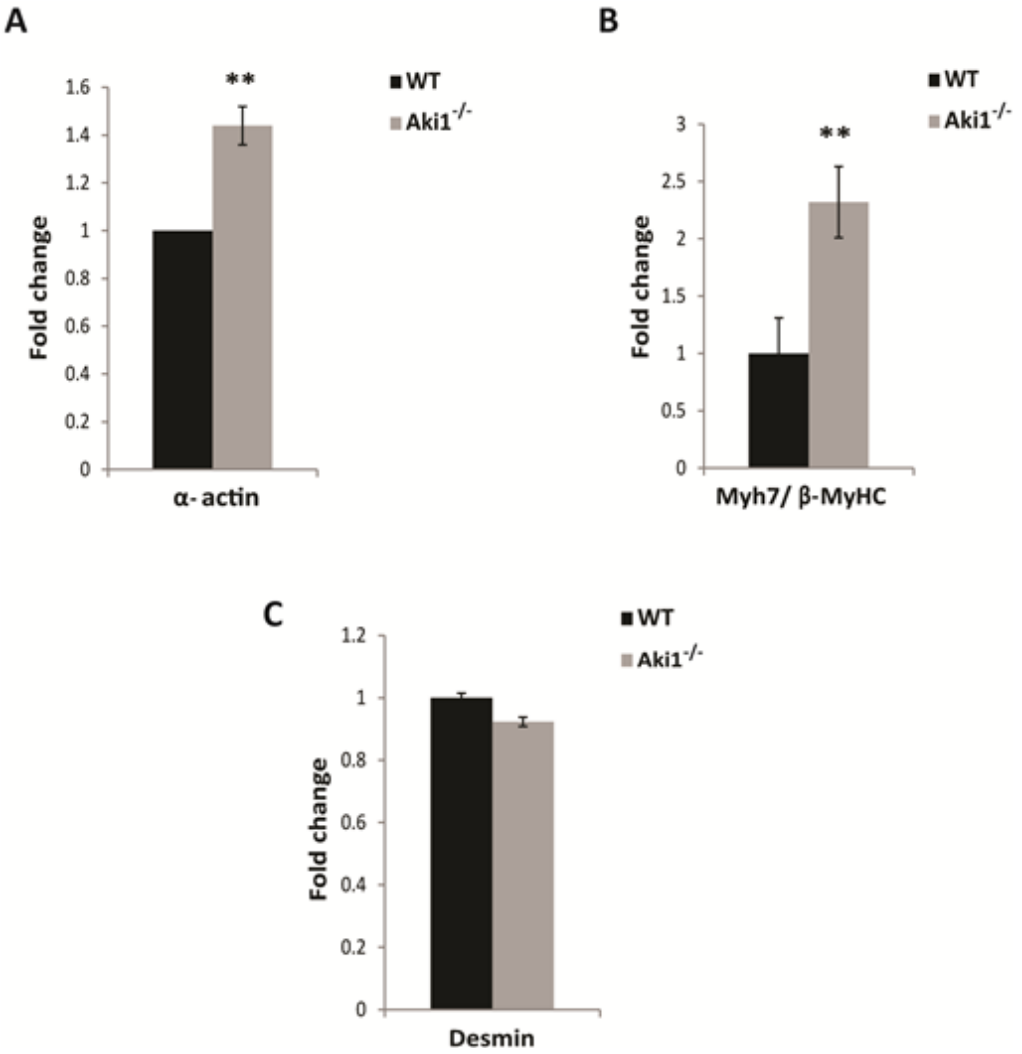

Figure 5.2.2 Akirin1 regulates the cytoskeletal and contractile genes post-transcriptionally in the cardiac muscle. mRNA expression of *α-actin, β-MyHC* and *desmin* was determined in Akirin1 knock-out and wild-type cardiac muscle. (A), (B) and (C) graphs showing the fold change mRNA expression of *α-actin, β-MyHC* and *desmin* in cardiac muscle respectively. The values are mean ± S.E. of four different animals (**p<0.01).

Figure 5.3 Lack of Akirin1 down-regulates the sarcomeric regulatory proteins in the cardiac muscle. Western blotting analysis was performed on Akirin1 knock-out and wild-type cardiac muscle protein lysates. A(i) A representative immunoblot showing the protein levels of various sarcomeric regulatory proteins (cardiac troponin T, cardiac troponin I and cardiac troponin C). GAPDH was used as an internal control for equal protein loading on the gel. A(ii), A(iii) and A(iv) Corresponding densitometry graphs of cardiac troponin T, cardiac troponin I and cardiac troponin C showing significant decrease or no change in protein content in Akirin1 cardiac muscle compared to the wild-type (*$p<0.05$ and **$p<0.01$). mRNA expression for *cardiac troponin T, cardiac troponin I* and *cardiac troponin C* was determined in Akirin1 knock-out and wild-type cardiac muscle. (B), (C) and (D) graphs showing the fold change mRNA expression of *cardiac troponin T, cardiac troponin* I and *cardiac troponin C* respectively. The values are mean ± S.E. of four different animals.

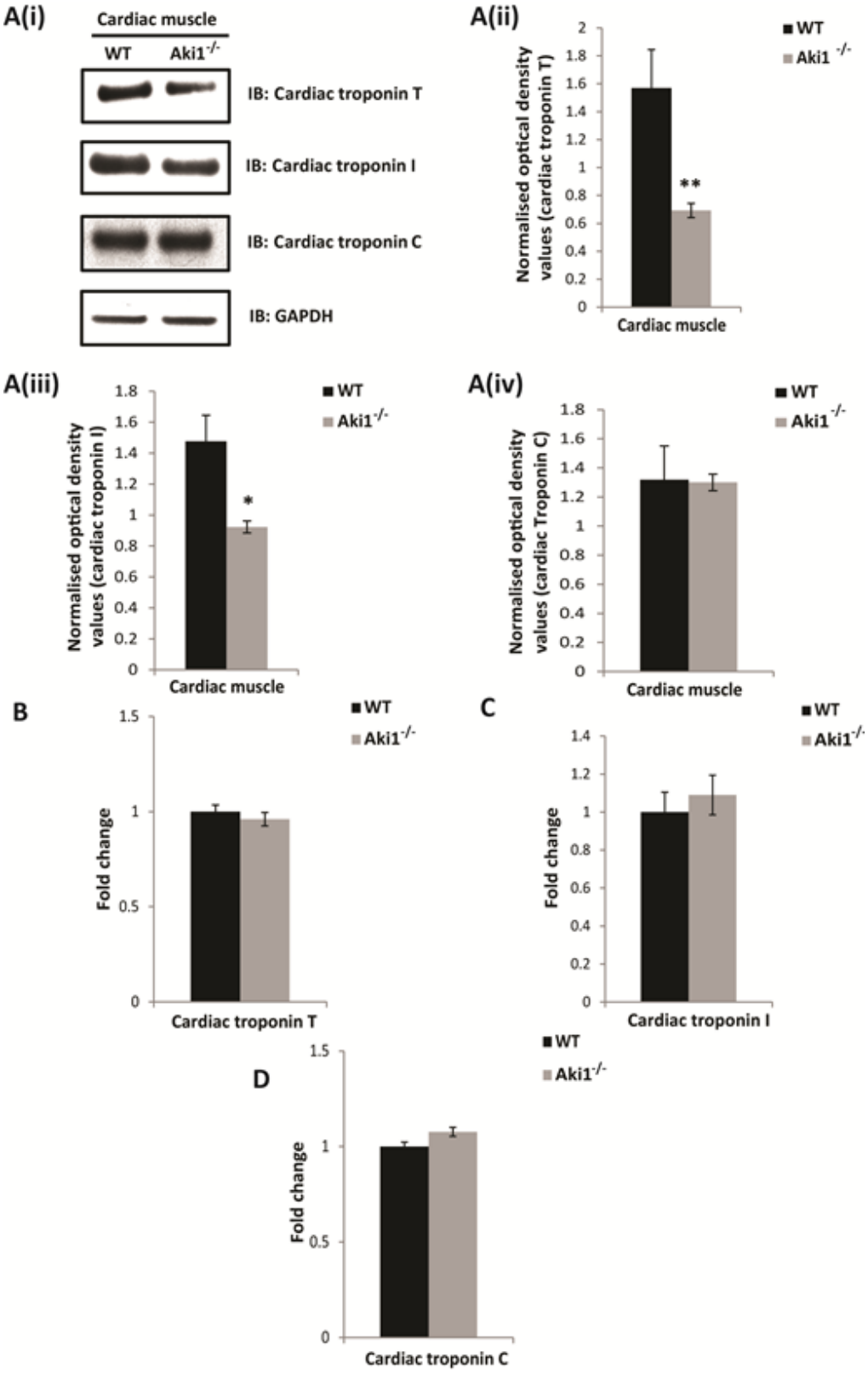
A(i)
Cardiac muscle
WT
Aki1-/-
IB: Cardiac troponin T
IB: Cardiac troponin I
IB: Cardiac troponin C
IB: GAPDH
A(ii)
WT
Aki1 -/-
Normalised optical density values (cardiac troponin T)
**
Cardiac muscle
A(iii)
WT
Aki1-/-
Normalised optical density values (cardiac troponin I)
*
Cardiac muscle
A(iv)
WT
Aki1 -/-
Normalised optical density values (cardiac Troponin C)
Cardiac muscle
B
WT
Aki1-/-
Fold change
Cardiac troponin T
C
WT
Aki1-/-
Fold change
Cardiac troponin I
D
WT
Aki1-/-
Fold change
Cardiac troponin C

5.3 Lack of Akirin1 down-regulates the sarcomeric regulatory proteins in the cardiac muscle.

The contraction of sarcomeres is mainly controlled by regulatory proteins like cardiac troponin T, cardiac troponin I and cardiac troponin C. It has been previously reported that the contractile ability of cardiac sarcomere reduced during pathological hypertrophy (James et al., 2000). So we determined the levels of these regulatory proteins by subjecting the protein lysates from Akirin1 knock-out and wild-type cardiac muscles to western blotting with anti-cardiac troponin T, anti-cardiac troponin I and anti-cardiac troponin C antibodies. The protein expression results showed that cardiac troponin T, known to bind to tropomyosin and facilitate sarcomere contraction, was significantly down-regulated in Akirin1 knock-out cardiac muscle compared to the wild-type cardiac muscle [Figure 5.3A(i) and A(ii)]. Another regulatory protein, cardiac troponin I, which regulates the contraction of the sarcomere by either turning on or off the interaction between the actin and myosin filaments, was also significantly down-regulated in the Akirin1 knock-out cardiac muscle compared to the wild-type cardiac muscle [Figure 5.3A(i) and A(iii)]. However the levels of cardiac troponin C which essentially binds to Ca^{2+} ions to initiate contraction was unchanged [Figure 5.3A(i) and A(iv)].

The mRNA transcription of these genes was analyzed by real-time qPCR in Akirin1 knock-out and wild-type cardiac muscle using *cyclophilin* as the normalising internal control. Gene expression analysis showed that there was no significant difference in the mRNA levels of *cardiac troponin T*, *cardiac troponin I* and *cardiac troponin C* between Akirin1 knock-out and wild-type

cardiac muscles [Figure 5.3B, C and D]. This result shows that the cardiac sarcomeric proteins are altered indicative of cardiac hypertrophy.

5.4 Lack of Akirin1 up-regulates Serum response factor (SRF) protein levels in cardiac muscle.

Cardiac hypertrophy program is known to be induced by various transcription factors expressed in the cardiac muscle like SRF, GATA4 and MEF2C (Zhang et al., 2011; Hasegawa et al., 1997; Molkentin et al., 1993). Over-expression of SRF in cardiac muscle is specifically known to activate the cardiac hypertrophy genes like Atrial natriuretic protein (ANP) and β-MyHC via regulating miR-1 expression (Zhang et al., 2001). As we observed an increase in the levels of sarcomeric contractile proteins and decrease in sarcomeric regulatory proteins in the Akirin1 knock-out cardiac muscle, we wanted to investigate if cardiac hypertrophy was induced by SRF in Akirin1 knock-out mice.

Firstly, we wanted to investigate the levels of SRF in both Akirin1 knock-out and wild-type cardiac muscle. Protein lysates of Akirin1 knock-out and wild-type cardiac muscles were probed with anti-SRF antibody. The western blotting results showed significantly increased levels of SRF protein in Akirin1 knock-out cardiac muscle compared to that of the wild-type [Figure 5.4A(i) and (ii)]. To see if the increase in cardiac SRF protein is due to increased *cardiac SRF* mRNA levels, we quantified the *cardiac SRF* mRNA levels using real-time qPCR with *cyclophilin* as the normalising internal control. No significant difference was observed in the *SRF* mRNA levels between Akirin1 knock-out and wild-type cardiac muscle (Figure 5.4B). These results suggest that Akirin1 regulates the expression of SRF post-transcriptionally in cardiac muscle.

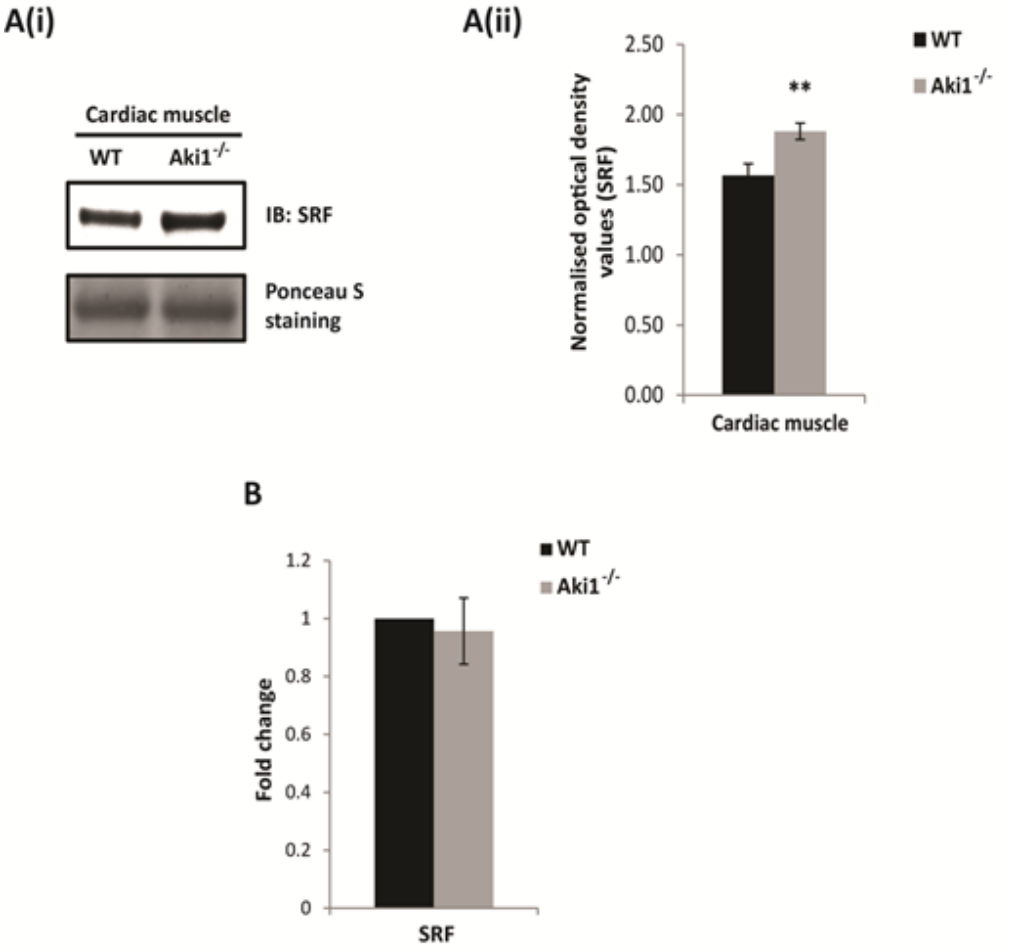

Figure 5.4 Lack of Akirin1 up-regulates Serum response factor (SRF) protein levels in cardiac muscle. Western blotting analysis was performed on Akirin1 knock-out and wild-type cardiac muscle protein lysates. A(i) A representative immunoblot showing the protein levels of SRF in Akirin1 knock-out and wild-type cardiac muscle. Ponceau S staining was used as an internal control for equal protein loading on the gel. A(ii) Corresponding densitometry graph of SRF showing significant increase in protein content in Akirin1 cardiac muscle compared to the wild-type (**$p<0.01$) (n=4). mRNA expression of *SRF* was determined in Akirin1 knock-out and wild-type cardiac muscle. (B) A graph showing the fold change in mRNA expression of *SRF* in Akirin1 knock-out compared to the wild-type cardiac muscle. The values are mean ± S.E. of four different animals.

5.5 Akirin1 regulates transcription of miR-1 in cardiac muscle.

Zhang et al. showed that over-expression of SRF in cardiac muscle induced cardiac hypertrophy by down-regulating the miR-1 transcription, thereby up-regulating the expression of miR-1 effector genes like ANP and β-MyHC (Zhang et al., 2011). The expression of primary miR-1 levels in both Akirin1 knock-out and wild-type cardiac muscle was quantified using real time-qPCR. The miR-1 Ct values were normalised to that of U6. Gene expression analysis revealed that Akirin1 knock-out cardiac muscle showed significantly reduced primary miR-1level compared to the wild-type cardiac muscle (Figure 5.5A). As mature miR-1 is the active form of miRNA that binds to target genes and regulate their expression, the levels of mature miR-1 were analyzed in Akirin1 knock-out and wild-type cardiac muscle. Similar to primary miR-1 levels, Akirin1 knock-out cardiac muscle showed significantly lower levels of mature miR-1 when compared to the wild-type cardiac muscle (Figure 5.5B).

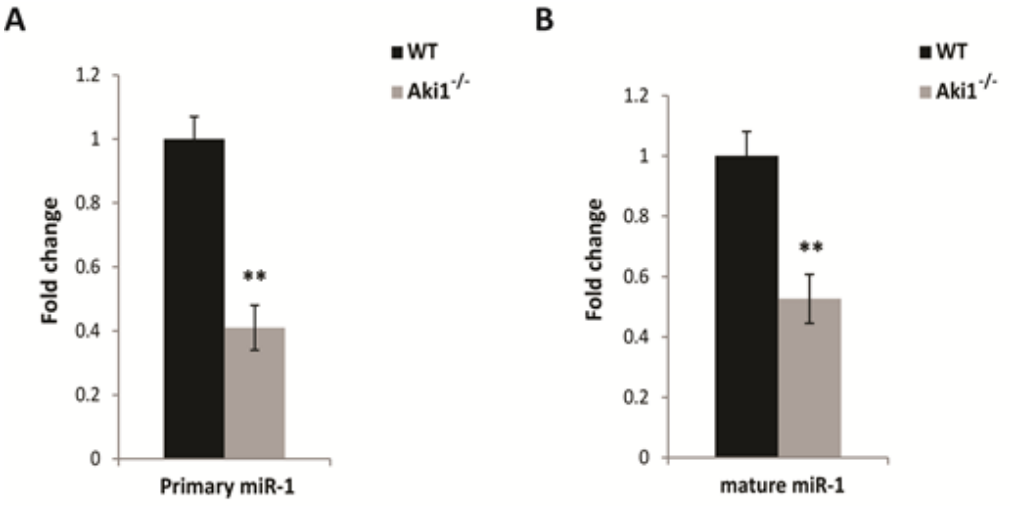

Figure 5.5 Akirin1 regulates transcription of miR-1 in cardiac muscle. Primary and mature miR-1 transcript levels in Akirin1 knock-out and wild-type cardiac muscle. mRNA expression analysis was performed on Akirin1 knock-out and wild-type cardiac muscle. (A) and (B) Representative graphs showing fold change expression of primary and mature miR-1 transcript levels in Akirin1 knock-out cardiac muscle respectively. The values are mean ± S.E. of four different animals (**$p<0.01$).

Figure 5.6 Absence of Akirin1 leads to increased expression of targets of miR-1: Atrial Natriuretic Peptide (ANP) and β-MyHC in cardiac muscle. Expression analysis of downstream targets of miR-1 namely ANP and β-MyHC in Akirin1 knock-out and wild-type cardiac muscle. Western blotting analysis was performed on Akirin1 knock-out and wild-type cardiac muscle protein lysates. A(i) and B(i) A representative immunoblot showing the protein levels of ANP and β-MyHC. GAPDH was used as an internal control for equal protein loading on the gel. A(ii) and B(ii) Corresponding densitometry graphs of ANP and β-MyHC showing significant increase in protein content in Akirin1 cardiac muscle compared to the wild-type (**$p<0.01$) (n=4). mRNA expression of *ANP* and *β-MyHC* was determined in Akirin1 knock-out and wild-type cardiac muscle. (C) and (D) Representative graphs showing the fold change mRNA expression of *ANP* and *β-MyHC* in cardiac muscle respectively. The values are mean ± S.E. of four different animals (**$p<0.01$).

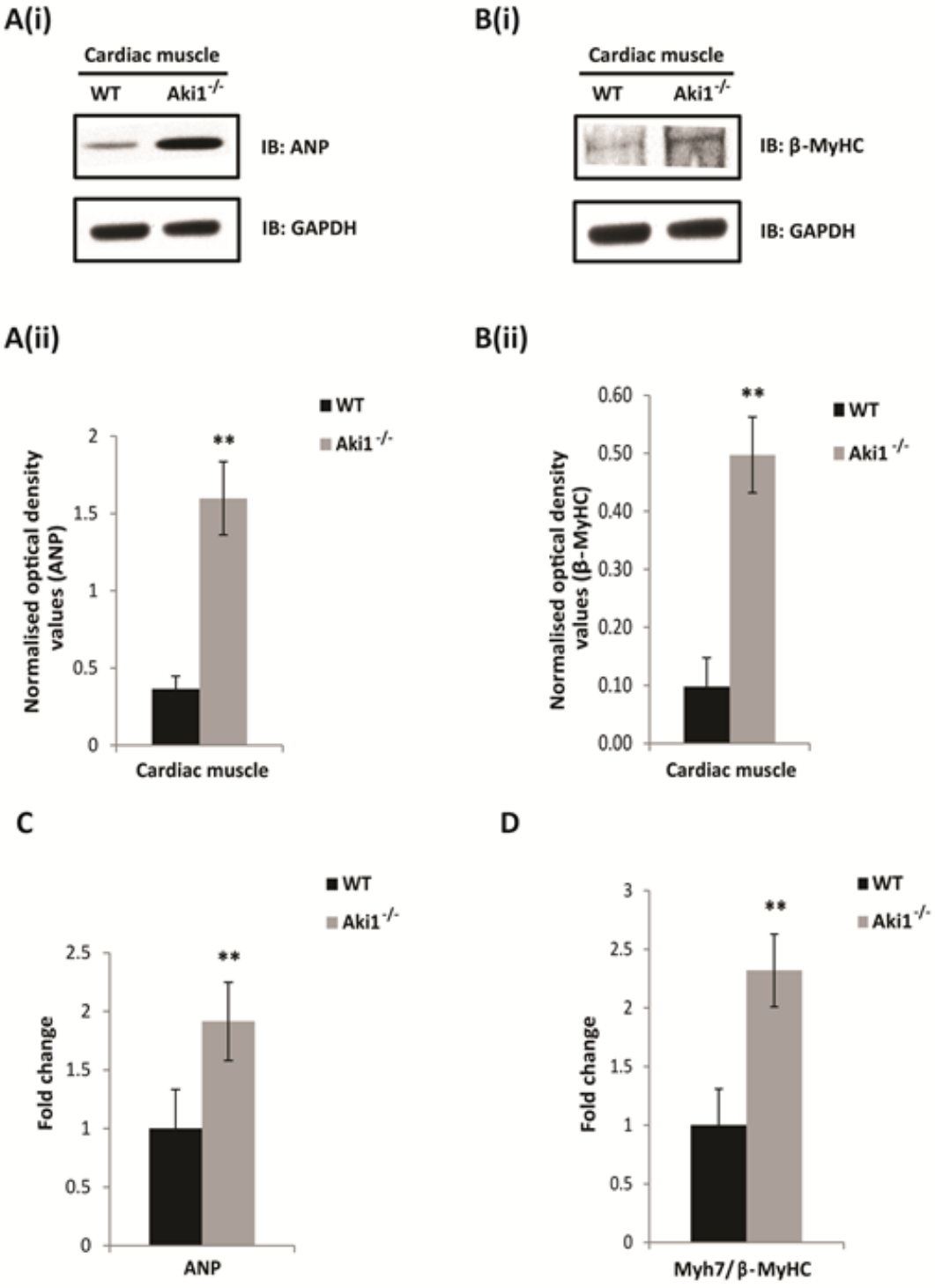
A(i)
Cardiac muscle
WT
Aki1-/-
IB: ANP
IB: GAPDH
B(i)
Cardiac muscle
WT
Aki1-/-
IB: β-MyHC
IB: GAPDH
A(ii)
WT
Aki1-/-
Normalised optical density values (ANP)
**
Cardiac muscle
B(ii)
WT
Aki1-/-
Normalised optical density values (β-MyHC)
**
Cardiac muscle
C
WT
Aki1-/-
Fold change
**
ANP
D
WT
Aki1-/-
Fold change
**
Myh7/β-MyHC

5.6 Absence of Akirin1 leads to increased expression of targets of miR-1: Atrial Natriuretic Peptide (ANP) and β-MyHC in cardiac muscle.

As miR-1 levels were down-regulated in Akirin1 knock-out cardiac muscle, we looked at the expression levels of some of the target genes regulated by miR-1 like Atrial natriuretic protein (ANP) and β-MyHC. Immunoblotting was performed on Akirin1 knock-out and wild-type cardiac muscle protein lysates with anti-ANP and anti-β-MyHC antibodies. The protein expression results showed that Akirin1 knock-out cardiac muscle expressed significantly increased levels of both ANP and β-MyHC protein compared to the wild-type cardiac muscle [Figure 5.6A(i), B(i), A(ii) and B(ii)]. To determine if the increase in ANP and β-MyHC protein levels is attributed to increased *ANP* and *β-MyHC* mRNA levels, gene expression analysis was performed to we quantify the *ANP* and *b-MyHC* mRNA level by real time-qPCR with *cyclophilin* as normalising internal control. The results indicated that Akirin1 knock-out cardiac muscle showed significantly higher levels of both *ANP* and *β-MyHC* mRNA compared to the wild-type cardiac muscle (Figure 5.6C and D).

5.7 Cardiac hypertrophy induced due to lack of Akirin1 may not be through MEF2C.

Another transcription factor, apart from SRF, that is known to induce cardiac hypertrophy is MEF2C (Molkentin et al., 1993). To see if MEF2C plays a role in inducing cardiac hypertrophy phenotype in the absence of Akirin1, western blotting was performed on protein lysates from Akirin1 knock-out and wild-type cardiac muscles with anti-phospho-MEF2C (thr300) and anti-MEF2C antibodies. The results showed that there was no difference in the protein levels of both phospho-MEF2C (thr300) and total MEF2C levels between Akirin1 knock-out and wild-type cardiac muscle [Figure 5.7A(i)]. Densitometry analysis also showed no significant difference in both phospho-MEF2C (thr300) and total MEF2C levels in Akirin1 knock-out and wild-type cardiac muscle [Figure 5.7A(ii) and A(iii)].

To determine if there were any changes in *Mef2c* mRNA levels, gene expression analysis was performed to quantify the *Mef2c* mRNA level by real time-qPCR with *cyclophilin* as normalising internal control. The results indicated that there was no difference in *Mef2c* mRNA levels between Akirin1 knock-out and wild-type cardiac muscle (Figure 5.7B).

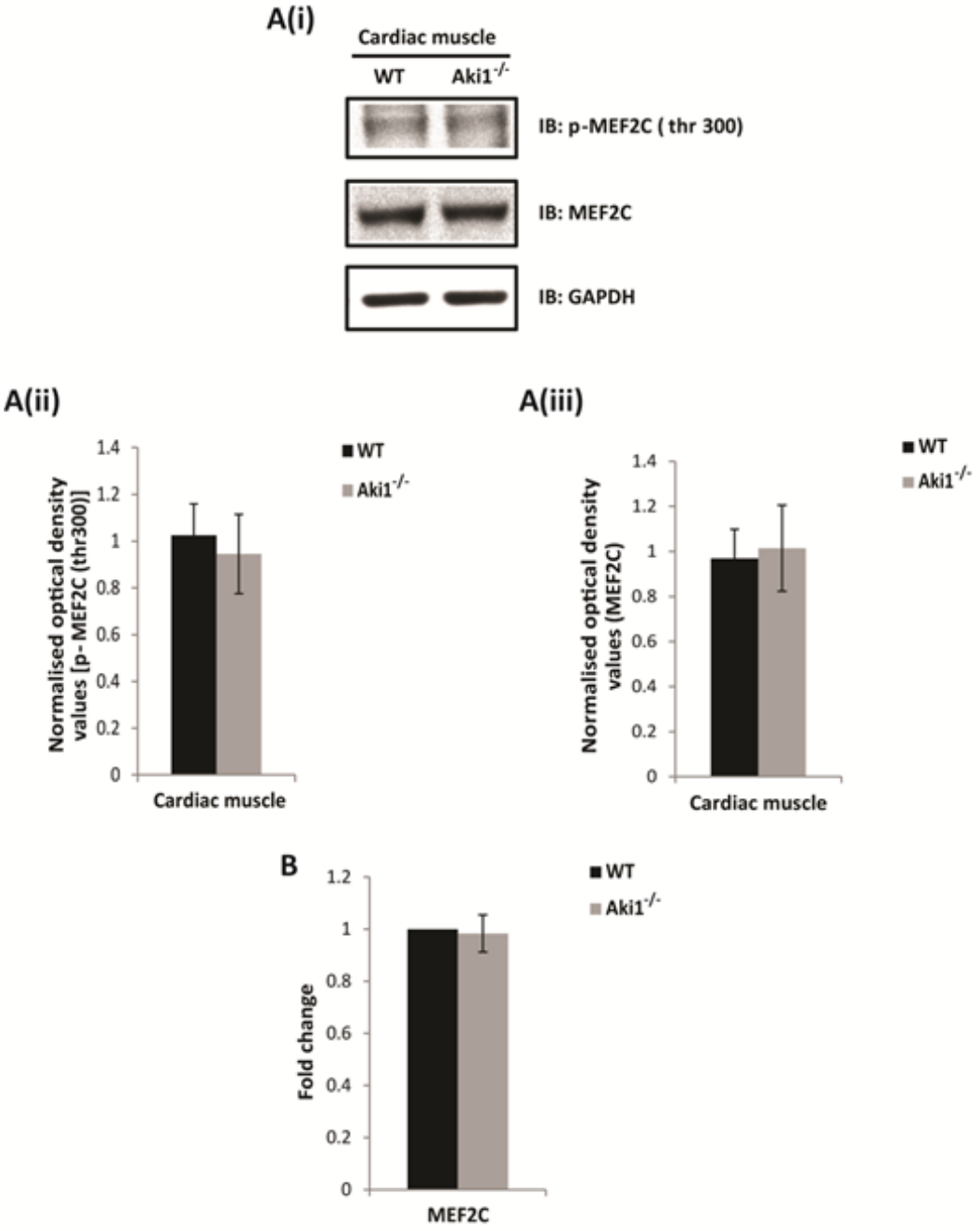

Figure 5.7 Cardiac hypertrophy induced due to lack of Akirin1 may not be through MEF2C. Expression profile of MEF2C in Akirin1 knock-out and wild-type cardiac muscle. Western blotting analysis was performed on protein lysates of Akirin1 knock-out and wild-type cardiac muscle. A(i) A representative immunoblot showing protein levels of both phospho-MEF2C (thr 300) and total MEF2C in Akirin1 knock-out and wild-type cardiac muscle. GAPDH was used as an internal control for equal protein loading on the gel. A(ii) and A(iii) Corresponding densitometry analysis graphs of phospho-MEF2C (thr300) and total MEF2C (n=4). (B) Graph showing fold change in mRNA expression for *MEF2C* in Akirin1 knock-out and wild-type cardiac muscle. The values are mean ±S.E. of four different animals.

5.8 Absence of Akirin1 in the cardiac muscle leads to activation of IGF-1/Akt/mTOR pathway leading to cardiac hypertrophy.

To investigate the mechanism behind cardiac hypertrophy seen in Akirin1 knock-out cardiac muscle, we investigated certain important cardiac hypertrophy inducing signaling pathways like IGF-1/Akt/mTOR pathway. This pathway involves cascade of intracellular components which together signal increased protein synthesis thus inducing cardiac hypertrophy (Haq et al., 2000; McMullen et al., 2003).

Firstly, we investigated the protein level of the IGF-1 growth factor. Protein lysates from Akirin1 knock-out and wild-type cardiac muscle were subjected to western blotting with anti-IGF-1 antibody. Western blotting results showed that Akirin1 knock-out cardiac muscle have significantly increased levels of intracellular IGF-1 levels compared to the wild-type cardiac muscle [Figure 5.8.1A(i)]. Densitometry analysis proved that the IGF-1 levels were significantly up-regulated in Akirin1 knock-out cardiac muscle compared to the wild-type [Figure 5.8.1A(ii)].

Binding of IGF-1 to its receptor activates its downstream target, phosphatidyl inositol-3-Kinase (PI3K). PI3K helps in phosphorylating membrane phospholipid phosphoinositide-4,5-biphosphate (PIP2) to phosphoinositide-3,4,5-triphoshate (PIP3). So we looked at the levels of both active phosphorylated PI3K p85 subunit levels and total pI3K p85 subunit levels using western blotting. Akirin1 knock-out and wild-type cardiac muscle protein lysates were probed with anti-phospho-PI3K p85 (tyr458)/p55 (tyr199) and anti-PI3K p85 antibodies. Protein expression analysis showed significantly increased levels of phosho-PI3K p85 (tyr458)/p55 (tyr199) level

in Akirin1 knock-out compared to the wild-type cardiac muscle. However, the total PI3K p85 level did not change between Akirin1 knock-out and wild-type cardiac muscle [Figure 5.8.1B(i)]. Densitometry analysis showed that Akirin1 knock-out cardiac muscle have significantly higher level of phospho-PI3K p85 (tyr458)/p55 (tyr199) compared to the wild-type cardiac muscle while the total PI3K p85 level did not change [Figure 5.8.1B(ii) and B(iii)]. The ratio of phospho-PI3K p85 (tyr458)/p55 (tyr199) to total PI3K p85 also was higher in Akirin1 knock-out cardiac muscle compared to that of the wild-type [Figure 5.8.1B(iv)].

Figure 5.8.1 Absence of Akirin1 in the cardiac muscle leads to increased levels of IGF-1 and PI3K proteins. Western blotting analysis was performed on Akirin1 knock-out and wild-type cardiac muscle protein lysates. A(i) A representative immunoblot showing the protein levels of IGF-1 in Akirin1 knock-out and wild-type cardiac muscle. GAPDH was used as an internal control for equal protein loading on the gel. A(ii) Densitometry graph of IGF-1 protein levels in Akirin1 knock-out and wild-type cardiac muscle. B(i) A representative immunoblot showing the protein levels of both phospho-PI3K p85 (tyr 458)/p55(tyr 199) and total PI3K p85 in Akirin1 knock-out and wild-type cardiac muscle. GAPDH was used as an internal control for equal protein loading on the gel. B(ii) and B(iii) Densitometry graphs of phospho-PI3K p85 (tyr 458)/p55(tyr 199) and total PI3K p85 protein levels in Akirin1 knock-out and wild-type cardiac muscle respectively. B(iv) Densitometry graph representing the ratio of phospho-PI3K p85 (tyr 458)/p55(tyr 199) to total PI3K p85 levels. All the graph values are mean ±S.E. of four different animals. Level of significance was compared to wild-type (*$p<0.05$ and **$p<0.01$).

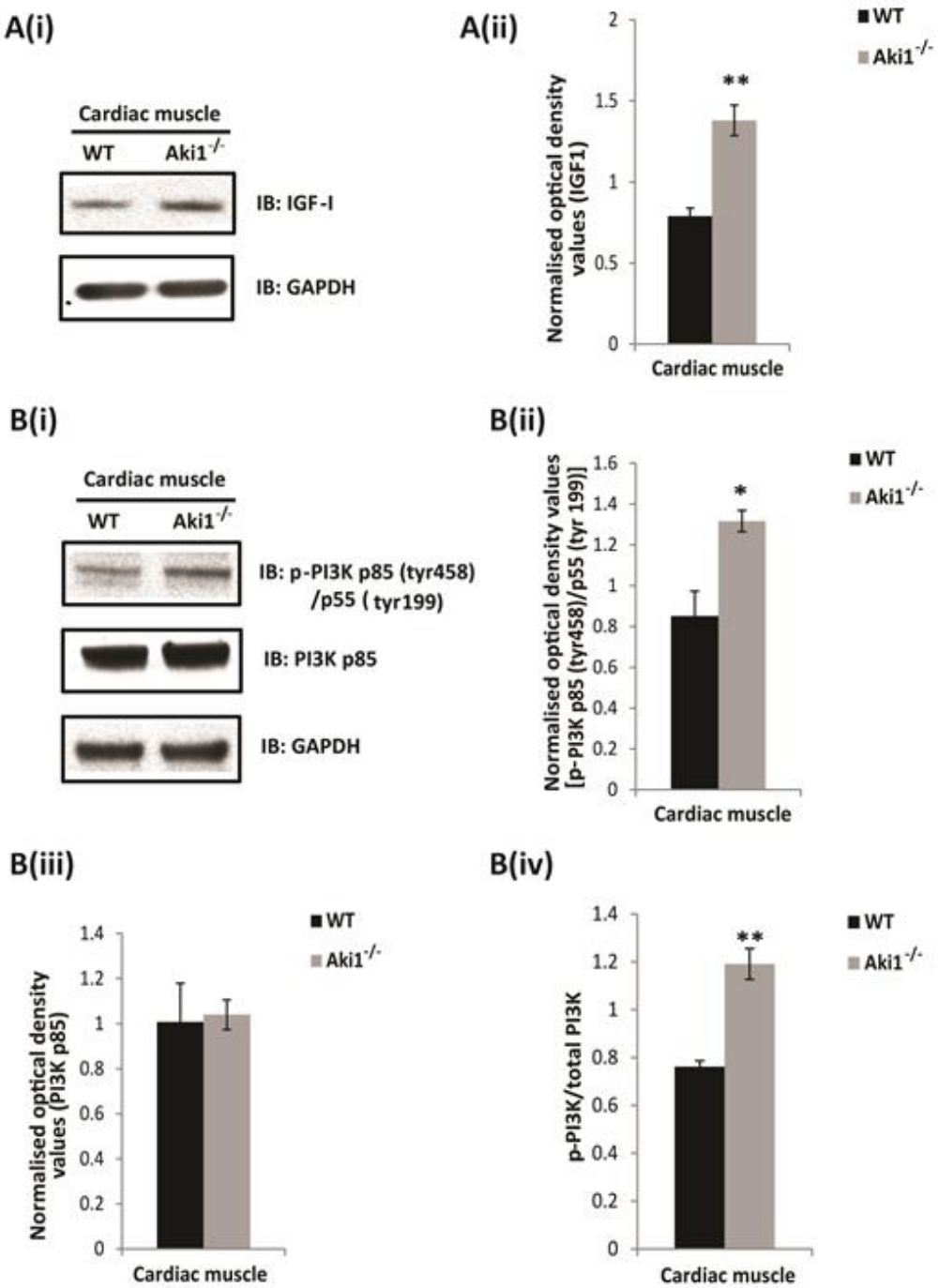
A(i)
Cardiac muscle
WT
Aki1-/-
IB: IGF-I
IB: GAPDH
A(ii)
WT
Aki1-/-
Normalised optical density values (IGF1)
**
Cardiac muscle
B(i)
Cardiac muscle
WT
Aki1-/-
IB: p-PI3K p85 (tyr458) /p55 (tyr199)
IB: PI3K p85
IB: GAPDH
B(ii)
WT
Aki1-/-
Normalised optical density values [p-PI3K p85 (tyr458)/p55 (tyr 199)]
*
Cardiac muscle
B(iii)
WT
Aki1-/-
Normalised optical density values (PI3K p85)
Cardiac muscle
B(iv)
WT
Aki1-/-
p-PI3K/total PI3K
**
Cardiac muscle

The signaling molecule that act downstream of PI3K is Akt. Akt also called protein kinase B is a serine/threonine protein kinase and is activated when phosphorylated at ser 473. We investigated the levels of both phospho-Akt (ser473) and total-Akt in Akirin1 knock-out and wild-type cardiac muscle. The immunoblotting results showed a significant increase in phosphorylation of Akt protein in Akirin1 knock-out cardiac muscle compared to the wild-type cardiac muscle, while the total Akt levels remained unchanged [Figure 5.8.2A(i)]. Densitometry analysis showed significant increase in Akt phosphorylation in Akirin1 knock-out cardiac muscle compared to the wild-type cardiac muscle with no changes in the total Akt levels [Figure 5.8.2A(ii) and A(iii)]. The ratio of phospho-Akt (ser473) to total Akt was higher in Akirin1 knock-out cardiac muscle compared to the wild-type cardiac muscle [Figure 5.8.2A(iv)].

Figure 5.8.2 Absence of Akirin1 in the cardiac muscle leads to increased levels of Akt and mTOR proteins. Western blotting analysis was performed on Akirin1 knock-out and wild-type cardiac muscle protein lysates. A(i) A representative immunoblot showing the protein levels of both phospho-Akt (ser 473) and total Akt in Akirin1 knock-out and wild-type cardiac muscle. GAPDH was used as an internal control for equal protein loading on the gel. A(ii) and C(iii) Densitometry graphs of phospho-Akt (ser 473) and total Akt protein levels in Akirin1 knock-out and wild-type cardiac muscle respectively. A(iv) Densitometry graph representing the ratio of phospho-Akt (ser 473) to total Akt levels. B(i) A representative immunoblot showing the protein levels of both phospho-mTOR (ser 2448) and total mTOR in Akirin1 knock-out and wild-type cardiac muscle. GAPDH was used as an internal loading control. B(ii) and B(iii) Densitometry graphs of phospho-mTOR (ser 2448) and total mTOR protein levels in Akirin1 knock-out and wild-type cardiac muscle respectively. B(iv) Densitometry graph representing the ratio of phospho-mTOR (ser 2448) to total mTOR levels. All the graph values are mean ±S.E. of four different animals. Level of significance was compared to wild-type (*$p<0.05$ and **$p<0.01$).

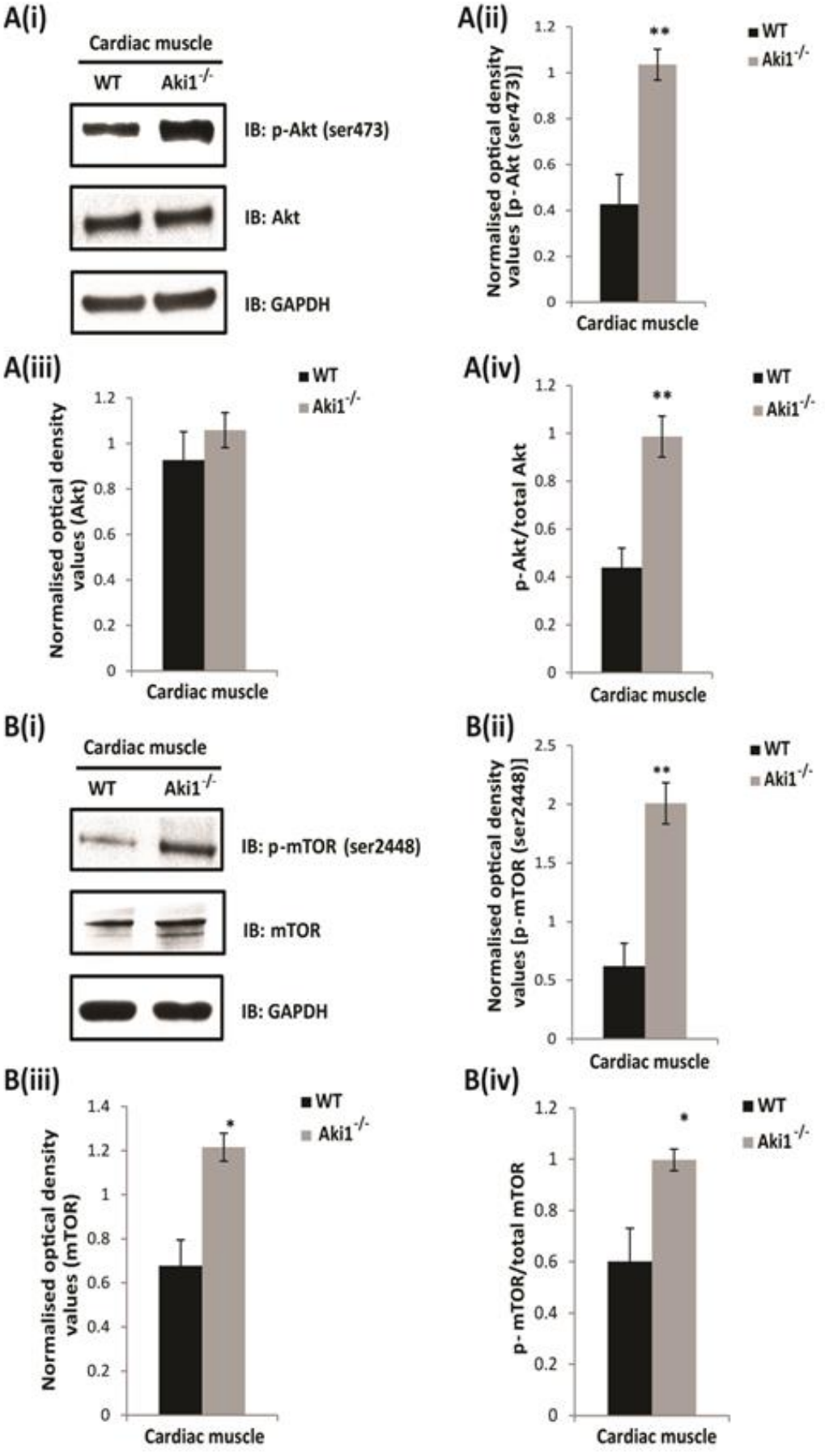
A(i)
Cardiac muscle
WT
Aki1-/-
IB: p-Akt (ser473)
IB: Akt
IB: GAPDH
A(ii)
Normalised optical density values [p-Akt (ser473)]
Cardiac muscle
WT
Aki1-/-
**
A(iii)
Normalised optical density values (Akt)
Cardiac muscle
WT
Aki1-/-
A(iv)
p-Akt/total Akt
Cardiac muscle
WT
Aki1-/-
**
B(i)
Cardiac muscle
WT
Aki1-/-
IB: p-mTOR (ser2448)
IB: mTOR
IB: GAPDH
B(ii)
Normalised optical density values [p-mTOR (ser2448)]
Cardiac muscle
WT
Aki1-/-
**
B(iii)
Normalised optical density values (mTOR)
Cardiac muscle
WT
Aki1-/-
*
B(iv)
p- mTOR/total mTOR
Cardiac muscle
WT
Aki1-/-
*

Akt can further stimulate protein synthesis pathway via mammalian target of rapamycin (mTOR) and Glycogen synthase kinase-3-beta (GSK3β). Akt promotes protein synthesis by phosphorylating mTOR at ser2448 while inactivates GSK3b by phosphorylating at ser9 (Manning et al., 2007). Hence, we estimated the phosphorylated and total levels of both mTOR and GSK3β in Akirin1 knock-out and wild-type cardiac muscle. Firstly, western blotting was performed on Akirin1 knock-out and wild-type cardiac muscle with anti-phospho-mTOR (ser2448) and anti-mTOR antibodies. Protein expression analysis showed that Akirin1 knock-out cardiac muscle have significantly increased levels of both phospho-mTOR (ser2448) and total mTOR compared to the wild-type cardiac muscle (Figure 5.8.2B(i), B(ii) and B(iii)]. The ratio of phospho-mTOR (ser2448) to total mTOR was also higher in Akirin1 knock-out cardiac muscle compared to the wild-type [Figure 5.8.2B(iv)].

Figure 5.8.3 Absence of Akirin1 in the cardiac muscle leads to increased levels of GSK3β and 4eBP1 proteins. Western blotting analysis was performed on Akirin1 knock-out and wild-type cardiac muscle protein lysates. A(i) A representative immunoblot showing the protein levels of both phospho-GSK3β (ser 9) and total GSK3β in Akirin1 knock-out and wild-type cardiac muscle. GAPDH was used as an internal loading control. A(ii) and A(iii) are densitometry graphs of phospho-GSK3β (ser 9) and total GSK3β protein levels in Akirin1 knock-out and wild-type cardiac muscle respectively. A(iv) Densitometry graph representing the ratio of phospho-GSK3β (ser 9) and total GSK3β levels. B(i) A representative immunoblot showing the protein levels of both phospho-4eBP1 (ser 65/thr 70) and total 4eBP1 in Akirin1 knock-out and wild-type cardiac muscle. GAPDH was used as an internal control for equal protein loading on the gel. B(ii) and B(iii) Densitometry graphs of phospho-4eBP1 (ser 65/thr 70) and total 4eBP1 protein levels in Akirin1 knock-out and wild-type cardiac muscle respectively. B(iv)] Densitometry graph representing the ratio of phospho-4eBP1 (ser 65/thr 70) to total 4eBP1 levels. All the graph values are mean ±S.E. of four different animals. Level of significance was compared to wild-type (*$p<0.05$, **$p<0.01$ and ***$p<0.001$).

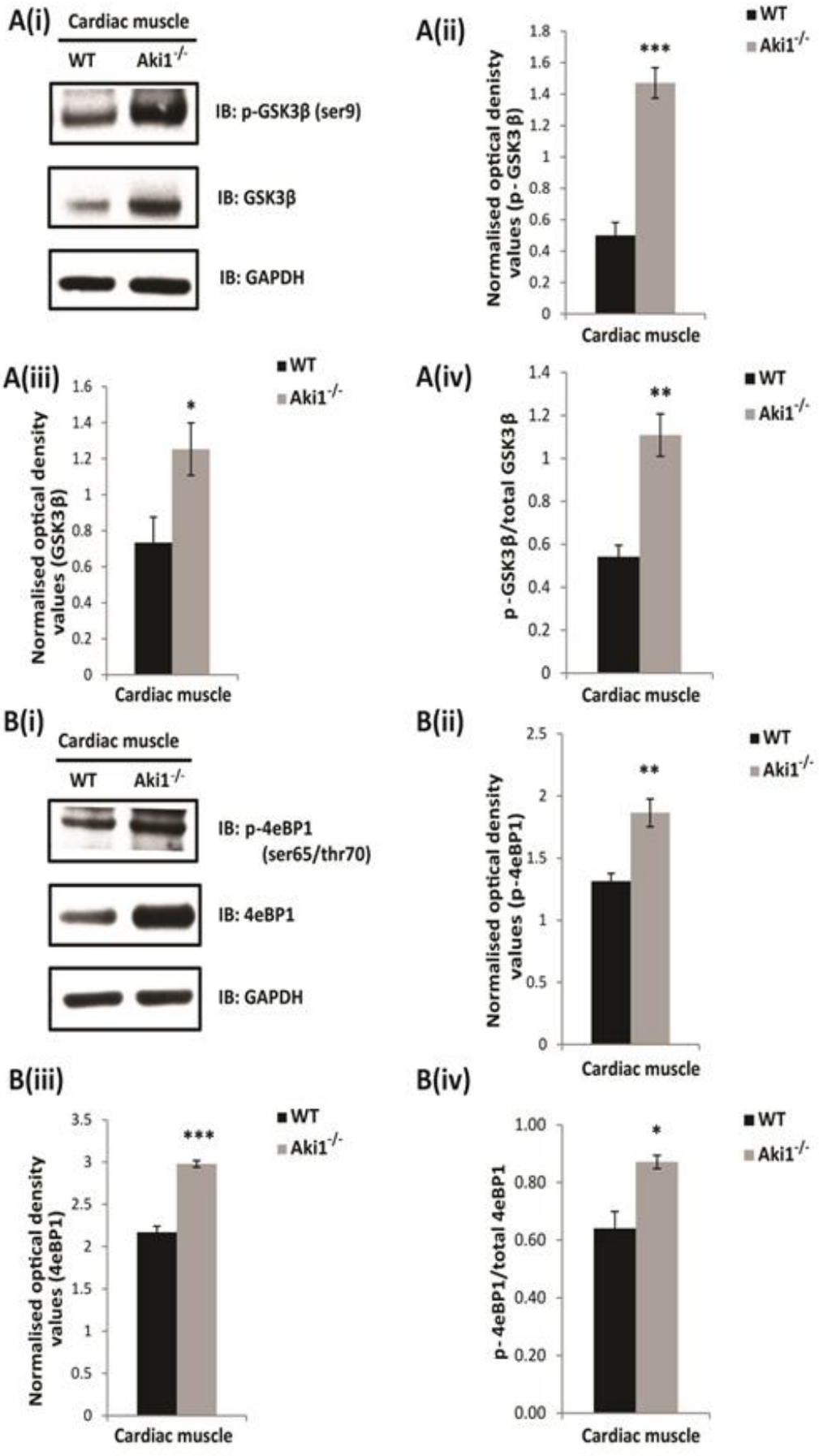
A(i)
Cardiac muscle
WT
Aki1-/-
IB: p-GSK3β (ser9)
IB: GSK3β
IB: GAPDH
A(ii)
WT
Aki1-/-
Normalised optical denisty values (p-GSK3β)
***
Cardiac muscle
A(iii)
WT
Aki1-/-
Normalised optical density values (GSK3β)
*
Cardiac muscle
A(iv)
WT
Aki1-/-
p-GSK3β/total GSK3β
**
Cardiac muscle
B(i)
Cardiac muscle
WT
Aki1-/-
IB: p-4eBP1 (ser65/thr70)
IB: 4eBP1
IB: GAPDH
B(ii)
WT
Aki1-/-
Normalised optical density values (p-4eBP1)
**
Cardiac muscle
B(iii)
WT
Aki1-/-
Normalised optical density values (4eBP1)
***
Cardiac muscle
B(iv)
WT
Aki1-/-
p-4eBP1/total 4eBP1
*
Cardiac muscle

Further, western blotting was performed on Akirin1 knock-out and wild-type cardiac muscle protein lysates with anti-phospho-GSK3β (ser9) and anti-GSK3β antibodies. Akirin1 knock-out cardiac muscle showed increased protein levels of both phospho-GSK3β (ser9) and total GSK3β compared to the wild-type cardiac muscle (Figure 5.8.3A(i), A(ii) and A(iii)]. The ratio of phospho-GSK3β (ser9) to total GSK3β was also significantly up-regulated in Akirin1 knock-out cardiac muscle compared to the wild-type cardiac muscle [Figure 5.8.3A(iv)].

mTOR activates translation of various cellular proteins by activating eukaryotic translation initiation 4E (eIF4E) by phosphorylating the inhibitory eIF4E-binding proteins called 4eBPs. So we investigated the protein levels of a predominantly used 4eBP protein in mammals like 4eBP1. Western blotting was performed on protein lysates from Akirin1 knock-out and wild-type cardiac muscle with anti-phospho-4eBP1 (ser65/thr70) and anti-4eBP1 antibodies. The levels of both phospho-4eBP1 (ser65/thr70) and total 4eBP1was up-regulated in Akirin1 knock-out cardiac muscle compared to the wild-type [Figure 5.8.3B(i), B(ii) and B(iii)]. The ratio of phospho-4eBP1 (ser65/thr70) to total 4eBP1 was also significantly increased in Akirin1 knock-out cardiac muscle compared to the wild-type cardiac muscle [Figure 5.8.3B(iv)]. All these results together suggest that in the absence of Akirin1, the signaling proteins involved in IGF-1/Akt/mTOR pathway are activated leading to cardiac hypertrophy phenotype.

5.9 Lack of Akirin1 leads to activation of JNK signaling pathway in the cardiac muscle.

Haq et al. showed that the three mitogen activated protein kinase (MAPK) pathways are activated during cardiac hypertrophy i.e., c-Jun N-terminal kinase (JNK), p38 and Extracellular signal-regulated kinase (ERK1/2) pathways (Haq et al., 2001). The protein levels of both phospho-JNK (T183/Y185) and total JNK in Akirin1 knock-out and wild-type cardiac muscles using anti-phospho-JNK (T183/Y185) and anti-JNK antibodies respectively were analyzed. Western blotting results showed that Akirin1 knock-out cardiac muscle showed increased levels of phospho-JNK (T183/Y185) compared to the wild-type cardiac muscle while the total JNK levels were unchanged between Akirin1 knock-out and wild-type cardiac muscle [Figure 5.9A(i), A(ii) and A(iii)]. The ratio of phospho-JNK (T183/Y185) to total JNK was also significantly increased in Akirin1 knock-out cardiac muscle compared to the wild-type cardiac muscle [Figure 5.9A(iv)].

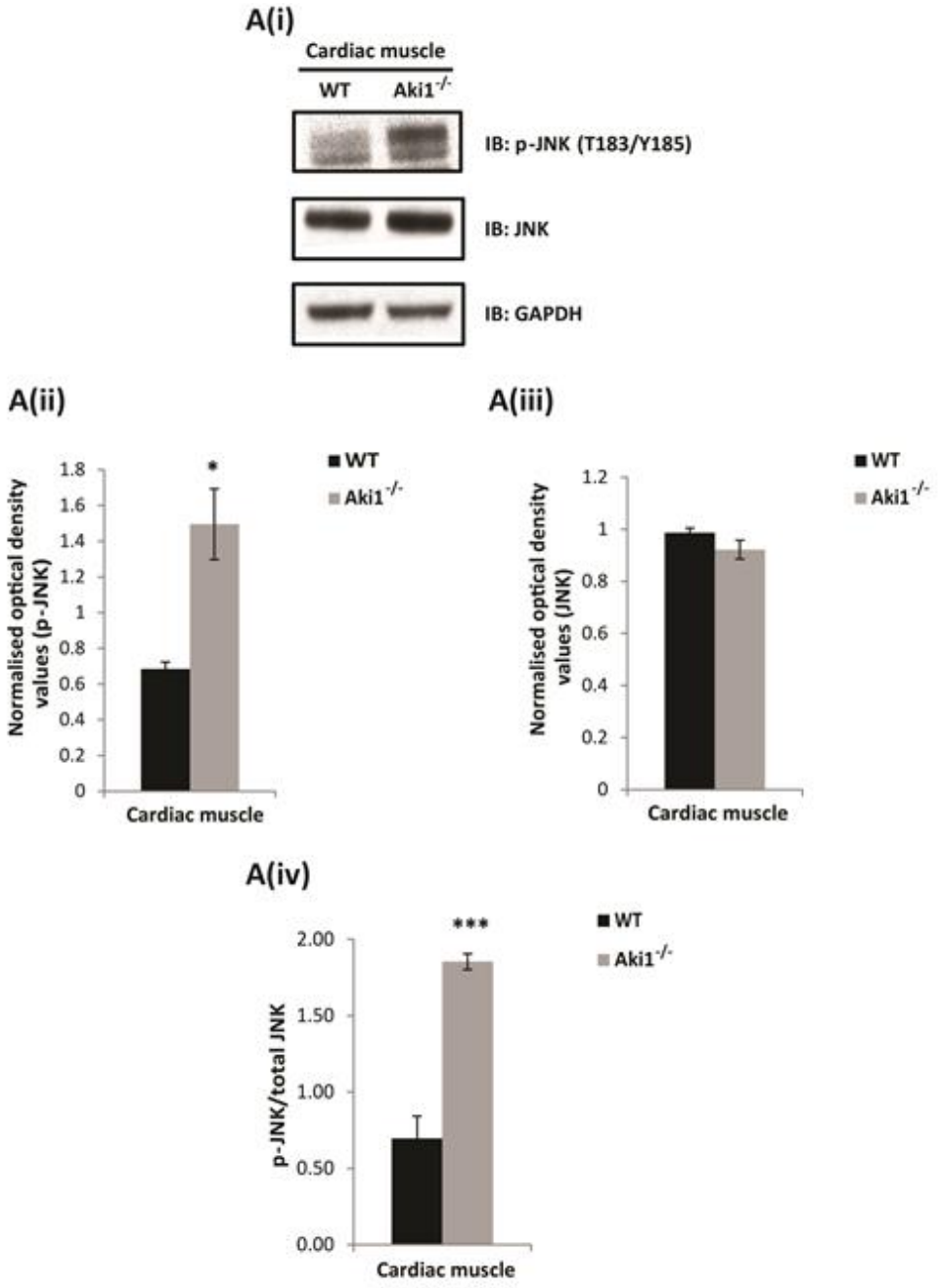

Figure 5.9 Lack of Akirin1 leads to activation of JNK signaling pathway in the cardiac muscle. Western blotting analysis was performed on Akirin1 knock-out and wild-type cardiac muscle protein lysates. A(i) A representative immunoblot showing the protein levels of both phospho-JNK(T183/Y185) and total-JNK in Akirin1 knock-out and wild-type cardiac muscle. GAPDH was used as an internal control for equal protein loading on the gel. A(ii) and A(iii) are corresponding densitometry graphs of phospho-JNK(T183/Y185) and total-JNK. A(iv) Densitometry graph representing the ratio of phospho-JNK(T183/Y185) to total-JNK levels. All the graph values are mean ±S.E. of four different animals (*$p<0.05$ and ***$p<0.001$).

5.10 Lack of Akirin1 leads to activation of p38 signaling pathway in the cardiac muscle.

Another important member of the MAPK pathways is p38 MAPK pathway. We wanted to investigate if p38 pathway was up-regulated in Akirin1 knock-out cardiac muscle as it was shown by Haq et al., 2001 that p38 pathway is up-regulated during cardiac hypertrophy. The protein lysates from Akirin1 knock-out and wild-type cardiac muscle were subjected to western blotting with anti-phospho-p38 MAPK (T180/Y182) and anti-p38 MAPK antibodies. Protein expression analysis showed that Akirin1 knock-out cardiac muscle showed increased levels of both phospho-p38 MAPK (T180/Y182) and p38 MAPK protein levels compared to the wild-type [Figure 5.10A(i)]. Densitometry analysis also showed that Akirin1 knock-out cardiac muscle showed increased levels of both phospho-p38 MAPK (T180/Y182) and p38 MAPK protein levels compared to the wild-type cardiac muscle [Figure 5.10A(ii) and A(iii)]. The ratio of phospho-p38 MAPK (T180/Y182) to p38 MAPK was also significantly up-regulated in Akirin1 knock-out cardiac muscle compared to the wild-type cardiac muscle [Figure 5.10A(iv)].

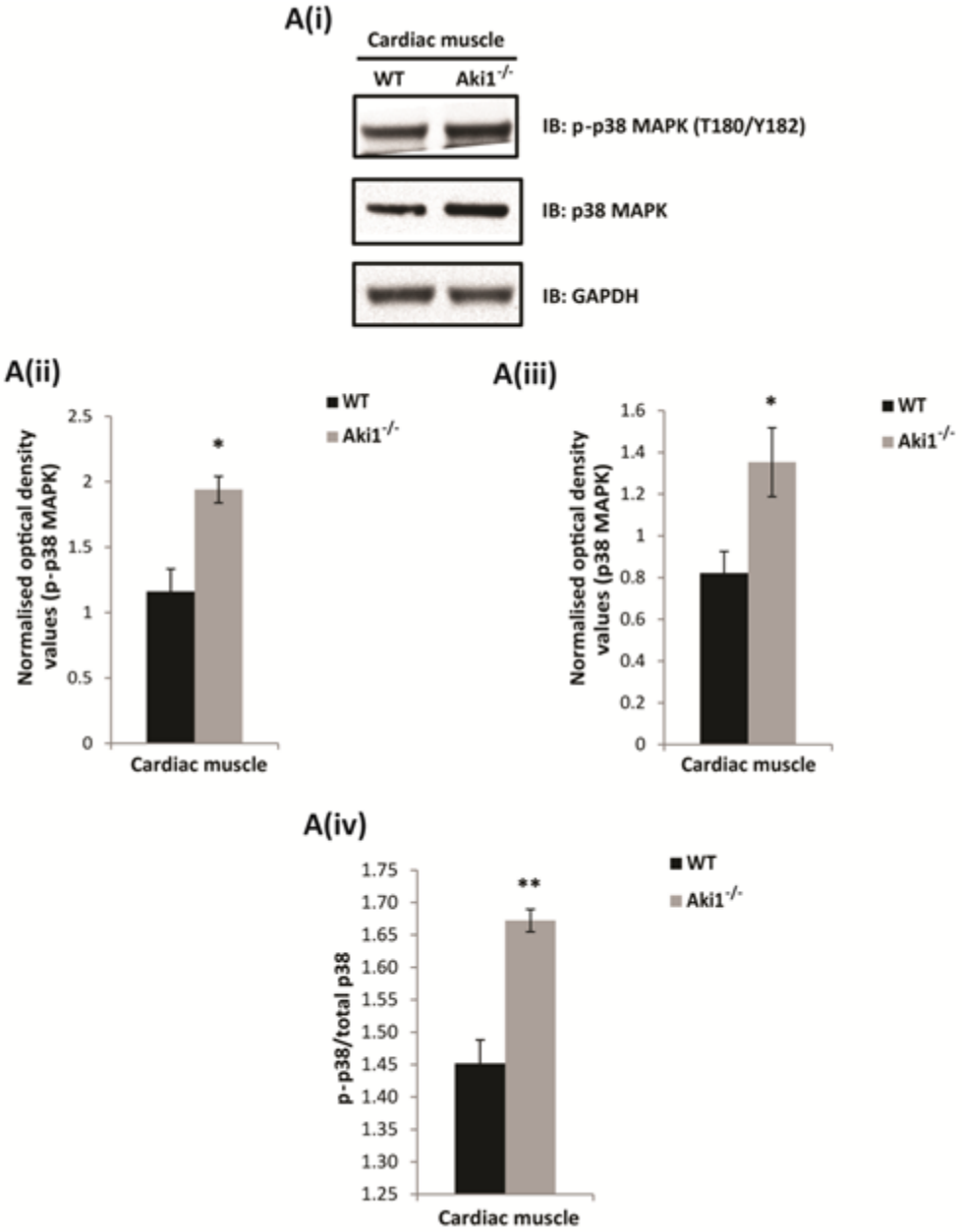

Figure 5.10 Lack of Akirin1 leads to activation of p38 MAPK signaling pathway in the cardiac muscle. Western blotting analysis was performed on Akirin1 knock-out and wild-type cardiac muscle protein lysates. A(i) A representative immunoblot showing the protein levels of both phospho-p38 MAPK (T180/Y182) and total-p38 MAPK in Akirin1 knock-out and wild-type cardiac muscle. GAPDH was used as an internal control for equal protein loading on the gel. A(ii) and A(iii) Corresponding densitometry graphs of phospho-p38 MAPK (T180/Y182) and total-p38 MAPK. A(iv) Densitometry graph representing the ratio of phospho-p38 MAPK (T180/Y182) to total-p38 MAPK levels. All the graph values are mean ±S.E. of four different animals (*$p<0.05$ and **$p<0.01$).

5.11 Lack of Akirin1 leads to activation of ERK1/2 signaling pathway in the cardiac muscle.

We investigated the levels of another member of MAPK pathway like ERK1/2, as it was shown by Haq et al., 2001 that ERK pathway is up-regulated during cardiac hypertrophy. Akirin1 knock-out and wild-type cardiac muscle protein lysates were probed with anti-phospho-ERK1/2 (thr202/tyr204) and ERK1/2 antibodies. Western blotting results showed that Akirin1 knock-out cardiac muscle showed increased levels of phospho-ERK1/2 (thr202/tyr204) compared to the wild-type cardiac muscle while the total ERK1/2 levels were unchanged between Akirin1 knock-out and wild-type cardiac muscle [Figure 5.11A(i), A(ii) and A(iii)]. The ratio of phospho-ERK1/2 (thr202/tyr204) to total ERK1/2 was also significantly increased in Akirin1 knock-out cardiac muscle compared to the wild-type cardiac muscle [Figure 5.11A(iv)]. These results together suggest that all the three main MAPK signaling pathways are activated in the absence of Akirin1 in cardiac muscle indicating cardiac hypertrophy.

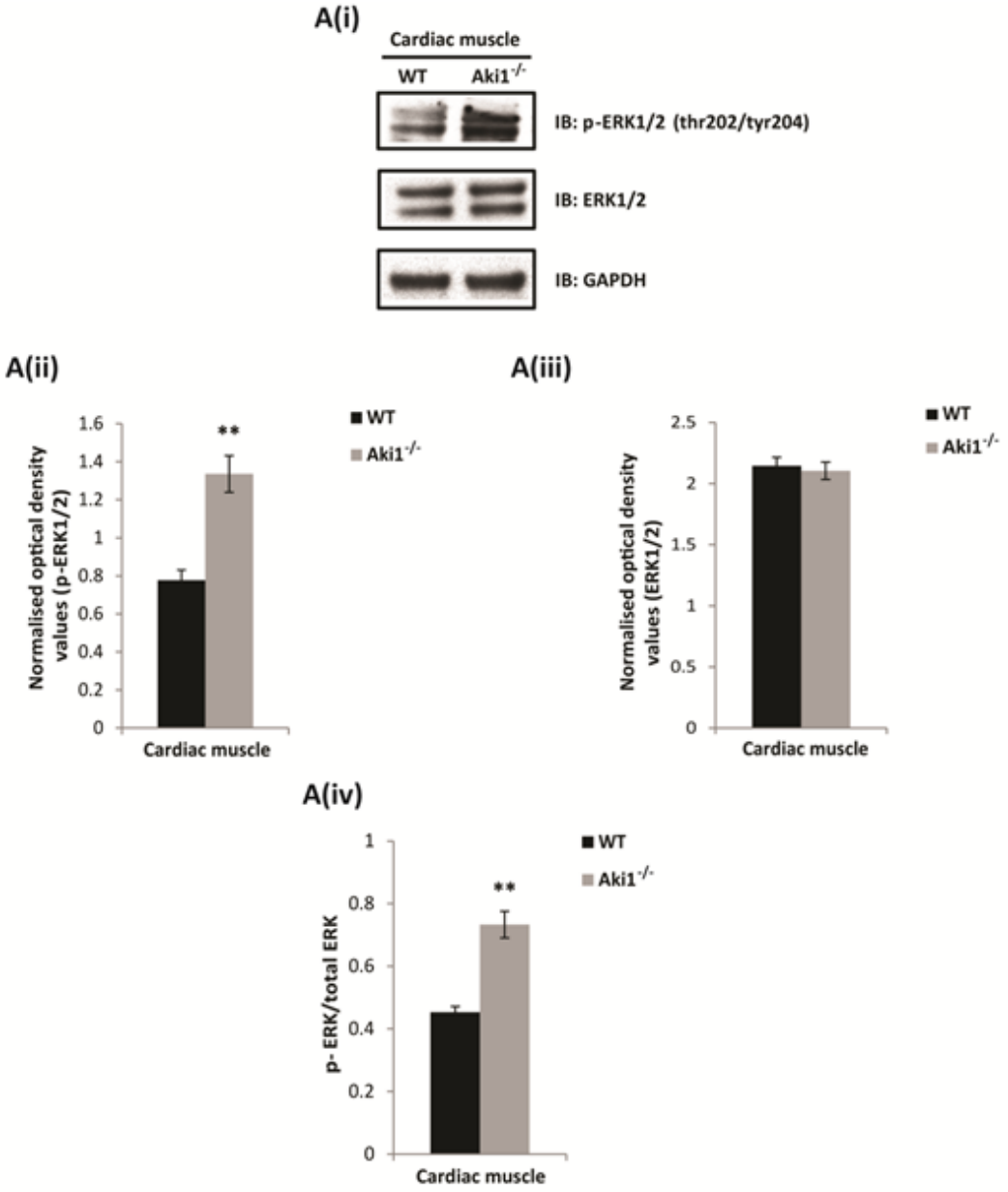

Figure 5.11 Lack of Akirin1 leads to activation of ERK1/2 signaling pathway in the cardiac muscle. Western blotting analysis was performed on Akirin1 knock-out and wild-type cardiac muscle protein lysates. A(i) A representative immunoblot showing the protein levels of both phospho-ERK1/2 (thr202/tyr204) and total-ERK1/2 in Akirin1 knock-out and wild-type cardiac muscle. GAPDH was used as an internal control for equal protein loading on the gel. A(ii) and A(iii) Corresponding densitometry graphs of phospho-ERK1/2 (thr202/tyr204) and total-ERK1/2. A(iv) Densitometry graph representing the ratio of phospho-ERK1/2 (thr202/tyr204) to total-ERK1/2 levels. All the graph values are mean ±S.E. of four different animals (**$p<0.01$).

5.12 Akirin1 does not regulate MuRF1 in cardiac muscle.

It has been shown that MuRF1 is an important regulator of cardiac hypertrophy by affecting the sarcomeric protein turnover in the cardiocytes (Willis et al., 2007). The results in skeletal muscle in section 4.7 showed that Akirin1 regulates the expression of MuRF1. So we wanted to investigate if Akirin1 regulates MuRF1 expression in cardiac muscle as well causing cardiac hypertrophy. For this, protein lysates from Akirin1 knock-out and wild-type cardiac muscle were probed with anti-MuRF1 antibody. The results showed no significant difference in the MuRF1 protein levels between Akirin1 knock-out and wild-type cardiac muscle [Figure 5.12A(i) and A(ii)]. The *MuRF1* mRNA levels were quantified by real time-qPCR and *MuRF1* Ct values were normalised to *Cyclophilin* Ct values. Consistent with the protein levels, Akirin1 knock-out cardiac muscle showed no significant difference in the *MuRF1* mRNA levels when compared to the wild-type cardiac muscle (Figure 5.12B).

As the expression of MuRF1 did not change in Akirin1 knock-out cardiac muscle, we wanted to investigate if the activity of MuRF1 as an E3 ubiquitin ligase changed. Western blotting was performed with anti-ubiquitin antibody. The results showed that the extent of ubiquitination of various cellular proteins were unchanged in Akirin1 knock-out cardiac muscle compared to the wild-type cardiac muscle [Figure 5.12C(i)]. Densitometry analysis confirmed that the extent of protein ubiquitination in Akirin1 knock-out and wild-type cardiac muscles were the same [Figure 5.12C(ii)]. This proves that Akirin1 does not regulate MuRF1 expression in cardiac muscle, unlike skeletal muscle.

Figure 5.12 Akirin1 does not regulate MuRF1 in cardiac muscle. Western blotting analysis was performed on protein lysates of Akirin1 knock-out and wild-type cardiac muscle. A(i) A representative immunoblot showing protein levels of MuRF1 in Akirin1 knock-out and wild-type cardiac muscle. α-tubulin was used as an internal control for equal protein loading on the gel. A(ii) Corresponding densitometry analysis of MuRF1 showing no significant change in protein content between Akirin1 knock-out and wild-type cardiac muscle (n=4). (B) Graph showing fold change in mRNA expression of *MuRF1* in Akirin1 knock-out and wild-type cardiac muscle. The values are mean ±S.E. of four different animals. C(i) A representative immunoblot showing the extent of ubiquitination of cellular proteins in Akirin1 knock-out and wild-type cardiac muscle. GAPDH was used as an internal control for equal protein loading on the gel. C(ii) Corresponding densitometry graph of ubiquitination in Akirin1 knock-out and wild-type cardiac muscle (n=4).

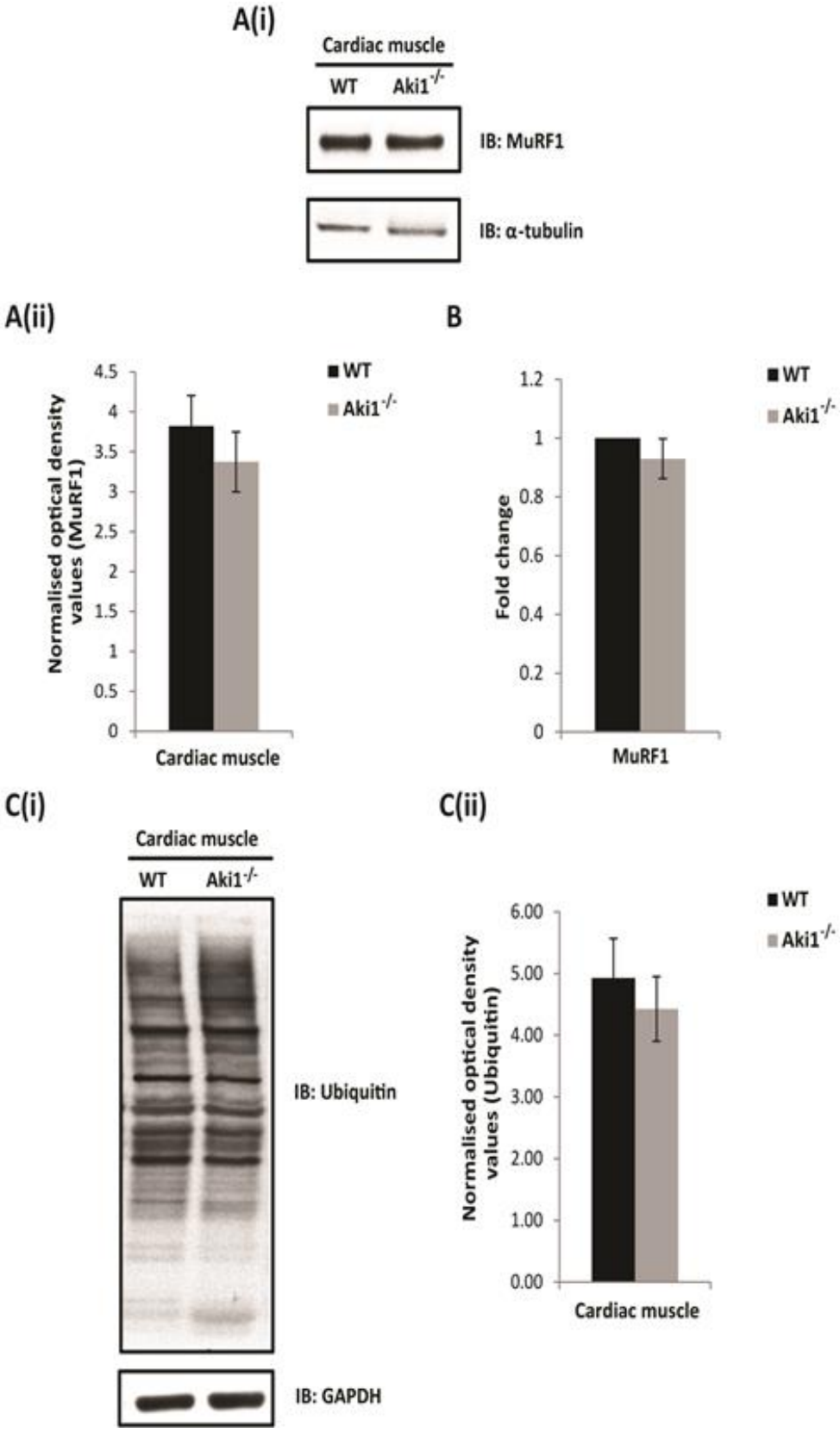
A(i)
Cardiac muscle
WT
Aki1-/-
IB: MuRF1
IB: α-tubulin
A(ii)
Normalised optical density values (MuRF1)
WT
Aki1-/-
Cardiac muscle
B
Fold change
WT
Aki1-/-
MuRF1
C(i)
Cardiac muscle
WT
Aki1-/-
IB: Ubiquitin
IB: GAPDH
C(ii)
Normalised optical density values (Ubiquitin)
WT
Aki1-/-
Cardiac muscle

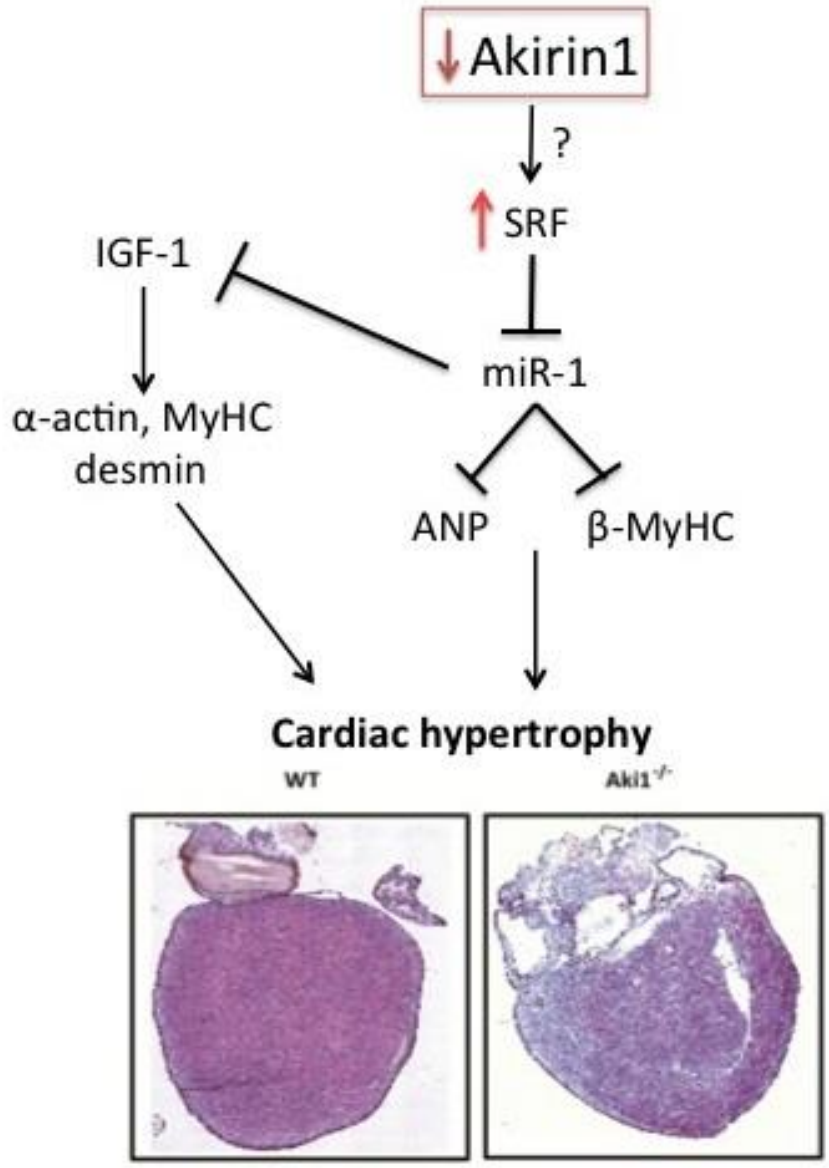

Figure 5.13 A schematic diagram summarizing the various results obtained in understanding the possible role of Akirin1 in inducing cardiac hypertrophy.

CHAPTER 6

DISCUSSION

6. DISCUSSION

Akirin1 is a recently known molecule that has not been extensively studied. Being a ubiquitously expressed nuclear protein, it can be speculated to have different functions in different tissues. Some of the important discoveries in the past revealed its role in myogenic differentiation (Marshall et al., 2008) and in satellite cell activation and skeletal muscle regeneration (Salerno et al., 2009).

To further elucidate the function of Akirin1 in striated muscle (skeletal and cardiac muscle), Akirin1 knock-out mouse model was used in this study.

The results obtained in this study show that Akirin1 knock-out mice did not show any obvious phenotypic change when compared to wild-type mice. The molecular analysis of important myogenic genes performed on Akirin1 knock-out skeletal muscle revealed that levels of myogenic genes were unchanged except for myogenin. Myogenin is known to play an important role in early differentiation (Venuti et al., 1995; Cserjesi et al., 1991) and thus a decrease in myogenin levels would lead to impaired differentiation (Sassoon et al., 1989). Also, another research group has recently shown that reduced myogenin levels in primary myotubes can reverse the process of myogenic terminal differentiation (Nikolaos et al., 2012). Thus, it can be expected that Akirin1 may be positively regulating myogenin levels and affecting myogenic differentiation. However, in Akirin1 knock-out primary cultures we did not observe reduced myogenic differentiation. In fact, the fusion index was higher in Akirin1 knock-out compared to the wild-type cultures. This phenotype could be an effect of increased SRF levels in the Akirin1 knock-out myoblasts (Figure 3.4 and 3.7). It also appears that SRF could be compensating for the reduced myogenin levels in differentiating primary myotubes. It has been

shown that SRF is known to be an important transcription factor essential for myogenic differentiation. So, it is likely that Akirin1 negatively regulates SRF during differentiation. Further, this regulation of SRF by Akirin1 was observed at post-transcriptional level as only the protein levels changed but not the mRNA levels. One of the mechanism by which Akirin1 may be post-transcriptionally regulating SRF levels is through MuRF1. It has been previously reported that SRF is targeted by MuRF1, an ubiquitin ligase, leading to its degradation, there by affecting myoblast differentiation (Lange et al., 2005; Soulez et al., 1996). Consistent with these reports, our results showed that Akirin1 regulates MuRF1 transcription during myogenic differentiation and in the the absence of Akirin1, MuRF1 levels were down-regulated (Figure 3.8 and 4.6). Thus, in the absence of Akirin1, it could be speculated that due to reduced MuRF1 levels, SRF is not being degraded to the wild-type levels leading to increased myoblast fusion. However, additional research is necessary to confirm this idea. Also, due to higher SRF and p21 levels, the Akirin1 knock-out myoblasts would withdraw from the cell cycle and differentiate earlier when compared to the wild-type myoblasts. Consistently, the results show an increased fusion of the myoblasts in the early stages of differentiation and thus no obvious phenotypic change in Akirin1 knock-out muscle was observed.

Besides having a role in myogenic differentiation, MuRF1 has a role in maintaining the integrity of the sarcomeres. MuRF1 is localized to the Z and M lines of sarcomere where it interacts with an array of proteins in the sarcomere and cytoskeleton (McElhinny et al., 2004). Our results have shown that lack of Akirin1 leads to reduced levels of MuRF1 in skeletal muscle

(Figure 4.6). Due to reduced MuRF1 protein level, important cytoskeletal proteins like desmin, actin and poly-glutamylated tubulin were also reduced when compared to the wild-type muscle (Figure 4.4 and 4.9). It has been previously reported that MuRF1 was involved in the glutamylation of tubulin (Spencer et al., 2000). Glutamylation renders stability to the microtubules, thus maintaining the sarcomeric integrity. Hence, it is quite possible that Akirin1 via MuRF1 regulates the stability of cytoskeletal proteins in muscle.

Molecular analysis of sarcomeric genes like α-actin, Myosin heavy chain and troponins showed that Akirin1 knock-out skeletal muscle showed reduced levels of these proteins compared to the wild-type (Figure 4.2 and 4.4). Reduced levels of these sarcomeric and cytoskeletal proteins in Akirin1 knock-out muscle may be compromising the sarcomeric stability and the effects of which can be extensively studied in a couple of ways. One is to study the detailed intra-cellular muscle fiber structure to directly assess the potential structural changes caused due to reduced levels of MuRF1 and other sarcomeric proteins using electron microscopy. Another way would be to study the extent of muscle regeneration after muscle injury by a myotoxin like notexin in Akirin1 knock-out mice compared to the wild-type mice.

Apart from stabilizing sarcomeric structure, MuRF1 being an E3 Ubiquitin ligase is known to regulate protein turnover in the skeletal muscle (Sacheck et al., 2004). A balance between synthesis and turnover of sarcomeric proteins is essential for maintenance of skeletal muscle structure and function. Our results showed that reduced MuRF1 levels lead to reduced ubiquitination of sarcomeric proteins (Figure 4.10). Reduced ubiquitination of sarcomeric proteins like MyHC has been previously reported to result in a myopathy characterized by

subsarcolemmal protein accumulation and reduced muscle contraction (Fielitz et al., 2007). So it may possible that lack of Akirin1 may be affecting the skeletal muscle function due to reduced MuRF1 levels. A detailed structure of Akirin1 knock-out sarcomere by electron microscopy would help in further understanding the effect of reduced ubiquitination of sarcomeric proteins.

Another important finding of this study is that the expression analysis showed that Akirin1 transcriptionally regulates the expression of different types of MyHC genes. Muscle fibers are made up of different types of MyHC like Myh7 in type I fibers (oxidative fibers), Myh2 in type IIa fibers (fast oxidative fibers) and Myh4 in type IIb fibers (fast glycolytic fibers). These different MyHC proteins have been shown to have different extent of ATPase activity thereby regulating energy metabolism in skeletal muscle (Edstrom et al., 1982, Rajab et al., 2000; Conjard et al., 1998). The proportion of different muscle fiber types are already established during embryogenic myogenesis. However in adults, they adapt to the metabolic energy demands by switching from one fiber type to another (Berchtold et al., 2000; Fluck et al., 2003). For example, a sprinter would require bursts of energy for fast contraction of muscles. Hence a sprinter's limb muscles would have higher proportion of fast twitch-glycolytic fibers. On the contrary, a marathon runner would require constant supply of energy to run long distances with slower muscle contraction compared to a sprinter. Hence a marathon runner's limb muscles would have higher proportion of slow twitch-oxidative fibers. Results obtained from our study showed that lack of Akirin1 down-regulated *Myh7* which encodes for MyHC in slow twitch and oxidative type I fibers and up-regulated *Myh2* which encodes for MyHC in fast twitch and less oxidative type IIa fibers. As a result of which, ablation of Akirin1 makes the

muscle less oxidative by increasing *Myh2* expression, leading to an increase in fast contracting type IIa muscle fibers and a decrease in *Myh7* expression, causing a decrease in slow contracting type I muscle fibers (Figure 4.15.1 and 4.15.2).

Another way to estimate the oxidative capacity in skeletal muscle is by SDH histochemistry. Akirin1 knock-out muscle showed reduced SDH staining with no difference in the α-GPD staining (measure of glycolytic capacity) indicating that lack of Akirin1 makes the muscle less oxidative while the glycolytic potential is unaffected (Figure 4.15). This further confirms the results that ablation of Akirin1 leads to fiber type switch from slow twitch oxidative type I myofibers to fast twitch less oxidative type IIa myofibers. Based on these results it can be inferred that Akirin1 plays a novel role in the determination of fiber type in the muscle which in turn would have a profound impact on the metabolic activity of the muscle.

In relevance to further comprehending the role of Akirin1 in energy metabolism, another aspect that would be worth exploring is the role of Akirin1 in regulating the mitochondrial DNA copy number and mitochondrial dynamics. We show herein that lack of Akirin1 leads to significant reduction in mitochondrial DNA copy number both during myogenic differentiation and in fully differentiated skeletal muscle (Figure 3.11 and 4.16). Reduced mitochondrial DNA copy number has been correlated to reduced ATP generation through oxidative phosphorylation thus serving as a read-out for mitochondrial function (Barazzoni et al., 2000). Furthermore, mitochondrial function and shape is dependent on two opposing processes called mitochondrial fission and fusion. An imbalance in these dynamic processes leads to impaired mitochondrial function eventually

leading to mitophagy (Bossy-Wetzel et al., 2003, Youle et al., 2012). Thus, it would be worth studying the role of Akirin1 in regulating the mitochondrial morphology by studying the expression profile of important marker genes involved in maintaining the balance between mitochondrial fission (e.g. Drp1, Fis1) and mitochondrial fusion (e.g. Mfn1, OPA1) (Lee et al., 2004; Chen et al., 2005). Also, mitochondrial number and morphology could be visualized by robust mitochondrial staining with Mito Tracker Red dye in Akirin1 knock-out and wild-type primary culture during differentiation and in skeletal muscle.

Furthermore we investigated the levels of proteins involved in the oxidative metabolic activity of skeletal muscle. For example, AMPK, a master regulator of cellular energy metabolism that maintains energy homeostasis in skeletal muscle was down-regulated in Akirin1 knock-out muscle (Figure 4.17). Consistently, its downstream targets CREB-1, PPARα and PGC1α levels were also reduced in the absence of Akirin1 (Figure 4.11 and 4.18). However, proteins like CREB-1 and PPARα were not up-regulated in differentiating Akirin1 over-expressing myoblasts (Figure 4.11.1 and 4.18.1). This could be due to differences in metabolic activity of fully differentiated skeletal muscle and differentiating myoblasts. Nonetheless, these results confirm a novel role of Akirin1 in regulating skeletal muscle metabolism. Research from other groups have established that reduced protein levels of CREB-1, PPARα and PGC1α leads to reduced mitochondrial function eventually leading to type 2 diabetes (Asmann et al., 2006).

Previous reports have also implicated MuRF1 in energy metabolism. Koyama et al. showed that MuRF1 links protein synthesis and energy metabolism mechanisms in skeletal muscle (Koyama et al., 2008). MuRF1 is also shown to

regulate carbohydrate metabolism by regulating blood glucose levels in mice (Hirner et al., 2008). As we observed reduced MuRF1 levels in the absence of Akirin1, it could be possible that carbohydrate metabolism may be affected in Akirin1 knock-out mice. However, additional research is necessary to establish the function of Akirin1 in regulating carbohydrate metabolism in mice.

This novel finding of effect of Akirin1 dysfunction on metabolic activity would be of significant clinical relevance as skeletal muscle is a highly metabolic tissue which plays an important role in maintaining energy metabolism homeostasis in the body. For example, Schuler et al. have shown that mice exhibiting fiber-type switch from slow contracting type I slow fibers to fast contracting type IIa fast fibers, developed metabolic disorders like obesity and Type 2 diabetes (Schuler et al., 2006). Thus, Akirin1 would have a significant role in maintaining a homeostatic balance in energy metabolism and would serve as a potential therapeutic target in the treatment of metabolic disorders like obesity and diabetes.

From the regulation point of view, we wanted to determine how Akirin1 regulates MuRF1. Firstly we analyzed the promoter region of MuRF1. The promoter analysis showed FoxO3 and CREB-1 binding sites on MuRF1 promoter. Previous reports have shown that FoxO3 transcription factor transcriptionally up-regulates MuRF1 in skeletal muscle (Zhao et al., 2007; Stitt et al., 2004). FoxO3 protein needs to be dephosphorylated to migrate to the nucleus to activate the transcription of MuRF1. The phosphorylated FoxO3 remains cytoplasmic and is in an inactive form. In fact, our results show that there was an increase in phosphorylated form of FoxO3 in Akirin1 knock-out skeletal muscle and during myogenic differentiation. Consistently, the levels of

FoxO3 were up-regulated when Akirin1 was over-expressed in C_2C_{12} myoblasts (Figure 3.9 and 4.8.1). Akirin1, a nuclear protein, is considered to act as co-factor. *In-silico* analysis of Akirin1 protein structure speculated that Akirin1 contains putative Forkhead interacting motif. So it may be possible that Akirin1 directly interacts with FoxO3 transcription factor, helping in the translocation of FoxO3 to the nucleus and leading to MuRF1 transcription. Transfection and band-shift assay results indicated that Akirin1 might be regulating the transcription of MuRF1 through CREB-1 also (Figure 4.7 and 4.12). The mechanism of CREB-1 mediated regulation of MuRF1 by Akirin1 is most likely an indirect one and hence is not clear yet.

Our work showed that absence of Akirin1 results in de-regulation of several genes that participate in skeletal muscle metabolism. It is also clear that Akirin1 regulates few genes like MuRF1 and Myh2 at transcriptional level while the others like AMPK, CREB-1, PPARα are regulated at post-transcriptional level. It is quite possible that some of the results we observe in this study due to lack of Akirin1 may be direct effects because of its interaction with transcription factors like FoxO3. This study clearly shows that Akirin1 regulates some molecules similarly both during differentiation and in fully differentiated muscle. However as the role of each of these molecules is different during myogenic differentiation and in fully differentiatiated muscle, we observe a different effect. Differential regulation of genes by Akirin1 can be further studied using a systems analysis approach to get more insights on understanding the exact mode of action of Akirin1 in regulating this array of genes.

Recent studies in Drosophila have shown that DmAkirin physically interacts with muscle transcription factor twist, and regulates transcription of twist-related

genes (Nowak et al., 2012). DmAkirin protein is also known to co-localise with Brahma SWI/SNF complex subunits which is a chromatin remodelling complex. Hence DmAkirin is predicted to link twist and chromatin remodelling complex affecting the expression of twist-regulated genes (Nowak et al., 2012). Our results herein show that lack of Akirin1 post-transcriptionally up-regulated HDAC4 which is known to play an important role in epigenetic regulation of many skeletal muscle genes (Figure 4.19). So, it may be possible that Akirin1 has a role directly or indirectly or both in epigenetically regulating the various genes that were observed in this study.

Akirin1 was found to have an interesting and distinct function in cardiac muscle. Our results showed that Akirin1 knock-out heart had larger ventricular cavity as seen in left ventricular hypertrophy (LVH) (Figure 5.1). One of the important pathways involved in both pathological and physiological hypertrophy is PI3K/Akt/GSK3β pathway and activation of PI3K leads to cardiac hypertrophy (Naga Prasad et al., 2000). Consistent to this finding, increase in PI3K protein was seen in Akirin1 knock-out cardiac muscle leading to activation of PI3-K/Akt/GSK3β pathway leading to increased protein synthesis (Figure 5.8). This increased protein synthesis was proven by increased protein levels of sarcomeric and cytosolic proteins like α-actin, MyHC and desmin in our study (Figure 5.2.1). It has been proven in pathological hypertrophy that the contractility of cardiac sarcomeres is affected due to reduced troponin I and troponin T levels (Varnava et al., 2001; Takeishi et al., 1998). In Akirin1 knock-out cardiac muscle also the troponin I and troponin T levels were down-regulated suggesting that Akirin1 knock-out hearts are undergoing pathological hypertrophy (Figure 5.3). Apart from PI3-K/Akt/GSK3β pathway, various other stress kinase

pathways are known to be activated during pathological cardiac hypertrophy like ERK pathway, p38 MAPK pathway and JNK pathway (Bueno et al., 2002; Bueno et al., 2000; Sugden et al., 1998; Wang et al., 1998; Wang et al., 1998; Zhang et al., 2003; Ramirez et al., 1997). The results from our study also showed that all the above pathways were activated in the absence of Akirin1 (Figure 5.9, 5.10 and 5.11). Thus showing that lack of Akirin1 affects the cardiac muscle mass homeostasis.

Zhang et al. showed that cardiac specific over-expression of SRF led to cardiomyopathy (Zhang et al., 2001). Later, the same research group in 2011 showed that this cardiac-specific over-expression of SRF led to down-regulation of miR-1 biogenesis (Zhang et al., 2011). In another study it was shown that miR-1 targets cardiac hypertrophy inducing genes like ANP and β-MyHC (Wei et al., 2014). Consistent with these findings, our study also showed that in the absence of Akirin1, SRF protein level was up-regulated in the cardiac muscle (Figure 5.4). This increase in SRF might be leading to down-regulation of miR-1 biogenesis due to which ANP and β-MyHC expression was up-regulated (Figure 5.6). Re-expression of fetal genes like ANP and β-MyHC are proven to induce Akt signaling pathway in the cardiac muscle leading to increased sarcomeric protein synthesis and pathological hypertrophy (Kato et al., 2005). Thus it can be speculated that Akirin1 post-transcriptionally regulates SRF levels in cardiac muscle leading to pathological cardiac hypertrophy through miR-1.

In summary, we have observed that Akirin1 regulates certain genes at transcription level and others post-transcriptionally. The exact mode of Akirin1 action is yet to be elucidated and it is quite possible that many of the observed differences are due to redundant or indirect processes to which Akirin1 is the

contributing factor. For example, Akirin1 may be regulating these genes post-transcriptionally either by affecting their RNA stability or through micro-RNAs that target the mRNA of the above genes and inhibit its translation. However, through this study, we have clearly established a striated muscle phenotype due to Akirin1 ablation, suggesting a novel role of Akirin1 in regulating metabolic activity in skeletal muscle and regulating cardiac muscle mass in cardiac muscle.

7. BIBLIOGRAPHY

- Akhter, S. A., Luttrell, L. M., Rockman, H. A., Iaccarino, G., Lefkowitz, R. J., & Koch, W. J. (1998). Targeting the receptor-Gq interface to inhibit in vivo pressure overload myocardial hypertrophy. *Science*, *280*(5363), 574-577.
- Alexandrides, T., Moses, A. C., & Smith, R. J. (1989). Developmental Expression of Receptors for Insulin, Insulin-like Growth Factor I (IGF-I), and IGF-II in Rat Skeletal Muscle. *Endocrinology*, *124*(2), 1064-1076.
- Allen, D. L., Sartorius, C. A., Sycuro, L. K., & Leinwand, L. A. (2001). Different pathways regulate expression of the skeletal myosin heavy chain genes. *Journal of Biological Chemistry*, *276*(47), 43524-43533.
- Alzghoul, M. B., Gerrard, D., Watkins, B. A., & Hannon, K. (2004). Ectopic expression of IGF-I and Shh by skeletal muscle inhibits disuse-mediated skeletal muscle atrophy and bone osteopenia in vivo. *The FASEB journal*, *18*(1), 221-223.
- Amacher, S. L., Buskin, J. N., & Hauschka, S. D. (1993). Multiple regulatory elements contribute differentially to muscle creatine kinase enhancer activity in skeletal and cardiac muscle. *Molecular and cellular biology*, *13*(5), 2753-2764.
- Amthor, H., Christ, B., Weil, M., & Patel, K. (1998). The importance of timing differentiation during limb muscle development. *Current biology*, *8*(11), 642-652.
- Asmann, Y. W., Stump, C. S., Short, K. R., Coenen-Schimke, J. M., Guo, Z., Bigelow, M. L., & Nair, K. S. (2006). Skeletal muscle mitochondrial functions, mitochondrial DNA copy numbers, and gene transcript profiles in type 2 diabetic and nondiabetic subjects at equal levels of low or high insulin and euglycemia. *Diabetes*, *55*(12), 3309-3319.
- Bagnato, P., Barone, V., Giacomello, E., Rossi, D., & Sorrentino, V. (2003). Binding of an ankyrin-1 isoform to obscurin suggests a molecular link between the sarcoplasmic reticulum and myofibrils in striated muscles. *The Journal of cell biology*, *160*(2), 245-253.
- Barazzoni, R., Short, K. R., & Nair, K. S. (2000). Effects of aging on mitochondrial DNA copy number and cytochromec oxidase gene expression in rat skeletal muscle, liver, and heart. *Journal of Biological Chemistry*, *275*(5), 3343-3347.
- Bartoli, M., Poupiot, J., Vulin, A., Fougerousse, F., Arandel, L., Daniele, N., & Richard, I. (2007). AAV-mediated delivery of a mutated myostatin

propeptide ameliorates calpain 3 but not α-sarcoglycan deficiency. *Gene therapy*, *14*(9), 733-740.

- Barton-Davis, E. R., Shoturma, D. I., Musaro, A., Rosenthal, N., & Sweeney, H. L. (1998). Viral mediated expression of insulin-like growth factor I blocks the aging-related loss of skeletal muscle function. *Proceedings of the National Academy of Sciences*, *95*(26), 15603-15607.
- Beck, F., Samani, N. J., Byrne, S., Morgan, K., Gebhard, R., & Brammar, W. J. (1988). Histochemical localization of IGF-I and IGF-II mRNA in the rat between birth and adulthood. *Development*, *104*(1), 29-39.
- Berchtold, M. W., Brinkmeier, H., & Müntener, M. (2000). Calcium ion in skeletal muscle: its crucial role for muscle function, plasticity, and disease. *Physiological reviews*, *80*(3), 1215-1265.
- Bischoff, R. (1997). Chemotaxis of skeletal muscle satellite cells. *Developmental dynamics*, *208*(4), 505-515.
- Bischoff, R., & Heintz, C. (1994). Enhancement of skeletal muscle regeneration. *Developmental dynamics*, *201*(1), 41-54.
- Black, B. L., Martin, J. F., & Olson, E. N. (1995). The mouse MRF4 promoter is trans-activated directly and indirectly by muscle-specific transcription factors. *Journal of Biological Chemistry*, *270*(7), 2889-2892.
- Bladt, F., Riethmacher, D., Isenmann, S., Aguzzi, A., & Birchmeier, C. (1995). Essential role for the c-met receptor in the migration of myogenic precursor cells into the limb bud. *Nature*, *376*(6543), 768-771.
- Bodine, S. C., Latres, E., Baumhueter, S., Lai, V. K. M., Nunez, L., Clarke, B. A., & Glass, D. J. (2001). Identification of ubiquitin ligases required for skeletal muscle atrophy. *Science Signaling*, *294*(5547), 1704.
- Bogdanovich, S., Krag, T. O., Barton, E. R., Morris, L. D., Whittemore, L. A., Ahima, R. S., & Khurana, T. S. (2002). Functional improvement of dystrophic muscle by myostatin blockade. *Nature*, *420*(6914), 418-421.
- Bondy, C., & Lee, W. H. (1993). Correlation between insulin-like growth factor (IGF)-binding protein 5 and IGF-I gene expression during brain development. *The Journal of neuroscience*, *13*(12), 5092-5104.
- Bossy-Wetzel, E., Barsoum, M. J., Godzik, A., Schwarzenbacher, R., & Lipton, S. A. (2003). Mitochondrial fission in apoptosis, neurodegeneration and aging. *Current opinion in cell biology*, *15*(6), 706-716.
- Breitbart, R. E., Liang, C. S., Smoot, L. B., Laheru, D. A., Mahdavi, V., & Nadal-Ginard, B. (1993). A fourth human MEF2 transcription factor, hMEF2D, is an early marker of the myogenic lineage. *Development*, *118*(4), 1095-1106.

- Buckingham, M., Bajard, L., Chang, T., Daubas, P., Hadchouel, J., Meilhac, S., & Relaix, F. (2003). The formation of skeletal muscle: from somite to limb. *Journal of Anatomy*, *202*(1), 59-68.
- Bueno, O. F., & Molkentin, J. D. (2002). Involvement of extracellular signal-regulated kinases 1/2 in cardiac hypertrophy and cell death. *Circulation research*, *91*(9), 776-781.
- Bueno, O. F., De Windt, L. J., Tymitz, K. M., Witt, S. A., Kimball, T. R., Klevitsky, R., & Molkentin, J. D. (2000). The MEK1–ERK1/2 signaling pathway promotes compensated cardiac hypertrophy in transgenic mice. *The EMBO Journal*, *19*(23), 6341-6350.
- Campbell, K. S., & Lakie, M. (1996, September). Sarcomere length measurement of thixotropic tension responses in relaxed amphibian muscle. *Journal of physiology-london* (vol. 495, pp. p162-p162).
- Campbell, K. S., & Lakie, M. (1998). A cross-bridge mechanism can explain the thixotropic short-range elastic component of relaxed frog skeletal muscle. *The Journal of physiology*, *510*(3), 941-962.
- Carlson, C. J., Booth, F. W., & Gordon, S. E. (1999). Skeletal muscle myostatin mRNA expression is fiber-type specific and increases during hindlimb unloading. *American Journal of Physiology-Regulatory, Integrative and Comparative Physiology*, *277*(2), R601-R606.
- Centner, T., Yano, J., Kimura, E., McElhinny, A. S., Pelin, K., Witt, C. C., & Labeit, S. (2001). Identification of muscle specific ring finger proteins as potential regulators of the titin kinase domain. *Journal of molecular biology*, *306*(4), 717-726.
- Centner, T., Yano, J., Kimura, E., McElhinny, A. S., Pelin, K., Witt, C. C., & Labeit, S. (2001). Identification of muscle specific ring finger proteins as potential regulators of the titin kinase domain. *Journal of molecular biology*, *306*(4), 717-726.
- Chargé, S., & Rudnicki, M. A. (2003). Fusion with the fused: a new role for interleukin-4 in the building of muscle. *Cell*, *113*(4), 422-423.
- Charvet, C., Houbron, C., Parlakian, A., Giordani, J., Lahoute, C., Bertrand, A., & Tuil, D. (2006). New role for serum response factor in postnatal skeletal muscle growth and regeneration via the interleukin 4 and insulin-like growth factor 1 pathways. *Molecular and cellular biology*, *26*(17), 6664-6674.
- Chen, H., & Chan, D. C. (2005). Emerging functions of mammalian mitochondrial fusion and fission. *Human molecular genetics*, *14*(suppl 2), R283-R289.

- Chin, E. R., Olson, E. N., Richardson, J. A., Yang, Q., Humphries, C., Shelton, J. M., & Williams, R. S. (1998). A calcineurin-dependent transcriptional pathway controls skeletal muscle fiber type. *Genes & development*, *12*(16), 2499-2509.
- Choi, J., Costa, M. L., Mermelstein, C. S., Chagas, C., Holtzer, S., & Holtzer, H. (1990). MyoD converts primary dermal fibroblasts, chondroblasts, smooth muscle, and retinal pigmented epithelial cells into striated mononucleated myoblasts and multinucleated myotubes. *Proceedings of the National Academy of Sciences*, *87*(20), 7988-7992.
- Clive R. Bagshaw. (1993). *Muscle contraction*. Springer.
- Conjard, A., Peuker, H., & Pette, D. (1998). Energy state and myosin heavy chain isoforms in single fibres of normal and transforming rabbit muscles. *Pflügers Archiv*, *436*(6), 962-969.
- Cornelison, D. D. W., & Wold, B. J. (1997). Single-cell analysis of regulatory gene expression in quiescent and activated mouse skeletal muscle satellite cells. *Developmental biology*, *191*(2), 270-283.
- Cornelison, D. D. W., Olwin, B. B., Rudnicki, M. A., & Wold, B. J. (2000). MyoD (-/-) Satellite Cells in Single-Fiber Culture Are Differentiation Defective and MRF4 Deficient. *Developmental biology*, *224*(2), 122-137.
- Cserjesi, P., & Olson, E. N. (1991). Myogenin induces the myocyte-specific enhancer binding factor MEF-2 independently of other muscle-specific gene products. *Molecular and cellular biology*, *11*(10), 4854-4862.
- Cusella-De Angelis, M. G., Molinari, S., Le Donne, A., Coletta, M., Vivarelli, E., Bouche, M., & Cossu, G. (1994). Differential response of embryonic and fetal myoblasts to TGF beta: a possible regulatory mechanism of skeletal muscle histogenesis. *Development*, *120*(4), 925-933.
- D'Angelo, D. D., Sakata, Y., Lorenz, J. N., Boivin, G. P., Walsh, R. A., Liggett, S. B., & Dorn, G. W. (1997). Transgenic Gαq overexpression induces cardiac contractile failure in mice. *Proceedings of the National Academy of Sciences*, *94*(15), 8121-8126.
- Daopin, S., Li, M., & Davies, D. R. (1993). Crystal structure of TGF-β2 refined at 1.8 Å resolution. *Proteins: Structure, Function, and Bioinformatics*, *17*(2), 176-192.

- Daston, G., Lamar, E., Olivier, M., & Goulding, M. (1996). Pax-3 is necessary for migration but not differentiation of limb muscle precursors in the mouse. *Development*, *122*(3), 1017-1027.
- Delling, U., Tureckova, J., Lim, H. W., De Windt, L. J., Rotwein, P., & Molkentin, J. D. (2000). A calcineurin-NFATc3-dependent pathway regulates skeletal muscle differentiation and slow myosin heavy-chain expression. *Molecular and Cellular Biology*, *20*(17), 6600-6611.
- Dickinson, A., Yeung, K. Y., Donoghue, J., Baker, M. J., Kelly, R. D., McKenzie, M., & John, J. S. (2013). The regulation of mitochondrial DNA copy number in glioblastoma cells. *Cell Death & Differentiation*, *20*(12), 1644-1653.
- Dong, Y., Pan, J. S., & Zhang, L. (2013). Myostatin suppression of Akirin1 mediates glucocorticoid-induced satellite cell dysfunction. *PloS one*, *8*(3), e58554.
- Dressel, U., Bailey, P. J., Wang, S. M., Downes, M., Evans, R. M., & Muscat, G. E. (2001). A dynamic role for HDAC7 in MEF2-mediated muscle differentiation. *Journal of Biological Chemistry*, *276*(20), 17007-17013.
- Durieux, A. C., Amirouche, A., Banzet, S., Koulmann, N., Bonnefoy, R., Pasdeloup, M., & Freyssenet, D. (2007). Ectopic expression of myostatin induces atrophy of adult skeletal muscle by decreasing muscle gene expression. *Endocrinology*, *148*(7), 3140-3147.
- Eckner, R., Yao, T. P., Oldread, E., & Livingston, D. M. (1996). Interaction and functional collaboration of p300/CBP and bHLH proteins in muscle and B-cell differentiation. *Genes & development*, *10*(19), 2478-2490.
- Edmondson, D. G., & Olson, E. N. (1989). A gene with homology to the myc similarity region of MyoD1 is expressed during myogenesis and is sufficient to activate the muscle differentiation program. *Genes & development*, *3*(5), 628-640.
- Edmondson, D. G., Cheng, T. C., Cserjesi, P., Chakraborty, T., & Olson, E. N. (1992). Analysis of the myogenin promoter reveals an indirect pathway for positive autoregulation mediated by the muscle-specific enhancer factor MEF-2. *Molecular and cellular biology*, *12*(9), 3665-3677.
- Edmondson, D. G., Lyons, G. E., Martin, J. F., & Olson, E. N. (1994). Mef2 gene expression marks the cardiac and skeletal muscle lineages during mouse embryogenesis. *Development*, *120*(5), 1251-1263.
- Edstrom, L., Hultman, E., Sahlin, K., & Sjoholm, H. (1982). The contents of high-energy phosphates in different fibre types in skeletal muscles

from rat, guinea-pig and man. *Journal of Physiology*, 332, 47-58.

- Elkasrawy, M. N., & Hamrick, M. W. (2010). Myostatin (GDF-8) as a Key Factor Linking Muscle Mass and Skeletal Form. *Journal of musculoskeletal & neuronal interactions*, *10*(1), 56.
- Emerson Jr, C. P. (1993). Embryonic signals for skeletal myogenesis: arriving at the beginning. *Current opinion in cell biology*, *5*(6), 1057-1064.
- Engert, J. C., Berglund, E. B., & Rosenthal, N. (1996). Proliferation precedes differentiation in IGF-I-stimulated myogenesis. *The Journal of Cell Biology*, *135*(2), 431-440.
- Erbay, E., Park, I. H., Nuzzi, P. D., Schoenherr, C. J., & Chen, J. (2003). IGF-II transcription in skeletal myogenesis is controlled by mTOR and nutrients. *The Journal of cell biology*, *163*(5), 931-936.
- Fagard, R. H. (1997). Impact of different sports and training on cardiac structure and function. *Cardiology clinics*, *15*(3), 397-412.
- Fickett, J. W. (1996). Coordinate positioning of MEF2 and myogenin binding sites. *Gene*, *172*(1), GC19-GC32.
- Fielitz, J., Kim, M. S., Shelton, J. M., Latif, S., Spencer, J. A., Glass, D. J., & Olson, E. N. (2007). Myosin accumulation and striated muscle myopathy result from the loss of muscle RING finger 1 and 3. *Journal of Clinical Investigation*, *117*(9), 2486-2495.
- Francis-West, P. H., Antoni, L., & Anakwe, K. (2003). Regulation of myogenic differentiation in the developing limb bud. *Journal of anatomy*, *202*(1), 69-81.
- Frey, N., Katus, H. A., Olson, E. N., & Hill, J. A. (2004). Hypertrophy of the heart a new therapeutic target?. *Circulation*, *109*(13), 1580-1589.
- Fuchs, E. (1994). Intermediate filaments and disease: mutations that cripple cell strength. *The Journal of cell biology*, *125*(3), 511-516.
- Fuchs, E., & Cleveland, D. W. (1998). A structural scaffolding of intermediate filaments in health and disease. *Science*, *279*(5350), 514-519.
- Fukada, S. I., Higuchi, S., Segawa, M., Koda, K. I., Yamamoto, Y., Tsujikawa, K., & Yamamoto, H. (2004). Purification and cell-surface marker characterization of quiescent satellite cells from murine skeletal muscle by a novel monoclonal antibody. *Experimental cell research*, *296*(2), 245-255.
- Fukushima, K., Badlani, N., Usas, A., Riano, F., Fu, F. H., & Huard, J. (2001). The use of an antifibrosis agent to improve muscle recovery after laceration. *The American journal of sports medicine*, *29*(4), 394-402.

- Gaddy-Kurten, D., Tsuchida, K., & Vale, W. (1994). Activins and the receptor serine kinase superfamily. *Recent progress in hormone research*, *50*, 109-129.
- Gal-Levi, R., Leshem, Y., Aoki, S., Nakamura, T., & Halevy, O. (1998). Hepatocyte growth factor plays a dual role in regulating skeletal muscle satellite cell proliferation and differentiation. *Biochimica et Biophysica Acta (BBA)-Molecular Cell Research*, *1402*(1), 39-51.
- Garrett, R. H., & Grisham, C. M. Biochemistry, 1999. *Saunder's College Publishing*.
- Gartel, A. L., & Radhakrishnan, S. K. (2005). Lost in transcription: p21 repression, mechanisms, and consequences. *Cancer research*, *65*(10), 3980-3985.
- Ge, X., McFarlane, C., Vajjala, A., Lokireddy, S., Ng, Z. H., Tan, C. K., & Kambadur, R. (2011). Smad3 signaling is required for satellite cell function and myogenic differentiation of myoblasts. *Cell research*, *21*(11), 1591-1604.
- Girgenrath, S., Song, K., & Whittemore, L. A. (2005). Loss of myostatin expression alters fiber-type distribution and expression of myosin heavy chain isoforms in slow-and fast-type skeletal muscle. *Muscle & nerve*, *31*(1), 34-40.
- Gojo, K., Abe, S., & Ide, Y. (2002). Characteristics of myofibres in the masseter muscle of mice during postnatal growth period. *Anatomia, histologia, embryologia*, *31*(2), 105-112.
- Goldspink, G. (2003). Gene expression in muscle in response to exercise. *Journal of Muscle Research & Cell Motility*, *24*(2-3), 121-126.
- Gossett, L. A., Kelvin, D. J., Sternberg, E. A., & Olson, E. N. (1989). A new myocyte-specific enhancer-binding factor that recognizes a conserved element associated with multiple muscle-specific genes. *Molecular and cellular biology*, *9*(11), 5022-5033.
- Goto, A., Matsushita, K., Gesellchen, V., El Chamy, L., Kuttenkeuler, D., Takeuchi, O., & Reichhart, J. M. (2008). Akirins are highly conserved nuclear proteins required for NF-κB-dependent gene expression in drosophila and mice. *Nature immunology*, *9*(1), 97-104.
- Graham, T. E., Yuan, Z., Hill, A. K., & Wilson, R. J. (2010). The regulation of muscle glycogen: the granule and its proteins. *Acta physiologica*, *199*(4), 489-498.
- Greene, E. A., & Allen, R. E. (1991). Growth factor regulation of bovine satellite cell growth in vitro. *Journal of animal science*, *69*(1), 146-152.

- Grefte, S., Kuijpers-Jagtman, A. M., Torensma, R., & Von den Hoff, J. W. (2007). Skeletal muscle development and regeneration. *Stem cells and development*, *16*(5), 857-868.
- Grobet, L., Poncelet, D., Royo, L. J., Brouwers, B., Pirottin, D., Michaux, C., & Georges, M. (1998). Molecular definition of an allelic series of mutations disrupting the myostatin function and causing double-muscling in cattle. *Mammalian genome*, *9*(3), 210-213.
- Grossman, W., Jones, D., & McLaurin, L. P. (1975). Wall stress and patterns of hypertrophy in the human left ventricle. *Journal of Clinical Investigation*, *56*(1), 56.
- Hannon, K., Smith II, C. K., Bales, K. R., & Santerre, R. F. (1992). Temporal and quantitative analysis of myogenic regulatory and growth factor gene expression in the developing mouse embryo. *Developmental biology*, *151*(1), 137-144.
- Haq, S., Choukroun, G., Kang, Z. B., Ranu, H., Matsui, T., Rosenzweig, A., & Force, T. (2000). Glycogen synthase kinase-3β is a negative regulator of cardiomyocyte hypertrophy. *The Journal of cell biology*, *151*(1), 117-130.
- Haq, S., Choukroun, G., Lim, H., Tymitz, K. M., del Monte, F., Gwathmey, J., & Molkentin, J. D. (2001). Differential activation of signal transduction pathways in human hearts with hypertrophy versus advanced heart failure. *Circulation*, *103*(5), 670-677.
- Hasegawa, K., Lee, S.J., Jobe, S.M., Markham, B.E., & Kitsis, R. N. (1997). cis-Acting sequences that mediate induction of beta-myosin heavy chain gene expression during left ventricular hypertrophy due to aortic constriction. *Circulation*, 96(11):3943-53.
- Hawke, T. J., Meeson, A. P., Jiang, N., Graham, S., Hutcheson, K., DiMaio, J. M., & Garry, D. J. (2003). p21 is essential for normal myogenic progenitor cell function in regenerating skeletal muscle. *American Journal of Physiology-Cell Physiology*, *285*(5), C1019-C1027.
- Hein, L., Stevens, M. E., Barsh, G. S., Pratt, R. E., Kobilka, B. K., & Dzau, V. J. (1997). Overexpression of angiotensin AT1 receptor transgene in the mouse myocardium produces a lethal phenotype associated with myocyte hyperplasia and heart block. *Proceedings of the National Academy of Sciences*, *94*(12), 6391-6396.
- Hidaka, K., Morisaki, T., Byun, S. H., Hashido, K., Toyama, K., & Mukai, T. (1995). The MEF2B Homolog Differentially Expressed in Mouse Embryonal Carcinoma Cells. *Biochemical and biophysical research communications*, *213*(2), 555-560.

- Hirner, S., Krohne, C., Schuster, A., Hoffmann, S., Witt, S., Erber, R., & Labeit, D. (2008). MuRF1-dependent regulation of systemic carbohydrate metabolism as revealed from transgenic mouse studies. *Journal of molecular biology*, *379*(4), 666-677.
- Holst, D., Luquet, S., Nogueira, V., Kristiansen, K., Leverve, X., & Grimaldi, P. A. (2003). Nutritional regulation and role of peroxisome proliferator-activated receptor δ in fatty acid catabolism in skeletal muscle. *Biochimica et Biophysica Acta (BBA)-Molecular and Cell Biology of Lipids*, *1633*(1), 43-50.
- Hoppeler, H., Vogt, M., Weibel, E. R., & Fluck, M. (2003). Response of skeletal muscle mitochondria to hypoxia. *Experimental physiology*, *88*(1), 109-119.
- Huang, Z., Chen, D., Zhang, K., Yu, B., Chen, X., & Meng, J. (2007). Regulation of myostatin signaling by c-Jun N-terminal kinase in C_2C_{12} cells. *Cellular signalling*, *19*(11), 2286-2295.
- Itoh, N., Mima, T., & Mikawa, T. (1996). Loss of fibroblast growth factor receptors is necessary for terminal differentiation of embryonic limb muscle. *Development*, *122*(1), 291-300.
- Jackson, M. F., Luong, D., Vang, D. D., Garikipati, D. K., Stanton, J. B., Nelson, O. L., & Rodgers, B. D. (2012). The aging myostatin null phenotype: reduced adiposity, cardiac hypertrophy, enhanced cardiac stress response, and sexual dimorphism. *Journal of Endocrinology*, *213*(3), 263-275.
- James, J., Zhang, Y., Osinska, H., Sanbe, A., Klevitsky, R., Hewett, T. E., & Robbins, J. (2000). Transgenic modeling of a cardiac troponin I mutation linked to familial hypertrophic cardiomyopathy. *Circulation research*, *87*(9), 805-811.
- James, P., Ellis, C. J., Whitlock, R. M. L., McNeil, A. R., Henley, J., & Anderson, N. E. (2000). Relation between troponin T concentration and mortality in patients presenting with an acute stroke: observational study. *BMJ: British Medical Journal*, *320*(7248), 1502.
- Joulia, D., Bernardi, H., Garandel, V., Rabenoelina, F., Vernus, B., & Cabello, G. (2003). Mechanisms involved in the inhibition of myoblast proliferation and differentiation by myostatin. *Experimental cell research*, *286*(2), 263-275.
- Kablar, B., Krastel, K., Ying, C., Asakura, A., Tapscott, S. J., & Rudnicki, M. A. (1997). MyoD and Myf-5 differentially regulate the development of limb versus trunk skeletal muscle. *Development*, *124*(23), 4729-4738.

- Kaliman, P., Canicio, J., Shepherd, P. R., Beeton, C. A., Testar, X., Palacín, M., & Zorzano, A. (1998). Insulin-like growth factors require phosphatidylinositol 3-kinase to signal myogenesis: dominant negative p85 expression blocks differentiation of L6E9 muscle cells. *Molecular Endocrinology*, *12*(1), 66-77.
- Kambadur, R., Sharma, M., Smith, T. P., & Bass, J. J. (1997). Mutations in myostatin (GDF8) in double-muscled Belgian Blue and Piedmontese cattle. *Genome research*, *7*(9), 910-915.
- Kato, T., Muraski, J., Chen, Y., Tsujita, Y., Wall, J., Glembotski, C. C., & Sussman, M. A. (2005). Atrial natriuretic peptide promotes cardiomyocyte survival by cGMP-dependent nuclear accumulation of zyxin and Akt. *Journal of Clinical Investigation*, *115*(10), 2716-2730.
- Kegley, K. M., Gephart, J., Warren, G. L., & Pavlath, G. K. (2001). Altered Primary Myogenesis in NFATC3 null Mice Leads to Decreased Muscle Size in the Adult. *Developmental biology*, *232*(1), 115-126.
- Kiess, W., Blickenstaff, G. D., Sklar, M. M., Thomas, C. L., Nissley, S. P., & Sahagian, G. G. (1988). Biochemical evidence that the type II insulin-like growth factor receptor is identical to the cation-independent mannose 6-phosphate receptor. *Journal of Biological Chemistry*, *263*(19), 9339-9344.
- Kirk, S., Oldham, J., Kambadur, R., Sharma, M., Dobbie, P., & Bass, J. (2000). Myostatin regulation during skeletal muscle regeneration. *Journal of cellular physiology*, *184*(3), 356-363.
- Kontrogianni-Konstantopoulos, A., Jones, E. M., van Rossum, D. B., & Bloch, R. J. (2003). Obscurin is a ligand for small ankyrin 1 in skeletal muscle. *Molecular biology of the cell*, *14*(3), 1138-1148.
- Koyama, S., Hata, S., Witt, C. C., Ono, Y., Lerche, S., Ojima, K., & Sorimachi, H. (2008). Muscle RING-finger protein-1 (MuRF1) as a connector of muscle energy metabolism and protein synthesis. *Journal of molecular biology*, *376*(5), 1224-1236.
- Koyama, S., Hata, S., Witt, C. C., Ono, Y., Lerche, S., Ojima, K., & Sorimachi, H. (2008). Muscle RING-finger protein-1 (MuRF1) as a connector of muscle energy metabolism and protein synthesis. *Journal of molecular biology*, *376*(5), 1224-1236.
- Lach-Trifilieff, E., Minetti, G. C., Sheppard, K., Ibebunjo, C., Feige, J. N., Hartmann, S., & Glass, D. J. (2014). An Antibody Blocking Activin Type II Receptors Induces Strong Skeletal Muscle Hypertrophy and Protects from Atrophy. *Molecular and cellular biology*, *34*(4), 606-618.

- Lalani, R., Bhasin, S., Byhower, F., Tarnuzzer, R., Grant, M., Shen, R., & Gonzalez-Cadavid, N. F. (2000). Myostatin and insulin-like growth factor-I and-II expression in the muscle of rats exposed to the microgravity environment of the NeuroLab space shuttle flight. *Journal of Endocrinology*, *167*(3), 417-428.
- Lange, S., Xiang, F., Yakovenko, A., Vihola, A., Hackman, P., Rostkova, E., & Gautel, M. (2005). The kinase domain of titin controls muscle gene expression and protein turnover. *Science*, *308*(5728), 1599-1603.
- Langley, B., Thomas, M., Bishop, A., Sharma, M., Gilmour, S., & Kambadur, R. (2002). Myostatin inhibits myoblast differentiation by down-regulating MyoD expression. *Journal of Biological Chemistry*, *277*(51), 49831-49840.
- Langley, B., Thomas, M., McFarlane, C., Gilmour, S., Sharma, M., & Kambadur, R. (2004). Myostatin inhibits rhabdomyosarcoma cell proliferation through an Rb-independent pathway. *Oncogene*, *23*(2), 524-534.
- Lawlor, M. A., & Rotwein, P. (2000). Coordinate control of muscle cell survival by distinct insulin-like growth factor activated signaling pathways. *The Journal of cell biology*, *151*(6), 1131-1140.
- Lee, S. J., & McPherron, A. C. (1999). Myostatin and the control of skeletal muscle mass: commentary. *Current opinion in genetics & development*, *9*(5), 604-607.
- Lee, S. J., & McPherron, A. C. (2001). Regulation of myostatin activity and muscle growth. *Proceedings of the National Academy of Sciences*, *98*(16), 9306-9311.
- Lee, Y. J., Jeong, S. Y., Karbowski, M., Smith, C. L., & Youle, R. J. (2004). Roles of the mammalian mitochondrial fission and fusion mediators Fis1, Drp1, and Opa1 in apoptosis. *Molecular biology of the cell*, *15*(11), 5001-5011.
- Li, H., & Capetanaki, Y. (1994). An E box in the desmin promoter cooperates with the E box and MEF-2 sites of a distal enhancer to direct muscle-specific transcription. *The EMBO journal*, *13*(15), 3580.
- Liu, D., Black, B. L., & Derynck, R. (2001). TGF-β inhibits muscle differentiation through functional repression of myogenic transcription factors by Smad3. *Genes & development*, *15*(22), 2950-2966.
- Liu, J. P., Baker, J., Perkins, A. S., Robertson, E. J., & Efstratiadis, A. (1993). Mice carrying null mutations of the genes encoding insulin-like growth factor I (*Igf1*) and type 1 IGF receptor (*Igf1r*). *Cell*, *75*(1), 59-72.

- Lokireddy, S., Mouly, V., Butler-Browne, G., Gluckman, P. D., Sharma, M., Kambadur, R., & McFarlane, C. (2011). Myostatin promotes the wasting of human myoblast cultures through promoting ubiquitin-proteasome pathway-mediated loss of sarcomeric proteins. *American Journal of Physiology-Cell Physiology*, *301*(6), C1316-C1324.
- Lokireddy, S., Wijesoma, I. W., Teng, S., Bonala, S., Gluckman, P. D., McFarlane, C., & Kambadur, R. (2012). The ubiquitin ligase Mul1 induces mitophagy in skeletal muscle in response to muscle-wasting stimuli. *Cell metabolism*, *16*(5), 613-624.
- Lompre, A. M., Nadal-Ginard, B., & Mahdavi, V. I. J. A. K. (1984). Expression of the cardiac ventricular alpha-and beta-myosin heavy chain genes is developmentally and hormonally regulated. *Journal of Biological Chemistry*, *259*(10), 6437-6446.
- Lu, J., McKinsey, T. A., Zhang, C. L., & Olson, E. N. (2000). Regulation of skeletal myogenesis by association of the MEF2 transcription factor with class II histone deacetylases. *Molecular cell*, *6*(2), 233-244.
- Luo, J., McMullen, J. R., Sobkiw, C. L., Zhang, L., Dorfman, A. L., Sherwood, M. C., & Cantley, L. C. (2005). Class IA phosphoinositide 3-kinase regulates heart size and physiological cardiac hypertrophy. *Molecular and cellular biology*, *25*(21), 9491-9502.
- Ma, K., Mallidis, C., Bhasin, S., Mahabadi, V., Artaza, J., Gonzalez-Cadavid, N., & Salehian, B. (2003). Glucocorticoid-induced skeletal muscle atrophy is associated with upregulation of myostatin gene expression. *American Journal of Physiology-Endocrinology and Metabolism*, *285*(2), E363-E371.
- Macqueen, D. J., & Johnston, I. A. (2009). Evolution of the multifaceted eukaryotic akirin gene family. *BMC evolutionary biology*, *9*(1), 34.
- Macqueen, D. J., Bower, N. I., & Johnston, I. A. (2010). Positioning the expanded *akirin* gene family of Atlantic salmon within the transcriptional networks of myogenesis. *Biochemical and biophysical research communications*, *400*(4), 599-605.
- Mal, A., Sturniolo, M., Schiltz, R. L., Ghosh, M. K., & Harter, M. L. (2001). A role for histone deacetylase HDAC1 in modulating the transcriptional activity of MyoD: inhibition of the myogenic program. *The EMBO journal*, *20*(7), 1739-1753.
- Manning, B. D., & Cantley, L. C. (2007). AKT/PKB signaling: navigating downstream. *Cell*, *129*(7), 1261-1274.

- Marshall, A., Salerno, M. S., Thomas, M., Davies, T., Berry, C., Dyer, K., & Sharma, M. (2008). Mighty is a novel promyogenic factor in skeletal myogenesis. *Experimental cell research*, *314*(5), 1013-1029.
- Martini, F. H. (2006), 7th edition, Fundamentals of Anatomy and Physiology.
- Massagué, J., & Chen, Y. G. (2000). Controlling TGF-β signaling. *Genes & development*, *14*(6), 627-644.
- Massagué, J., Cheifetz, S., Endo, T., & Nadal-Ginard, B. (1986). Type beta transforming growth factor is an inhibitor of myogenic differentiation. *Proceedings of the National Academy of Sciences*, *83*(21), 8206-8210.
- Mastroyiannopoulos, N. P., Nicolaou, P., Anayasa, M., Uney, J. B., & Phylactou, L. A. (2012). Down-regulation of myogenin can reverse terminal muscle cell differentiation. *PloS one*, *7*(1), e29896.
- Masuda, S., Hayashi, T., Egawa, T., & Taguchi, S. (2009). Evidence for differential regulation of lactate metabolic properties in aged and unloaded rat skeletal muscle. *Experimental gerontology*, *44*(4), 280-288.
- Mathews, L. S., Enberg, B., & Norstedt, G. (1989). Regulation of rat growth hormone receptor gene expression. *Journal of Biological Chemistry*, *264*(17), 9905-9910.
- McCroskery, S. M., Platt, L., Hennebry, A., Nishimura, T., McLeay, L., & Kambadur, R. (2005). Improved muscle healing through enhanced regeneration and reduced fibrosis in myostatin-null mice. *Journal of cell science*, *118*(15), 3531-3541.
- McCroskery, S., Thomas, M., Maxwell, L., Sharma, M., & Kambadur, R. (2003). Myostatin negatively regulates satellite cell activation and self-renewal. *The Journal of cell biology*, *162*(6), 1135-1147.
- McElhinny, A. S., Perry, C. N., Witt, C. C., Labeit, S., & Gregorio, C. C. (2004). Muscle-specific RING finger-2 (MURF-2) is important for microtubule, intermediate filament and sarcomeric M-line maintenance in striated muscle development. *Journal of cell science*, *117*(15), 3175-3188.
- McFarlane, C., Plummer, E., Thomas, M., Hennebry, A., Ashby, M., Ling, N., & Kambadur, R. (2006). Myostatin induces cachexia by activating the ubiquitin proteolytic system through an NF-κB-independent, FoxO1-dependent mechanism. *Journal of cellular physiology*, *209*(2), 501-514.

- McFarlane, C., Sharma, M., & Kambadur, R. (2008). Myostatin is a procachectic growth factor during postnatal myogenesis. *Current Opinion in Clinical Nutrition & Metabolic Care*, *11*(4), 422-427.
- McKinnell, I. W., & Rudnicki, M. A. (2004). Molecular mechanisms of muscle atrophy. *Cell*, *119*(7), 907-910.
- McKinsey, T. A., Zhang, C. L., & Olson, E. N. (2001). Control of muscle development by dueling HATs and HDACs. *Current opinion in genetics & development*, *11*(5), 497-504.
- McLennan, I. S. (1996). Degenerating and regenerating skeletal muscles contain several subpopulations of macrophages with distinct spatial and temporal distributions. *Journal of anatomy*, *188*(Pt 1), 17.
- McMullen, J. R., Shioi, T., Zhang, L., Tarnavski, O., Sherwood, M. C., Kang, P. M., & Izumo, S. (2003). Phosphoinositide 3-kinase (p110α) plays a critical role for the induction of physiological, but not pathological, cardiac hypertrophy. *Proceedings of the National Academy of Sciences*, *100*(21), 12355-12360.
- McPherron, A.C., Lawler, A.M., & Lee, S.J. (1997). Regulation of skeletal muscle mass in mice by a new TGF-beta superfamily member. *Nature*, 387(6628), 83-90.
- Megeney, L. A., Kablar, B., Garrett, K., Anderson, J. E., & Rudnicki, M. A. (1996). MyoD is required for myogenic stem cell function in adult skeletal muscle. *Genes & Development*, *10*(10), 1173-1183.
- Mehra, A., & Wrana, J. L. (2002). TGF-β and the Smad signal transduction pathway. *Biochemistry and cell biology*, *80*(5), 605-622.
- Mihaylova, M. M., Vasquez, D. S., Ravnskjaer, K., Denechaud, P. D., Yu, R. T., Alvarez, J. G., & Shaw, R. J. (2011). Class IIa histone deacetylases are hormone-activated regulators of FOXO and mammalian glucose homeostasis. *Cell*, *145*(4), 607-621.
- Miner, J. H., & Wold, B. (1990). Herculin, a fourth member of the MyoD family of myogenic regulatory genes. *Proceedings of the National Academy of Sciences*, *87*(3), 1089-1093.
- Molkentin, J. D., & Markham, B. E. (1993). Myocyte-specific enhancer-binding factor (MEF-2) regulates alpha-cardiac myosin heavy chain gene expression in vitro and in vivo. *Journal of Biological Chemistry*, *268*(26), 19512-19520.
- Molkentin, J. D., Black, B. L., Martin, J. F., & Olson, E. N. (1996). Mutational analysis of the DNA binding, dimerization, and transcriptional

activation domains of MEF2C. *Molecular and cellular biology*, *16*(6), 2627-2636.

- Mone, S. M., Sanders, S. P., & Colan, S. D. (1996). Control mechanisms for physiological hypertrophy of pregnancy. *Circulation*, *94*(4), 667-672.
- Mosher, D. S., Quignon, P., Bustamante, C. D., Sutter, N. B., Mellersh, C. S., Parker, H. G., & Ostrander, E. A. (2007). A mutation in the myostatin gene increases muscle mass and enhances racing performance in heterozygote dogs. *PLoS genetics*, *3*(5), e79.
- Mrosek, M., Labeit, D., Witt, S., Heerklotz, H., von Castelmur, E., Labeit, S., & Mayans, O. (2007). Molecular determinants for the recruitment of the ubiquitin-ligase MuRF-1 onto M-line titin. *The FASEB Journal*, *21*(7), 1383-1392.
- Muir, A. R. (1965). Further observations on the cellular structure of cardiac muscle. *Journal of anatomy*, *99*(Pt 1), 27.
- Murre, C., McCaw, P. S., Vaessin, H., Caudy, M., Jan, L. Y., Jan, Y. N., & Baltimore, D. (1989). Interactions between heterologous helix-loop-helix proteins generate complexes that bind specifically to a common DNA sequence. *Cell*, *58*(3), 537-544.
- Musaro, A., McCullagh, K. J., Naya, F. J., Olson, E. N., & Rosenthal, N. (1999). IGF-1 induces skeletal myocyte hypertrophy through calcineurin in association with GATA-2 and NF-ATc1. *Nature*, *400*(6744), 581-585.
- Naidu, P. S., Ludolph, D. C., To, R. Q., Hinterberger, T. J., & Konieczny, S. F. (1995). Myogenin and MEF2 function synergistically to activate the MRF4 promoter during myogenesis. *Molecular and cellular biology*, *15*(5), 2707-2718.
- Nowak, S. J., Aihara, H., Gonzalez, K., Nibu, Y., & Baylies, M. K. (2012). Akirin links twist-regulated transcription with the Brahma chromatin remodeling complex during embryogenesis. *PLoS genetics*, *8*(3), e1002547.
- Ohsawa, M., Liewluck, T., Ogata, K., Iizuka, T., Hayashi, Y., Nonaka, I., & Nishino, I. (2007). Familial reducing body myopathy. *Brain and Development*, *29*(2), 112-116.
- Olguin, H. C., & Olwin, B. B. (2004). Pax-7 up-regulation inhibits myogenesis and cell cycle progression in satellite cells: a potential mechanism for self-renewal. *Developmental biology*, *275*(2), 375-388.
- Oliver, M. H., Harrison, N. K., Bishop, J. E., Cole, P. J., & Laurent, G. J. (1989). A rapid and convenient assay for counting cells cultured in

microwell plates: application for assessment of growth factors. *Journal of cell science*, *92*(3), 513-518.

- Olivetti, G., Abbi, R., Quaini, F., Kajstura, J., Cheng, W., Nitahara, J. A., & Anversa, P. (1997). Apoptosis in the failing human heart. *New England Journal of Medicine*, *336*(16), 1131-1141.
- Olson, E. N., & Williams, R. S. (2000). Remodeling muscles with calcineurin. *Bioessays*, *22*(6), 510-519.
- Ott, M. O., Bober, E., Lyons, G., Arnold, H., & Buckingham, M., (1991). Early expression of the myogenic regulatory gene, myf-5, in precursor cells of skeletal muscle in the mouse embryo. *Development*, *111*(4), 1097-1107.
- Oustanina, S., Hause, G., & Braun, T. (2004). Pax7 directs postnatal renewal and propagation of myogenic satellite cells but not their specification. *The EMBO journal*, *23*(16), 3430-3439.
- Patterson, C., Willis, M. S., & Portbury, A. (2011). Rise Above: Muscle Ring-Finger-1 (MURF1) Regulation of Cardiomyocyte Size and Energy Metabolism. *Transactions of the American Clinical and Climatological Association*, *122*, 70.
- Paul, A. C., & Rosenthal, N. (2002). Different modes of hypertrophy in skeletal muscle fibers. *The Journal of cell biology*, *156*(4), 751-760.
- Person, V., Kostin, S., Suzuki, K., Labeit, S., & Schaper, J. (2000). Antisense oligonucleotide experiments elucidate the essential role of titin in sarcomerogenesis in adult rat cardiomyocytes in long-term culture. *Journal of cell science*, *113*(21), 3851-3859.
- Philip, B., Lu, Z., & Gao, Y. (2005). Regulation of GDF-8 signaling by the p38 MAPK. *Cellular signalling*, *17*(3), 365-375.
- Pirskanen, A., Kiefer, J.C., Hauschka, S.D. (2000). IGFs, insulin, Shh, bFGF and TGF-beta1 interact synergistically to promote somite myogenesis in vitro. *Developmental biology*, 224(2), 189-203.
- Pizon, V., Iakovenko, A., van der Ven, P. F., Kelly, R., Fatu, C., Fürst, D. O., & Gautel, M. (2002). Transient association of titin and myosin with microtubules in nascent myofibrils directed by the MURF2 RING-finger protein. *Journal of cell science*, *115*(23), 4469-4482.
- Pluim, B. M., Zwinderman, A. H., van der Laarse, A., & van der Wall, E. E. (2000). The athlete's heart a meta-analysis of cardiac structure and function. *Circulation*, *101*(3), 336-344.

- Powell-Braxton, L., Hollingshead, P., Giltinan, D., Pitts-Meek, S., & Stewart, T. (1993). Inactivation of the IGF-I Gene in Mice Results in Perinatal Lethality. *Annals of the New York Academy of Sciences*, *692*(1), 300-301.
- Puri, P. L., Iezzi, S., Stiegler, P., Chen, T. T., Schiltz, R. L., Muscat, G. E., & Sartorelli, V. (2001). Class I histone deacetylases sequentially interact with MyoD and pRb during skeletal myogenesis. *Molecular cell*, *8*(4), 885-897.
- Rajab, P., Fox, J., Riaz, S., Tomlinson, D., Ball, D., & Greenhaff, P. L. (2000). Skeletal muscle myosin heavy chain isoforms and energy metabolism after clenbuterol treatment in the rat. *American Journal of Physiology-Regulatory, Integrative and Comparative Physiology*, *279*(3), R1076-R1081.
- Ramirez, M. T., Sah, V. P., Zhao, X. L., Hunter, J. J., Chien, K. R., & Brown, J. H. (1997). The MEKK-JNK Pathway Is Stimulated by α1-Adrenergic Receptor and Ras Activation and Is Associated with in Vitroand in Vivo Cardiac Hypertrophy. *Journal of Biological Chemistry*, *272*(22), 14057-14061.
- Reardon, K. A., Davis, J., Kapsa, R. M., Choong, P., & Byrne, E. (2001). Myostatin, insulin-like growth factor-1, and leukemia inhibitory factor mRNAs are upregulated in chronic human disuse muscle atrophy. *Muscle & nerve*, *24*(7), 893-899.
- Rebbapragada, A., Benchabane, H., Wrana, J. L., Celeste, A.J., & Attisano, L. (2003). Myostatin signals through a transforming growth factor beta-like signaling pathway to block adipogenesis. *Molecular Cell Biology*, 23(20), 7230-42.
- Reiss, K., Cheng, W., Ferber, A., Kajstura, J., Li, P., Li, B., & Anversa, P. (1996). Overexpression of insulin-like growth factor-1 in the heart is coupled with myocyte proliferation in transgenic mice. *Proceedings of the National Academy of Sciences*, *93*(16), 8630-8635.
- Reshef, R., Maroto, M., & Lassar, A. B. (1998). Regulation of dorsal somitic cell fates: BMPs and Noggin control the timing and pattern of myogenic regulator expression. *Genes & development*, *12*(3), 290-303.
- Rios, R., Carneiro, I., Arce, V. M., & Devesa, J. (2001). Myostatin regulates cell survival during C_2C_{12} myogenesis. *Biochemical and biophysical research communications*, *280*(2), 561-566.
- Rios, R., Carneiro, I., Arce, V. M., & Devesa, J. (2002). Myostatin is an inhibitor of myogenic differentiation. *American Journal of Physiology-Cell Physiology*, *282*(5), C993-C999.

- Robertson, T. A., Maley, M. A. L., Grounds, M. D., & Papadimitriou, J. M. (1993). The role of macrophages in skeletal muscle regeneration with particular reference to chemotaxis. *Experimental cell research*, *207*(2), 321-331.
- Robson, L. G., & Hughes, S. M. (1996). The distal limb environment regulates MyoD accumulation and muscle differentiation in mouse-chick chimaeric limbs. *Development*, *122*(12), 3899-3910.
- Rodgers, B. D., Interlichia, J. P., Garikipati, D. K., Mamidi, R., Chandra, M., Nelson, O. L., & Santana, L. F. (2009). Myostatin represses physiological hypertrophy of the heart and excitation–contraction coupling. *The Journal of physiology*, *587*(20), 4873-4886.
- Rudnicki, M. A., Schnegelsberg, P. N., Stead, R. H., Braun, T., Arnold, H. H., & Jaenisch, R. (1993). MyoD or Myf-5 is required for the formation of skeletal muscle. *Cell*, *75*(7), 1351-1359.
- Sacheck, J. M., Ohtsuka, A., McLary, S. C., & Goldberg, A. L. (2004). IGF-I stimulates muscle growth by suppressing protein breakdown and expression of atrophy-related ubiquitin ligases, atrogin-1 and MuRF1. *American Journal of Physiology-Endocrinology and Metabolism*, *287*(4), E591-E601.
- Sahlin, K., Tonkonogi, M., & Söderlund, K. (1998). Energy supply and muscle fatigue in humans. *Acta Physiologica Scandinavica*, *162*(3), 261-266.
- Sajko, Š., Kubínová, L., Cvetko, E., Kreft, M., Wernig, A., & Eržen, I. (2004). Frequency of M-cadherin-stained satellite cells declines in human muscles during aging. *Journal of Histochemistry & Cytochemistry*, *52*(2), 179-185.
- Salerno, M. S., Dyer, K., Bracegirdle, J., Platt, L., Thomas, M., Siriett, V., & Sharma, M. (2009). *Akirin1* (*Mighty*), a novel promyogenic factor regulates muscle regeneration and cell chemotaxis. *Experimental cell research*, *315*(12), 2012-2021.
- Sarker, K. P., & Lee, K. Y. (2004). L6 myoblast differentiation is modulated by Cdk5 via the PI3K–AKT–p70S6K signaling pathway. *Oncogene*, *23*(36), 6064-6070.
- Sartorelli, V., Webster, K. A., & Kedes, L. (1990). Muscle-specific expression of the cardiac alpha-actin gene requires MyoD1, CArG-box binding factor, and Sp1. *Genes & development*, *4*(10), 1811-1822.
- Sassoon, D., Lyons, G., Wright, W. E., Lin, V., Lassar, A., Weintraub, H., & Buckingham, M. (1989). Expression of two myogenic regulatory

factors myogenin and MyoD1 during mouse embryogenesis. *Nature*, *341*(6240), 303-307.

- Sato, M., Muragaki, Y., Saika, S., Roberts, A. B., & Ooshima, A. (2003). Targeted disruption of TGF-β1/Smad3 signaling protects against renal tubulointerstitial fibrosis induced by unilateral ureteral obstruction. *Journal of Clinical Investigation*, *112*(10), 1486-1494.
- Schiaffino, S., & Reggiani, C., (1994). Myosin isoforms in mammalian skeletal muscle. *Journal of Applied Physiology*, *77*(2), 493-501.
- Schuelke, M., Wagner, K. R., Stolz, L. E., Hübner, C., Riebel, T., Kömen, W., & Lee, S. J. (2004). Myostatin mutation associated with gross muscle hypertrophy in a child. *New England Journal of Medicine*, *350*(26), 2682-2688.
- Schuler, M., Ali, F., Chambon, C., Duteil, D., Bornert, J. M., Tardivel, A., & Metzger, D. (2006). PGC1α expression is controlled in skeletal muscles by PPARβ, whose ablation results in fiber-type switching, obesity, and type 2 diabetes. *Cell metabolism*, *4*(5), 407-414.
- Schulte, J. N., & Yarasheski, K. E. (2001). Effects of resistance training on the rate of muscle protein synthesis in frail elderly people. *International journal of sport nutrition and exercise metabolism*, *11*, 111-118.
- Schultz, E., Jaryszak, D. L., & Valliere, C. R. (1985). Response of satellite cells to focal skeletal muscle injury. *Muscle & nerve*, *8*(3), 217-222.
- Schulz, R. A., & Yutzey, K. E. (2004). Calcineurin signaling and NFAT activation in cardiovascular and skeletal muscle development. *Developmental biology*, *266*(1), 1-16.
- Seelay, R.R., T.D. Stephens and P. Tate. 7th Edition. Anatomy and Physiology.
- Seidman, J. G., & Seidman, C. (2001). The genetic basis for cardiomyopathy: from mutation identification to mechanistic paradigms. *Cell*, *104*(4), 557-567.
- Semsarian, C., Wu, M. J., Ju, Y. K., Marciniec, T., Yeoh, T., Allen, D. G., & Graham, R. M. (1999). Skeletal muscle hypertrophy is mediated by a Ca^{2+}dependent calcineurin signalling pathway. *Nature*, *400*(6744), 576-581.
- Shah, O. J., Anthony, J. C., Kimball, S. R., & Jefferson, L. S. (2000). 4E-BP1 and S6K1: translational integration sites for nutritional and hormonal information in muscle. *American Journal of Physiology-Endocrinology And Metabolism*, *279*(4), E715-E729.

- Sharma, M., Kambadur, R., Matthews, K. G., Somers, W. G., Devlin, G. P., Conaglen, J. V., & Bass, J. J. (1999). Myostatin, a transforming growth factor-β superfamily member, is expressed in heart muscle and is upregulated in cardiomyocytes after infarct. *Journal of cellular physiology*, *180*(1), 1-9.
- Sharma, M., Langley, B., Bass, J., & Kambadur, R. (2001). Myostatin in muscle growth and repair. *Exercise and sport sciences reviews*, *29*(4), 155-158.
- Shioi, T., Kang, P. M., Douglas, P. S., Hampe, J., Yballe, C. M., Lawitts, J., & Izumo, S. (2000). The conserved phosphoinositide 3-kinase pathway determines heart size in mice. *The EMBO journal*, *19*(11), 2537-2548.
- Shyu, K. G., Ko, W. H., Yang, W. S., Wang, B. W., & Kuan, P. (2005). Insulin-like growth factor-1 mediates stretch-induced upregulation of myostatin expression in neonatal rat cardiomyocytes. *Cardiovascular research*, *68*(3), 405-414.
- Siriett, V., Salerno, M. S., Berry, C., Nicholas, G., Bower, R., Kambadur, R., & Sharma, M. (2007). Antagonism of myostatin enhances muscle regeneration during sarcopenia. *Molecular Therapy*, *15*(8), 1463-1470.
- Slager, H. G., Van Inzen, W., Freund, E., van den Eijnden-Van Raaij, A. J. M., & Mummery, C. L. (1993). Transforming growth factor-β in the early mouse embryo: Implications for the regulation of muscle formation and implantation. *Developmental genetics*, *14*(3), 212-224.
- Soulez, M., Rouviere, C. G., Chafey, P., Hentzen, D., Vandromme, M., Lautredou, N., & Tuil, D. (1996). Growth and differentiation of C2 myogenic cells are dependent on serum response factor. *Molecular and cellular biology*, *16*(11), 6065-6074.
- Spencer, J. A., Eliazer, S., Ilaria, R. L., Richardson, J. A., & Olson, E. N. (2000). Regulation of microtubule dynamics and myogenic differentiation by MURF, a striated muscle RING-finger protein. *The Journal of cell biology*, *150*(4), 771-784.
- Sriram, S., Subramanian, S., Sathiakumar, D., Venkatesh, R., Salerno, M. S., McFarlane, C. D., & Sharma, M. (2011). Modulation of reactive oxygen species in skeletal muscle by myostatin is mediated through NF-κB. *Aging cell*, *10*(6), 931-948.
- Stitt, T. N., Drujan, D., Clarke, B. A., Panaro, F., Timofeyva, Y., Kline, W. O., & Glass, D. J. (2004). The IGF-1/PI3K/Akt pathway prevents expression of muscle atrophy-induced ubiquitin ligases by inhibiting FOXO transcription factors. *Molecular cell*, *14*(3), 395-403.

- St-Pierre, J., Lin, J., Krauss, S., Tarr, P. T., Yang, R., Newgard, C. B., & Spiegelman, B. M. (2003). Bioenergetic analysis of peroxisome proliferator-activated receptor γ coactivators 1α and 1β (PGC-1α and PGC-1β) in muscle cells. *Journal of Biological Chemistry*, *278*(29), 26597-26603.
- Sugden, P. H., & Clerk, A. (1998). Cellular mechanisms of cardiac hypertrophy. *Journal of molecular medicine*, *76*(11), 725-746.
- Tajbakhsh, S., Rocancourt, D., Cossu, G., & Buckingham, M. (1997). Redefining the Genetic Hierarchies Controlling Skeletal Myogenesis: Pax-3 and Myf-5 Act Upstream of MyoD. *Cell*, *89*(1), 127-138.
- Takeishi, Y., Chu, G., Kirkpatrick, D. M., Li, Z., Wakasaki, H., Kranias, E. G., & Walsh, R. A. (1998). In vivo phosphorylation of cardiac troponin I by protein kinase Cbeta2 decreases cardiomyocyte calcium responsiveness and contractility in transgenic mouse hearts. *Journal of Clinical Investigation*, *102*(1), 72.
- Talmadge, R. J., Roy, R. R., & Edgerton, R. V. (1993). Muscle fiber types and function. *Current opinion in rheumatology*, *5*(6), 695-705.
- Thomas, M., Langley, B., Berry, C., Sharma, M., Kirk, S., Bass, J., & Kambadur, R. (2000). Myostatin, a negative regulator of muscle growth, functions by inhibiting myoblast proliferation. *Journal of Biological Chemistry*, *275*(51), 40235-40243.
- Thomson, D. M., Herway, S. T., Fillmore, N., Kim, H., Brown, J. D., Barrow, J. R., & Winder, W. W. (2008). AMP-activated protein kinase phosphorylates transcription factors of the CREB family. *Journal of Applied Physiology*, *104*(2), 429-438.
- Tidball, J. G., Albrecht, D. E., Lokensgard, B. E., & Spencer, M. J. (1995). Apoptosis precedes necrosis of dystrophin-deficient muscle. *Journal of cell science*, *108*(6), 2197-2204.
- Tobimatsu, K., Noguchi, T., Hosooka, T., Sakai, M., Inagaki, K., Matsuki, Y., & Kasuga, M. (2009). Overexpression of the transcriptional coregulator Cited2 protects against glucocorticoid-induced atrophy of C_2C_{12} myotubes. *Biochemical and biophysical research communications*, *378*(3), 399-403.
- Toker, A., & Cantley, L. C. (1997). Signalling through the lipid products of phosphoinositide-3-OH kinase. *Nature*, *387*(6634), 673-676.
- Tortora G. J. & Derrickson B.(2007) 13^{th} edition, Principles of Anatomy and Physiology.
- Trendelenburg, A. U., Meyer, A., Rohner, D., Boyle, J., Hatakeyama, S., & Glass, D. J. (2009). Myostatin reduces Akt/TORC1/p70S6K signaling,

inhibiting myoblast differentiation and myotube size. *American Journal of Physiology-Cell Physiology*, *296*(6), C1258-C1270.

- Tse, J., Powell, J. R., Baste, C. A., Priest, R. E., & Kuo, J. F. (1979). Isoproterenol-induced cardiac hypertrophy: modifications in characteristics of β-adrenergic receptor, adenylate cyclase, and ventricular contraction. *Endocrinology*, *105*(1), 246-255.
- Tskhovrebova, L., & Trinick, J. (2003). Titin: properties and family relationships. *Nature Reviews Molecular Cell Biology*, *4*(9), 679-689.
- Vaidya, T. B., Rhodes, S. J., Taparowsky, E. J., & Konieczny, S. F. (1989). Fibroblast growth factor and transforming growth factor beta repress transcription of the myogenic regulatory gene MyoD1. *Molecular and cellular biology*, *9*(8), 3576-3579.
- Van der Ven, P. F., Bartsch, J. W., Gautel, M., Jockusch, H., & Furst, D. O. (2000). A functional knock-out of titin results in defective myofibril assembly. *Journal of Cell Science*, *113*(8), 1405-1414.
- Varnava, A. M., Elliott, P. M., Baboonian, C., Davison, F., Davies, M. J., & McKenna, W. J. (2001). Hypertrophic cardiomyopathy histopathological features of sudden death in cardiac troponin T disease. *Circulation*, *104*(12), 1380-1384.
- Venuti, J. M., Morris, J. H., Vivian, J. L., Olson, E. N., & Klein, W. H. (1995). Myogenin is required for late but not early aspects of myogenesis during mouse development. *The Journal of cell biology*, *128*(4), 563-576.
- Vitt, U. A., & Hsueh, A. J. (2001). Stage-dependent role of growth differentiation factor-9 in ovarian follicle development. *Molecular and cellular endocrinology*, *183*(1), 171-177.
- Volders, P. G., Willems, I. E., Cleutjens, J. P., Aren, J. W., Havenith, M. G., & Daemen, M. J. (1993). Interstitial collagen is increased in the non-infarcted human myocardium after myocardial infarction. *Journal of molecular and cellular cardiology*, *25*(11), 1317-1323.
- Wagner, K. R., Liu, X., Chang, X., & Allen, R. E. (2005). Muscle regeneration in the prolonged absence of myostatin. *Proceedings of the National Academy of Sciences of the United States of America*, *102*(7), 2519-2524.
- Wakabayashi, K., Sugimoto, Y., Takezawa, Y., Oshima, K., Matsuo, T., Ueno, Y., & Irving, T. C. Muscle Contraction Mechanisms: Use of Synchrotron X-ray Diffraction. *eLS*.

- Wakatsuki, T., Schlessinger, J., & Elson, E. L. (2004). The biochemical response of the heart to hypertension and exercise. *Trends in biochemical sciences*, *29*(11), 609-617.
- Wallimann, T. (1996). 31P-NMR-measured creatine kinase reaction flux in muscle: a caveat! *Journal of Muscle Research & Cell Motility*, *17*(2), 177-181.
- Wan, B., & Moreadith, R. W. (1995). Structural characterization and regulatory element analysis of the heart isoform of cytochrome c oxidase VIa. *Journal of Biological Chemistry*, *270*(44), 26433-26440.
- Wang, Y., Huang, S., Sah, V. P., Ross, J., Brown, J. H., Han, J., & Chien, K. R. (1998). Cardiac muscle cell hypertrophy and apoptosis induced by distinct members of the p38 mitogen-activated protein kinase family. *Journal of Biological Chemistry*, *273*(4), 2161-2168.
- Wang, Y., Su, B., Sah, V. P., Brown, J. H., Han, J., & Chien, K. R. (1998). Cardiac hypertrophy induced by mitogen-activated protein kinase kinase 7, a specific activator for c-Jun NH2-terminal kinase in ventricular muscle cells. *Journal of Biological Chemistry*, *273*(10), 5423-5426.
- Webb, S. E., Lee, K. K. H., Tang, M. K., & Ede, D. A. (1997). Fibroblast growth factors 2 and 4 stimulate migration of mouse embryonic limb myogenic cells. *Developmental dynamics*, *209*(2), 206-216.
- Wei, Y., Peng, S., Wu, M., Sachidanandam, R., Tu, Z., Zhang, S., & Zhao, Y. (2014). Multifaceted roles of miR-1s in repressing the fetal gene program in the heart. *Cell Research*.
- Wentworth, B. M., Donoghue, M., Engert, J. C., Berglund, E. B., & Rosenthal, N. (1991). Paired MyoD-binding sites regulate myosin light chain gene expression. *Proceedings of the National Academy of Sciences*, *88*(4), 1242-1246.
- Westerbald,H., Bruton, J.D., Katz, A. (2010). Skeletal muscle: energy metabolism, fiber types, fatigue and adaptability. *Experimental Cell Research*, 316(8), 3093-3099.
- Wettschureck, N., Rütten, H., Zywietz, A., Gehring, D., Wilkie, T. M., Chen, J., & Offermanns, S. (2001). Absence of pressure overload induced myocardial hypertrophy after conditional inactivation of Gαq/Gα11 in cardiomyocytes. *Nature medicine*, *7*(11), 1236-1240.
- Willis, M. S., Ike, C., Li, L., Wang, D. Z., Glass, D. J., & Patterson, C. (2007). Muscle ring finger 1, but not muscle ring finger 2, regulates cardiac hypertrophy in vivo. *Circulation research*, *100*(4), 456-459.

- Wright, W. E., Sassoon, D. A., & Lin, V. K. (1989). Myogenin, a factor regulating myogenesis, has a domain homologous to MyoD. *Cell*, *56*(4), 607-617.
- Yaffe, D., & Saxel, O. (1977). A myogenic cell line with altered serum requirements for differentiation. *Differentiation*, *7*(1-3), 159-166.
- Yaffe, D., & Saxel, O. R. A. (1977). Serial passaging and differentiation of myogenic cells isolated from dystrophic mouse muscle. *Nature*, *270*(5639), 725-727.
- Yang, C. G., Wang, X. L., Wang, L., Zhang, B., & Chen, S. L. (2011). A new Akirin1 gene in turbot (Scophthalmus maximus): Molecular cloning, characterization and expression analysis in response to bacterial and viral immunological challenge. *Fish & shellfish immunology*, *30*(4), 1031-1041.
- Yang, S. Y., & Goldspink, G. (2002). Different roles of the IGF-I Ec peptide (MGF) and mature IGF-I in myoblast proliferation and differentiation. *FEBS letters*, *522*(1), 156-160.
- Yarasheski, K. E., Welle, S., & Nair, K. S. (2002). Muscle protein synthesis in younger and older men. *Jama*, *287*(3), 317-318.
- Ye, J., Cippitelli, M., Dorman, L., Ortaldo, J. R., & Young, H. A. (1996). The nuclear factor YY1 suppresses the human gamma interferon promoter through two mechanisms: inhibition of AP1 binding and activation of a silencer element. *Molecular and cellular biology*, *16*(9), 4744-4753.
- Yoshiko, Y., Hirao, K., & Maeda, N. (2002). Differentiation in C_2C_{12} myoblasts depends on the expression of endogenous IGFs and not serum depletion. *American Journal of Physiology-Cell Physiology*, *283*(4), C1278-C1286.
- Youle, R. J., & Van Der Bliek, A. M. (2012). Mitochondrial fission, fusion, and stress. *Science*, *337*(6098), 1062-1065.
- Young, P., Ehler, E., & Gautel, M. (2001). Obscurin, a giant sarcomeric Rho guanine nucleotide exchange factor protein involved in sarcomere assembly. *The Journal of cell biology*, *154*(1), 123-136.
- Zachwieja, J. J., Witt, T. L., & Yarasheski, K. E. (2000). Intravenous glutamine does not stimulate mixed muscle protein synthesis in healthy young men and women. *Metabolism*, *49*(12), 1555-1560.
- Zentella, A., & Massague, J. (1992). Transforming growth factor beta induces myoblast differentiation in the presence of mitogens. *Proceedings of the National Academy of Sciences*, *89*(11), 5176-5180.

- Zhang, C. L., McKinsey, T. A., Chang, S., Antos, C. L., Hill, J. A., & Olson, E. N. (2002). Class II histone deacetylases act as signal-responsive repressors of cardiac hypertrophy. *Cell*, *110*(4), 479-488.
- Zhang, S., Weinheimer, C., Courtois, M., Kovacs, A., Zhang, C. E., Cheng, A. M., & Muslin, A. J. (2003). The role of the Grb2–p38 MAPK signaling pathway in cardiac hypertrophy and fibrosis. *Journal of Clinical Investigation*, *111*(6), 833-841.
- Zhang, X., Azhar, G., Chai, J., Sheridan, P., Nagano, K., Brown, T., & Wei, J. Y. (2001). Cardiomyopathy in transgenic mice with cardiac-specific overexpression of serum response factor. *American Journal of Physiology-Heart and Circulatory Physiology*, *49*(4), H1782.
- Zhang, X., Azhar, G., Helms, S. A., & Wei, J. Y. (2011). Regulation of cardiac microRNAs by serum response factor. *J Biomed Sci*, *18*(1), 15.
- Zhao, J., Brault, J. J., Schild, A., Cao, P., Sandri, M., Schiaffino, S., & Goldberg, A. L. (2007). FoxO3 coordinately activates protein degradation by the autophagic/lysosomal and proteasomal pathways in atrophying muscle cells. *Cell metabolism*, *6*(6), 472-483.
- Zhao, P., & Hoffman, E. P. (2004). Embryonic myogenesis pathways in muscle regeneration. *Developmental Dynamics*, *229*(2), 380-392.
- Zheng, Z., Wang, Z. M., & Delbono, O. (2004). Ca2+ calmodulin kinase and calcineurin mediate IGF-1-induced skeletal muscle dihydropyridine receptor α1S transcription. *The Journal of membrane biology*, *197*(2), 101-112.
- Zhou, X., Richon, V. M., Rifkind, R. A., & Marks, P. A. (2000). Identification of a transcriptional repressor related to the noncatalytic domain of histone deacetylases 4 and 5. *Proceedings of the National Academy of Sciences*, *97*(3), 1056-1061.
- Zimmers, T. A., Davies, M. V., Koniaris, L. G., Haynes, P., Esquela, A. F., Tomkinson, K. N., & Lee, S. J. (2002). Induction of cachexia in mice by systemically administered myostatin. *Science*, *296*(5572), 1486-1488.
- Zivkovic, Z., Torina, A., Mitra, R., Alongi, A., Scimeca, S., Kocan, K. M., & De la Fuente, J. (2010). Subolesin expression in response to pathogen infection in ticks. *BMC immunology*, *11*(1), 7.

THE END